

Cement-Bitumen Treated Materials (CBTM) for Cold
Regions: RAP Aggregate Source and
Low Production Temperatures

by

Simone RASCHIA

MANUSCRIPT-BASED THESIS PRESENTED TO ÉCOLE DE
TECHNOLOGIE SUPÉRIEURE IN PARTIAL FULFILLMENT OF THE
DEGREE OF DOCTOR OF PHILOSOPHY
Ph.D.

MONTREAL, SEPTEMBER 28, 2020

ÉCOLE DE TECHNOLOGIE SUPÉRIEURE
UNIVERSITÉ DU QUÉBEC



Simone RASCHIA, 2020



This [Creative Commons](https://creativecommons.org/licenses/by-nc-nd/4.0/) licence allows readers to download this work and share it with others as long as the author is credited. The content of this work can't be modified in any way or used commercially

BOARD OF EXAMINERS

THIS THESIS HAS BEEN EVALUATED

BY THE FOLLOWING BOARD OF EXAMINERS

Mr. Daniel Perraton, thesis director
Department of construction engineering at École de technologie supérieure

Mr. Alan Carter, thesis co-director
Department of construction engineering at École de technologie supérieure

Mr. Andrea Graziani, thesis co-director
Department of civil and building engineering, and architecture at Università Politecnica delle Marche

Mr. Éric David, President of the Board of Examiners
Department of mechanical engineering at École de technologie supérieure

Mr. Michel Vaillancourt, Member of the jury
Department of construction engineering at École de technologie supérieure

Mr. Emmanuel Chailleux, Member of the jury
Institut français des sciences et technologies des transports, de l'aménagement et des réseaux

THIS THESIS WAS PRESENTED AND DEFENDED

IN THE PRESENCE OF A BOARD OF EXAMINERS AND PUBLIC

ON SEPTEMBER 9, 2020

AT ÉCOLE DE TECHNOLOGIE SUPÉRIEURE

ACKNOWLEDGMENTS

There are no good students, only good teachers, and I can certainly say that mine were not only leaders to refer to, but real guides who have enlightened the way in the past years. Thanks to Prof. Daniel Perraton, who with his wisdom and fighting spirit hasn't let me doubt of myself even one day. Thanks to Prof. Alan Carter, who taught me that having a messy office is simply a symbol of great passion. Last but not the least, thanks to Prof. Andrea Graziani, for having initially thought of me to send to Canada, and teaching me over time the importance of the details that really make the difference. Everything you have taught me will not be lost and I promise to always follow your example.

Thanks to Mr. Emmanuel Chailleux, Mr. Michel Vaillancourt, and the jury president Mr. Éric David for being jury members for my doctoral thesis.

My family never imagined they'd find themselves in such an adventure, I know that. And for that I thank them tremendously, for always supporting me and opening their minds to understand how to make me feel better. Thanks to Marta, probably the person who listened to me the most and understood me for all these years. Everyone deserves to have their loved one by their side, and while I will miss my life here in Canada, I am sure an even more exciting life is waiting for me with you.

Thanks to all the friends of ÉTS, Francis, Sylvain, Sébastien, Appu, Marc-André, Mounir, Amir, Djalil, Ehsan, Quentin, Charles, Reza, Saeed B., Saeed S., for making every day of work a party, and for making these three years fly. I will never forget you.

Thanks to my italian support team, Davide, Chiara M, Chiara O, Petala, Patty and Giorgio, which were always there for everything and became my family on the other side of the ocean.

Matériaux traités au ciment et bitume (MTCB) pour les régions froides: source de granulats GBR et basses températures de production

Simone RASCHIA

RÉSUMÉ

L'augmentation du prix du bitume due à la crise énergétique des dernières années a entraîné le développement de technologies rentables de recyclage des revêtements en enrobé bitumineux. La disponibilité limitée de granulats naturels, l'augmentation des coûts d'élimination des matériaux provenant des chaussées et la sensibilisation politique croissante aux questions environnementales favorisent fortement les techniques de recyclage, telles que le recyclage à froid (*cold recycling* - CR) et la réutilisation des granulats bitumineux recyclés (GBR). Dans ce contexte, les matériaux traités au ciment et bitume (MTCB) sont prometteurs en termes de fiabilité, de rentabilité et de développement durable. La principale différence entre le MTCB et l'enrobé bitumineux à chaud (*hot mix asphalt* - HMA) est que l'effet lubrifiant dans le premier cas est donné principalement par l'eau, tandis que dans le second cas il est donné par le bitume chauffé. De plus, la cohésion du MTCB est assurée par l'effet combiné de l'émulsion de bitume (ou de la mousse de bitume) et du ciment comme agents de liaison. Puisque les GBR représentent la composante principale du squelette granulaire du MTCB, une étude portant sur l'effet des différentes sources de GBR quant à l'ouvrabilité et aux propriétés thermo-mécaniques du MTCB est nécessaire pour éclairer le processus de formulation de ce type de matériaux. Par ailleurs, l'expérience terrain a montré que la mise en oeuvre de MTCB à basse température (pendant les saisons froides) semble changer les propriétés mécaniques de ce matériau à long terme. Par conséquent, l'objectif principal de cette thèse est de comprendre l'effet des sources de GBR et des basses températures de mise en oeuvre sur les propriétés du MTCB. Les résultats ont montré que la source GBR influence effectivement plusieurs propriétés des MTCB. En fait, les caractéristiques du liant du GBR, ainsi que son affinité avec le bitume résiduel de l'émulsion, affectent les propriétés des MTCB lors de la production (maniabilité et compactabilité), et aussi pendant et après la cure, où on a observé une influence sur les propriétés mécaniques dans les domaines de petite et de grande déformation. En outre, les caractéristiques de l'émulsion de bitume influencent le processus de production à basse température. Les résultats ont montré que la production de ces matériaux à 5 °C (malaxage, transport, mise en place, compactage et cure) était possible. De cette manière, le temps disponible pour la production de MTCB au cours de l'année augmente, mais, par contre, une perte de rigidité à long terme de 30% a été observée par rapport aux MTCB produits à 25 °C. Il convient d'en tenir compte lors de la conception des chaussées.

Mots clés : Recyclage à froid, Source du GBR, Production, Cure, Basses températures, Propriétés mécaniques

Cement-bitumen treated materials (CBTM) for cold regions: RAP aggregate source and low production temperatures

Simone RASCHIA

ABSTRACT

The increase of asphalt price due to the energy crisis of the last years drove the development of cost-effective asphalt pavement recycling technologies. The limited availability of natural aggregates, the growing awareness about the environment and the increasing costs for handling milled materials, required innovative sustainable technics, such as cold in-place recycling (CIR) and the reuse of reclaimed asphalt pavement (RAP). In this context, cement-bitumen treated materials (CBTM) ensure benefits in terms of reliability, cost-effectiveness and environmental sustainability. The main difference between CBTM and Hot Mix Asphalt (HMA) is that the lubricant effect in the first is given mostly by the water, while in the second case it is given by the heated bitumen. At the same time, the cohesion of CBTM is granted by the cooperation of bitumen emulsion (or foamed bitumen) and cement as binding agents. Since the RAP aggregate are the major component of the aggregate volume, it is believed that a study on the effect of different RAP sources is needed to improve the mix design process. Moreover, field experience shows that CBTM laydown at low temperatures (during cold seasons) seems to suffer a loss in mechanical properties. Hence, the main objective of this thesis is to understand the effect of RAP sources and of low production temperatures on CBTM properties. Results have shown that the RAP source does influence several CBTM properties. In fact, the RAP binder characteristics, as well as its affinity with the residual bitumen used in the emulsion, affect the properties of cold recycled materials not only during production (workability and compactability), but also during and after the curing period, where influence on the mechanical properties in the small strain and large strain domains were observed. Furthermore, the bitumen emulsion characteristics influence the production process at low temperatures. Results showed that the production of such materials at 5 °C (intended as mixing, transportation, laydown, compaction and curing) was possible. In this way the time available for production during the year increases, but, on the other hand, a stiffness loss of 30% was observed compared to mixtures produced at 25 °C. This should be taken into account during pavement design.

Keywords : Cold recycling, RAP source, Production, Curing, Low temperatures, Mechanical properties

TABLE OF CONTENTS

	Page
INTRODUCTION	1
CHAPTER 1 LITERATURE REVIEW	5
1.1 Cold Recycling (CR).....	5
1.1.1 Cold Recycled Mixtures (CRM).....	6
1.1.2 Bitumen emulsions.....	8
1.1.3 Foamed bitumen.....	16
1.1.4 Reclaimed asphalt pavement (RAP).....	17
1.1.5 Ordinary Portland Cement	18
1.2 Interaction of bitumen emulsion with mineral aggregates.....	21
1.3 Role of mineral additions.....	22
1.4 CBTM production and curing.....	24
1.4.1 Introduction.....	24
1.4.2 Mixing and compaction	26
1.4.3 Curing protocols.....	31
1.4.4 Field curing studies	32
1.4.5 Laboratory curing for bitumen emulsion mixes.....	33
1.5 Modelling of CBTM properties	36
1.5.1 Evolutive behaviour	36
1.5.2 Visco-elastic behaviour of bituminous materials.....	37
1.5.3 Rheological modelling.....	42
CHAPTER 2 RESEARCH OBJECTIVES AND EXPERIMENTAL PROGRAM.....	49
2.1 Research problem.....	49
2.2 Objectives	50
2.3 Experimental approach	51
2.3.1 Physical properties	52
2.3.2 Mechanical properties.....	53
2.4 Materials	56
2.5 Thesis structure	57
CHAPTER 3 VOLUMETRIC APPROACH FOR CBTM.....	61
3.1 Overview on the volumetric approach for HMA.....	61
3.2 Volumetric approach for CBTM mixtures.....	62
3.2.1 CBTM composition during compaction	63
3.2.2 CBTM composition at the long-term state.....	66
3.3 Practical validation of the volumetric approach	70
CHAPTER 4 SECTION 1: EVALUATION OF CEMENT-BITUMEN TREATED MATERIALS COMPOSITION	73

CHAPTER 5	RECYCLED GLASS FILLER IN COLD RECYCLED MATERIALS TREATED WITH BITUMINOUS EMULSION	75
5.1	Abstract	75
5.2	Introduction	76
5.3	Objectives	78
5.4	Materials	78
	5.4.1 RAP	78
	5.4.2 Bituminous emulsion and active fillers	79
	5.4.3 Mix design	80
5.5	Test equipment and procedures	84
	5.5.1 Indirect Tensile Strength (ITS) Test	84
	5.5.2 Indirect tensile stiffness modulus (ITSM) test	85
5.6	Results analysis	86
	5.6.1 Indirect Tensile Strength (ITS) Test	86
	5.6.2 Indirect tensile stiffness modulus (ITSM) test	88
5.7	Conclusions	91
CHAPTER 6	EFFECT OF WATER AND CEMENT CONTENT ON THE MECHANICAL PROPERTIES OF COLD RECYCLED MIXTURES (CRM) WITH BITUMEN EMULSION	93
6.1	Abstract	93
6.2	Introduction	94
6.3	Materials and methodology	95
	6.3.1 Materials	95
	6.3.2 Mixtures	96
6.4	Results analysis	99
6.5	Conclusions	102
CHAPTER 7	SUMMARY OF SECTION 1 AND INTRODUCTION OF SECTION 2: INFLUENCE OF RAP AGGREGATE ON CBTM PROPERTIES	105
7.1	Summary of Section 1	105
7.2	Section 2: study of the RAP aggregate effect on CBTM properties	106
CHAPTER 8	EFFECT OF GRADATION ON VOLUMETRIC AND MECHANICAL PROPERTIES OF COLD RECYCLED MIXTURES (CRM)	109
8.1	Abstract	109
8.2	Introduction	110
8.3	Materials and methods	113
	8.3.1 Mixtures composition	113
	8.3.2 Mixing and compaction	117
	8.3.3 Laboratory testing	118

8.4	Results and discussion	120
8.4.1	Workability and compactability.....	120
8.4.2	Mechanical properties and water loss	126
8.5	Conclusions.....	127
CHAPTER 9	LABORATORY MECHANICAL CHARACTERISATION OF COLD RECYCLED MIXTURES PRODUCED WITH DIFFERENT RAP SOURCES	131
9.1	Abstract.....	131
9.2	Introduction.....	132
9.3	Materials and methods	133
9.3.1	Materials	133
9.3.2	Mixtures	135
9.3.3	Specimens compaction and curing.....	136
9.3.4	Testing.....	140
9.4	Results and discussion	143
9.4.1	Water Loss	143
9.4.2	Indirect Tensile Strength Modulus.....	145
9.4.3	Indirect Tensile Strength.....	146
9.4.4	Semi-Circular Bending Test	147
9.5	Conclusions.....	149
CHAPTER 10	EFFECT OF RAP SOURCE ON COMPACTABILITY AND BEHAVIOUR OF CRM MIXTURES IN THE SMALL STRAIN DOMAIN	153
10.1	Abstract.....	153
10.2	Introduction.....	154
10.3	Analytical models	156
10.3.1	Compressible Packing Model (CPM).....	156
10.3.2	Di Benedetto-Neifar (DBN) model.....	159
10.4	Mixtures and methods.....	163
10.4.1	Materials and mixtures.....	163
10.4.2	Mixing, compaction and curing	165
10.4.3	Experimental program	167
10.5	Results and discussion	169
10.6	Conclusions.....	175
CHAPTER 11	SUMMARY OF SECTION 2 AND INTRODUCTION OF SECTION 3: INFLUENCE OF LOW PRODUCTION TEMPERATURES ON CBTM PROPERTIES.....	177
11.1	Summary of Section 2.....	177
11.2	Section 3: study of the effect of low production temperatures on CBTM properties	178

CHAPTER 12	INFLUENCE OF LOW PRODUCTION TEMPERATURE ON COMPACTABILITY AND MECHANICAL PROPERTIES OF COLD RECYCLED MIXTURES	183
12.1	Abstract.....	183
12.2	Introduction.....	183
12.3	Experimental approach	187
12.4	Materials and methodology.....	188
12.4.1	Materials and mixtures.....	188
12.4.2	Mixtures production.....	190
12.4.3	Testing program.....	192
12.4.3.1	Workability and compactability.....	192
12.4.3.2	Water loss.....	194
12.4.3.3	Indirect Tensile Strength (ITS)	195
12.5	Results analysis.....	196
12.5.1	Workability and compactability.....	196
12.5.1.1	Correlation between $V_m(10)$, k and CEI^+_T	197
12.5.1.2	Effect of mixing and transportation temperatures on CEI^+_T	199
12.5.2	Water Loss	201
12.5.3	Indirect Tensile Strength (ITS).....	203
12.5.4	Indirect Tensile Stiffness Modulus	206
12.5.5	Scanning Electron Microscope (SEM)	208
12.6	Conclusions.....	209
CHAPTER 13	THERMO-RHEOLOGICAL MODELLING IN THE SMALL STRAIN DOMAIN OF CEMENT-BITUMEN TREATED MATERIALS.....	211
13.1	Abstract.....	211
13.2	Introduction.....	212
13.3	Thermo-rheological modelling of HMA and CBTM.....	213
13.3.1	2S2P1D model	216
13.3.2	DBN model	217
13.4	Materials and methodology.....	222
13.4.1	Materials and mixtures.....	222
13.4.2	Mixtures production.....	224
13.4.3	Experimental devices	225
13.5	Results analysis.....	226
13.5.1	Time-Temperature Superposition Principle (TTSP).....	227
13.5.2	The 2S2P1D model.....	229
13.5.3	The DBN model.....	232
13.6	Discussion.....	233
13.7	Conclusions.....	235

CHAPTER 14	VISCO-ELASTO-PLASTIC CHARACTERIZATION IN THE SMALL STRAIN DOMAIN OF CEMENT-BITUMEN TREATED MATERIALS PRODUCED AT LOW TEMPERATURES	239
14.1	Abstract.....	239
14.2	Introduction.....	240
14.3	Materials and methodology.....	242
14.3.1	Materials and mixtures.....	242
14.3.2	Mixing, compaction and curing	244
14.3.3	Complex modulus test.....	247
14.3.4	Rheological modelling.....	248
14.4	Results Analysis.....	252
14.4.1	Rheological Modelling.....	252
14.4.2	Characteristic Time τ_{0E}	257
14.4.3	Glassy Modulus E_0	259
14.4.4	Analysis in the frequency range.....	261
14.5	Conclusions.....	263
CHAPTER 15	SUMMARY OF SECTION 3.....	267
CONCLUSION	269
RECOMMENDATIONS	273
ANNEX I	PROPERTIES OF MATERIALS EMPLOYED IN THE THESIS.....	277
ANNEX II	GRAPHIC REPRESENTATION OF THE RESULTS FOR COMPLEX MODULUS TESTS TO EVALUATE THE EFFECT OF LOW PRODUCTION TEMPERATURES ON CBTM MECHANICAL PROPERTIES	285
ANNEX III	REPEATABILITY STUDY ON THE LABORATORY PRODUCTION PROCESS OF CEMENT BITUMEN TREATED MATERIALS WITH FOAMED BITUMEN	297
ANNEX IV	EXPERIMENTAL INVESTIGATION ON WATER LOSS AND STIFFNESS OF CBTM USING DIFFERENT RA SOURCES.....	309
ANNEX V	INFLUENCE OF CURING ON THE MECHANICAL PROPERTIES OF CEMENT-BITUMEN TREATED MATERIALS USING FOAMED BITUMEN: AN INTERLABORATORY TEST PROGRAM.....	317

ANNEX VI	THERMO-RHEOLOGICAL MODELLING IN THE SMALL STRAIN DOMAIN OF CEMENT-BITUMEN TREATED MATERIALS.....	331
	LIST OF BIBRIOGAPHICAL REFERENCES	333

LIST OF TABLES

	Page
Table 1.1	Bitumen emulsion identification (AkzoNobel, 2017).....12
Table 1.2	Level of use of typical emulsifiers (AkzoNobel, 2000).....12
Table 1.3	Advantages and disadvantages of bituminous and cementitious additions (taken from Xiao et al. (2018)).....25
Table 1.4	Mixing procedures for CRM mixtures with added bitumen (RAP, cement or lime and emulsion) (Tebaldi et al., 2014)26
Table 1.5	Compaction methods used for CRM mixtures containing RAP (Tebaldi et al., 2014).....27
Table 3.1	CBTM loose mixture composition (SSD condition)70
Table 3.2	CBTM loose mixture G_{mm}^{PVC} measurements.....71
Table 3.3	CBTM loose mixture composition (apparent specific gravity)71
Table 5.1	Characteristics of the bituminous emulsion.....79
Table 5.2	Main physical properties of the fillers used for the experimental program.....80
Table 5.3	Main physical properties of the fillers used for the experimental program.....80
Table 5.4	Stiffness modulus results89
Table 5.5	Water loss in the specimen after curing.....90
Table 6.1	RAP aggregate properties95
Table 6.2	Bitumen emulsion properties95
Table 6.3	Volumetric composition of the studied mixtures.....98
Table 8.1	Granular composition of the aggregate blends113
Table 8.2	Main properties of aggregates used115

Table 8.3	Main properties of bitumen emulsions and bitumen residue	116
Table 8.4	Linear regression parameters: average value (standard error)	122
Table 9.1	RAP sources classification (PCS index)	134
Table 9.2	Properties of RAP sources used	134
Table 9.3	Bitumen emulsion properties	134
Table 9.4	Volumetric characterization of the compacted mixes	138
Table 9.5	Fitting parameters of the water loss model	145
Table 10.1	Properties of RAP sources used	164
Table 10.2	Bitumen emulsion properties	165
Table 10.3	Volumetric composition of the mixtures after compaction to reach $V_m = 10.8\%$	167
Table 10.4	CPM model results	170
Table 10.5	Morphological parameters of RAP sources fractions	171
Table 10.6	DBN model parameters	175
Table 12.1	RAP aggregate properties	189
Table 12.2	Bitumen emulsions properties	189
Table 12.3	Mixtures naming and production process	191
Table 12.4	Results of two-way ANOVA for CEI_T^+	200
Table 12.5	Water loss model fitting parameters	203
Table 12.6	Results of two-way ANOVA for ITS results (Emulsion A)	204
Table 13.1	RAP aggregate properties	223
Table 13.2	Bitumen emulsions properties	223
Table 13.3	Mixtures naming and curing process	225

Table 13.4	WLF parameters.....	229
Table 13.5	Rheological modelling parameters for the studied mixtures	234
Table 14.1	RAP aggregate properties	244
Table 14.2	Bitumen emulsion properties	244
Table 14.3	Mixtures code, production steps (laboratory time), conditioning temperatures and number of specimens.....	246
Table 14.4	WLF shifting parameters ($T_0 = 20\text{ }^\circ\text{C}$)	254
Table 14.5	DBN model parameters for the studied mixtures ($T_0 = 20\text{ }^\circ\text{C}$)	256
Table 14.6	Single Factor ANOVA analysis for τ_{0E} in mixtures produced at low temperatures.....	259
Table 14.7	Single Factor ANOVA analysis for E_0 in mixtures produced at low temperatures.....	261
Table 14.8	Two-Factor with replication ANOVA analysis for E_0 to evaluate production temperatures.....	261

LIST OF FIGURES

		Page
Figure 1.1	Conceptual composition of pavement mixtures (readapted from Grilli, Graziani & Bocci, 2012)	7
Figure 1.2	Types of emulsions: a) O/W emulsion; b) W/O emulsion; c) W/O/W emulsion (Salomon, 2006)	8
Figure 1.3	Manufacturing layout of bitumen emulsion (AkzoNobel, 2017).....	9
Figure 1.4	Types of emulsion charges: a) Anionic emulsion (negative charge); b) Cationic emulsion (positive charge) (AkzoNobel, 2017).....	11
Figure 1.5	The two possible breaking cases for the bitumen emulsion (Lesueur & Potti, 2004).....	14
Figure 1.6	Determination of Optimum Foamant Water Content (Asphalt Academy, 2009).....	17
Figure 1.7	Volumetric composition development during cement hydration for $w/c = 0.42$	20
Figure 1.8	Optical images of fresh emulsified asphalt with cement (Wang et al., 2014)	23
Figure 1.9	Energy consumption of production steps for different techniques (taken from Xiao et al., 2018).....	25
Figure 1.10	Proctor compaction test results (Grilli et al., 2012)	29
Figure 1.11	SGC Test results (Grilli et al., 2012)	30
Figure 1.12	Compactability of cold mix asphalt using emulsified bitumen—void and normalized water extruded (Wendling et al., 2014).....	30
Figure 1.13	Normalized strength along curing related to literature (taken from (Dolzycki et al., 2017))	33
Figure 1.14	Microtomography details of an asphalt and cement composite (García et al., 2013)	35

Figure 1.15	Example of experimental points and model related to a material property (Raschia, Graziani, et al., 2019b)	37
Figure 1.16	Behaviours typically observed in bituminous mixtures (Strain vs Number of loading) (Di Benedetto et al., 2001)	38
Figure 1.17	Stress-strain trend for complex modulus test in only-compression configuration	39
Figure 1.18	Isothermal curves for CBTM mixtures (6 temperatures, 6 frequencies) (Godenzoni, Graziani, et al., 2016)	40
Figure 1.19	Master curves for a CBTM mixture at $T_s = 20^\circ\text{C}$ (5 frequencies, 7 temperatures)	41
Figure 1.20	Huet-Sayegh model	42
Figure 1.21	Representation of the 2S2P1D model (readapted from Olard & Di Benedetto (2003))	44
Figure 1.22	Unidirectional representation of the DBN model for bituminous mixtures	45
Figure 1.23	Cycling response of the EP bodies (taken from Di Benedetto et al., 2011)	45
Figure 1.24	Representation of the DBN model for small number of cycles in the small strain domain	46
Figure 1.25	Calibration of the GKV model (5, 15, 25 elements) on the Cole-Cole diagram (taken from Tiouajni et al., 2011)	48
Figure 2.1	Overview of the experimental plan	52
Figure 2.2	a) Example of material sample for SEM; b) SEM device used (Hitachi TM3000)	53
Figure 2.3	a) ITSM testing setup; b) PUNDIT device; c) Complex modulus setup	54
Figure 2.4	a) ITS test setup; b) SCB test setup	55
Figure 2.5	Materials employed in the different chapters of the thesis	56
Figure 2.6	Schematic representation of the thesis structure	57

Figure 3.1	Volumetric composition of a HMA compacted specimens	62
Figure 3.2	CBTM volumetric composition in the fresh state.....	63
Figure 3.3	Example of compaction curves of CBTM from SGC.....	66
Figure 3.4	CBTM volumetric composition in the long-term state (no intergranular water).....	67
Figure 3.5	Effect of hydration degree on CBTM volumetric properties.....	69
Figure 5.1	Gradation of the design mix compared to the reference curve	79
Figure 5.2	Influence of water content on the compactability of CRM: a) Voids in the mixture Vi; b) Voids filled with Liquids (VFL)	82
Figure 5.3	ITS device and specimen	84
Figure 5.4	ITSM test setup with MTS device inside the environmental chamber	86
Figure 5.5	Indirect tensile strength of mixtures	87
Figure 5.6	Comparison of the stiffness modulus for the mixes at different temperatures	88
Figure 6.1	Gradation of the studied granular material	96
Figure 6.2	Indirect Tensile Strength test results in dry and wet conditions	99
Figure 6.3	Indirect Tensile Stiffness Modulus test results	100
Figure 6.4	Dynamic Modulus test results (PUNDIT at 40°C)	101
Figure 6.5	Scanning Electron Microscope images	102
Figure 8.1	Aggregate blend gradations studied at: a) ÉTS; b) UNIVPM	114
Figure 8.2	Compaction curves for the six mixtures at: a) ÉTS; b) UNIVPM.....	121
Figure 8.3	Results for k and $V_m(10)$ parameters	123
Figure 8.4	G/G _{lim} and S/S _{lim} values	124
Figure 8.5	Correlation between gradation, workability and compactability parameters	125

Figure 8.6	Mechanical tests results: a) ITS and ITR at ÉTS; b) ITS and ITSM at UNIVPM.....	127
Figure 9.1	Aggregate blend gradations of the studied mixes	135
Figure 9.2	Volumetric characterization of CBTM mixtures	139
Figure 9.3	Determination of Y_1 factor for different notch depths (25 mm, 32 mm and 38 mm) for a $s/D = 0.847$	143
Figure 9.4	Water Loss model and results	144
Figure 9.5	Indirect Tensile stiffness modulus results.....	146
Figure 9.6	Indirect Tensile Strength results	147
Figure 9.7	Strain Energy to Failure U results.....	148
Figure 9.8	Critical Energy Release Rate J_c results	148
Figure 9.9	Critical Stress Intensity Factor K_{IC} results	149
Figure 10.1	Effect of finer and coarser fractions on an intermediate fraction (readapted from (De Larrard, 1999))	158
Figure 10.2	DBN model for bituminous mixtures	160
Figure 10.3	Schematic representation of the DBN model for small strain and small cycles.....	161
Figure 10.4	Complex shear modulus results on the RAP residual binder: a) Black space; b) Cole-Cole plan.....	163
Figure 10.5	Aggregate distribution of the mixtures studied.....	165
Figure 10.6	Specimens employed for testing	167
Figure 10.7	Experimental results: a) Cole-Cole plan and, b) Black space.....	172
Figure 10.8	Master curves at $T_s = 20^\circ\text{C}$: a) Norm of the complex modulus and, b) Phase angle	172
Figure 10.9	Shift factors and WLF model for the studied mixtures.....	173

Figure 10.10	Experimental results modelled with the DBN model ($n = 40$): a) Cole-Cole plan, b) Black space, c) Master curve of the norm of the complex modulus at $T_s = 20^\circ\text{C}$ and, d) Master curve of the phase angle at $T_s = 20^\circ\text{C}$	174
Figure 11.1	Laboratory production simulation and experimental program	180
Figure 12.1	Target aggregate blend.....	188
Figure 12.2	Graphic meaning of CEI_T^+ , $V_m(10)$ and k parameters	194
Figure 12.3	Compaction curves.....	197
Figure 12.4	a) Relationship between $V_m(10)$ and k ; b) Relationship between CEI_T^+ and k ; c) Relationship between CEI_T^+ and $V_m(10)$	198
Figure 12.5	Relationship between CEI_T^+ , mixing temperature and transportation temperature	199
Figure 12.6	Water loss experimental data and superposed model for mixtures with: a) Emulsion A and b) Emulsion B.....	202
Figure 12.7	Effect of mixing and transportation temperatures on Indirect Tensile Strength (28 days).....	204
Figure 12.8	Correlation between residual water and Indirect Tensile Strength (at 14 and 28 days of curing).....	205
Figure 12.9	ITSM results.....	207
Figure 12.10	SEM images captured for mixes produced with Emulsion A after 28 days of curing.....	208
Figure 13.1	2S2P1D analogical representation (taken from Gayte et al., 2016).....	216
Figure 13.2	a) DBN model for bituminous mixtures, b) Generalized Kelvin-Voigt model, which gives an asymptotic representation of the DBN model when strain tends to 0	218
Figure 13.3	Cyclic loading behaviour of elasto-plastic element for small number of cycles (path ABCB).....	219
Figure 13.4	Representation of the DBN model applied in the small strain domain, EP are represented by a spring (modulus, E) and a non-viscous dissipation (D).....	220

Figure 13.5	Energy dissipation during cyclic loading in the small strain domain (experimental data superposed to an equivalent sinusoidal loading).....	221
Figure 13.6	Correlation between: a) GKV model, and b) 2S2P1D model (taken from Di Benedetto, Delaporte et al., 2007).....	221
Figure 13.7	Maximum density curve, RAP and blend gradations	222
Figure 13.8	SGC specimen of Ø100 mm x 140mm: a) un-sealed condition, b) sealed condition and, c) coring and sawing to obtain the testing specimens of Ø75 x 120mm	225
Figure 13.9	View of a specimen with measurement system in: a) MTS press and, b) AMPT PRO press	226
Figure 13.10	Experimental results showed in: a) Cole-Cole plan and, b) Black space.....	227
Figure 13.11	At $T_{ref} = 20^{\circ}\text{C}$, master curves of: a) The norm of the complex modulus $ E^* $ and, b) The phase angle φ	228
Figure 13.12	Shift factors, a_T , and WLF model related to the studied mixtures.....	229
Figure 13.13	Optimization of the 2S2P1D model for B_Unsealed mixture according to: a) Cole-Cole plan, b) Black space, c) phase angle master curve and, d) complex modulus master curve ($T_{ref} = 20^{\circ}\text{C}$).....	231
Figure 13.14	Application of 2S2P1D model fitted on the master curve of the norm of the complex modulus (calibration : 2S2P1D_> E*) for: a) Cole-Cole plan, b) Black space, c) phase angle master curve and, d) complex modulus master curve ($T_{ref} = 20^{\circ}\text{C}$).....	232
Figure 13.15	Application of the 2S2P1D (dashed line) and DBN (continuous line) models to the studied mixtures ($n = 40$): a) Cole-Cole plan, b) Black space, c) phase angle master curve and, d) complex modulus master curve ($T_{ref} = 20^{\circ}\text{C}$)	233
Figure 13.16	Accuracy of the DBN model for: a) norm of complex modulus and, b) phase angle	234
Figure 14.1	Gradation of RAP and aggregate blend	243

Figure 14.2	Laboratory production and experimental program: a) mixture A_5_25, b) mixture A_5_5, c) mixture A_25_25 and, d) mixture A_25_5.....	245
Figure 14.3	SGC specimen of Ø100mm x 140mm: a) unsealed condition, b) sealed condition and, c) coring and sawing for testing specimens of Ø75 x 120mm	247
Figure 14.4	Representation of the DBN model applied in the small strain domain (few cycles).....	250
Figure 14.5	Experimental data from complex modulus tests: a) Cole-Cole plan and, b) Black space	253
Figure 14.6	Master curves at reference temperature $T_0 = 20^\circ\text{C}$ of: a) norm of the complex modulus and, b) phase angle	254
Figure 14.7	Experimental data and DBN model ($T_0 = 20^\circ\text{C}$) for $n = 40$: a) Cole-Cole plan, b) Black space, c) master curve of the norm of the complex modulus $ E^* $ and, d) master curve of the phase angle φ_{EP} (φ_{EP} is shown and represents the elasto-plastic phase angle).....	255
Figure 14.8	Accuracy of the DBN model according to experimental results ($T_0 = 20^\circ\text{C}$): a) norm of the complex modulus and, b) phase angle.....	257
Figure 14.9	Effect of production temperatures on τ_{0E} : a) unsealed specimens and, b) sealed specimens.....	259
Figure 14.10	Effect of production temperatures on E_0 : a) unsealed specimens and, b) sealed specimens.....	260
Figure 14.11	Relative difference values between mixtures cured in sealed conditions and unsealed conditions: a) norm of the complex modulus and, b) phase angle.....	262
Figure 14.12	Relative difference values between mixtures produced at low and standard temperatures: a) norm of the complex modulus and, b) phase angle.....	263

LIST OF ABBREVIATIONS

2S2P1D	2 Springs, 2 Parabolic elements, 1 Dashpot
AASHTO	American Association of State Highway Transportation Officials
AC	Asphalt Concrete
AMPT	Asphalt Mixture Performance Tester
ANOVA	ANalysis Of VAriance
ARRA	Asphalt Recycling & Reclaiming Association
ASTM	American Society for Testing and Materials
BBS	Binder Bond Strength
BSM	Bitumen-Stabilized Material
CAM	Cold Asphalt Material
CBTM	Cement-Bitumen Treated Material
CCPR	Cold Central Plant Recycling
CEI	Compaction Energy Index
CFS	Closed-Form Shifting
CIPR	Cold In-Plant Recycling
CIR	Cold In-place Recycling
COV	Coefficient Of Variance
CPM	Compressive Packing Model
CR	Cold Recycling
CRM	Cold Recycled Material
CSS	Cationic Slow-Setting
CTM	Cement-Treated Material
DBN	Di Benedetto & Neifar
EP	Elasto-Plastic
EPFM	Elasto-Plastic Fracture Mechanic
ÉTS	<i>École de Technologie Supérieure</i>
FB	Foamed Bitumen

XXX

FEM	Finite Element Method
FHWA	Federal Highway Administration
FSD	Free Surface Drying
GKV	Generalized Kelvin-Voigt
GU	General Use
HIR	Hot In-place Recycling
HMA	Hot Mix Asphalt
HPAC	High-Performance Asphalt Concrete
ILTP	Inter-Laboratory Testing Program
ITS	Indirect Tensile Strength
ITSM	Indirect Tensile Stiffness Modulus
LCMB	<i>Laboratoire sur les Chaussées et Matériaux Bitumineux</i>
LEFM	Linear-Elastic Fracture Mechanic
LVE	Linear Visco-Elastic
ML	Moisture Loss
MTQ	<i>Ministère des Transports du Québec</i>
MTS	Material Testing System
NMAS	Nominal Maximum Aggregate Size
OMC	Optimum Moisture Content
OPC	Ordinary Portland Cement
PCC	Portland Cement Concrete
PCS	Passing to a Control Sieve
PSD	Partially Sealed (or Surface) Drying
PUNDIT	Portable Ultrasonic Non-destructive Digital Indicating Tester
RA	Reclaimed Asphalt
RAP	Reclaimed Asphalt Pavement
RCD	Roller Compacted concrete
RILEM	<i>Réunion Internationale des Laboratoires et Experts des Matériaux, systèmes de construction et ouvrages</i>

RRT	Round Robin Test
RSD	Restrained Surface Drying
SCB	Semi-Circular Bending
SCC	Self-Compacting Concrete
SEM	Scanning Electron Microscope
SGC	Shear (or Superpave) Gyrotory Compactor
SMA	Stone Mastic Asphalt
SSD	Saturated Surface Dried
TC	Technical Committee
TG	Task Group
TRB	Transportation Research Board
TTSP	Time-Temperature Superposition Principle
UNIVPM	<i>UNIVersità Politecnica delle Marche</i>
UPV	Ultrasonic Pulse Velocity
VA _g	Virgin Aggregate
VFL	Voids Filled with Liquids
V _m	Voids in the mixture
VMA	Voids in the Mineral Aggregate
WLF	William-Landel-Ferry
WMA	Warm Mix Asphalt

INTRODUCTION

Nowadays, road pavements rehabilitation is a very important topic, since it faces the increasing issue of new infrastructure demand together with the decrease of funds, with a new, safe, reliable and cost-effective road system (ARRA, 2001; Bocci et al., 2011; Cardone et al., 2014; Ezenwa et al., 2013; Grilli et al., 2012; Stroup-Gardiner, 2011). First recycling and rehabilitation cases go back to the 1930s (Hot In-place Recycling, HIR), even though the majority of the results in the scientific and technical fields were achieved around the mid 1970s (ARRA, 2001).

A significant improvement of energy and materials saving was given by the increasing use of the Reclaimed Asphalt Pavement (RAP), which partially or completely replace the natural aggregates in asphalt mixtures. Furthermore, production temperatures were gradually decreased thanks to the employment of warm mix additives (WMA), bitumen emulsion and foamed bitumen. Thanks to these tools, asphalt industries were able to guarantee a strong environmental involvement.

Five main recycling techniques are defined by ARRA (2001), according to the damage of the pavement, operations management and level of traffic:

- Cold Planing;
- Hot Recycling;
- Hot In-Place Recycling (HIR);
- Cold Recycling (CR):
 - Cold In-Place Recycling (CIR);
 - Cold Central Plant Recycling (CCPR);
- Full-Depth Reclamation:
 - Pulverization
 - Mechanical and/or bituminous and/or chemical stabilization

If necessary, all the recycling methods just mentioned can be employed together in the same project. This thesis focuses its attention on materials produced with CR techniques, which are carried out at ambient temperature (with no heat addition), allow the use of non-renewable resources, and in general they allow energy savings compared to other construction methods.

CR technology is considered a powerful rehabilitation system when the following issues are observed (Davidson & Eng, 2003):

- Pavement cracking: age cracking, thermal cracking, fatigue cracking, and reflective cracking;
- Permanent deformation: rutting due to unstable asphalt mixture, shoving, rough pavement;
- Loss of integrity in the existing asphalt pavement, ravelling, stripping, flushing, loss of bond between bituminous layers, and presence of potholes.

The CR techniques were introduced in Canada in the late 1980s and has grown continuously. The regional municipality of Ottawa-Carleton (now known as the City of Ottawa) was the first agency to utilize the process as a rehabilitation tool. Nowadays CR process is used almost in every province of Canada. The interesting point to be made is that each province uses different choices for the binder: British Columbia uses a rejuvenator or blends, Ontario uses high floats as well as cationic emulsions, Québec uses cationic emulsions and the Maritimes use high float and cationic emulsions (Davidson, 2005).

This thesis deals with issues related to the production of CR (CCPR and CIR) mixtures, characterized by the use of ordinary Portland cement and bitumen emulsion as binders. In particular, the experimental plan is oriented towards the study of the aggregate phase composing the mixture, and on how low production temperatures influence mechanical properties, in both the short and the long term.

CHAPTER 1 presents an update review of the scientific literature specifically related to the thesis subject, which led to the problem statement and research objectives described in CHAPTER 2. CHAPTER 3 gives both a theoretical and practical description of a typical mix

design approach used for HMA, the volumetric approach, which in this thesis has been applied to CBTM mixtures. CHAPTERS 4, 5 and 6, which contain two papers, analyze aspects useful for the CBTM composition, i.e. the use of cement as mineral addition in CBTM mixtures (CHAPTER 5), and the effect of water and cement content on the mechanical properties (CHAPTER 6). CHAPTERS 7, 8, 9 and 10 collect three papers that deal with the aggregate structure of CBTM, in particular with granular distribution, Nominal Maximum Aggregate Size (NMAS) and RAP source. CHAPTERS 11, 12, 13 and 14 are composed of three papers which assess the influence of low production temperatures on short and long-term mechanical properties of CBTM mixtures, with a limited analysis also carried out on a different bitumen emulsion. CHAPTER 15 contains some global considerations about the previous four chapters. Concluding, the main findings of this thesis are described as well as some useful recommendations for future works.

CHAPTER 1

LITERATURE REVIEW

This research thesis aims to cover several aspects of a particular type of cold recycled material, the cement-bitumen treated materials (CBTM). In particular, the study will focus on components (water, cement and RAP aggregate), as well as on the production process performed at low temperatures. Consequently, the literature review will highlight the most important findings from the scientific community to support the objectives of this thesis.

1.1 Cold Recycling (CR)

Road pavements constructed with CR technology using either bitumen emulsion or foamed bitumen are environmentally sustainable and cost-effective. They are suitable in particular for pavement rehabilitation using in situ recyclers and/or conventional construction equipment (Giani et al., 2015; Thenoux et al., 2007).

CR process can be performed either in production plants (Cold Central Plant Recycling—CCPR) and in situ (Cold In-Place Recycling—CIR). In case of CCPR, the process takes place in a stationary or mobile recycling plant, which can be a real production center or a CIR train, less the milling machine. In this manner, the material is controlled and sometimes pre-treated before the new laydown, giving in return a lower variability and a higher reliability of the final product (ARRA, 2001; Godenzoni, 2017).

On the other hand, CIR process generally uses 100% of the RAP generated during the milling process since only asphalt layers are used; also, Virgin Aggregates (VAg) can be included to reach the target gradation. The CIR treatment depth is typically within the 50 to 100 mm range when the binding phase is only composed of bitumen emulsion. Treatment depths of 125 to 150 mm are possible when co-binders (or active fillers), such as Portland cement, lime, kiln dust or fly ash are used to improve the early strength gain and resistance to moisture damage

(ARRA, 2001). If lime or Portland cement is added to the recycled mix, they can be added in dry form or as slurry. The slurry method eliminates potential dust problems and permits greater control of the amount of recycling modifier being added (ARRA, 2001).

1.1.1 Cold Recycled Mixtures (CRM)

In order to ensure workability and compactability at ambient temperature during CR processes, a water dosage normally ranging between 3% and 6% by mixture mass is added, which allows to reach a final air voids rate between 10% and 15% (Tebaldi et al., 2014; Xiao et al., 2018). The compacted CR mixture (CRM) must be adequately cured before a wearing surface is placed, to let the water evaporation occur. The rate of curing is quite variable and depends on several factors, including environmental conditions and drainage, as well as moisture characteristics of the mix. Obviously, the mechanical properties of the final product highly depend on the curing process, which can be severely hindered in cold climates. Typical curing periods are several hours to 2 weeks, depending on the above-mentioned factors, the site location and the binding agent used (foamed bitumen or bitumen emulsion) (ARRA, 2001).

It has been observed that CRM properties in the early life (first days) and in the long term (after few years) can be improved with the introduction in the mixture of mineral additions. For mineral addition it is intended a filler-sized granular material which can have or not have the ability of chemically or physically bond with water. In the literature, terms like *active fillers* or *co-binders* can be found to express the same component inside the CRM mixture, like cement, hydrated lime, kiln dust, fly ash, etc. With this terminology, the identification of the mineral addition used can be misunderstood. For example, hydrated lime ($\text{Ca}(\text{OH})_2$) reacts with the carbon dioxide (CO_2) in the air to give limestone, even though it needs to be mixed with water to start the reaction (Colleparidi, 1991). So, it can be considered as an active filler only from this point of view. On the other hand, ordinary Portland cement has the ability to create bonds when combined with water, keeping trapped a certain amount required by the

hydration reaction. In this thesis, cement is used as mineral addition (or co-binder), since the term *active filler* is considered too generic.

According to the contemporary presence of bitumen and cement, CRM materials can be named differently and divided in several categories (Figure 1.1):

- Cement Treated Materials (CTMs): no bitumen is employed and the structural cohesion is conferred only by the hydration of the cement, that is used between 1 and 6% generally;
- Cement Bitumen Treated Materials (CBTMs): these mixes are an improved version of the CTMs, since virgin bitumen binder (from 1 to 3%) is used in order to confer a more asphalt-like behaviour to the mix (less brittle and more flexible). Cement content decreases between 1 and 3%. This category is considered in this thesis;
- Bitumen Stabilized Materials (BSMs): they are characterized by granular unbound aggregates (mostly recycled) stabilized by using low percentages of bitumen (1 to 3%) and up to 1% of cement.

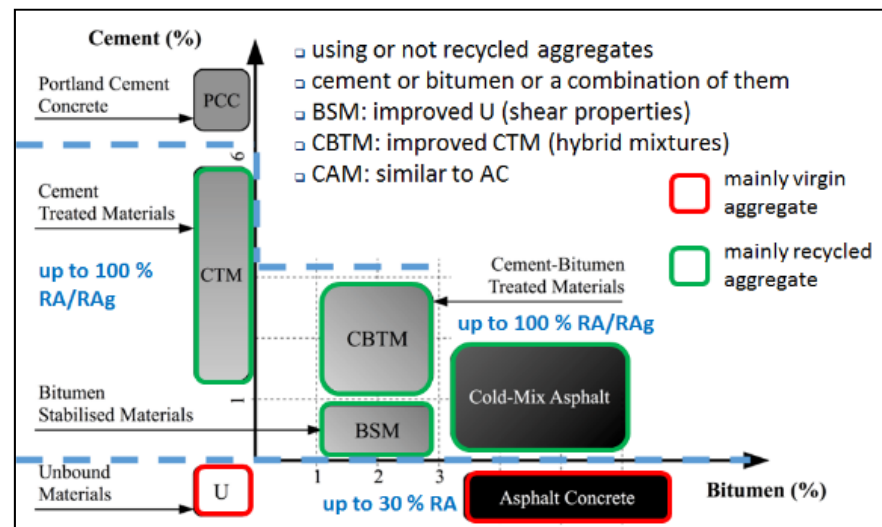


Figure 1.1 Conceptual composition of pavement mixtures (readapted from Grilli, Graziani & Bocci, 2012)

Bitumen emulsion and foamed bitumen are methods to reduce bitumen viscosity, allowing a better mixing with the cold moist material and to improve workability at ambient temperature. They are produced in two complete different methods (Asphalt Academy, 2009).

1.1.2 Bitumen emulsions

Bitumen emulsions are dispersion of small droplets of one liquid in another liquid. Emulsions in general can be formed by any two immiscible liquids, but in most emulsions one of the phases is water. Oil-in-water (O/W) emulsions are those in which the continuous phase is water and the disperse (droplet) phase is an “oily” liquid. Water-in-oil (W/O) or “inverted” emulsions are those in which the continuous phase is an oil and the disperse phase is water (Salomon, 2006). In addition, emulsions can have more complex structures, such as W/O/W, where the disperse phase contains another phase which may not have the same composition as the continuous phase (Figure 1.2).

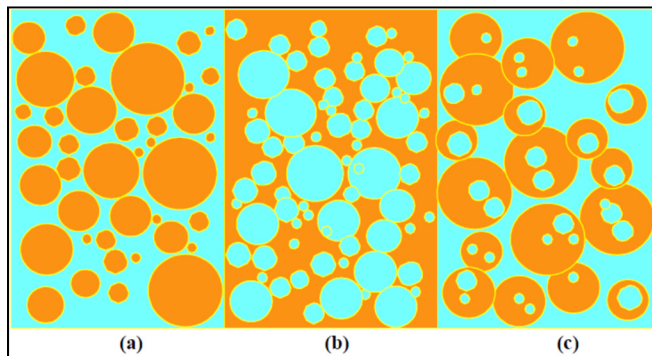


Figure 1.2 Types of emulsions: a) O/W emulsion; b) W/O emulsion; c) W/O/W emulsion (Salomon, 2006)

Standard bitumen emulsions are normally considered to be the O/W type. They usually contain from 40% to 75% of bitumen, 0.1% to 2.5% of emulsifier, 25% to 60% of water plus some minor components (Salomon, 2006). Bitumen droplets in the bitumen emulsion are

characterized by a size distribution, and this distribution is influenced by the bitumen emulsion recipe and the mechanics and operating conditions of the emulsion manufacturing plant.

The particle size (usually between 1 and 30 μm diameter) and the particle size distribution of the bitumen emulsion droplets strongly influence the physical properties of the emulsion, such as viscosity and storage stability; larger average particle size leads to lower emulsion viscosity, as does a broad or bimodal particle size distribution (Salomon, 2006).

Emulsions are made by mixing hot bitumen with water containing emulsifying agents and applying sufficient mechanical energy to break up the bitumen into droplets. Emulsions are produced in a colloid mill, containing a high-speed (1000–6000 rev/min) rotor. The typical manufacturing of a bitumen emulsion is illustrated in Figure 1.3.

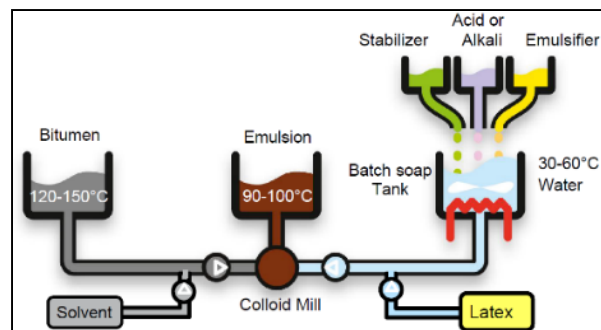


Figure 1.3 Manufacturing layout of bitumen emulsion (AkzoNobel, 2017)

Elements listed in the picture are described as follows (AkzoNobel, 2017):

- **Bitumen**: Similar material used in HMA but the choice depends on the application;
- **Water**: Generally potable water without suspended solids. Some emulsions could require softened water;
- **Polymer**: Emulsions may contain polymers which can be used as a water dispersion (latex-natural rubber latex or Styrene Butadiene latex), or solids (like Styrene Butadiene Styrene-

SBS) which are dissolved in the bitumen. The polymer modifies the elastic and flow properties of bitumen to improve performance;

- Solvent: may be included in the emulsion to improve emulsification, to reduce settlement, improve curing rate at low temperatures, or to provide the right binder viscosity after curing;
- Emulsifier: The emulsifier is a chemical compound which is used to stabilize the emulsion. They are mostly derived from natural fats and oils like beef fat, or from wood products like tall oils and lignins;
- Thickeners: water-soluble polymers which improve the storage stability of the emulsion;
- Salts: Used to control viscosity changes in the emulsion.

In addition, other chemical elements could be included: calcium and sodium chlorides, included to reduce the osmosis of water into the bitumen due to the presence of small amounts of salt in asphalt, and adhesion promoters, that are surface-active amine compounds added to promote sufficient adhesion between cured anionic emulsions (and occasionally cationic) and the aggregates (AkzoNobel, 2017).

Emulsifiers are chemical elements with surface activity that, when dissolved in a liquid (especially water), decrease the surface tension by adsorption on the liquid/vapour interface or other surfaces. Emulsifiers molecules have a nonpolar lipophilic tail and a polar hydrophilic head group, which is balanced by the counter-ion (SFERB, 1991). The molecules concentrate at the interface between water and bitumen, orientated with the polar group in the water and the nonpolar parts of the molecule in the oil (Figure 1.4). Emulsifiers can be classified into anionic, cationic, ampholytic and non-ionic types depending on the charge their head groups adopt in water, although this charge may depend on pH.

Anionic emulsifiers ionize in water to create negatively charged ions, and they usually contain negatively charged oxygen atoms in head group. At opposite, cationic emulsifiers ionize in water to create positively charged ions. In the head group, they usually have nitrogen atoms

positively charged. Ampholytic emulsifiers are characterized by two or more functional groups, which can ionize together in an aqueous phase, according to the pH. At the end, non-ionic emulsifiers do not produce ions in aqueous phases.

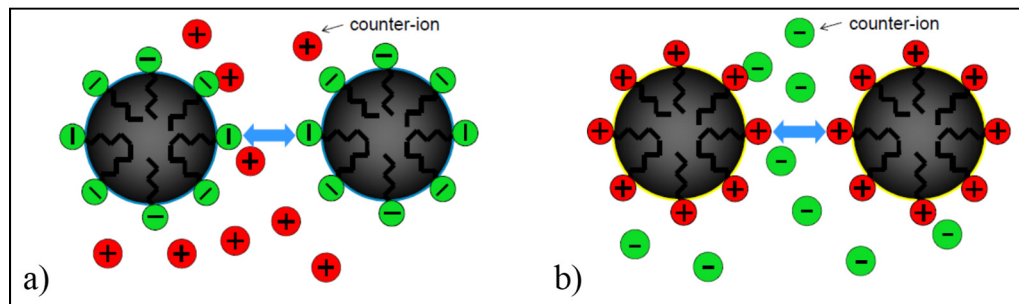


Figure 1.4 Types of emulsion charges: a) Anionic emulsion (negative charge); b) Cationic emulsion (positive charge) (AkzoNobel, 2017)

Emulsifiers are often supplied in a water-insoluble form and need to be “activated” (or de-protonated) with acid or alkali to have the final surface-active cationic or anionic water-soluble form used to prepare the soap solution. The choice of the acid or alkali (and the final emulsion pH, subsequently), strongly influence its properties. Hydrochloride and phosphoric acids are used for cationic emulsions, while sodium and potassium hydroxide are the most common alkalis used for anionic emulsions (SFERB, 1991).

Although a large amount of emulsifier in an emulsion resides at the bitumen/water interface, a certain amount is dispersed in the water phase (free part). As emulsifier molecules are partially hydrophobic, they are most likely to exist as colloids. When an emulsion comes into contact with aggregates, the free emulsifier will be attracted to charged sites. Of course, if these sites are used by free emulsifier, the emulsion will not break as quickly. Therefore, the higher the level of (free) emulsifier, the slower the breaking rate of the emulsion. It can also be hypothesized that a large amount of free emulsifier in an emulsion can rapidly attach to the aggregate surface, preventing the bitumen breaking on the same spot. In this way, bitumen droplets will coalesce far from the aggregate surface, leading to poor binding of the final

mixture. Table 1.1 gives a correlation between the type of the emulsion and its typical use in asphalt industry, while Table 1.2 illustrates the typical level of emulsifiers used.

Table 1.1 Bitumen emulsion identification (AkzoNobel, 2017)

	Reference standard	Rapid-setting	Medium-setting	Slow-setting
Cationic (+)	ASTM D977 and D2397	CRS	CMS	CSS
	UNI EN 13808:2013	C60B1 C60B2 C60B3	C60B4 C60B5 C60B6	C60B7 C60B8 C60B9 C60B10
Anionic (-)	ASTM D977 and D2397	RS	MS	SS
	UNI EN 13808:2013	A60B1 A60B2 A60B3	A60B4 A60B5 A60B6	A60B7 A60B8 A60B9 A60B10
Used for:		Chip-seal	Open-graded mix	Dense-graded mix

Table 1.2 Level of use of typical emulsifiers (AkzoNobel, 2000)

Emulsion type	Emulsifier level [%]	Emulsion pH	Typical emulsifier
Cationic Rapid Setting	0.15-0.25	2-3	Tallow diamine
Cationic Medium Setting	0.3-0.6	2-3	Tallow diamine
Cationic Slow Setting	0.8-2.0	2-5	Quaternary amine
Anionic Rapid Setting	0.2-0.4	10.5-12	Tally acid
Anionic Medium Setting	0.4-0.8	10.5-12	Tally acid
Anionic Slow Setting	1.2-2.5	7.5-12	Nonionic+lignosulphonate

The principle of employing asphalt emulsion technology is to match the reactivity of the emulsion with the reactivity of the aggregate; rapid set emulsions shall be used with low-reactive (low surface area) aggregates, while slow set emulsions are better suited for reactive (high surface area) aggregates. In particular, some aggregates, like carbonates and fillers (as cement, that is highly basic), may neutralize acid in cationic emulsions causing the pH to rise and the emulsion to be destabilized. At opposite, anionic emulsions may be destabilized by soluble multivalent ions (Salomon, 2006).

On a physicochemical point of view, emulsion stability is obtained thanks to the repulsive forces between bitumen droplets (electrostatic forces). These interparticle forces can be described by the so-called DLVO theory, named by Derjaguin-Landau-Verwey-Overbeek (Israelachvili, 2015). According to this theory, inter-droplet interactions are the sum of an electrostatic repulsion and a Van der Waals attraction. When the repulsion overcomes the attraction, the droplets are prevented from approaching each other and the emulsion is stable, i.e., no coalescence occurs. On the opposite, when the attraction overcomes the repulsion, the droplets tend to contact and then coalesce. Hence, the breaking of the emulsion can be described in rational terms as a consequence of two causes (Figure 1.5) (Lesueur & Potti, 2004):

- Very high bitumen concentration of droplets (film forming): the bitumen droplets retain their identity up to a high concentration, which can be higher than 98% for slow setting emulsions. From then, the pressure becomes high enough to generate the breaking of the films between the bitumen droplets and coalescence occur. The kinetics of the film formation is then imposed by the water evaporation rate;
- Disappearance of the electrostatic repulsion between droplets (gel contraction): this breaking mode is activated by the action of the aggregates or of an additive, such as Portland cement or lime. Chemical reactions or changes in the pH will promote the coalescence of the bitumen droplets (electrostatic attraction and/or chemical reactions);

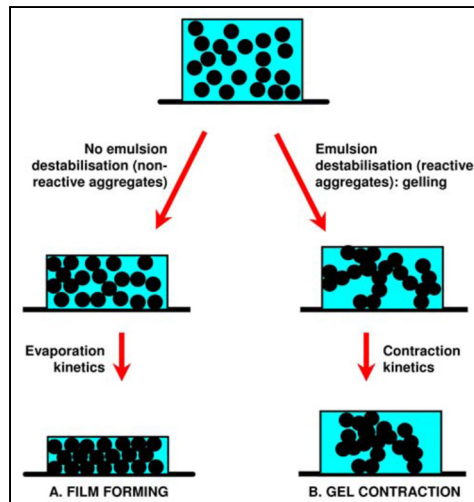


Figure 1.5 The two possible breaking cases for the bitumen emulsion (Lesueur & Potti, 2004)

According to Wates and James (Wates & James, 1993) there are three breaking mechanisms for cationic emulsions in contact with negatively charged siliceous materials:

- Emulsifier abstraction: in which the emulsifier moves from the bitumen/water interface to the aggregate surface, leading to the coalescence of the emulsion;
- Deprotonation of the acidified emulsifier: protons are adsorbed by aggregates basic surface, deactivating the emulsifier and thus causing the emulsion breaking;
- Droplet migration: bitumen droplets are attracted to the negatively charged aggregate surface, due to the positively charged emulsifier. The final situation is beneficial as the bitumen is bound on the aggregates by the emulsifier, which subsequently acts as adhesion agent.

Another mechanism has been proposed by Plotnikova (Plotnikova, 1993). This theory claims that the free emulsifier is firstly adsorbed on the aggregate surface. In the same way, the emulsifier spread on the bitumen particles is abstracted and absorbed on the aggregate; the

aggregate surface becomes then hydrophobic, and the bitumen is attracted being hydrophobic too because of the emulsifier desorption.

Gaestel assessed that there are two breaking mechanisms in the case of anionic emulsions (Gaestel, 1967):

- In combination with calcareous aggregates, which are positively charged, the emulsifier forms a salt with the calcium ions contained in the aggregate, removing it from the bitumen/water interface and leading the emulsion to break;
- In combination with negatively charged siliceous aggregates, the inorganic cation is adsorbed on the aggregate surface. This causes the deactivation of the emulsifier through the loss of the counter-ion, thus the emulsion is destabilized and breaks.

Needham (Needham, 1996) conducted a wide study on coalescence properties of emulsions during compaction, and especially its behaviour depending on several parameters. The factors that showed a strong effect on bitumen particles coalescence during compaction are the bitumen penetration grade, the compaction load, the cement content, and the polymer addition combined with cement. Softer bitumen droplets deform more easily during compaction, especially when the pressure to which they are subject is higher. Moreover, it seems to exist an electrostatic or steric boundary between droplets which must be overcome in order to join them together. The higher the cement content, employed alone or with polymers, the higher the coalescence increase, due to the chemical reaction that deactivates the emulsifier, although rapid-setting cements do not lead to a faster coalescence. Nonetheless, emulsions with high resistance to hydration reaction ions OH^- and Ca^{2+} show much better mixing stability (Ouyang et al., 2018). At the same time, it is important the type of emulsifier used as well, since different emulsifier types seem to have retarding effect on cement hydration (Tan et al., 2013).

Results showed that a higher emulsifier level leads to a slower coalescence, caused by a high concentration of free emulsifier, such as a strong repulsive force between bitumen particles. Same result is obtained with the use of polymers without cement (Needham, 1996).

Overall, the compaction process seems to be fundamental to start the coalescence process and the cohesion development, since un-compacted mixes did not show cohesive behaviour in the first 24h. On the other hand, what is not crucial is the compaction temperature, since results showed that an increase from 3°C to 45°C lead to a low coalescence increase from 37% to 53% (Needham, 1996).

1.1.3 Foamed bitumen

The thesis treats only of CBTM mixtures produced with bitumen emulsion but a general overview on the foamed bitumen mixtures is provided. Foamed bitumen is produced by injecting water into hot bitumen, resulting in spontaneous foaming. The physical properties of the bitumen are temporarily altered when the injected water, on contact with the hot bitumen, is turned into vapour, which is trapped in thousands of tiny bitumen bubbles. The foam dissipates in less than a minute and the foaming process occurs in an expansion chamber.

To produce a CBTM with this technique on site, the bitumen is foamed in that context and incorporated into the aggregate while still in its foamed state. The greater the volume of the foam, the better the distribution of the bitumen in the aggregates.

During the mixing process, the bitumen bubbles burst, producing tiny bitumen particles, that disperse throughout the aggregate by adhering to the finer particles (fine sand and smaller) to form a mastic. The moisture in the mix prior to the addition of the foamed bitumen plays an important role in dispersing the bitumen during mixing. On compaction, the bitumen particles in the mastic are physically pressed against the larger aggregate particles resulting in localized non-continuous bonds (Asphalt Academy, 2009).

The properties of the foam are characterized by means of the expansion ratio and the half-life values. These values are calculated as follows:

- Expansion Ratio = Maximum volume of foamed bitumen/Original volume of bitumen;

- Half-life = Time measured in seconds for the foamed bitumen to subside from the maximum volume to half of the maximum volume.

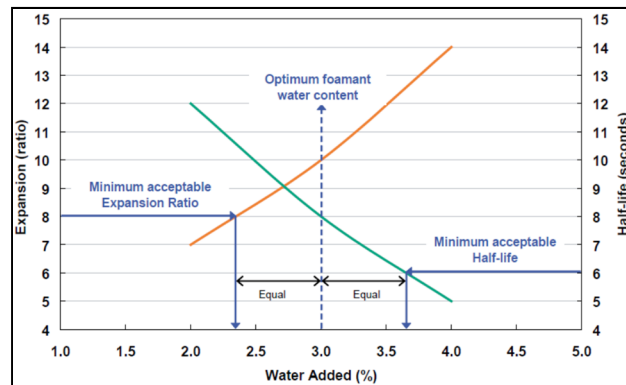


Figure 1.6 Determination of Optimum Foamant Water Content (Asphalt Academy, 2009)

Such parameters are measured in laboratory simply spraying the bitumen foam in a standardized bucket with different foaming water contents. By varying the application rate of the foamant water, a plot such as Figure 1.6 is obtained for a specific temperature. In this manner, it is possible to choose the optimum foaming water content. Standard specifications for ER_m and $\tau_{1/2}$ are non-existent but recommended values of $ER_m > 8$ and $\tau_{1/2} > 6$ seconds are observed from South African experience (technical guidelines) (Jenkins, 2000b).

1.1.4 Reclaimed asphalt pavement (RAP)

The increasing use of RAP in the last years is mainly due to the exponential improvement of the techniques adopted, as well as the advancements in the scientific field. In fact, recycling asphalt pavements have technical, economical and environmental advantages. For these reasons, the majority of design and rehabilitation projects worldwide are characterized by the employment of RAP aggregate in percentages from 10% to 100%, depending especially on the road class and the traffic level (Al-Qadi et al., 2007).

After that RAP is obtained from the pavement milling, it is usually stockpiled in production plants before being re-used in construction or rehabilitation projects. At this stage, the material is completely exposed to air and ambient factors, which lead to oxidation and ageing. As a consequence, the characterization of the RAP when implemented in a new mixture is an extremely important step. Normally, when RAP is employed in HMA mixture, the extracted RAP binder is extracted and analyzed to determine the degree of blending with the virgin binder at the target mixing temperature. However, it is reasonable to assume that when RAP is implemented in a CRM (or CBTM) mixture, no blending occurs between the bitumen emulsion residual bitumen and the RAP binder, because of the low production temperatures. In such case, one crucial aspect is the RAP gradation. RAP is a heterogeneous material and is not always composed of aggregates covered by old bitumen. At the same time, it is possible to find conglomerates of small aggregates glued together by a mastic. Such aspects could cause a drastic change in the gradation when a new mixture is put in place, therefore it is important to keep the RAP gradation under control (Perraton, Tebaldi, et al., 2016). In the framework of the RILEM TC 237-SIB TG6, a protocol by Perraton at École de technologie supérieure was proposed to perform a Round Robin Test (RRT) in order to characterize RAP sources by a fragmentation test. This procedure resulted to be suitable to differentiate different RAP classes based on their fragmentation resistance, but additional studies were needed to evaluate the relationship between the fragmentation test classification and the properties of the CBTM mixture produced (Perraton, Tebaldi, et al., 2016; Tebaldi et al., 2019).

1.1.5 Ordinary Portland Cement

Cement is a hydraulic binder which is generally employed to produce concrete. When it is combined in his unhydrated form with water, it forms the cement paste. The cement paste is the binding phase in concrete which holds the aggregate structure together. A particular type of cements are the calcium silicate cements, also known as Portland cements. At present, five types of Portland cements exist (types I-V), and the main differences among them are due to the production process, especially in terms of cement minerals used and the fineness to which

the cement is ground. These five types are defined as Ordinary Portland Cements (OPC) and they are the most commonly used for typical concrete applications (Thomas & Jennings, 2009).

The reaction between OPC and water forms various products, among which the most important is called calcium-silicate hydrate (C-S-H) gel, which grows between particles giving strength to the cement paste. The volumetric composition of the cement paste is strongly related to the degree of the hydration reaction α , which varies from 0 (unhydrated cement) to 1 (cement completely hydrated). The formulation of the volumetric properties evolution with α is possible thanks to the Powers' model (Powers, 1958). Powers' model is largely based on a comprehensive study of water vapour sorption isotherms and chemically bound water in hardening cement pastes. The water involved in a cement paste can be classified in three parts: capillary water, gel water and chemically bound water. The capillary water is the free water present in the coarse capillary pores. The gel water is the water physically bound to the surface of the gel solid, equal to approximately 0.19 g per gram of cement reacted. The gel solid structure is composed of the chemically bound water, which is approximately 0.23 g per gram of cement reacted. Therefore, a complete OPC hydration is only possible at a water/cement (w/c) ratio above 0.42 (= 0.23 + 0.19). If a lower w/c ratio is used some cement will remain unhydrated ($\alpha < 1$), whereas if a higher w/c ratio is used cement will totally hydrate ($\alpha = 1$) and some capillary water will still be available (Jensen & Hansen, 2001; Powers, 1958).

The products formed by the reaction have a lower volume compared to the total volume of cement and capillary water initially used, due to chemical shrinkage. The volume of capillary pores is around 6.4 ml per 100 g of cement reacted. Based on such assumptions and assuming an air-free cement paste, the following volumes can be defined (Jensen et al., 2001):

- Volume of capillary pores V_{cp} :

$$V_{cp} = 0.20 \cdot V_C \cdot \alpha \quad (1.1)$$

- Volume of capillary water V_{cw} :

$$V_{cw} = V_{cw,0} - 1.32 \cdot V_C \cdot \alpha \quad (1.2)$$

- Volume of gel water V_{gw} :

$$V_{gw} = 0.60 \cdot V_C \cdot \alpha \quad (1.3)$$

- Volume of gel solid V_{gs} :

$$V_{gs} = 1.52 \cdot V_C \cdot \alpha \quad (1.4)$$

- Volume of unhydrated cement V_{UNC} :

$$V_{UNC} = V_C \cdot (1 - \alpha) \quad (1.5)$$

All the volumes just described are illustrated in Figure 1.7. In the figure, the w/c ratio is fixed at 0.42 in order to have a full cement hydration and the evolution of the volumetrics for α as a function of time is shown. It can be observed that the volumes of capillary water and cement when $\alpha = 0$ ($V_{cw,0}$ and V_C) are 57% and 43%, respectively. It is also highlighted that if $\alpha = 1$ in Equations (1.1) — (1.5) the total volume of the cement paste is still equal to 1, even though approximately 8.6% ($= 0.20 \times 0.43$) of the hydrated cement paste is capillary pores. The remaining solid structure of the cement paste, V_{gw} and V_{gs} , is approximately 2.12 ($= 1.52 + 0.6$) times the initial cement volume.

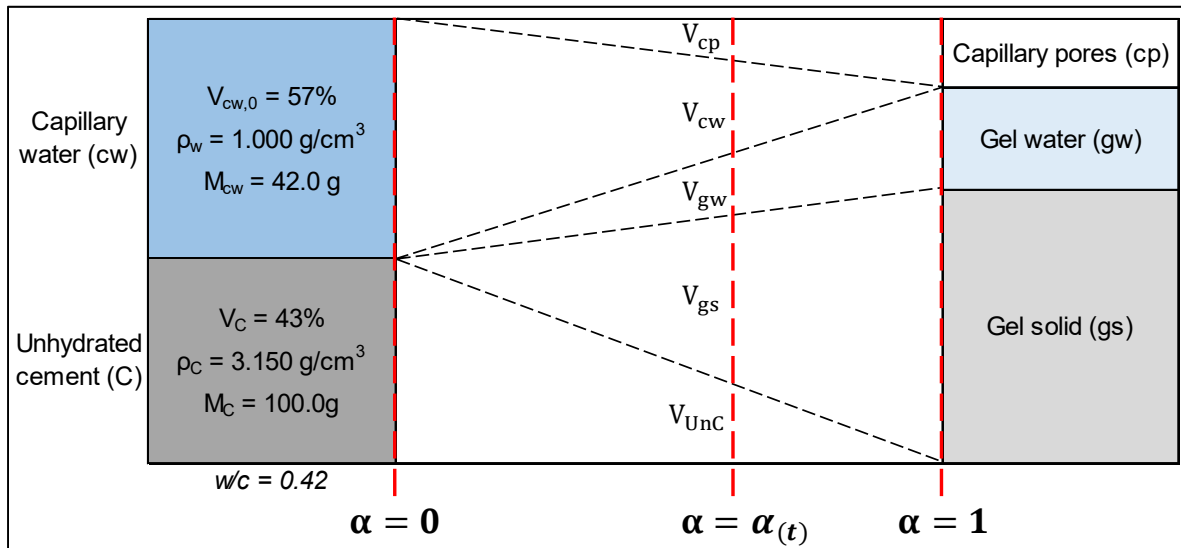


Figure 1.7 Volumetric composition development during cement hydration for w/c = 0.42

1.2 Interaction of bitumen emulsion with mineral aggregates

As mentioned in chapter 1.1.2, the bitumen emulsion can show different ways to flocculate and eventually break on the aggregate surface, depending especially on the chemical attraction between bitumen droplets and aggregate. In more practical situations and in lack of specific laboratory equipment, it is difficult to precisely evaluate both the aggregate and bitumen emulsion composition. Regarding the aggregates, the identification becomes more difficult when dealing with stockpiled RAP, since its random nature makes it composed of many variables. Same goes for bitumen emulsions supplied by industrial producers that often are not willing to share all the details regarding the composition. In this manner, some important aspects of the emulsion chemistry are totally unknown. Of course both issues lead to some uncertainties at the moment of mix-design, since the mechanical properties of CBTM mixtures could change drastically for different aggregate-emulsion combinations.

When a bitumen emulsion is combined with RAP, such as in CBTM mixtures, the assumption that the aged RAP binder does not reactivate, to act as a co-binder, is reasonable. In fact, generally RAP is considered as a “black rock”, i.e. an aggregate phase composed by a reclaimed aggregate partly coated by stiff aged binder. The aged binder is unlikely reactivating at the usual production temperatures of CBTM. Yan, Zhu, Zhang, Gao, & Charmot (2014) evaluated the effect of the presence of RAP in CBTM mixtures mechanical properties and by a finite elements analysis (FEM) analysis. Both protocols confirmed that the presence of RAP improved Indirect Tensile Strength (ITS), high temperature stability, moisture resistance and fatigue performance. According to the analysis, the aged binder in the RAP could act as a cushion between the aggregate phase and the virgin binder, reducing stress and strain fields.

In other researches, the bonding resistance at the interface between bitumen emulsion and aggregate surface was evaluated by means of the Binder Bond Strength test (BBS) (Cardone et al., 2018; Graziani, Virgili, et al., 2018; Miller et al., 2010). The test consists in gluing a stub on a mineral flat surface by means of the virgin binder (in this case bitumen emulsion). After a certain period of curing and/or conditioning, the stub is pneumatically pulled out and the

adhesive strength necessary to remove the stub is measured. Results from BBS test showed a quite good repeatability, even though the test was not born to test bitumen emulsions (Miller et al., 2010). Moreover, it was observed that when bitumen emulsion is combined to a limestone surface, this penalizes the moisture sensitivity if compared to a basalt surface (Graziani, Virgili, et al., 2018). An attempt was done to evaluate the RAP/bitumen emulsion adhesion strength, by coating the mineral surface with a virgin binder and simulate a laboratory ageing to reproduce the RAP characteristic (Cardone et al., 2018). The main failure type was cohesive (rather than adhesive), meaning a good bond between the residual emulsion bitumen and the artificial RAP surface. When the mastic composed of bitumen emulsion and filler was tested instead of the simple residual binder, the main failure type was adhesive. Testing the mastic is more realistic, since in CBTM mixture it is the mastic (bitumen emulsion, filler and cement) that coats the larger RAP aggregates. An adhesive failure type is an index of the poor bonding between the two components.

1.3 Role of mineral additions

It is important to remark that bitumen and other co-binders (cement, calcium carbonate, etc.) do not create a new unique binder, but they act separately. However, the addition of these elements produces suitable structural and durability properties (Brown & Needham, 2000; Raschia et al., 2018; Stroup-Gardiner, 2011; Yan et al., 2017).

The dosage of residual bitumen and cement control the stiffness and thermal sensitivity of CBTMs, while the quality and amount of fines (passing at 0.063mm sieve) are extremely important for the production of the binding mastic. In particular, when a bitumen emulsion is employed, the amount of fines is less critical, since the bitumen partially coats the coarser aggregates.

According to the proportions in which bitumen and cement are mixed, the mechanical response of a CBTM is extremely variable. In general, the addition of cement increases strength,

stiffness and permanent deformation resistance but, at high cement content, mixture could be affected by premature cracking (Grilli et al., 2012; Yan et al., 2017).

Cement hydration takes place thanks to the watery phase that is introduced in the mixture as part of the bitumen emulsion or water itself used for improvement of compactability (Brown et al., 2000; Giuliani, 2001; Montepara & Giuliani, 2001). The presence of bitumen with the cement does not prevent the formation of cement hydrated compounds. Nevertheless, different types of emulsifier have different effect on cement hydration rate (Li et al., 2015; Tan et al., 2013). In other cases, for example when the emulsifier content is low, the water retained in the mixture evaporates quickly and the cement hydration is arrested or prevented (Miljković et al., 2017). Figure 1.8 shows that when cement is added, the emulsified bitumen particles split gradually. The asphalt membrane sticks to the surface of the cement, which can block cement particle hydration (Wang et al., 2014).

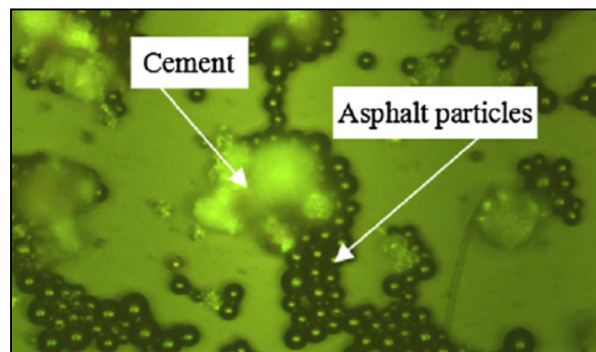


Figure 1.8 Optical images of fresh emulsified asphalt with cement (Wang et al., 2014)

It was found that other mineral additions (such as slag and rock flour) had no influence on the dry or soaked ITS results compared with CBTM produced with any filler. On the other hand, cementitious binders resulted in higher ITS values, as expected (Hodgkinson & Visser, 2004). Similar results were achieved by different authors (Brown et al., 2000; Lachance et al., 2012; Niazi & Jalili, 2009), which concluded with the general mechanical enhancement given by ordinary Portland cement in CBTMs. In fact, it can be seen that hydrated lime and calcium

chloride (CaCl_2) can give a contribution on stiffness, but not as high as Portland cement (Raschia et al., 2018). Nevertheless, Chandra et al. (2013) showed that mixtures with 1% of cement compared with mixtures treated with 2% of hydrated lime gave similar performance at ITS. Moreover, Du (2014) demonstrated that hydrated lime combined with slag forms a cementitious binder that is able to give acceptable moisture resistance, even though not as high as with cement addition. However, the application of cement is more popular while producing lime slurry is much more difficult (Sebaaly et al., 2004). Grilli et al. (2012) clarified the behaviours of cement and bitumen acting at the same time by considering the weight ratio between the residual emulsion bitumen in the mix (B_R) and the cement dosage used (C). Indeed, if $B_R/C < 1$, it implies CBTMs with high stiffness and low ITS values, whereas when B_R/C is approximately 1 the mixture provided both high stiffness and ITS values. Finally, if $B_R/C > 1$, the mixture showed low stiffness and ITS values. This means that the cement allows high stiffness to be reached and, increasing the residual bitumen dosage (B_R), high fracture resistance can be provided, too. However, when a higher dosage of bitumen emulsion is used, the mixture becomes more ductile and the stiffness decreases. Table 1.3 shows important aspects to consider when bituminous binders, such as bitumen emulsion, and cementitious binders, such as cement, are used.

1.4 CBTM production and curing

1.4.1 Introduction

Mix design is the process which leads to the production of construction materials with the necessary quality and consistency to fulfil their intended functions. The production process consists in many aspects, such as the choice of materials, as well as transportation, laying and compaction procedures. A production process carried out in an efficient way optimizes the energy consumption of each aspect, influencing directly the project final costs (Figure 1.9) (Xiao et al., 2018).

Table 1.3 Advantages and disadvantages of bituminous and cementitious additions (taken from Xiao et al. (2018))

Binder	Advantages	Disadvantages
Bitumen emulsion	<ol style="list-style-type: none"> 1) Flexibility (viscoelastic type of material) 2) Ease of application and acceptance 3) Quick strength development 4) (traffic can be open soon) 	<ol style="list-style-type: none"> 1) Relatively empirical (not uniform distribution) 2) Rutting as main distress
Cement	<ol style="list-style-type: none"> 3) Availability, cost saving and ease of application 5) Specifications are usually available 6) Compressive strength and durability improved 	<ol style="list-style-type: none"> 4) Shrinkage cracking failure 5) Requires curing and protection from early traffic

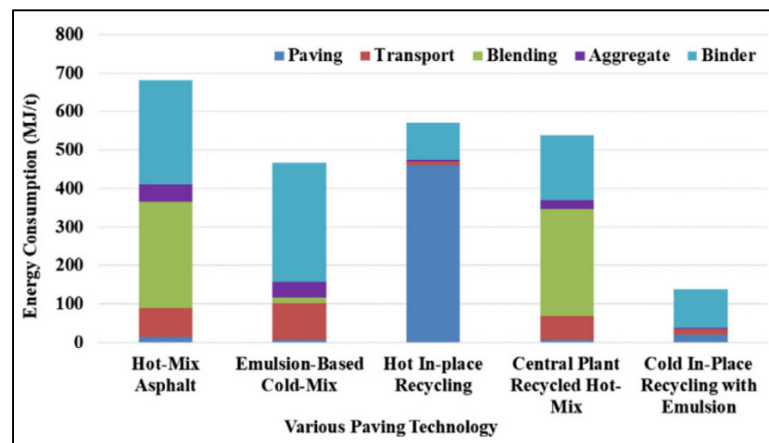


Figure 1.9 Energy consumption of production steps for different techniques (taken from Xiao et al., 2018)

Mix design of CBTMs is particularly challenging because of the number and the different types of “ingredients” that build these materials. Each component, VAg or RAP, water, bitumen and cement, with its own variability, availability and cost, needs to be blended and processed to formulate a composite product (Asphalt Academy, 2009).

1.4.2 Mixing and compaction

Tebaldi et al. (2014) provided a large synthesis of mixing procedures for specimen preparation for CBTM made with emulsion (Table 1.4).

Table 1.4 Mixing procedures for CRM mixtures with added bitumen (RAP, cement or lime and emulsion) (Tebaldi et al., 2014)

Design method	Emulsion temperature (°C)	Mixing order	Mixing method
Minnesota procedure	60	RAP and water mixed. Then mixed with emulsion	Manual
Norway procedure	Room temperature	RAP, water and emulsion mixed at once.	Manual/Mechanical
Italian procedure	Room temperature	RAP and aggregates, water, cement, emulsion	Manual
Wirtgen procedure	Room temperature	RAP, cement, water and emulsion mixed at once. RAP, lime and water mixed at least 4h prior to mixing with emulsion.	Mechanical mixer
NYS DOT-proposed specification	25	RAP mixed with water. Then with emulsion	Manual/Mechanical one specimen mixed at a time, mixing time $\leq 60s$
South Africa guidelines using vibratory compaction	Field temperature	RAP and cement or lime mixed. Then mixed with water and stored for 15–30 min. Mix with emulsion and store for 40–60 min before compaction	Pug-mill mixer

In the current state of practice, there are four main types of laboratory compaction procedure for CBTM mixtures: impulsive (Marshall hammer and Proctor rammer), static (Duriez compactor), static and kneading (Shear Gyrotory Compactor—SGC) and vibratory (Vibratory Hammer). The selection among these methods depends mainly on the specific role of CBTM in the pavement structure and technical experiences. When CBTM are used as an improved granular material impulsive compaction could be more reliable, whereas when they are used as a surrogate of a bound mixture the kneading or vibratory compaction could be more effective.

CRMs without added bitumen are mainly compacted using the Proctor or by the AASHTO T-180 method while mixtures with added bitumen are mainly compacted using the Marshall or gyratory or vibratory compaction. Table 1.5 shows a summary of some of the compaction methods used for CRM with and without bitumen. One of the aims of specimen preparation in the laboratory is to compact specimens in a similar manner to field compaction. However, the extent to which any of these mix design methods simulate field compaction is not clear (Tebaldi et al., 2014).

Table 1.5 Compaction methods used for CRM mixtures containing RAP (Tebaldi et al., 2014)

Design method	Mixture without added bitumen	Mixture with added bitumen	Specimen size (mould size) for bituminous mixes
California procedure—foam bitumen	AASHTO T-180 (method D)	Marshall 75x2 blows	100 x 64 mm (diameter x height)
California procedure—emulsion	-	Marshall 75x2 blows/30 gyrations	
Minnesota procedure	-	Gyratory 600 kPa, 1.25°	101.6mm diameter

Table 1.5 Compaction methods used for CRM mixtures containing RAP (Tebaldi et al., 2014) (continued)

Norway procedure	Modified Proctor	Gyratory 600 kPa, 10, 30 rpm, specimens compacted to 96% of density at 200 gyrations.	100mm diameter
South Africa procedure—foam bitumen Level 1	Modified AASHTO	Marshall/vibratory hammer	100mm diameter
South Africa procedure—foam bitumen Level 2	Modified AASHTO	Vibratory hammer	150mm diameter by 127mm height Proctor mould
Wirtgen procedure	AASHTO T-180	Marshall 75x2 blows or vibratory compaction	-
Modified Marshall procedure	-	Marshall 50x2 blows	4 inches diameter
NYS DOT-proposed specification	-	Marshall 75x2 blows or 30 gyrations at 250°C	4 inches diameter
Italian guidelines	-	Gyratory 600 kPa, 30 rpm, specimens compacted at 200 gyrations.	150mm diameter

One of the issues of CRM is the laboratory simulation of the field mix since the equipment used in lab and the specimen size differs than in the field. Air voids distribution within the mix is a function of many factors such as mix composition, compaction method and aggregate properties. The choice among the different compaction methods and energy are also important to well represent field conditions. Moreover, the influence of compaction energy and the

resulting density (air voids content) in CBTM is of extreme importance for the curing and mechanical behaviour of the mix (Jiang et al., 2019).

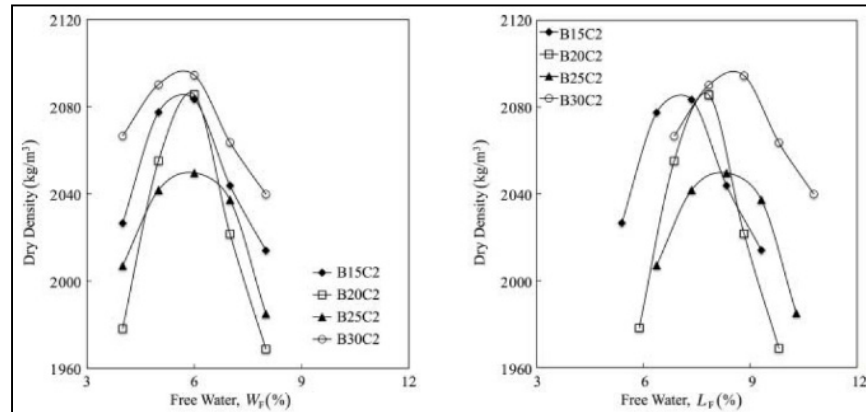


Figure 1.10 Proctor compaction test results (Grilli et al., 2012)

However, it was observed that volumetric characterization of CBTM mixtures brings to a better control of the compaction process itself, if the dosage and the mix design are made thoroughly. The basic concepts are explained in CHAPTER 3. In accordance to this approach Grilli et al. (2012) studied the compactability and the optimum liquid (water and bitumen) content of these mixtures produced with bitumen emulsion. Two compaction methods were employed: Proctor and Shear Gyratory Compactor. The “bell-shaped” curves obtained by means of Proctor compaction (Figure 1.10) showed an optimum free water content for all mixtures. The term free water is used to indicate the amount of water that is not absorbed by the aggregates. At the same time, a unique value of optimum free liquid content was not found. This indicates that even before emulsion breaking, the effective bitumen did not contribute to the compaction process. When the SGC is employed, two types of compaction curves were identified: mainly linear (at a low water content) and bilinear (at a high water content) (Figure 1.11). The point of inflection of the bilinear trend is located at the number of gyrations corresponding to a level of void saturation (by water and bitumen) of about 90%, indicating that as air voids are reduced, liquids tend to fill them (mixture approaches saturation); then part of the compaction energy is spent to increase the pore liquid pressure.

Another research project was performed by Wendling et al. (2014) in order to adapt the current French SGC to allow the compaction of cold mixes by adding the functionality of collecting extruded water due to pore saturation (Figure 1.12).

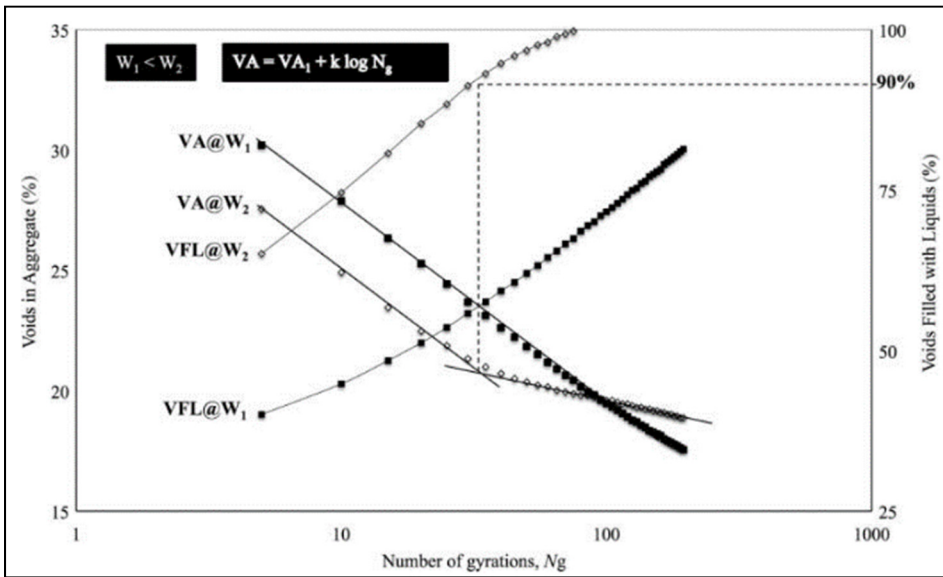


Figure 1.11 SGC Test results (Grilli et al., 2012)

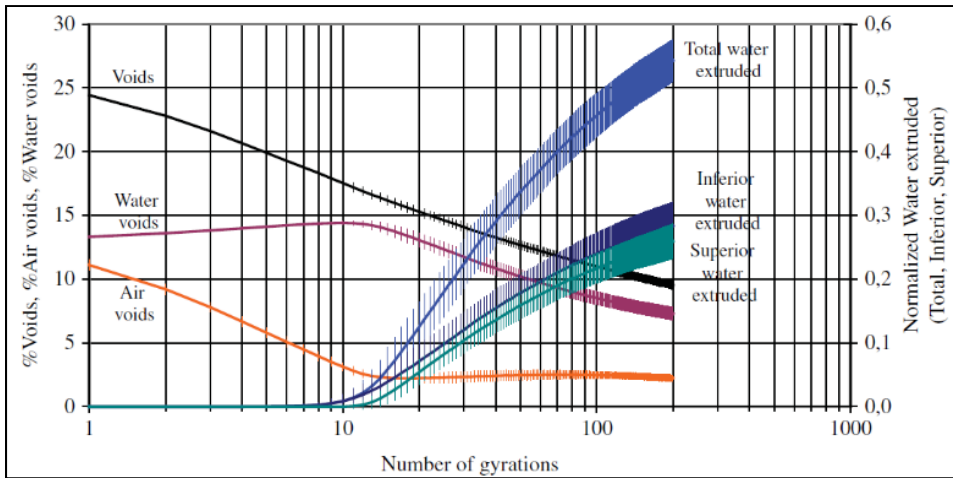


Figure 1.12 Compactability of cold mix asphalt using emulsified bitumen—void and normalized water extruded (Wendling et al., 2014)

Also in this case, it can be observed that water starts to flow out and be collected when the air voids reach a constant value (around 2–3%). The collection of water occurred from both the upper and lower sides of the compaction mould, where the water was flowing in the same amount. The results obtained from both researches would suggest that both the measurement and study of water extrusion kinetics could become valuable tools in assessing the onsite behaviour of cold bituminous mixes and, in particular, their drainage properties during compaction.

1.4.3 Curing protocols

Curing of CBTM is an evolutive process during which the material loses water through evaporation, and improves its mechanical properties through cement hydration and emulsion breaking. Because of this, it is important to have reliable laboratory (and field) procedures to control the curing process during time.

Laboratory curing of CBTM aims to simulate field curing conditions while trying to accelerate the achievement of the long-term properties (Jenkins & Moloto, 2008). With the term “long-term properties” it is intended the condition of the material for which the evolution of its properties is almost stable. In fact, it is quite impossible to establish whether CBTM mixtures are totally cured or not. However, the factors that influence lab and field curing are extremely difficult to standardize and reproduce because they are related to mixture composition (binder types and dosage), construction parameters (degree of compaction, layer thickness, drainage conditions, construction phases) and environmental factors (temperature, humidity, wind).

When both bitumen emulsion and mineral additions are employed, the curing process actually results from more mechanism: emulsion breaking, moisture loss and hydration of eventual cementitious binders. Therefore, a laboratory simulated curing protocol should consider the single curing mechanism characterizing the components used (emulsion breaking/moisture loss and cement hydration), paying attention to specimen shape, dimensions and boundary

conditions as well as controlling curing temperature and relative humidity (Cardone et al., 2014).

In particular, initial curing rate and residual water of CBTM are extremely important during construction activities because they control when upper layers can be laid down and therefore when the rehabilitated pavement can be reopened to traffic.

1.4.4 Field curing studies

In many European countries, the residual moisture content is used to determine the right moment for an HMA overlay, ranging from 1.0% to 1.5% of the cold mixture (Kim et al., 2011). According to the Federal Highway Administration (FHWA) survey in 2009, each US state has different moisture content and curing time requirements: Arizona, Iowa, South Dakota, Vermont and Washington state require that the CIR layer cures until the moisture is reduced to 1.5% or less. Colorado requires a moisture content of 1.0%, while Kansas 2.0%. Delaware, Idaho, Maine, Maryland, Nebraska, Nevada, New Hampshire, New York, Ohio, Ontario, and Pennsylvania require a 4–45 days curing (Kim et al., 2011).

Although many manuals do not specify different curing requirements for CIR produced with foamed bitumen or bitumen emulsions, generally a higher moisture content for foamed bitumen compared to mixes with emulsion is allowed. They recommend between 1.0% and 1.5% of residual water for emulsion layers before a new layer is laid, but at least 2.0% less than the optimum moisture content (OMC) if the cold mixture is produced with foam.

Lee (1980) highlighted that curing behaviour of such mixtures is dependent on the mixture composition, hence it is important to consider also water dosage as a fundamental parameter in terms of mix design. In the literature, it is common to find residual water contents of less than 0.5% after oven curing at 60°C (Jenkins et al., 2008). Moreover, 60°C temperature is often above the softening point temperature of the base binder and may cause a different dispersion of the bitumen if compared to field conditions.

Subsequently, curing temperatures of 40 ± 5 °C were commonly used as an accelerated laboratory curing simulation of field moisture conditions. Plus, depending on the curing period, it can represent between 12 months and 3 years of field curing (Jenkins et al., 2008; Serfass et al., 2004).

1.4.5 Laboratory curing for bitumen emulsion mixes

It is widely known that it is not possible to establish a unique laboratory curing protocol for bitumen emulsion mixtures. In addition, many mix-designs use a combination of curing times and temperatures. The early strength of the cold recycled pavements, immediately after compaction, can be simulated using a curing time of 6 hours (Lee et al., 2002). At the same time, a curing period of 24 hours is widely accepted as a reference for quality control of the mixture just laid; it also particularly fits the project time scheduling. Figure 1.13 shows normalized values of strength development along curing.

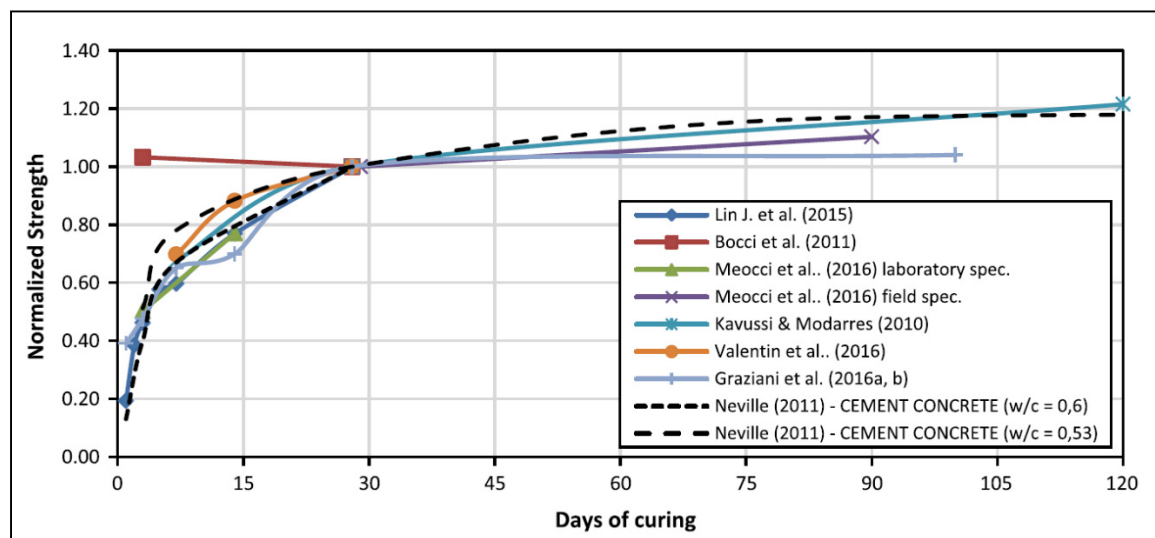


Figure 1.13 Normalized strength along curing related to literature (taken from (Dolzycki et al., 2017))

The authors normalized the strength development assuming as reference value the one obtained at 28 days. As already mentioned, the curing process depends on many different variables (raw materials, mixture composition and binder dosage, environmental conditions, etc.), but from the data collected in the figure it can be observed that the increase in strength between 28 and 120 days reached a maximum of 20%. This indicates that 28 days of curing does not allow to reach a perfectly stable condition of mechanical properties, but it can be a good compromise between laboratory timing operations and the need to investigate long-term cured materials, since the increase observed afterwards is quite small.

A particular aspect of curing in CBTMs is the presence of bituminous and hydraulic binders, which are characterized by the interaction of different physical and chemical mechanisms. Curing mechanisms related to the bituminous phase basically involve emulsion breaking and water expulsion. Initially, flocculation and coalescence of bitumen droplets lead to the formation of bituminous films incorporating part of the finer aggregate particles (filler and fine sand), cement and water. Afterwards, cohesion is ensured by moisture loss through evaporation and pore pressure-induced flow paths. Curing also involves chemical reactions linked to cement hydration. At low cement dosage, the hydration products disperse inside the fresh bitumen films increasing mixture viscosity and improving the resistance to permanent deformations. At higher cement dosage, the volume of hydration products grows forming a stiffer matrix that connects coarser aggregates. In addition, because cement hydration reactions require the presence of water, the use of cement accelerates the emulsion curing process by reducing the amount of free water. Strength and stiffness are normally increasing in relation to the amount of water loss during curing. Cement usually reacts almost completely in the mixture (Cardone et al., 2014; Graziani, Iafelice, et al., 2018), and the final amount of free water is reduced by the water involved in the reaction; on the other hand, even if the material is cured for more than 28 days, a small amount of evaporable water still remains in the mixture (Figure 1.14) (García et al., 2013). In fact, it has been shown that after 3 days of curing at 20 ± 1 °C cement in CBTM mixtures with cationic emulsion had a degree of hydration of around 70%, and that such value was also likely increasing (Fang et al., 2016).

Bocci et al. (2011) investigated the influence of curing conditions, temperature and moisture on the mechanical behaviour of these materials. They analyzed stiffness modulus on three curing temperature representing typical seasonal conditions: 40°C, 20°C and 5°C. Results showed that higher curing temperatures resulted in higher rates of stiffness increase and higher maximum values. Nevertheless, even though low temperatures slowed down the curing process, they did not penalize the mixture potential performance. Moreover, these mixtures showed an overall good moisture resistance regardless of the curing temperature.

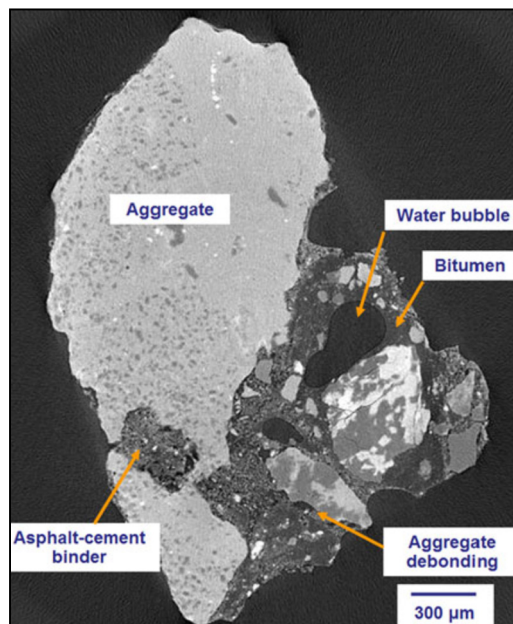


Figure 1.14 Microtomography details of an asphalt and cement composite (García et al., 2013)

Specific results about the role of cement in low-term curing is collected in Graziani et al. (2016), who modelled curing effects using a statistical regression analysis. In particular, it is highlighted that the initial strength development was faster than the stiffness development. This suggests that curing of the bituminous emulsion mainly contributes to the evolution of ITS, whereas the evolution of Indirect Tensile Stiffness Modulus (ITSM) is more linked to the formation of hydration products, which do not entail any moisture loss (Graziani et al., 2016).

Different curing procedures were investigated in Ojum et al. (2014), taking into account the effect of temperature and cement under different curing regimes. In particular, they performed three different curing conditions: unconfined, partially wrapped (the circular surface of the specimens were wrapped with aluminum foil) and fully wrapped specimens. As results, the ratio of 28-days stiffness values between specimens cured unwrapped and those cured fully wrapped is typically 2-2.5, independently by the curing temperature. Moreover, the inclusion of 1% of cement in the fully wrapped case leads to strength and stiffness results approximately equal to those of unwrapped specimens without cement, suggesting that 1% cement addition is an appropriate means to avoid the effects of adverse weather during curing, i.e. excessive residual water in the mixture.

1.5 Modelling of CBTM properties

1.5.1 Evolutive behaviour

The curing process in CBTM mixtures is characterized by a mass loss due to water evaporation and an increase of the mechanical properties, which is partly caused by the cement hydration (Dolzycki et al., 2017). Water loss and cement reaction have an evolutive trend along time, which can be observed by recording the parameter in an experimental way. Such parameters can be easily modelled to predict long-term values (after the last measured point), and at the same time model parameters can be used to compare different CBTM mixtures analyzed (Figure 1.15).

Initially, the Michaelis-Menten model was used for CBTM mixtures to evaluate the material property trend according to time, using two parameters: y_A , representing the asymptotic value, and K_c , representing the short-term rate increase (Graziani et al., 2016; Michaelis & Menten, 2007). The issue related to this model is the time interval in which it is applied; in fact, it has been observed that considering all the experimental data from 0 days led to a poor prediction of the long-term values. This is caused by the fact that it is difficult to predict the values after

1 day of curing and at long-term simply because the process is happening in two distinct steps, for which the threshold is somewhere close to 1 day. For this reason, a modified version of the Michaelis-Menten model was proposed to analyze experimental results starting from 1 day (Raschia, Graziani, et al., 2019b). Now, it is a three-parameters model: y_A is the asymptotic value, y_1 is the material property after 1 day of curing, and H is the time (expressed in days) required by the property to reach half of the difference between y_A and y_1 . The application of this model is represented in Figure 1.15. However, other models are present in the literature, such as the maturity method. It consists in measuring the concrete temperature history during curing, which allows the estimation of the hydration degree and hence of the strength development (Galobardes et al., 2015).

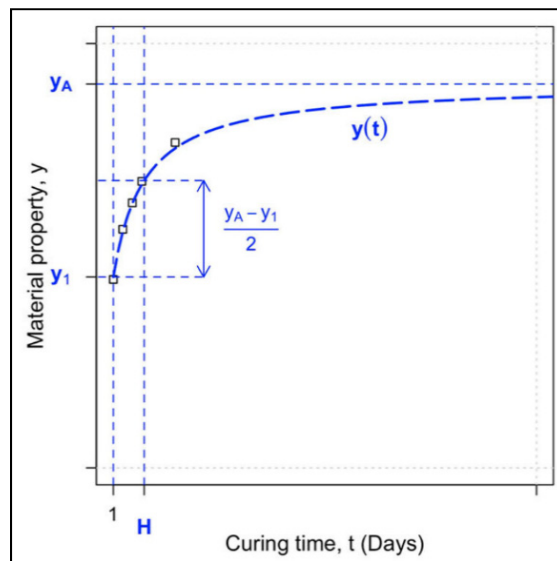


Figure 1.15 Example of experimental points and model related to a material property (Raschia, Graziani, et al., 2019b)

1.5.2 Visco-elastic behaviour of bituminous materials

In case that a repeated load (for example traffic) is applied to a bituminous material, a 3D strain field is observed, which can be simplified in 2D along the longitudinal and transversal

directions of the load applied. Depending on the strain amplitude transmitted to the material, as well as the number of cycles of the load application, the pavement shows different types of behaviour and eventually failure (Figure 1.16).

When both the strain and the number of cycles applied are low, the material is not supposed to damage and to behave as a linear viscoelastic (LVE) material. The viscous contribution is given by the bituminous binder present in the mixture. The general behaviour of a LVE material is comprised in two limits: at high load application rates (high frequencies), or very low temperatures, it behaves as a perfectly elastic material, whereas at very low frequencies or high temperatures it behaves as a perfectly viscous material. As a consequence, the material response in between these two extremes is governed by the LVE theory (Corte & Di Benedetto, 2004).

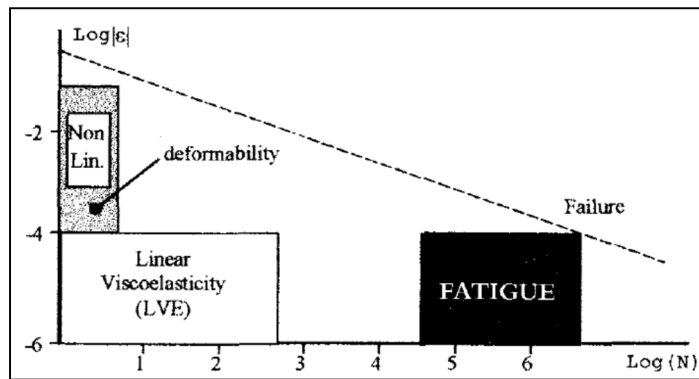


Figure 1.16 Behaviours typically observed in bituminous mixtures (Strain vs Number of loading) (Di Benedetto et al., 2001)

The LVE characterization of a bituminous material can be assessed through complex modulus tests. The complex modulus E^* of a material is a complex unit composed of a real part, or storage modulus E_1 , and an imaginary part, or loss modulus E_2 :

$$E^* = E_1 + iE_2 \quad (1.6)$$

where i is the imaginary number. For bituminous mixtures, E^* is dependent on temperature and loading rate.

The norm of the complex modulus $|E^*|$ can be measured by the application of a sinusoidal stress which corresponds to a sinusoidal response of the strain, which is normally delayed with respect to the stress by a quantity defined as phase angle, Φ_E (Figure 1.17).

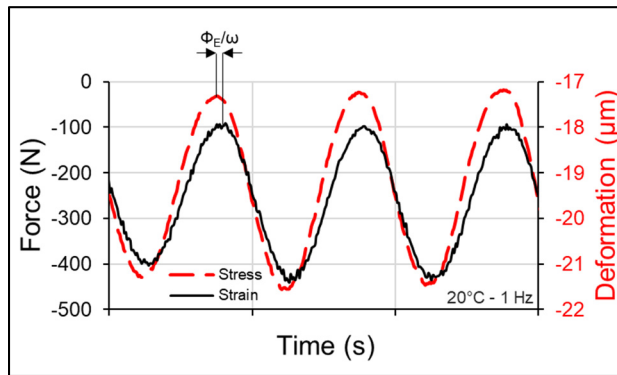


Figure 1.17 Stress-strain trend for complex modulus test in only-compression configuration

The equations that describe stress and strain functions ($\sigma(t)$ and $\varepsilon(t)$), as well as the complex modulus E^* are:

$$\sigma(t) = \sigma_0 \cdot \sin(\omega t) \quad (1.7)$$

$$\varepsilon(t) = \varepsilon_0 \cdot \sin(\omega t - \phi_E) \quad (1.8)$$

$$E^* = \frac{\sigma_0}{\varepsilon_0} \cdot e^{i\phi_E} = |E^*| \cdot e^{i\phi_E} \quad (1.9)$$

where $\omega = 2\pi f$ represents the pulsation and f the frequency.

The phase angle can vary from 0° , typical for perfectly elastic material, to $\pi/2$, typical of perfectly viscous material. This parameter represents the rotation of the vector with norm $|E^*|$ in the Cole-Cole imaginary plan (E_1 vs E_2). Consequently, the norm of the complex modulus $|E^*|$ can be determined as:

$$|E^*| = \sqrt{E_1^2 + E_2^2} \quad (1.10)$$

Both $|E^*|$ and ϕ_E material properties in LVE materials are strongly influenced by temperature and load frequency. In general, for the same material subject to a sinusoidal stress, $|E^*|$ tends to increase when the temperature decreases (or frequency increases), whereas ϕ_E tends to increase when temperature increases (or frequency decreases). This behaviour is usual in HMA mixtures, but it is also respected in CBTM mixtures (Figure 1.18).

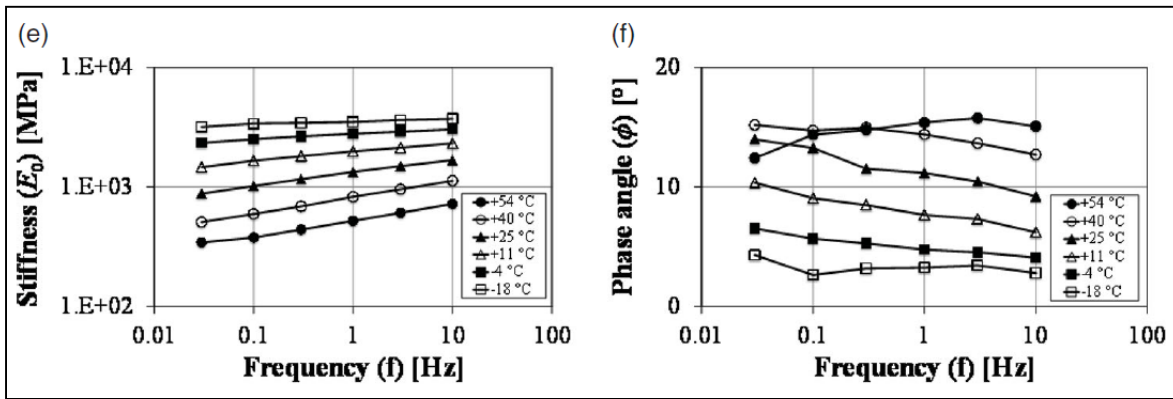


Figure 1.18 Isothermal curves for CBTM mixtures (6 temperatures, 6 frequencies)
(Godenzoni, Graziani, et al., 2016)

Moreover, due to their physical composition (low bitumen dosage, high air voids, low aggregate coating), CBTM generally show lower values of stiffness $|E^*|$ and phase angle ϕ_E if compared to HMA (Graziani et al., 2020).

From the isothermal curves obtained by experimental results, it can be clearly observed that the same value of $|E^*|$ or ϕ_E can be obtained at different temperatures or frequencies. If this is the case, it means that the material respects the Time-Temperature Superposition Principle (TTSP). This can also be assumed if the experimental points follow a unique curve in the Cole-Cole plan or the Black space ($|E^*|$ vs ϕ_E). For example, polymer modified binders do not respect the TTSP due to the presence of polymers in the blend (Olard & Di Benedetto, 2003).

When the TTSP applies, it is possible to describe the norm of the complex modulus $|E^*|$ or the phase angle ϕ_E as properties depending only by the frequency, called in this case reduced frequency f_{red} . After selecting a reference temperature T_S and its related isothermal curve, the remaining isothermal curves can be shifted by a certain quantity on the frequency axis to follow the reference curve. The new position of the isothermal curves are characterized by the same values of $|E^*|$ or ϕ_E , but the frequency is translated by a shift factor a_T :

$$f_{red} = f \cdot a_T \quad (1.11)$$

It is obvious that for the reference temperature isothermal curve, $a_T = 1$. Results expressed in this way are called “master curves” (Figure 1.19).

The William, Landel and Ferry (WLF) model is often used to estimate the trend of the shift factors a_T according to temperature (Ferry, 1980):

$$\log(a_T) = -\frac{C_1(T - T_S)}{C_2 + T - T_S} \quad (1.12)$$

where C_1 and C_2 are material constants at the reference temperature.

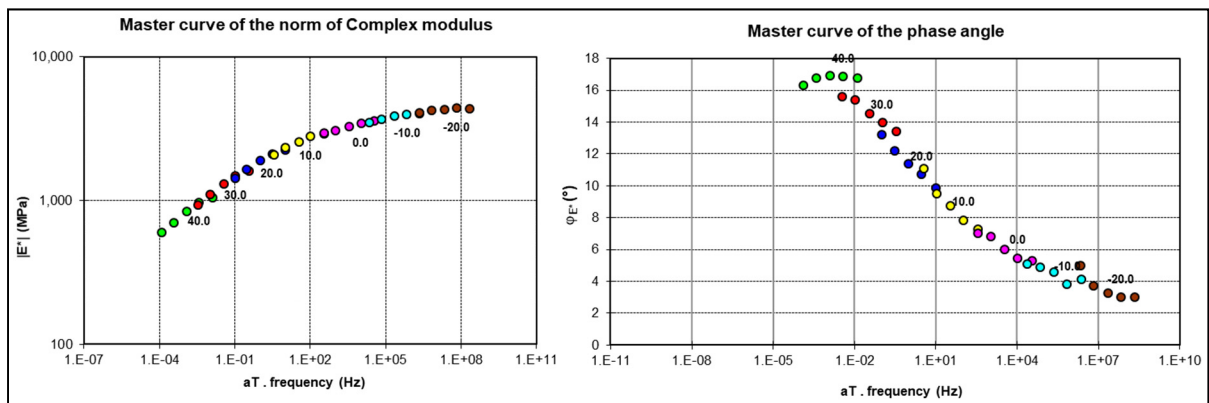


Figure 1.19 Master curves for a CBTM mixture at $T_S = 20^\circ\text{C}$ (5 frequencies, 7 temperatures)

1.5.3 Rheological modelling

The LVE nature of materials allow to represent them in form of analogical models, which are composed of a combination of springs (elastic elements) and linear dashpots (Ferry, 1980). The importance of analogical models is represented by their ability to describe physical phenomena of the material, which, on the other hand, is not possible with empirical mathematical functions. The simplest models for LVE materials are the Maxwell and the Kelvin-Voigt models. In the first, a spring and a linear dashpot are placed in series, whereas in the second they are placed in parallel. Since such models are not advanced enough to describe bituminous materials behaviour, they acted as starting point for the development of efficient models. One is the Huet-Sayegh model, where a combination in series of a spring (stiffness E_0) and two parabolic dashpot (k and h) is in parallel with a second spring (stiffness E_{00}) (Figure 1.20).

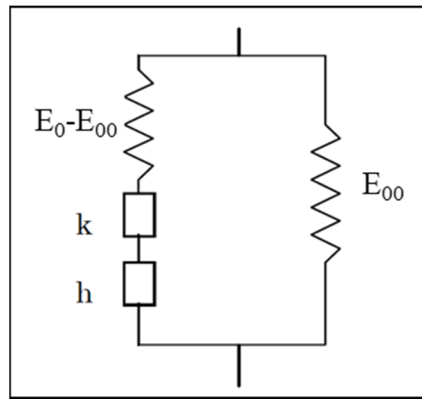


Figure 1.20 Huet-Sayegh model

The complex modulus E^* with the Huet-Sayegh model is calculated as:

$$E_{HS}^*(i\omega\tau) = E_{00} + \frac{E_0 - E_{00}}{1 + \delta(i\omega\tau)^{-k} + (i\omega\tau)^{-h}} \quad (1.13)$$

where E_{00} is the modulus when $\omega \rightarrow 0$ (static modulus), E_0 is the modulus when $\omega \rightarrow \infty$ (glassy modulus), τ is the characteristic time, which value varies only with temperature T ($\tau(T) =$

$a_T(T) \cdot \tau(T_S)$), k and h are the parabolic exponent such as $0 < k < h < 1$, and δ is a calibration constant.

In this way, the determination of 6 constants (E_{00} , E_0 , τ , k , h and δ) allows a good description of the LVE behaviour of the material. Graziani et al. (2020) observed that in CBTM mixtures the Huet-Sayegh model is able to well model the master curve of the norm of the complex modulus. On the other hand, the phase angle values measured experimentally were always higher than the model values. This difference was almost constant regardless temperature and frequency, meaning that the model underestimates the phase angle. They explained this finding introducing the concept of frictional dissipation, which is reasonable to assume in CBTM mixtures due to the low aggregate coating. Moreover, such phenomenon is not supposed to be influenced by temperature and frequency. As a consequence, a correction was proposed by Graziani et al. (2020) to correct the Huet-Sayegh model:

$$E_{HSq}^*(i\omega\tau) = E_{HS}^*(i\omega\tau) \cdot e^{iq\left(\frac{\pi}{2}\right)} \quad (1.14)$$

The term $e^{iq\left(\frac{\pi}{2}\right)}$ adds a time-temperature independent phase angle $q\left(\frac{\pi}{2}\right)$ to the Huet-Sayegh model phase angle, without changing the complex modulus value. More simply, if $q = 0$, it gives the Huet-Sayegh model. This approach resulted quite useful to have a better fitting with experimental data and model values in CBTM, even if it adds a variable to the model optimization.

Olard & Di Benedetto (2003) pointed out that the Huet-Sayegh model is suitable for bituminous mixtures modelling, even though it is not efficient at low frequencies (high temperatures) in case of binders. This is caused by the approximation that the model assumes, reducing at a parabolic element instead of a linear dashpot. To overcome this issue, a new model was proposed, the 2S2P1D (2 springs, 2 parabolic elements, 1 dashpot), which is represented in Figure 1.21 and described by the equation:

$$E_{2S2P1D}^*(i\omega\tau) = E_{00} + \frac{E_0 - E_{00}}{1 + \delta(i\omega\tau)^{-k} + (i\omega\tau)^{-h} + (i\omega\beta\tau)^{-1}} \quad (1.15)$$

where some parameters were already described and a Newtonian viscosity is introduced, $\eta = (E_0 - E_{00})\beta\tau$. β is dimensionless and it is a model parameter. In this case, as in the case of the modified Huet-Sayegh model, 7 constants are necessary to determine the LVE behaviour of a frequency and temperature dependent material. Being β linked to the dashpot viscosity, it appears to be normally lower in HMA mixtures if compared to CBTM mixtures (Gandi et al., 2017; Lachance-Tremblay et al., 2017; Olard & Perraton, 2010). It must be highlighted that the LVE characterization of CBTM mixtures is still an open issue and analogical models are rarely used.

When different types of behaviour of bituminous materials need to be described (beyond the LVE field), the DBN model is a suitable rheological model. The DBN model (named after the authors Di Benedetto and Neifar) is very versatile and its formulation can be adapted to be very simple (for LVE or elastic fields) or more complicated (for fatigue, permanent deformation or non linearity) (Di Benedetto, Mondher, et al., 2007). The unidirectional representation of the DBN model is shown in Figure 1.22. The model is composed of elasto-plastic (EP) and purely viscous bodies. The EP bodies represent any non-viscous behaviour (i.e. rate-independent behaviour), whereas the viscous bodies, with viscosity η_i , take into account the temperature sensitivity and the viscous irreversibility (Di Benedetto, Mondher, et al., 2007).

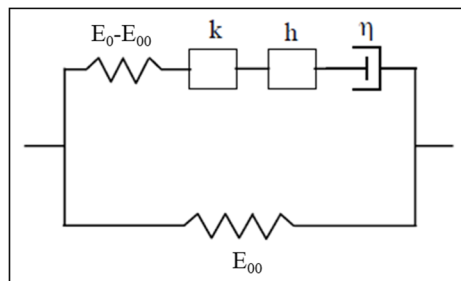


Figure 1.21 Representation of the 2S2P1D model (readapted from Olard & Di Benedetto (2003))

The behaviour of EP bodies is quite identical to that of granular materials (non-cohesive). In the unidirectional case, the law describing the EP bodies correlates the stress increase $\Delta\sigma$ to the strain increase $\Delta\varepsilon$:

$$\Delta\sigma = f(\Delta\varepsilon) \quad (1.16)$$

The function f is composed of the two virgin curves, loading and unloading (Figure 1.23).

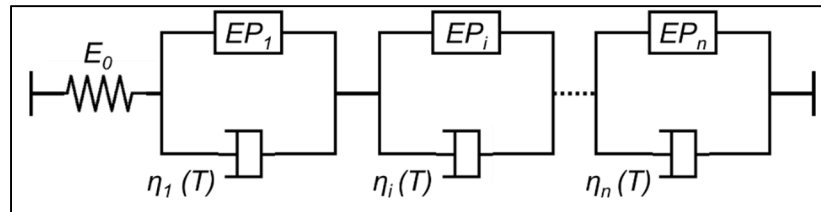


Figure 1.22 Unidirectional representation of the DBN model for bituminous mixtures

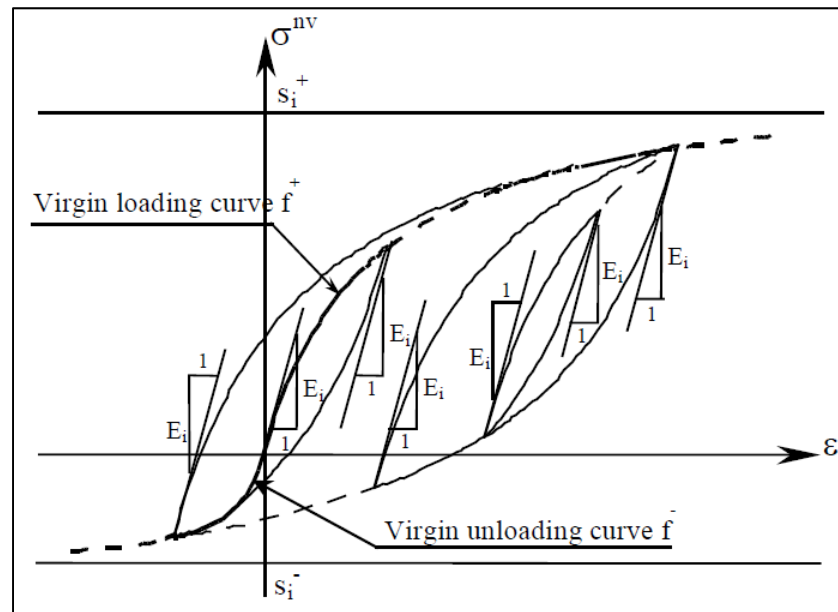


Figure 1.23 Cycling response of the EP bodies (taken from Di Benedetto et al., 2011)

In the small strain domain and for small number of cycles, the material behaviour is considered linear visco-elastic. Hence, the schematic representation corresponds to a Generalized Kelvin-Vöigt (GKV) with additional plastic dissipation in the springs D (Figure 1.24) (Attia, 2020).

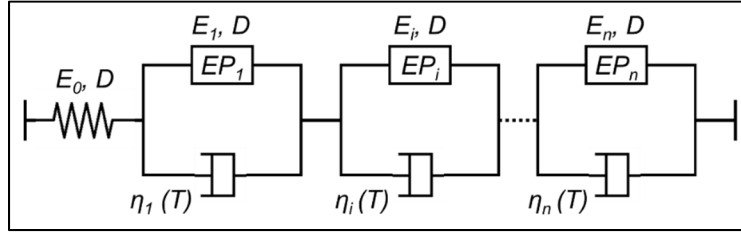


Figure 1.24 Representation of the DBN model for small number of cycles in the small strain domain

When a cyclic loading is applied to a visco-elastic material, the energy dissipated per unit volume during one cycle \mathcal{W}_v is calculated as:

$$\mathcal{W}_v = \pi \varepsilon_0 \sigma_0 \sin \varphi \quad (1.17)$$

where ε_0 is the strain amplitude, σ_0 is the stress amplitude and φ is the phase angle of the complex modulus. When plastic dissipation is added by means of the non-viscous elements, the plastic energy per unit volume dissipated in the EP bodies is:

$$\mathcal{W}_{ep} = 2\pi \varepsilon_0 \sigma_0 D \quad (1.18)$$

where D is the damping ratio. At small strain level, the damping ratio can be considered the same in all the elements of the DBN model, and it can be approximated using an equivalent phase angle φ_{ep} , obtained by Eq. 1.17 and 1.18:

$$\pi \varepsilon_0 \sigma_0 \sin \varphi = 2\pi \varepsilon_0 \sigma_0 D \quad (1.19)$$

$$D = \frac{\sin \varphi_{ep}}{2} \quad (1.20)$$

It is assumed that the damping ratio does not affect the norm of the complex modulus, which can be calculated as for the GKV model:

$$|E^*|_{\text{GKV}} = \left| \frac{1}{E_0} + \sum_{i=1}^n \frac{1}{E_i + i\omega\eta_i} \right|^{-1} \quad (1.21)$$

where E_0 is the stiffness of the spring, E_i and η_i are the elastic modulus and viscosity of each element, respectively. The energies dissipated in the linear dashpot and in the EP bodies can be also expressed as:

$$\mathcal{W}_v = \pi\varepsilon\sigma \cdot \frac{\omega\eta_i}{E_i^2 + (\omega\eta_i)^2} \cdot |E^*| \quad (1.22)$$

$$\mathcal{W}_{\text{ep}} = \pi\varepsilon\sigma \cdot \frac{2 \cdot D \cdot E_i}{E_i^2 + (\omega\eta_i)^2} \cdot |E^*| \quad (1.23)$$

Consequently the expression of the phase angle φ_{DBN} , considering both viscous and non-viscous dissipation, is:

$$\sin(\varphi_{\text{DBN}}) = \frac{\mathcal{W}_v + \mathcal{W}_{\text{ep}}}{\pi\varepsilon\sigma} = \sum_{i=0}^n \left(\frac{\omega\eta_i}{E_i^2 + (\omega\eta_i)^2} + \frac{2 \cdot D \cdot E_i}{E_i^2 + (\omega\eta_i)^2} \right) \cdot |E^*| \quad (1.24)$$

The calibration of the DBN model first requires the calibration of the 2S2P1D on the experimental data. Then, the GKV model is calibrated on the 2S2P1D model by choosing the right number of elements n (Figure 1.25). If necessary, the additional parameter D is used to take into account eventual non-viscous phenomena, by the introduction of the additional phase angle φ_{ep} (Tiouajni et al., 2011).

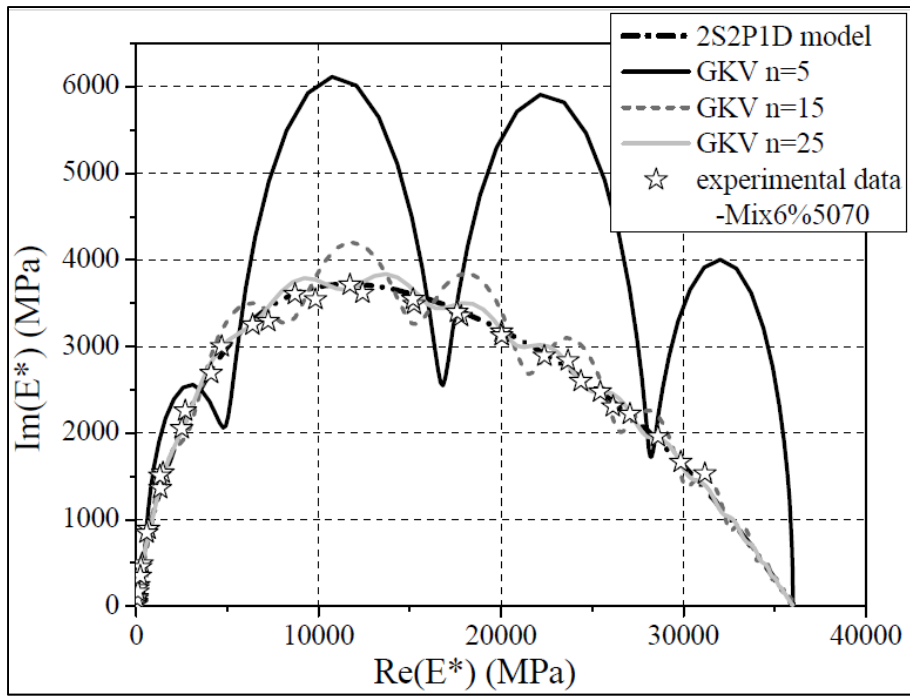


Figure 1.25 Calibration of the GKV model (5, 15, 25 elements) on the Cole-Cole diagram (taken from Tiouajni et al., 2011)

CHAPTER 2

RESEARCH OBJECTIVES AND EXPERIMENTAL PROGRAM

2.1 Research problem

In Quebec, cold recycling techniques are largely employed, thanks to their contribution in terms of economic and environmental sustainability. Many projects are realized following this new path, and scientific researches focused on such materials are increasing considerably in the last years. Nevertheless, the pavement design of rehabilitation and the realization itself are often based on the acquired experience, and not following standard guidelines or scientific principles.

So far, the laboratory simulation of what really happens in the field (and vice versa) is still a complex issue (Serfass et al., 2004). The production of CBTM and the replication of their time-dependent behaviour are tricky topics, which require several hypotheses. The presence of binders highly sensitive to environmental conditions (temperature and relative humidity), such as bitumen emulsion and cement, raises many questions and problematics about what might ensure an adequate cohesion between mastic and aggregate blend, or about the mixture strength, especially at short-term (García et al., 2013). The behaviour of these materials is evolutive and the mechanical properties change with the curing time; for this reason, it is important to design a good material, preventing a permanent lack in the long-term strength and the waste of millions of dollars.

When bitumen emulsion is used in CBTM mixtures, it is important to consider the chemical aspects that characterize the relationship between the binder (bitumen droplets dispersed in water and emulsifier) and the aggregates surface. Currently, bitumen emulsions are present in the market according to a specific standardized classification, which normally indicates their electrochemical charge (positive or negative), the amount of residual bitumen, and their breaking speed, i.e. the speed at which the emulsion coalesces and breaks on a random

aggregate surface (rapid, medium or slow setting). Nevertheless, it is believed that this is not enough to ensure an adequate bond between the emulsion and the aggregate phase. It is reasonable to think that using a single bitumen emulsion (for example cationic) and varying the aggregate source (with about the same charge), this will not lead to the same final product in terms of mechanical properties. The same could be valid adopting one aggregate source in combination with several bitumen emulsions. In the same way, different combinations of bitumen emulsions and aggregate source could vary the workability of the mixture. For this reason, a part of this research will focus to evaluate the influence of different aggregate gradations used, as well as what is the impact of using two different RAP sources.

Another practical problem related to CBTM mixtures is their strong dependence to environmental conditions, which are the main responsible of the curing process (water evaporation, emulsion breaking and cement hydration). It is demonstrated that if the cold recycled layer is produced and compacted at average ambient temperatures above 20°C, it should not experience any kind of structural and mechanical issue in the future, provided that the project is performed accurately (Bocci et al., 2011; Gandi, 2018). In case of cold climates, where average temperatures suitable for CBTM mixtures are limited to few months of the year, the possibility to produce a low performance material is high, because of the strict timelines. The production of such mixes at low temperatures have not been deeply studied yet, hence a part of this research focuses on this aspect, considering workability, short and long-term mechanical properties.

2.2 Objectives

This research aims to investigate three main problematic aspects of the production of CBTM mixtures; thus, the thesis is divided in three main sections:

- Section 1: Study of the influence of the CBTM composition (mineral addition, water content) on the mechanical properties of mixtures. It is introduced in CHAPTER 4 and it is developed as follows:
 - Investigate a valid alternative for Portland cement in CRMs (CHAPTER 5);

- Understand how the water content employed to satisfy compaction requirements affects the mechanical properties of the CRMs (CHAPTER 6).
- Section 2: Study of the effect of RAP aggregate on CBTM properties. It is introduced in CHAPTER 7 and it is developed as follows:
 - Investigate the effect that the aggregate distribution (gradation) of CRMs has on workability and compactability (CHAPTER 8);
 - Study the influence of different RAP sources on the mechanical properties of the CBTM mixtures produced (CHAPTER 9);
 - Evaluate the effect of the RAP source on compactability and LVE properties of CBTM (CHAPTER 10).
- Section 3: Study on the laboratory simulation of the production of CBTM at low temperatures. It is introduced in CHAPTER 11 and it is developed as follows:
 - Studying the effect on the mechanical properties of CBTM produced with two emulsion sources (CHAPTER 12);
 - Evaluating the effect of low production temperatures and emulsion source on the long-term mechanical properties of CBTM mixtures, cured under different conditions (CHAPTER 13 and 14).

It is important to remark that only CBTM mixtures produced with bitumen emulsion are studied in this research.

2.3 Experimental approach

In order to achieve a good level of knowledge regarding the above-mentioned goals of the thesis, several physical and mechanical properties of the investigated CBTM mixtures were considered. This part provides a general overview of the measured properties that are present also in the rest of the thesis. Figure 2.1 shows a summary of the measurements or tests carried out, specifically limited to the chapters containing results.

2.3.1 Physical properties

The analysis of CBTM physical properties is possible through simple protocols and allows at the same time an efficient way to study specific aspects of the material. More exactly, the physical parameters investigated in this thesis are: workability, compactability, water loss and microscope image capturing.

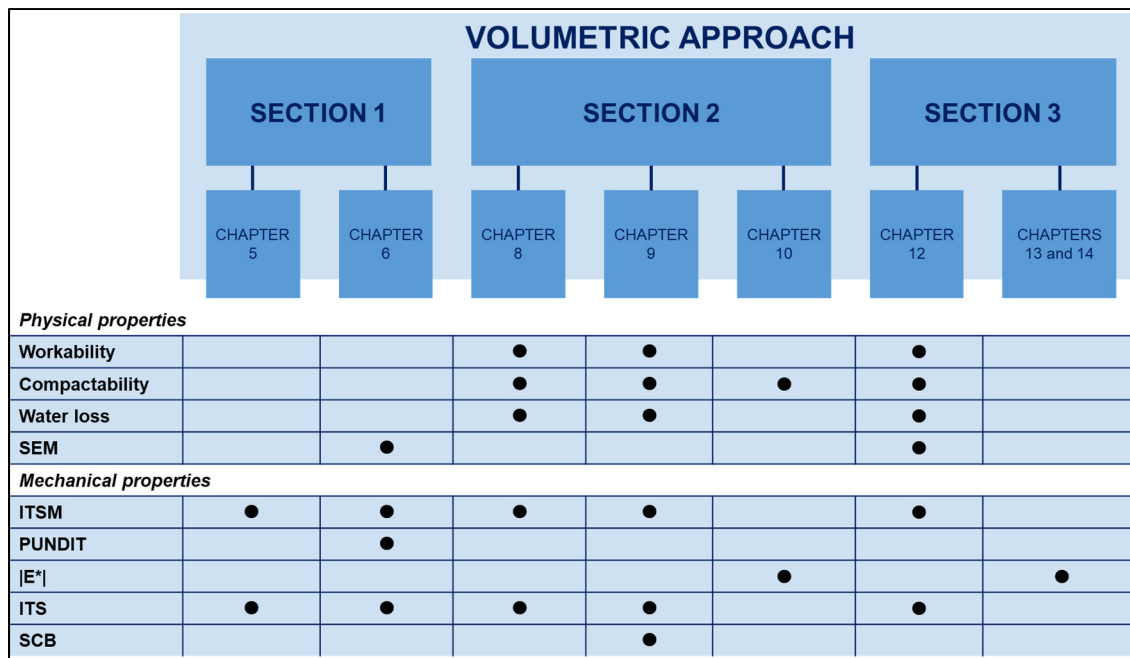


Figure 2.1 Overview of the experimental plan

When bituminous binders are involved, workability and compactability are normally related to the mixture composition and temperature. In this thesis, both characteristics are linked to laboratory compaction by means of a Shear Gyrotory Compactor (SGC). The combination of both properties gives an idea of the compaction effort required to lay down and compact the material. Regarding curing, a practical way to monitor the process in the laboratory is to record the mass loss of the specimen on a regular basis. This approach is totally preventing any damage of the specimen, since it can be performed without touching the material. The mass

loss during the curing period corresponds to the water loss if particular attention is paid to avoid any material loss during compaction and curing.

Image capturing with a Scanning Electron Microscope (SEM) is particularly useful to confirm or disprove results obtained according to other tests. This procedure can be performed on specimen parts obtained after destructive tests or on samples specifically prepared. The analysis with a SEM is possible until a magnitude value of around $\times 10.000$, after which the material starts to burn if not previously treated with a surface protection (Figure 2.2).

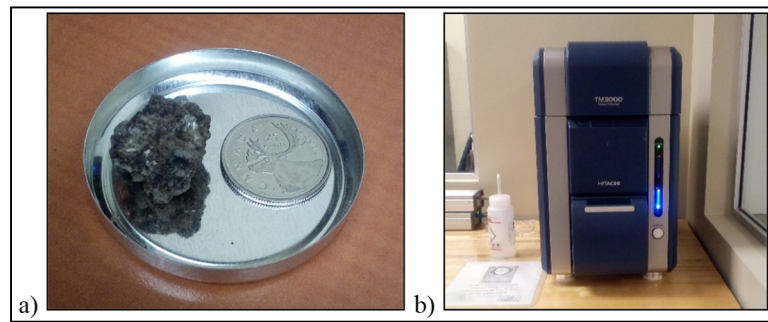


Figure 2.2 a) Example of material sample for SEM; b) SEM device used (Hitachi TM3000)

2.3.2 Mechanical properties

The mechanical characterization of CBTM mixtures is possible through several tests at all deformation levels: small deformation (Young's modulus, dynamic modulus, complex modulus), failure point (tensile strength) and crack propagation. In each of the listed case, a specific test was chosen throughout this work to study and compare the mixtures produced.

The Young modulus (or stiffness modulus) E is evaluated with the Indirect Tensile Stiffness Modulus (ITSM) test (Figure 2.3 a). The test consists in loading a circular specimen along one diameter and measuring the deformation along the transversal diameter. The type of load is impulsive and its amplitude does not cause any damage inside the material structure. The

stiffness modulus E is then calculated at a certain temperature in relation to the applied load and the measured deformation.

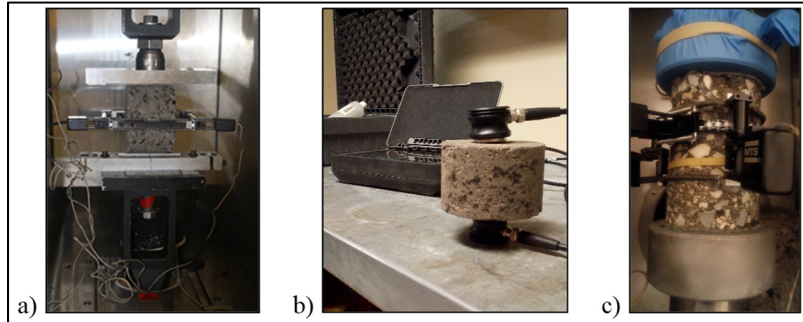


Figure 2.3 a) ITSM testing setup; b) PUNDIT device; c) Complex modulus setup

The dynamic modulus is measured with a Portable Ultrasonic Non-destructive Digital Indicating Tester (PUNDIT) (Figure 2.3 b). With this equipment is possible to propagate compression and shear waves inside the material between two shear transducers. The time employed by the waves to cover the gap between the transducers is used to calculate shear modulus, Poisson ratio and eventually the dynamic modulus.

To investigate the linear viscoelastic (LVE) properties of CBTM mixtures, complex modulus tests were performed at different temperatures and frequencies (Figure 2.3 c). The test consists in applying an haversine load (only compression) at more frequencies and measuring the related axial deformation by means of three extensometers placed on the lateral surface of the specimens 120° apart. The stiffness modulus measured in this manner is temperature and frequency dependent. The results obtained were modelled with the 2S2P1D model and the main parameters were used as a tool to study and compare different materials.

The failure point of bituminous mixtures, and in this case of CBTM, is normally measured by the Indirect Tensile Strength (ITS) test (Figure 2.4 a). The test applies the load at a constant speed rate along one diametral plane of the cylindrical specimen, causing the tensile failure along the transversal diameter. As a result, the correlation between load and vertical

displacement is obtained, even though normally only the force peak value is used as an indicator. The test is normally conducted at room temperature and on both dry and wet conditioned specimens.

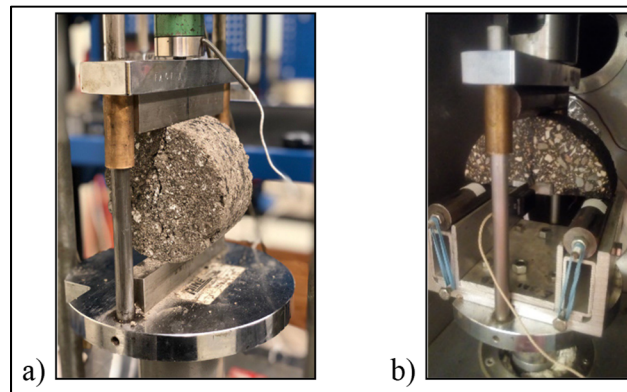


Figure 2.4 a) ITS test setup; b) SCB test setup

The cracking propagation behaviour of CBTM mixtures has been evaluated with the Semi-Circular Bending (SCB) test (Figure 2.4 b). Cylindrical specimens are cut to obtain semi-circular specimens in which a notch is made on the flat surface with precise width and depth. This notch causes the crack initiation and propagation under a constant speed rate load applied on the circular surface. The test can be performed at different temperatures but it is often related to low temperatures cracking behaviour.

In terms of mix design for CBTM mixtures, a volumetric approach has been studied and adopted in every step of the experimental plan. Basically, every component of the mixture (aggregates, cement, bitumen emulsion and water) is characterized by a mass and volume inside the final product. If such properties are well known and the production process is accurately performed, it is possible to estimate with good precision the volumetric properties of the mixture (at the beginning and during curing). This methodology is currently used for HMA mix design, and this research attempts to prove its efficiency also when applied to CBTM. CHAPTER 3 gives the theoretical background and the basic explanation of this concept.

2.4 Materials

For the development of this thesis, several raw materials were used and investigated depending on the goal of each section. In particular, different RAP aggregates, virgin aggregates, cements and bitumen emulsions were involved. Figure 2.5 shows which materials were used to produce specific mixtures in the related thesis chapter. Annex I contains basic characteristics for each of the material listed.

CHAPTER	Mixes name	RAP source	Virgin aggregate	Filler	Cement	Bitumen emulsion
5	M-C	RAP Chambly (CA)		Limestone (CA)	Cement GU (CA)	CSS-1 (CA)
	M-L					
	M-VL					
	M-V					
6	0C_2W	RAP-CBR (IT)	-			CSS-1 (UK)
	0C_4W					
	15C_2W					
	15C_4W					
8	CA_FT	RAP Chambly (CA)	Limestone sand 0/2 (IT)	Limestone (CA)	Cement GU (CA)	CSS-1 (CA)
	CA_HPAC	RAP Chambly (CA)				
	CA_MTQ	RAP St. Isidore (CA)				
	IT_FT	RAP-CBR (IT)		Limestone (IT)	Cement II/B-S (IT)	C60B10 (IT)
	IT_SMA					
	IT_FINE					
9	R1_16	RAP-CBR (IT)	-	Limestone (CA)	Cement GU (CA)	CSS-1 (UK)
	R1_10					
	R2_10	RAP-NCAT (USA)				
10	RAP1	RAP-CBR (IT)	-	Limestone (CA)	Cement GU (CA)	CSS-1 (UK)
	RAP2	RAP-NCAT (USA)				
12	A_T ₁ T ₂ C	RAP-CBR (IT)	-	Limestone (CA)	Cement GU (CA)	CSS-1 (UK)
13	B_T ₁ T ₂ C					C60B10 (IT)
14						

Figure 2.5 Materials employed in the different chapters of the thesis

2.5 Thesis structure

As previously explained, this thesis is divided in three main sections, each one developed in several chapters. A schematic representation is given in Figure 2.6.

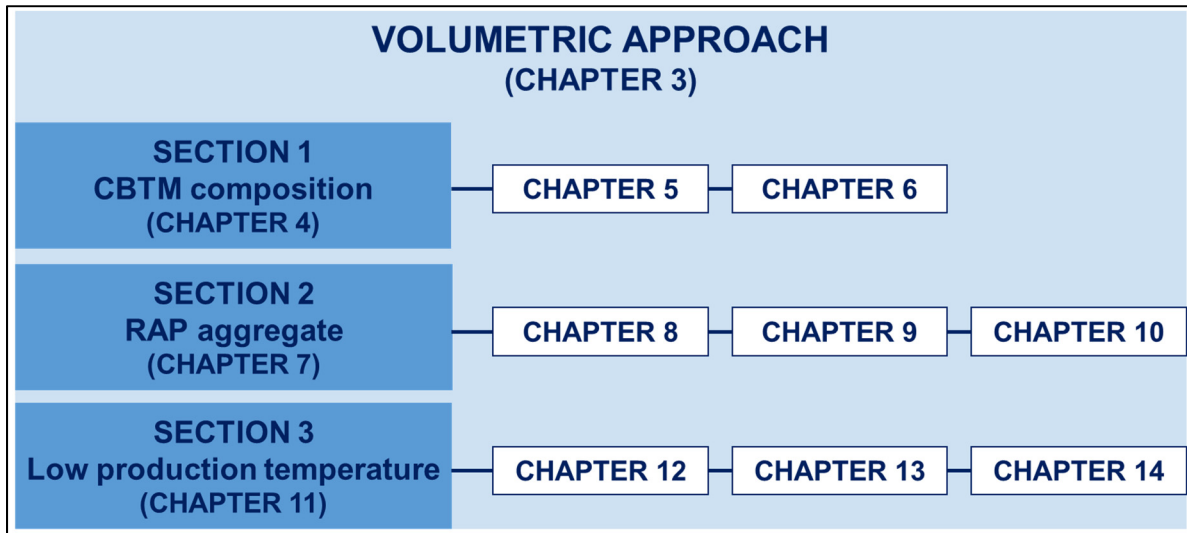


Figure 2.6 Schematic representation of the thesis structure

The following CHAPTER 3 treats the application of the volumetric approach for the CBTM mixtures mix design. This chapter is extremely important for the definition of some parameters that are widely used in every chapter containing the experimental investigation. The following part of the thesis contains experimental results.

CHAPTER 4 introduces Section 1, and collects findings regarding CBTM composition. Two conference papers follow this chapter: “*Recycled Glass Filler In Cold Recycled Materials Treated with Bituminous Emulsion*” (CHAPTER 5) and “*Effect of water and cement content on the mechanical properties of Cold Recycled Mixtures (CRM) with bitumen emulsion*” (CHAPTER 6). The first analyzes different mineral additions to be used in CBTM together with bitumen emulsion, especially looking at the employment of pulverized recycled glass to obtain a 100% recycled material. The second paper treats different water and cement contents

in CBTM mixtures to clarify the best combination of the two components in terms of mechanical properties. The first paper has been presented at the 97th Transportation Research Board (TRB) Annual Meeting in 2018 as a poster, whereas the second is published in the indexed journal *Lecture Notes in Civil Engineering* and presented for the 5th International Symposium on Asphalt Pavement & Environment.

CHAPTER 7 provides a summary of Section 1 and an introduction to Section 2, regarding the effect of RAP aggregate on CBTM mixtures properties. More specifically, three papers are dedicated to this goal: the influence of several aggregate distributions (gradations) (CHAPTER 8) and the effect of two sources of RAP also constituted by different NMAS (CHAPTERS 9 and 10). CHAPTER 8 is a journal paper entitled “*Effect of gradation on volumetric and mechanical properties of cold recycled mixtures (CRM)*” published in *Road Materials and Pavement Design*. This part is the result of a fruitful cooperation between the École de Technologie Supérieure (ÉTS) and the Università Politecnica delle Marche (UNIVPM). In fact, the paper collects data from both universities, which studied the influence of a total of 6 different aggregate distributions on the mechanical properties of CBTM. As a consequence of these results, a fixed distribution was selected and followed in the remaining part of the thesis. CHAPTER 9 deals with the influence of two RAP sources on water loss and mechanical properties of CBTM mixtures. It is important to note that the two RAP sources were characterized by different NMAS, and for this reason one of the two materials was modified to reduce its NMAS. Hence, a total of 3 mixtures were studied. CHAPTER 10 contains results which give further informations about the effect of the RAP source. In this paper, in fact, the analysis is focused on the workability of the mixtures and their rheological properties. CHAPTER 9 is published in the indexed journal *Road Materials and Pavement Design* as a Special Issue of the 8th European Asphalt Technology Association (EATA) conference held in 2019 (title “*Laboratory mechanical characterisation of cold recycled mixtures produced with different RAP sources*”). CHAPTER 10, entitled “*Effect of RAP source on compactability and visco-elastic behaviour of CRM mixtures*”, is submitted to a peer-reviewed scientific journal but currently under review.

CHAPTER 11 provides a summary of Section 2 and an introduction to Section 3, regarding the production at low temperatures of CBTM mixtures. In particular, the production was divided in 4 steps: mixing, transportation and compaction, first curing and second curing. Each steps was characterized by a specific temperature and different combinations were planned setting 5 °C, 25 °C and 40 °C as values. A total of 5 mixtures were produced with one emulsion source, and 2 additional mixtures with a different emulsion source. In CHAPTER 12, physical and mechanical properties of these mixtures were investigated in the short term (after about one month of curing in laboratory). After this part, specimens were stored for a year in two conditions: sealed in wax, to prevent any light and air exposure, and unsealed, to have a long-term cured material. In particular, the first condition simulates the material in-situ when an upper layer (normally HMA) is laid as surface course. The related results are shown in CHAPTERS 13 and 14. In the first, only some results are analyzed, since the section focuses on the introduction of a new methodology proposed for the thermo-rheological modelling of CBTM mixtures. The new approach is then applied to the rest of the mixtures produced and the analysis is contained in CHAPTER 14. CHAPTER 12 is a scientific paper entitled “*Influence of low production temperatures on compactability and mechanical properties of cold recycled mixtures*” published in the journal *Construction and Building Materials*, whereas CHAPTERS 13 and 14 are submitted to peer-reviewed scientific journals but currently under review. CHAPTER 15 provides a collection of the main findings and recommendations regarding the last three papers.

Annex I collects the main properties of all the raw materials used in this thesis (RAP aggregates, virgin aggregates, cements, bitumen emulsions). Annexes III, IV, and V presents three papers related to the contribution given to the Task Group 1 (TG1) on Cold Recycling of the RILEM Technical Committee 264-RAP. In this framework, an Inter-Laboratory Testing Program (ILTP) was launched by the TG leaders Prof. Daniel Perraton and Prof. Alan Carter to investigate different variables characterizing CBTM mixtures, produced with both foamed bitumen and bitumen emulsion. The objectives of the ILTP were:

- Implementing volumetric approach in CBTM mix design;

- Study the influence of two RAP sources discriminated by the Fragmentation Test;
- Evaluate the influence of free-surface drying (FSD) and partially-surface drying (PSD) curing protocols;
- Analyse different laboratory compaction methods (SGC, Marshall hammer, Proctor rammer).

The ILTP was a big opportunity to exchange with 12 laboratories from 10 different countries on the problematics linked to the laboratory production of CBTM and to share a common procedure to enhance reproducibility.

CHAPTER 3

VOLUMETRIC APPROACH FOR CBTM

This chapter deals with the application of the volumetric approach to bituminous materials. In particular, it has been developed to perform volumetric mix design for HMA mixture and it is now widely applied as a standard procedure. Nonetheless, it is possible to apply the same concepts to CRM (and CBTM) materials in order to improve various aspects related to their industrial production such as: optimizing the mix design (avoiding excessive usage of materials), ensuring better mechanical properties, providing a new tool for quality control protocols.

3.1 Overview on the volumetric approach for HMA

Volumetric characteristics are extremely important in terms of mix design and quality control since they significantly influence mechanical performance and durability of the mixtures (Cominsky et al., 1994). The volumetric analysis of HMA considers generally three main parameters that are related to Figure 3.1:

- Air voids content (V_i), that is the air volume expressed as percentage of the bulk volume of the HMA compacted specimen (V_{mb});

$$V_i(\%) = \frac{V_i}{V_{sb} + V_{bit,e} + V_i} \cdot 100\% = \frac{G_{mm} - G_{mb}}{G_{mm}} \cdot 100\% \quad (3.1)$$

- Voids of the mineral aggregate (VMA), that is the porosity of the aggregate skeleton and which is filled by effective bitumen (not considering the amount absorbed by the aggregate) and air. It is also expressed as a percentage of the bulk volume of the compacted specimen (V_{mb});

$$VMA(\%) = 100\% - \frac{G_{mb}P_s(\%)}{G_{sb}} \quad (3.2)$$

- Voids filled with bitumen (VFB), that is the VMA fraction occupied by effective bitumen;

$$VFB(\%) = \frac{VMA(\%) - V_i(\%)}{VMA(\%)} \cdot 100\% \quad (3.3)$$

where M_{sb} is the bulk mass of the aggregates; P_s is the mass percentage of the aggregates; $M_{bit,e}$ is the effective bitumen mass; V_{sb} is the aggregate bulk volume; $V_{bit,e}$ is the effective bitumen volume; V_i is the volume of air voids; V_{mm} is the dry volume (aggregates and effective bitumen), V_{mb} is the bulk volume of the compacted mixture, G_{sb} is the bulk specific gravity of the aggregate, G_{mm} is the maximum specific gravity of the mixture; G_{mb} is the bulk specific gravity of the compacted mixture.

	Mass	Volume			Specific gravity			
Air		V_i						VMA (VFB)
Effective bitumen	$M_{bit,e}$	$V_{bit,e}$						
Absorbed bitumen								
Aggregate	M_{sb} (P_s)	V_{sb}	V_{mm}	V_{mb}	G_{sb}	G_{mm}	G_{mb}	

Figure 3.1 Volumetric composition of a HMA compacted specimens

3.2 Volumetric approach for CBTM mixtures

Grilli et al. (2012, 2016) proposed that the volumetric approach usually used for HMAs can be extended to CBTM mixtures, even if some assumptions and corrections need to be made essentially for the introduction of cement and water in the system.

CBTMs produced with emulsion pass through two completely different states: the initial state, where water plays a key role driving the bitumen into the mixture and acting as a lubricant, and the long-term state, when its volumetric properties can be determined as HMAs.

3.2.1 CBTM composition during compaction

During the compaction process of the CBTM mixtures (initial state—indicated with the subscript “0”), *VMA* are represented by the non-solid part of the mixture, while *VFL* (Voids filled with liquids) are introduced instead of the *VFB*. In fact, *VFL* consider both water and bitumen contents to indicate the level of the *VMA* saturation. Figure 3.2 shows the CBTM composition in the initial state.

	<i>Mass</i>	<i>Volume</i>		<i>Specific gravity</i>		
Air		V_{air}				
Intergranular water	$M_{w,i}$	$V_{w,i}$				VMA^0 V_m^0 (VFL^0)
Residual bitumen	M_{bit} (P_{bit})	V_{bit}				
Absorbed water				V_{mb}^0		
Aggregates	M_{SSD}	V_{SSD}	V_{mm}^0		G_{SSD}	
					G_{mm}^0	
Cement	M_C	V_C			G_C	
					G_{mb}^0	

Figure 3.2 CBTM volumetric composition in the fresh state

In Figure 3.2, M_C is the mass of cement; M_{SSD} is the aggregates mass in saturated surface dried (SSD) condition; M_{bit} is the residual bitumen mass (from bitumen emulsion); $M_{w,i}$ is the mass of intergranular water; V_C is the volume of cement; V_{SSD} is the aggregates volume in SSD condition; V_{bit} is the residual bitumen volume; $V_{w,i}$ is the volume of intergranular water; V_{air} is the volume of air; V_{mm}^0 is the dry volume during compaction (cement, aggregates and residual bitumen); V_{mb}^0 is the bulk volume of the mixture during compaction; G_{SSD} is the SSD specific gravity of the aggregate; G_C is the specific gravity of cement; G_{mm}^0 is the maximum specific gravity of the mixture during compaction; G_{mb}^0 is the bulk specific gravity of the mixture during

compaction; V_m^0 are the voids in the mixture during compaction; VMA^0 are the voids in the mineral aggregate during compaction; VFL^0 are the voids filled with liquids during compaction.

Some observations are necessary at this stage. The cement is initially employed in the mixture as a filler, in his unhydrated form. For this reason, it is not totally considered as an aggregate because its composition (mass M_C and volume V_C) is going to change due to the formation of the hydrates products.

Regarding the bitumen emulsion, it can be considered as a perfect two-phases composite: residual bitumen (M_{bit} , V_{bit}) and water. As a consequence, knowing the bitumen/water ratio of the emulsion used, it is possible to calculate the mass of each component. This step is important because it allows to exclusively consider the bitumen phase as a stand-alone component, even if it is introduced in form of emulsion. Furthermore, the residual bitumen is considered totally effective, meaning that no bitumen absorption occurs in the aggregate permeable voids. This is due to the fact that in cold recycling aggregates are already wet, hence superficial pores are usually saturated with water. In addition, bitumen comes in a solid state (little droplets) and it is reasonable to assume that at room temperature the bitumen does not flow in the permeable voids of the aggregate. In particular cases, when RAP aggregates are used, the RAP binder is not active (for the low production temperatures) and the particles are considered as black rocks.

The water dosage fixed for the mix design is conferred by two parts: water provided from the bitumen emulsion, as already mentioned, and additional water, which is normally added to the mixture to improve workability and compactability of the mixture. These two contributions constitute the total water content of the CBTM mixture. In some cases the aggregates are employed in wet conditions, especially in field applications, and the aggregate moisture should be considered as part of the total water. In other cases, such as in laboratory applications, aggregates are totally dry (oven-dried) and the permeable voids are responsible for water absorption when the mixture is produced. Hence, this amount of water is considered part of

the aggregates volume, which are in SSD condition (M_{SSD} , V_{SSD}). The volume of water present in the mixture that is not absorbed is called intergranular water ($M_{w,i}$, $V_{w,i}$).

With this background, referring to Figure 3.2, the following volumetric parameters during compaction can be defined: Voids in the mixture (V_m^0), Voids in the mineral aggregate (VMA^0) and Voids filled with Liquids (VFL^0).

$$V_m^0(\%) = \frac{V_{air} + V_{W,i}}{V_C + V_{SSD} + V_{bit} + V_{air} + V_{W,i}} \cdot 100\% \quad (3.4)$$

$$= \frac{G_{mm}^0 - G_{mb}^0}{G_{mm}^0} \cdot 100\%$$

$$VMA^0(\%) = V_m^0(\%) + \frac{G_{mb}^0 \cdot P_{bit}(\%)}{G_{bit}} \quad (3.5)$$

$$VFL^0(\%) = \frac{V_{W,i} + V_{bit}}{V_{bit} + V_{air} + V_{W,i}} \cdot 100\% \quad (3.6)$$

Specific gravities G_{mm}^0 and G_{mb}^0 in the initial state are defined as follows:

$$G_{mb}^0 = \frac{M_{SSD} + M_C + M_{bit}}{\frac{M_{SSD}}{G_{SSD}} + \frac{M_C}{G_C} + \frac{M_{bit}}{G_{bit}} + \frac{M_{W,i}}{G_W} + V_{air}} = \frac{M_{SSD} + M_C + M_{bit}}{V_{mb}^0} \quad (3.7)$$

$$G_{mm}^0 = \frac{M_{SSD} + M_C + M_{bit}}{\frac{M_{SSD}}{G_{SSD}} + \frac{M_C}{G_C} + \frac{M_{bit}}{G_{bit}}} = \frac{M_{SSD} + M_C + M_{bit}}{V_{mm}^0} \quad (3.8)$$

where all the notations are previously explained.

VFL^0 is a particularly important parameter, since it indicates the level of saturation of the VMA^0 . As long as VFL^0 is less than 100%, the mixture contains air voids and hence is unsaturated. However, when VFL^0 reaches or exceeds 100%, water is squeezed out of the mixture together with parts of fine aggregates and bitumen droplets, which will change significantly the mixture composition. In particular it has been shown that CBTMs produced with bitumen emulsion having VFL^0 above 90% generally imply a visible loss of liquids and fines from the compaction mould (Grilli et al., 2012). However, parameters V_m^0 , VMA^0 and

VFL^0 as defined above are purely theoretical. When a CBTM mixture is compacted, the device used to carry out the compaction allows to know such values after or during compaction. For example, employing an SGC, it is possible to measure the volumetric parameters V_m^0 , VMA^0 and VFL^0 at each gyration (Figure 3.3), thanks to the constant registration of the specimen height (volume). On the contrary, if other compaction techniques such as Marshall hammer or Proctor rammer are employed, it is possible to know the bulk volume of the compacted mixture G_{mb}^0 and all the volumetric properties only after compaction.

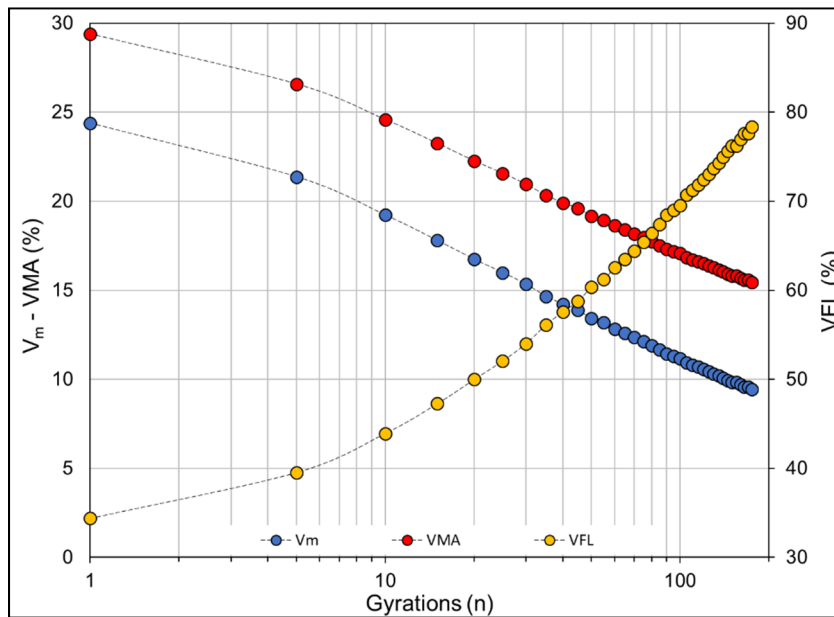


Figure 3.3 Example of compaction curves of CBTM from SGC

3.2.2 CBTM composition at the long-term state

The volumetric concepts explained in the previous section are useful when a mix design for CBTM is performed and valid at the initial stage of CBTM mixtures. However, the material will change its volumetric properties during curing, until a long-term condition is reached (Figure 3.4). From a theoretical point of view, volumetric properties of the compacted mixture should not change from the initial state to the long-term state, since intergranular water volume

is considered as a void in the mixture. However, when cement hydration takes place it affects volumetric properties according to the degree of hydration. Hence, the superscript α appears in Figure 3.4, to identify those volumetric properties which are going to change according to the cement hydration. In particular, in the figure, M_{HC}^α is the mass of hydrated cement; M_{SSD} is the aggregates mass considered in SSD condition because of the entrapped water; M_{bit} is the residual bitumen mass (from bitumen emulsion); V_{HC}^α is the volume of hydrated cement; V_{SSD} is the aggregates volume in SSD condition; V_{bit} is the residual bitumen volume; V_{air} is the volume of air; V_{mm}^α is the dry volume related to cement hydration; V_{mb}^α is the bulk volume of the mixture related to cement hydration; G_{SSD} is the SSD specific gravity of the aggregate; G_{HC} is the specific gravity of hydrated cement; G_{mm}^α is the maximum specific gravity of the mixture related to cement hydration; G_{mb}^α is the bulk specific gravity of the mixture related to cement hydration; V_m^α are the voids in the mixture related to cement hydration; VMA^α are the voids in the mineral aggregate related to cement hydration; VFL^α are the voids filled with liquids related to cement hydration.

	<i>Mass</i>	<i>Volume</i>		<i>Specific gravity</i>		
Air		V_{air}				VMA^α V_m^α
Residual bitumen	M_{bit}	V_{bit}				(VFL^α)
Entrapped water				V_{mb}^α		
Aggregates	M_{SSD}	V_{SSD}	V_{mm}^α	G_{SSD}	G_{mm}^α	
Hydrated cement	M_{HC}^α	V_{HC}^α		G_{HC}		

Figure 3.4 CBTM volumetric composition in the long-term state (no intergranular water)

The major part of the water will evaporate from the connected pores structure leaving space to the air. In case that some water particles are dispersed in the mastic or at the interface between

mastic and aggregates (absorbed water), it is highly probable that such amount of water will never evaporate (entrapped water). At the same time, a part of the intergranular water will react with cement to form the C-S-H products. The C-S-H products are characterized by a solid structure (gel solid) and gel water. Taking into account the considerations made in chapter 1.1.5 it is thus possible to define the expression for M_{HC}^α and V_{HC}^α . The mass of hydrated cement M_{HC}^α is simply the mass of cement M_C plus the mass of water reacted as a function of α :

$$M_{HC}^\alpha = M_C + M_C \cdot 0.42 \cdot \alpha \quad (3.9)$$

It needs to be highlighted that if $\alpha < 1$ and the hydration reaction is incomplete, the remaining capillary water is considered as a part of the intergranular water of the CBTM mixture, hence it will evaporate.

The volume of hydrated cement V_{HC}^α is considered as the volume of only the solid part of the cement paste, and the capillary pores are not considered in this volume but are included in the volume of air in the mixture. Therefore, it is composed of the volume of cement unhydrated, the volume of gel water and the volume of gel solid:

$$V_{HC}^\alpha = V_{UnC} + V_{gw} + V_{gs} \quad (3.10)$$

Using Equations (1.3) — (1.5):

$$V_{HC}^\alpha = V_C \cdot (1 - \alpha) + 2.12 \cdot V_C \cdot \alpha \quad (3.11)$$

$$V_{HC}^\alpha = \frac{M_C}{G_C} \cdot (1 + 1.12 \cdot \alpha) \quad (3.12)$$

With such considerations, different equations should be provided for the CBTM mixture volumetric properties in function of hydration degree α :

$$\begin{aligned} G_{mb}^\alpha &= \frac{M_{SSD} + M_{bit} + M_{HC}^\alpha}{\frac{M_{SSD}}{V_{SSD}} + \frac{M_{bit}}{G_{bit}} + \frac{M_C}{G_C} + \frac{M_{W,i}}{G_{W,i}} + V_{air}} = \frac{M_{SSD} + M_{bit} + M_{HC}^\alpha}{V_{mb}^\alpha} \quad (3.13) \\ &= \frac{M_{SSD} + M_{bit} + M_{HC}^\alpha}{V_{mb}^0} \end{aligned}$$

$$G_{mm}^{\alpha} = \frac{M_{SSD} + M_{bit} + M_{HC}^{\alpha}}{\frac{M_{SSD}}{V_{SSD}} + \frac{M_{bit}}{G_{bit}} + \frac{M_C}{G_C} \cdot (1 + 1.12\alpha)} = \frac{M_{SSD} + M_{bit} + M_{HC}^{\alpha}}{V_{mm}^{\alpha}} \quad (3.14)$$

The term representing the volume in Eq. (3.13) is assumed same as the one in Eq. (3.7), $V_{mb}^0 = V_{mb}^{\alpha}$. This assumption is always valid also in case of cement hydration: even though its volume increases the air voids decreases, but the bulk volume does not change.

Figure 3.5 shows the trend of the last two equations as a function of the cement hydration degree. It was applied to a CBTM mixture with initial $V_m^0 = V_m^{\alpha} = 14.7\%$ and 1.5% of cement by dry aggregates mass. It is observed that G_{mm}^{α} tends to decrease due to the increase in volume of cement, whereas G_{mb}^{α} tends to increase because of the mass of water entrapped by the hydration reaction (while the bulk volume does not change). In general, the air voids content in the CBTM mixture tends to decrease proportionally with the increase of the cement hydration degree. This is explained by the fact that the increase in volume of cement is always higher than the capillary voids created, regardless the value of α . Hence, if at the moment of production a certain V_m^0 value is target, such value could reduce up to around 7% if cement completely hydrates.

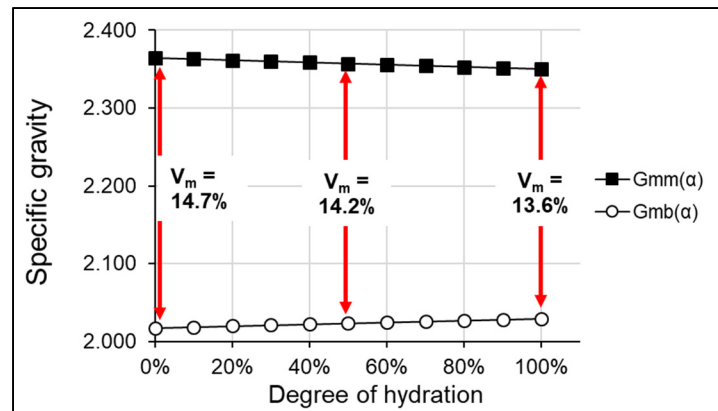


Figure 3.5 Effect of hydration degree on CBTM volumetric properties

3.3 Practical validation of the volumetric approach

In this section, the validation of the volumetric approach is provided with the help of experimental tests. In particular, the maximum dry specific gravity is initially determined in a theoretical way (considering SSD and apparent specific gravity of the aggregates), and verified afterwards with the laboratory measurement of the same parameter. Regarding the validation of the bulk specific gravity value G_{mb} , it is practically complicated to perform laboratory measurements, since the test is carried out in water and an excessive particle loss would occur during the manipulation.

The CBTM mixture considered is composed by RAP and filler as aggregates, in proportion of 94% and 6% by mass, respectively. A cement dosage of 1.5% by aggregate mass is added as co-binder, together with 3.0% of residual bitumen by aggregate mass (5.0% of bitumen emulsion). Table 3.1 lists the loose mixture composition for an aggregate mass of 1024.6 g in SSD condition. According to such composition, $G_{mm}^{SSD} = \frac{1070.7}{452.9} = 2.364$.

Table 3.1 CBTM loose mixture composition (SSD condition)

Component	Mass (g)		Density (g/cm ³)		Volume (cm ³)	
RAP	M_{SSD}	963.1	G_{SSD}	2.441	V_{SSD}	394.6
Filler		61.5	G_{sb}	2.650		23.2
Cement	M_C	15.4	G_C	3.150	V_C	4.9
Bitumen	M_{bit}	30.7	G_{bit}	1.015	V_{bit}	30.2
Total	1070.7				452.9	

In order to validate this value, the same mixture was prepared in lab, considering also the intergranular water to allow a good aggregate coating by the bitumen and to simulate the actual CBTM mixture. After mixing, the material was spread on a pan on a thin layer with thickness of an aggregate particle and placed in an environmental chamber at 40 °C for 24 hours to dry. The G_{mm}^{pyc} was then measured according to the LC 26–045 procedure on three samples,

obtaining the results in Table 3.2. Such measurements give an average $G_{mm}^{pyc} = 2.412$. The higher value obtained with the experimental measurement could be explained by the fact that the aggregate component is not in SSD condition, but it is totally dry. If the calculations for the theoretical G_{mm} are repeated considering the aggregate apparent specific gravity (G_{app}) instead of the SSD condition, a value of $G_{mm}^{app} = 2.399$ is obtained (Table 3.3).

Table 3.2 CBTM loose mixture G_{mm}^{pyc} measurements

Sample	Dry mass (g) A	Mass of pycnometer and water (g) D	Mass of pycnometer, material and water (g) E	$G_{mm}^{pyc} = \frac{A}{A + D - E}$
#1	1059.5	5658.9	6279.3	2.413
#2	1012.8	5663.3	6255.8	2.410
#3	1107.8	5664.2	6313.2	2.415

Table 3.3 CBTM loose mixture composition (apparent specific gravity)

Component	Mass (g)		Density (g/cm ³)		Volume (cm ³)	
RAP	M_{app}	963.1	G_{app}	2.482	V_{app}	388.0
Filler		61.5	G_{app}	2.650		23.2
Cement	M_c	15.4	G_c	3.150	V_c	4.9
Bitumen	M_{bit}	30.7	G_{bit}	1.015	V_{bit}	30.2
Total	1070.7				446.3	

Such value is much closer to the result obtained with the experimental measurements. Hence, it is reasonable to assume that the definition of the G_{mm} by means of a pycnometer does not consider the aggregate in SSD conditions, meaning that the aggregate permeable voids are considered as voids in the mixture. Nevertheless, what happens in reality can be different. Aggregates are used in the CBTM mixtures already in SSD conditions (moist aggregates), and then coated by a mastic composed of cement and bitumen emulsion. During curing, it is

difficult to assess if the absorption water will evaporate or not, but it will most likely be entrapped in the mastic. Consequently, the G_{mm}^{SSD} could give the more realistic value of the maximum specific gravity for a CBTM mixture, even though the volumetric approach can be validated considering G_{mm}^{pyc} and G_{mm}^{app} .

From this, it is possible to conclude that the volumetric approach can be applied to CBTM mixtures, if particular attention is paid at the moment of production, especially in terms of components dosage and compaction processes. Initial material characterization is also important.

CHAPTER 4

SECTION 1: EVALUATION OF CEMENT-BITUMEN TREATED MATERIALS COMPOSITION

One important aspect of CBTM mixtures is the limited environmental and economic impact. Despite the mixtures in this thesis are almost totally composed of RAP and produced at ambient temperature, a further improvement could be achieved by reducing as much as possible the Portland cement dosage with an alternative recycled mineral addition. In CHAPTER 5, recycled glass powder is employed, because of its high availability and application for concrete production in Québec.

Moreover, the role of water in CBTM mixtures is often not considered when evaluating the mechanical properties, and it is only linked to the density of the mixture. It is mainly employed to improve aggregate bitumen coating and to obtain a workable mix in order to reduce the compaction effort. A part of the water is reacting with mineral additions according to the hydration degree (if it is the case), another part will evaporate, whereas a small part will still be in the mixture. The water dosage in CBTM mixtures with bitumen emulsion should be considered in two limits: the lower limit, represented by the water contained in the emulsion (which is directly related to the residual bitumen content), and the higher limit, represented by the maximum saturation of the air voids in the mixture. Beyond the higher limit, expulsion of water bitumen droplets and fine particles occurs if the compaction energy and the water dosage are not balanced. In CHAPTER 6, these two limits are investigated, keeping similar air voids content in the mixtures studied.

CHAPTER 5

RECYCLED GLASS FILLER IN COLD RECYCLED MATERIALS TREATED WITH BITUMINOUS EMULSION

Simone Raschia^a, Saeed Badeli^a, Alan Carter^a, Andrea Graziani^b, Daniel Perraton^a

^a Construction Engineering department, École de technologie supérieure (ÉTS) 1100, Notre-Dame Street West, Montreal, Canada

^b Department of Civil and Building Engineering, and Architecture, Università Politecnica delle Marche, Via Brecce Bianche, 60131 Ancona, Italy

Paper presented at the poster session of the 97th Transportation Research Board Annual meeting in 2018

5.1 Abstract

Cold recycling techniques in road engineering had a wide success in last decades, since they allow the rehabilitation of pavement structures at reduced cost while considerably reducing the environmental footprint. Such techniques can be employed with up to 100% of the old pavement, although recent studies have assessed that the moderate use of other binding agents, such as cement, in the final mixture is fundamental to confer acceptable cohesion and rigidity in the early stage. This study is on the inclusion of an alternative material in the mixture, instead of cement, such as micronized recycled glass.

The research involved four different mixtures, in order to well understand the impact of the micronized glass in the mixture performance. Consequently, mixtures were respectively produced with cement, lime, lime plus glass powder, and glass powder. After a curing process of 3 days, an investigation of resilient modulus and mechanical performance in wet and dry conditions was carried out.

Results showed that mixes stabilized with glass powder rather than hydraulic binders do not reach comparable performance level, because of the poor reactivity of the silica with the system bitumen/water. On the other hand, if recycled glass is combined with lime, an improved material is obtained, if compared to the mix stabilized with only lime; this can be explained by the reaction between silica and hydroxide calcium, that results in something similar to cement composition. On a side, the 3-days curing protocol resulted in an incomplete curing of the material, highlighting the fundamental importance of this aspect.

5.2 Introduction

Cold recycling techniques are a reliable manner to preserve the consumption of construction materials, to reduce maintenance and rehabilitation costs as well as environmental emissions during construction process (ARRA, 2001; Stroup-Gardiner, 2011).

In Cold Recycling (CR) processes, reclaimed asphalt pavement (RAP) coming from the old pavement is re-used with no addition of heat, with the purpose to obtain a Cold Recycled Mixture (CRM). The binding action in this kind of mixes is ensured by the asphalt, in form of bitumen emulsion or foamed bitumen, with the involvement of Portland cement. In this way, it is possible to obtain acceptable stiffness, strength and durability. Good workability and compaction are ensured by the presence of water in the mix (Grilli et al., 2012).

Cold In-place Recycling (CIR) is characterized by all production activities (milling, mixing and compaction) performed directly in the field, leading to a lower control of the employed materials and of the process quality. Nevertheless, these aspects are balanced by higher economic benefits and shorter production times. In this manner, binder or base layers are usually built.

CIR with bitumen emulsions starts to develop strength as the emulsion in the mixture begins to break, turning from brown to black. When asphalt emulsions or emulsified recycling additives are used, this can take from 30 minutes to 2 hours, depending on the characteristics

of the asphalt emulsion, thickness of the CR mix, and environmental conditions. The compacted CIR mixture must be adequately cured before a wearing surface is placed. The rate of curing is quite variable and depends on several factors, including environmental conditions and drainage, and moisture characteristics of the mix. Typical curing periods are several days to 2 weeks, depending on the above-mentioned factors, and the recycling additive or modifiers used. Moreover, it is possible for the mixes to follow an accelerated curing, which allows the achievement of the same final mechanical properties with shorter time (Bocci et al., 2011).

As already mentioned, the employment of cement in presence of bitumen emulsion allows a remarkable development of initial stiffness, and, at the same time, it reduces the water susceptibility, since it acts as a dewatering agent. Small amounts of ordinary cement do not create cementitious matrix with other materials and the final product has an asphalt-like behavior (more ductile) (Grilli et al., 2012).

It is important to note that not all filler reacts with the binder; some fillers are active while others are simply mineral filler in the gradation. According to the FHWA (Kandhal & Mallick, 1998), the use of lime in recycled materials helps to reduce water damage and increases the tensile and compressive strength of the materials; furthermore, studies about lime kiln dust and hydrated lime showed that such materials can be definitely used in cold recycling process in order to achieve results similar to those obtained with cement (Lachance et al., 2012).

The use of cement as binding agent in CRMs can considerably improve bitumen emulsion mixtures. Different authors have shown the cementitious binders resulted in increased stiffness of the mixture: this effect is basically due to the emulsion setting and the hydration of cement (Brown et al., 2000; Niazi et al., 2009; Oruc et al., 2007).

Commonly, cement is composed mainly of calcium oxide (CaO), silica (SiO₂), aluminum oxide (Al₂O₃) and ferrous oxide (Fe₂O₃), but the composition is usually described as a mix of C₃S, C₂S, C₃A, and C₄AF (Pigeon, 1981).

5.3 Objectives

The aim of this study is to investigate a valid alternative for cement presence in CRMs, in order to obtain a final mixture even more economical and environmentally sustainable. For this purpose, several mixtures are studied, to compare effects between cement and lime (hydrated lime – $\text{Ca}(\text{OH})_2$), or by the combination of lime and micronized glass (silica – SiO_2). The rationale behind the combination of lime and micronized glass is that this combination should result in a pozzolanic reaction similar to the one we have with cement. Moreover, mixtures with only silica is produced to understand the chemical and mechanical behavior in presence of bitumen emulsion (water and bitumen). As a consequence, a new totally sustainable material could be obtained, since the production micronized glass is relatively simple, and requires less energy than the production of cement.

5.4 Materials

5.4.1 RAP

The reclaimed asphalt pavement (RAP) has been sampled from a plant stockpile in Montreal Area (Canada). The RAP has been characterized in terms of density, gradation and absorption. Apparent density was evaluated as 2.577 g/cm^3 and the water absorption WA24 as 1% (EN 1097-6). Also, the asphalt content of the RAP was established at 6.1% with an ignition oven. In accordance with (EN 13108-8), the RAP used is classified as 14 RA 0/10. The target aggregate gradation is the maximum density Fuller-Thompson curve and, to ensure similar values, the initial RAP gradation (used at 80%) was divided in the 0/5 and 5/10 fractions, employed at 10% each (Figure 5.1).

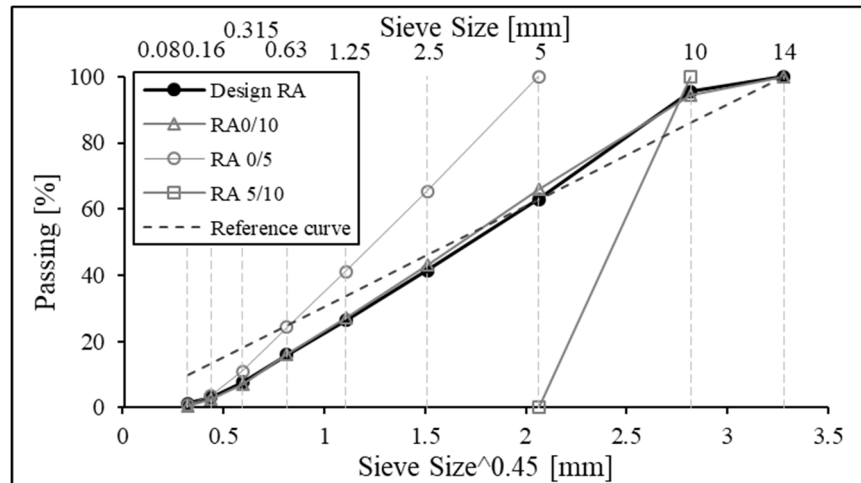


Figure 5.1 Gradation of the design mix compared to the reference curve

5.4.2 Bituminous emulsion and active fillers

The emulsion employed is a cationic slow setting CSS1 emulsion which contains 60% bitumen. This emulsion (Table 5.1) has a slow setting behavior and acts as a lubricant during compaction phase. Its special formulation was designed to mix high fine contents; therefore, long workability times and stability can be achieved. The dosage of the binding agents (bitumen from the emulsion) is the same for all mixes (2% of residual bitumen), and the dosage of the stabilizing agent (active filler) is set at 1% for all mixes (Table 5.2).

Table 5.1 Characteristics of the bituminous emulsion

Emulsion characteristic	Standard	Value
Retained on the 850 μm sieve (% mass)	ASTM D6933	0.01
Storage stability at 24h (%)	ASTM D6930	0.10
Viscosity Saybolt-Furol at 25°C (sec)	ASTM D7496	28.1
Distillation residue at 260°C (%)	ASTM D6997	62.8
Penetration, 25°C, 100g, 5s (0.1mm)	ASTM D5	170
Particles charge	-	POSITIVE

Table 5.2 Main physical properties of the fillers used for the experimental program

Materials	Absorption (%)	Particle density (g/cm ³)	Particle maximum size
Cement	0	3.015	80 μm
Hydrated lime	0	2.240	80 μm
Micronized glass	0	2.560	4 μm

5.4.3 Mix design

Stabilizing agents used and compared in all the mixes are cement, hydrated lime and micronized glass. The dosage of the binding agents in the mixtures is given with respect to the dry aggregate weight in Table 5.3. The free water content shown in Table 5.3, is the total water in the mix that is not absorbed by the solid particles.

Table 5.3 Main physical properties of the fillers used for the experimental program

	Mix with cement	Mix with hydrated lime	Mix with hydrated lime and glass	Mix with glass
Aggregate blend	M-C	M-L	M-VL	M-V
RAP 0/10 (%)	80	80	80	80
RAP 0/5 (%)	10	10	10	10
RAP 5/10 (%)	10	10	10	10
Binding agents				
Cement, C (%)	1.0	-	-	-
Hydrated lime, L (%)	-	1.0	0.5	-
Micronized glass, V (%)	-	-	0.5	1.0
Residual bitumen, B _R (%)	2.0	2.0	2.0	2.0
Free water (%)	2.0	2.0	2.0	2.0

The total water content optimization is based on the volumetric characteristics of the compacted specimen of CRM produced with bituminous emulsion. The procedure was adapted from that currently adopted for the determination of void characteristics of bituminous specimens. In this case, the following parameters are evaluated:

- Voids in the mixture V_i , which designates the percentage of total mixture volume that is occupied by air and free water (water not absorbed by the aggregate);
- Voids in the aggregate V_A , which designates the percentage of total mixture that is occupied by air, free water and fresh bitumen;
- Voids filled with liquids V_{FL} , which designates the percentage of V_A that is occupied by water and fresh bitumen.

V_i represents the volume of the non-structural part of the specimen and is evaluated as:

$$V_i = \frac{G_{mm} - G_{mb}}{G_{mm}} \cdot 100 \quad (5.1)$$

Where G_{mm} is the maximum specific gravity of the loose mixture whereas G_{mb} is the dry specific gravity of the compacted mixture (i.e. the ratio between the total mass of solids to the total volume of the mixture). In this case, even if, during compaction, the emulsion is not yet broken, residual bitumen should be considered as a stand-alone material, as it is going to be after the emulsion breaking. G_{mm} is calculated considering only aggregates, cement and bitumen (not including water) while G_{mb} is calculated together with the height data recorded by the SGC.

Voids filled with liquids V_{FL} are evaluated as follows:

$$V_{FL} = \frac{V_{WF} + V_{B,R}}{V_A} \cdot 100 \quad (5.2)$$

Where V_{WF} is the volume occupied by the free water (not adsorbed water) and $V_{B,R}$ is the volume occupied by the emulsion residual bitumen. V_A indicates the voids in the aggregate mixture (i.e. the ratio between the volume of air, free water and fresh bitumen to the total

volume of the mixture). Additional details on the calculation procedures are reported in (Grilli et al., 2016; Grilli et al., 2012).

The specimen used in the mix design was composed by the same blend for M-C, that means stabilized with 1% of cement and 3.33% of bitumen emulsion (which results in 2% residual bitumen since the emulsion contains 60% of bitumen). More specimens were compacted by means of SGC (protocol previously illustrated) at 2% and 3% of free water content up to 180 gyrations. Figure 5.2 reports the average compaction curves obtained for each water content in terms of V_i and VFL as functions of number of gyrations, on a logarithmic scale.

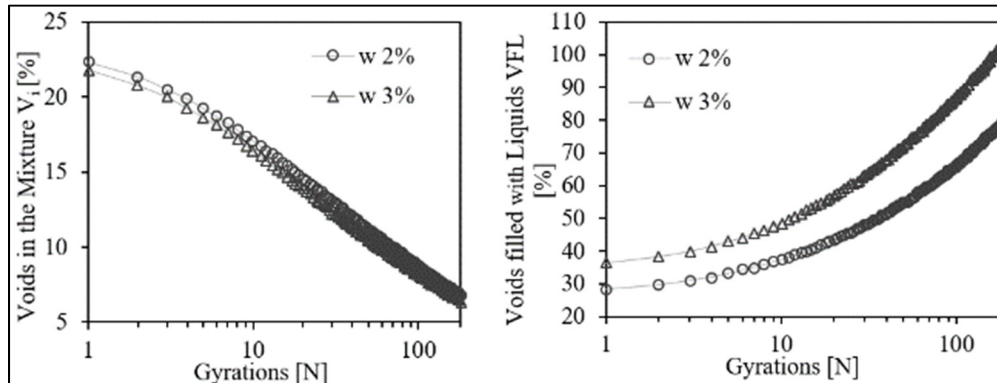


Figure 5.2 Influence of water content on the compactability of CRM:
a) Voids in the mixture V_i ; b) Voids filled with Liquids (VFL)

The first graph shows how voids in the mixture, V_i , decrease when number of gyrations increases. It can be noticed that the increase of water content leads to a low difference in the final value of air voids between the two mixes. This can be explained by the VFL trend: the second graph indicates that during compaction water progressively fills the voids volume available. VFL computed with Eq. (4.2) is representative of the degree of saturation, it means that the value of 100% represents the maximum saturation rate achievable by the mixture; continuing with compaction could lead to squeezing water out of the specimen from the bottom and the top of the mould. This phenomenon was actually observed at the end of the compaction process regarding the mixture with 3% of free water, which reached a VFL level of 103%. The

small amount of squeezed material caused the lower air voids content. Similar results have been observed in previous experimental studies carried out on both bitumen emulsion (Graziani et al., 2016; Grilli et al., 2012) and foamed bitumen mixes.

In case VFL exceeds 90%, it generally implies a visible loss of liquids and fines (as well as bitumen particles). In this case, the final composition of the compacted specimen can be significantly different from the initial design composition. In the present study, according to the results obtained and considering the limit of $VFL < 90\%$, a value of free water of 2% is selected, along with a compaction energy of $N = 180$.

In order to facilitate the control of the water content, oven-dried aggregates were employed. The drying temperature was $40^{\circ}\text{C} \pm 2^{\circ}\text{C}$. The total water content (w_{tot}) of each mixture is composed by the emulsion water content (w_{emu}) and additional water (w_{add}), which has been added in two steps. The first part, corresponding, to the absorption water, was added to the dry aggregates the day before mixing. The wet mixture was sealed and stored for 24h in a plastic bag to reach a homogeneous moisture condition and to allow a complete absorption by the aggregates. Subsequently, the mix was thoroughly blended, gradually adding the respective active filler, the remaining part of the additional water and the emulsion. Samples were mixed manually at room temperature for at least one minute for each addition step, the time required to ensure a good particle coating.

Immediately after mixing, specimens were compacted with a Superpave gyratory compactor (SGC) following this protocol: 100mm diameter mold, constant pressure of 600 kPa, gyration rate of 30 rpm and angle of inclination of 1.25° . After compaction, specimens were stable enough to allow demolding. At this point, a curing protocol at $38^{\circ}\text{C} \pm 2^{\circ}\text{C}$ and 60% of relative humidity (LC 26-002) was applied for 3 days to all produced mixtures.

5.5 Test equipment and procedures

5.5.1 Indirect Tensile Strength (ITS) Test

The indirect tensile strength (ITS) was determined by using the standard ASTM D 6931. Tensile characteristics of the mixes were measured by loading the cylindrical specimens with a compressive load along a vertical diametric plane at a constant rate (Figure 5.3).

In this test, tensile failure occurs in the specimen rather than a compressive failure. A constant tensile stress perpendicular to the diametrical plane was developed by the loading configuration and ultimately causing the specimen to fail by the creation of the crack which eventually split the specimen along the vertical diameter. This test was performed at room temperature (25 °C) with a loading rate of 51mm/minute. The strength of the tested material is calculated by using the Eq. (4.3).



Figure 5.3 ITS device and specimen

$$S_t = \frac{2000 \cdot P}{\pi \cdot t \cdot D} \quad (5.3)$$

Where S_t is the tensile strength of the mix (kPa), P describes maximum load, (N), t is specimen height immediately before the test (mm), and D is the specimen diameter (mm). 16 specimens were tested for ITS (2 wet and 2 dry each mixture), and the air voids of the tested specimens were at $7.4 \pm 0.4\%$.

5.5.2 Indirect tensile stiffness modulus (ITSM) test

To measure the stiffness of the mixes, an indirect tensile stiffness modulus (ITSM) test was performed with an MTS device based on the standard EN 12697-26 (Annex C). The stiffness modulus is considered as one of the most important performance characteristics of the pavement structures. Indirect tensile stiffness modulus test on cylindrical specimens gives information on the viscoelastic behavior of asphalt mixes. The cold mixes in this study have similar composition and volumetric characteristics as hot mixes. This made it possible to exclusively focus on the influence of the several additives (especially recycled glass) on the mix properties.

ITSM test measured the stiffness modulus by a series of repeated application of vertical load pulses. The tests are performed in strain control mode with a precise recovery time. According to the standard, the average of 5 load pulses determines the stiffness modulus of the mix. For each of pulses the stiffness modulus is obtained with Eq. (4.4):

$$S_m = \frac{F \cdot (R + 0.27)}{L \cdot H} \quad (5.4)$$

Where S_m represents the stiffness modulus (MPa), F is the peak value of the applied repeated vertical load (N), H represents mean amplitude of the horizontal deformation obtained from five applications of the load pulse expressed (mm), L is mean thickness of the specimen (mm), and R is the Poisson's ratio (assumed to be 0.35).

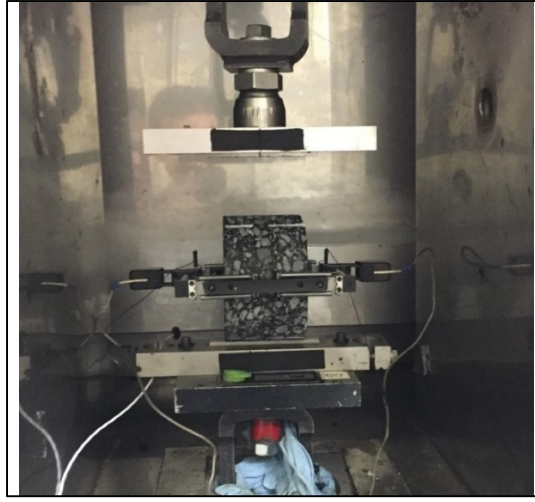


Figure 5.4 ITSM test setup with MTS device inside the environmental chamber

To determine the effect of the recycled glass as an additive on the temperature susceptibility of the mix, an environmental chamber was used for thermal conditioning. ITSM test was conducted at three different temperatures ($-10\text{ }^{\circ}\text{C}$, $0\text{ }^{\circ}\text{C}$, $10\text{ }^{\circ}\text{C}$). The modulus also needs to be defined along the perpendicular diameter. It should be 80 to 110% of the first value to accept the validity of the test. The final value of the modulus is the mean value of both diameters (vertical and horizontal). 1 specimen for each mixture was tested for ITSM, and the air voids of the tested specimens were at $7.0 \pm 0.5\%$.

5.6 Results analysis

5.6.1 Indirect Tensile Strength (ITS) Test

The value of ITS is used to determine the tensile strength of asphalt mix which can be further associated to the cracking resistance of the mix. Figure 5.5 compares the results of tensile strength for the mixes in dry and wet conditions.

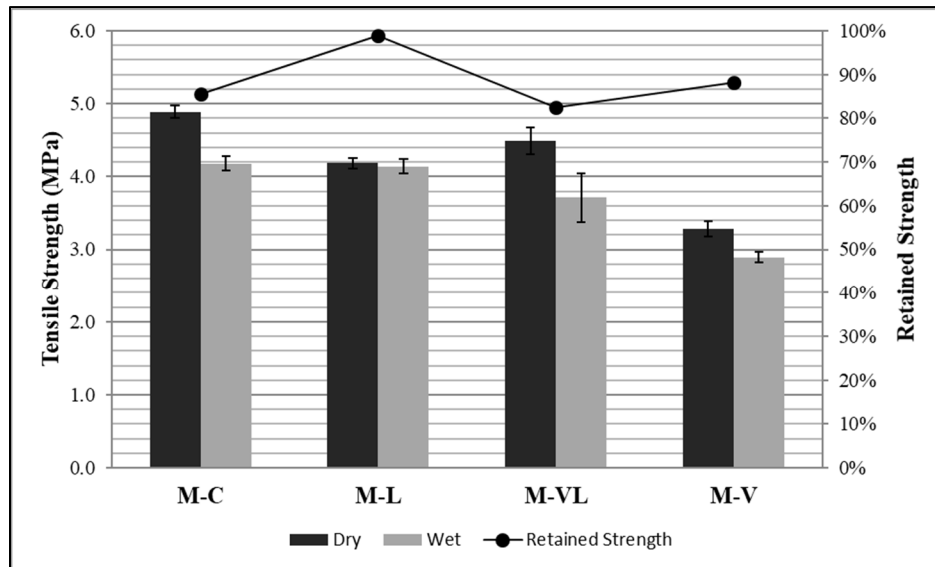


Figure 5.5 Indirect tensile strength of mixtures

As can be observed, use of cement (M-C) results in highest value of tensile strength. It is also demonstrated that the addition of recycled glass as only additive (M-V) caused a serious reduction, over 30% lower than with cement, in the tensile strength of the mix. This important point highlights that recycled micronized glass is sensibly less reactive than cement with the free water in the system. This is probably due to the total absence of calcium oxide that is normally provided by cement and which is necessary in order to start hydration reactions.

In contrast, the use of recycled glass combined with hydrated lime in M-VL results in a significant increase in tensile strength for both wet and dry conditions compare to the mix with glass only. It can be noticed that in dry conditions, the mix shows roughly same good performance if compared with M-C. In particular, silica components provided by recycled glass can increase the dry performance of mixes compare to only hydrated lime (M-L). In fact, whereas presence of water seems to not affect M-L, it has an opposite behavior if recycled glass is added. Also, all mixes have acceptable retained strength (>80%), but with M-V at the lowest level, the M-L mix at the highest, and the M-C and M-VL at similar level.

5.6.2 Indirect tensile stiffness modulus (ITSM) test

Table 5.4 presents the result of the indirect tensile stiffness modulus tests. Figure 5.6 indicates the final comparisons of the stiffness modulus for different mixes at various temperatures (-10 °C, 0 °C, 10 °C).

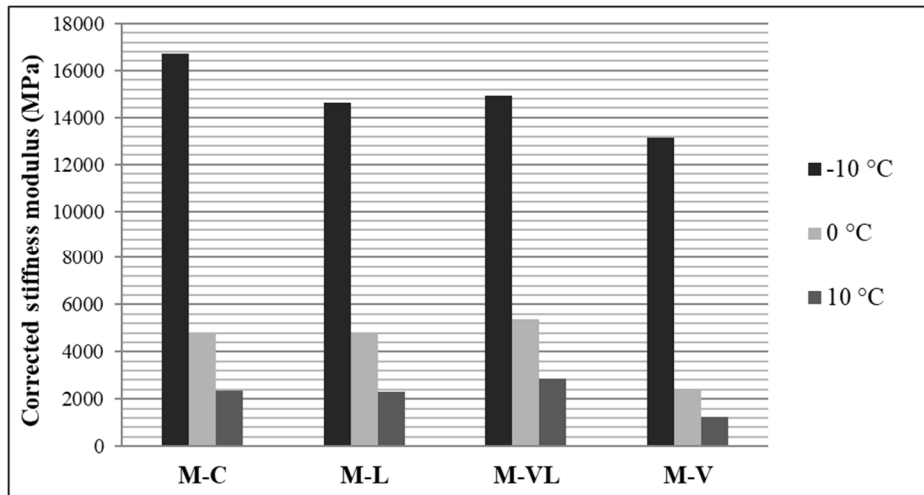


Figure 5.6 Comparison of the stiffness modulus for the mixes at different temperatures

Results demonstrate that the use of cement results in globally higher tensile stiffness modulus than mixes with only hydrated lime or only glass. It is also shown that the addition of the glass to asphalt mixes and its influence on the temperature susceptibility of the mix indicated that M-VL (hydrated lime plus glass) had higher stiffness modulus value than the M-L and M-V mixes. It can be noted that M-VL has closer modulus value to M-C containing only cement. This confirms the result of the ITS test.

As it is indicated in Figure 5.6, regardless the temperature, M-V (containing only recycled glass as additive) has the lowest performance in terms of stiffness modulus (79%, 51% and 53% of the stiffness of the mix with cement at -10°C, 0°C and 10°C respectively). Glass powder used as a stand-alone agent in bitumen emulsion mixes is not able to develop

acceptable adhesion with the mineral components of the material. Since the recycled glass used here is composed of particles with high surface area, it is believed that it acts as a dewatering agent in the mix by adsorbing water on its surface. However, this process alone does not seem to be enough to grant the mix high stiffness at young age.

Table 5.4 Stiffness modulus results

	Temperature (°C)	Load Factor	Rise time (ms)	Deformation (µm)	Stiffness modulus (MPa)	Corrected Stiffness modulus ⁽¹⁾ (MPa)
M-C	-10	0.6	124.9	3.21	16 652	16 711
	0	0.59	123.6	5.23	4 843	4 795
	10	0.6	132.1	4.89	2 353	2 350
M-L	-10	0.6	125.7	2.91	14 615	14 614
	0	0.59	129.5	5.20	4 861	4 827
	10	0.6	132.6	4.71	2 318	2 312
M-VL	-10	0.59	126.0	3.00	15 157	14 938
	0	0.6	129.5	4.76	5 327	5 358
	10	0.61	132.0	4.00	2 854	2 880
M-V	-10	0.6	131.0	3.70	13 002	13 123
	0	0.6	125.0	5.20	2 523	2 452
	10	0.6	130.0	4.50	1 247	1 240
⁽¹⁾ Corrected stiffness modulus for a load of 0.6						

At medium and high temperature (0 °C, and 10 °C), mixes with calcium hydroxide components (M-C, M-L, M-VL) have almost the same appreciable value of the stiffness modulus. At a lower temperature (-10 °C), the mix with cement has the highest modulus, with the three other mixes having stiffness values equivalent to 87%, 89% and 79% of the stiffness of the mix with cement for the M-L, M-VL and M-V mixes respectively. In fact, the 3-days curing protocol followed in the research did not lead to a complete development of internal chemical reactions and water evaporation, with a sensible amount of free water still available in the mixture. As

shown in Table 5.5, there was still water left in the specimen after three days of curing since water loss is less than 2% (free water in the mix), and this amount of water is higher than the amount theoretically used by the cement or hydrated lime hydration. It can also be seen that since there is no hydration with the mix containing only glass, the water loss is higher. As a consequence, presence of water at -10°C still plays an important role in the material stiffness, which at the same time does not seem to be fully-cured. It is important to remember that high stiffness values sometimes cause the crack reflection in the pavement in cold climate (Navarro & Gámez, 2011); this means that curing time is a fundamental parameter to be taken into account for further studies, especially for low-temperatures performance analysis.

Table 5.5 Water loss in the specimen after curing

Specimen	Weight before curing (kg)	Weight after curing (kg)	Water loss (%)
M-C	1.035	1.016	1.836
M-L	1.033	1.014	1.839
M-VL	1.035	1.016	1.836
M-V	1.033	1.013	1.936

In general, considering ITS and ITSM results, it is indicated that mixes containing hydraulic additives (cement or hydrated lime) show higher values of stiffness modulus and tensile strength than mix stabilized by micronized glass. These results indicate that such materials are able to withstand larger stress prior to failure. The contribution of recycled glass combined with hydrated lime has to be highlighted; from both tests, it is clear how it has beneficial effects, improving general performance of the mix. It means that probably hydrated lime and glass powder are able to create chemical bonds, although still not comparable with cement composition.

5.7 Conclusions

The present research aimed to study the behavior of recycled glass which can replace cement in the production of cold recycled mixtures with bituminous emulsion. For this purpose, a reference mixture stabilized with 1% of cement is compared with other possible solutions: in particular, cement is replaced with 1% of hydrated lime, 1% of glass powder and 0.5% of hydrated lime plus 0.5% of glass powder.

From the results, it is clear how the employment of recycled glass as stabilizing agent does not lead to comparable performance level if referred to the reference mixture. Actually, from ITS dry results, it seems to be the less performant, even if its water susceptibility is reasonably low. Better results were achieved when glass powder is combined with hydrated lime. The presence of calcium hydroxide and amorphous silica in the mixture started a similar reaction than cement, sensibly increasing stiffness and resistance values. In dry conditions and regardless the temperature, mechanical performances of the mentioned mixture are closer to the reference mix. At last, the use of hydrated lime instead of cement conferred to the material lower strength, although it showed the lowest water susceptibility, around 1%.

Three days of curing in specific conditions did not allow a complete mechanical characteristics development in the material, there is simply not enough time for a complete water evaporation and chemical reactions, extremely important aspects in this kind of mixes. Such feature, as well as the optimization of hydrated lime and glass content, especially from a chemical point of view, can be considered for deeper studies.

CHAPTER 6

EFFECT OF WATER AND CEMENT CONTENT ON THE MECHANICAL PROPERTIES OF COLD RECYCLED MIXTURES (CRM) WITH BITUMEN EMULSION

Simone Raschia^a, Tushar Chauhan^b, Shalu Panwar^b, Alan Carter^a, Andrea Graziani^c, Daniel Perraton^a

^a Construction Engineering department, École de technologie supérieure (ÉTS) 1100, Notre-Dame Street West, Montreal, Canada

^b Department of Civil Engineering, Indian Institute of Technology, Bombay, India

^c Department of Civil and Building Engineering, and Architecture, Università Politecnica delle Marche, Via Brecce Bianche, 60131 Ancona, Italy

Paper published in proceeding of the 5th International Symposium on Asphalt Pavements & Environment (APE), September 2019

6.1 Abstract

Cold recycled mixtures (CRM) treated with bitumen emulsion are innovative materials in road pavement construction industry which gained visibility in the last decades. They are produced at ambient temperatures thanks to the employment of bitumen emulsion, water and additional hydraulic binders. In this research, four CRM mixes are studied analysing the effect of two water contents and two cement dosages. The mechanical properties of the mixes were studied in terms of Indirect Tensile Ratio (ITR), Indirect Tensile Stiffness Modulus (ITSM) test and dynamic modulus test, after a curing period of 14 days. Moreover, results analysis is improved by images obtained at the scanning electron microscope (SEM). From the results, the presence of more water decreased the indirect tensile strength (ITS) in both dry and wet conditions, even if the water susceptibility was generally low (ITR > 80%). The PUNDIT measurements along curing highlighted the progressive increase of the dynamic modulus, which after curing was higher in the mixtures with cement. At the end, SEM images highlighted the effect of the water

content in the dispersion of the bituminous phase, as well as the presence of cement hydration products.

6.2 Introduction

Cold recycled mixtures (CRMs) are gaining interest in the road pavement construction industry thanks to the possibility to produce reliable materials for the pavement structure at ambient temperature (Davidson, 2005; Tebaldi et al., 2014; Xiao et al., 2018). The bituminous phase is replaced by the use of bitumen emulsion, a two-phase suspension constituted by bitumen droplets suspended in an aqueous phase. In order to increase the short-term and long-term mechanical properties, some Ordinary Portland cement is normally added, which allows also a faster breaking process of the bitumen emulsion (ARRA, 2001; Asphalt Academy, 2009; Brown et al., 2000). It is important to highlight that additional water is often considered in the production process to enhance the workability and compactability of the mix (Grilli et al., 2016; Raschia, Graziani, et al., 2019a). It is clearly demonstrated that the water content is of extreme importance for the reduction of the internal friction during compaction, as well as for the cement hydration. In fact, many studies demonstrated that with a higher amount of water in the mix, it is possible to reach higher density with less compaction effort (Cross, 2003; Gaudefroy et al., 2008; Martínez et al., 2007). Once that the curing process starts, a small part of the water is employed by the cement for the formation of hydration products, whereas the major part is expelled by evaporation depending on the environmental conditions (temperature and humidity) (Cardone et al., 2014; Godenzoni, Cardone, et al., 2016; Kim et al., 2011). As curing proceeds, water partially evaporates, partially reacts with cement and partially remains in the solid structure of the mixture. In fact, it is often showed that it is difficult to reach the total loss of the water inside the mix (Cardone et al., 2014; Garcia et al., 2013).

The objective of this study is to understand how the water content employed to satisfy compaction requirements affects the mechanical properties of the CRM with bitumen emulsion. To achieve this goal, mixtures with same volumetric properties are produced

changing water content, and repeating the experimental plan with and without the addition of Ordinary Portland cement.

6.3 Materials and methodology

6.3.1 Materials

The reclaimed asphalt pavement (RAP) used to produce the CRMs in this study was stockpiled in a production plant in Italy. The main physical properties of the RAP aggregate are collected in Table 6.1. The bitumen emulsion used is a CSS-1 type (ASTM D2397) and its properties, as well as the ones of the residual bitumen, are listed in Table 6.2. The cement used was a GU type (CSA A3000) with compressive strength at 28 days of 43.9 MPa (ASTM C109).

Table 6.1 RAP aggregate properties

Property	Standard	Unit	Value
Binder content	ASTM D6307	%	5.51
Nominal maximum particle dimension	ASTM D448-03	mm	16
Maximum specific gravity	ASTM C127-128	-	2.482

Table 6.2 Bitumen emulsion properties

Bitumen emulsion property	Standard	Unit	Value
Density	ASTM D6397-16	g/cm ³	1.0
Residue content	ASTM D6997-12	%	60.3
Storage stability @ 24 hours	ASTM D6930-10	%	0.6
Residual bitumen property			
Needle penetration @ 25°C	ASTM D5-13	mm	4.1
Softening point	ASTM D36-14	°C	48.6

6.3.2 Mixtures

In the present study, four mixtures were produced with the same gradation, which is represented in Figure 6.1. The target distribution was the Fuller-Thompson maximum density curve, with exponent 0.45. In order to obtain the target gradation, the final aggregate blend was composed of 94.4% of RAP aggregate and 5.6% of limestone filler. The bitumen emulsion content was fixed at 5.0% by aggregate mass, which means a residual bitumen content of 3.0% by aggregate mass. Two cement contents were tested, as well as two different dosages of intergranular water: the mixtures 0C_2W and 0C_4W do not contain cement, and are produced with 2% and 4% of intergranular water, respectively; the mixtures 15C_2W and 15C_4W contain 1.5% of cement by aggregate mass and 2% and 4% of intergranular water, respectively. Water contents of 2% and 4% were chosen because the first is the amount of minimum water coming from the bitumen emulsion addition, whereas the second allows to employ half of the compaction energy compared to the first one to obtain the same amount of air voids.

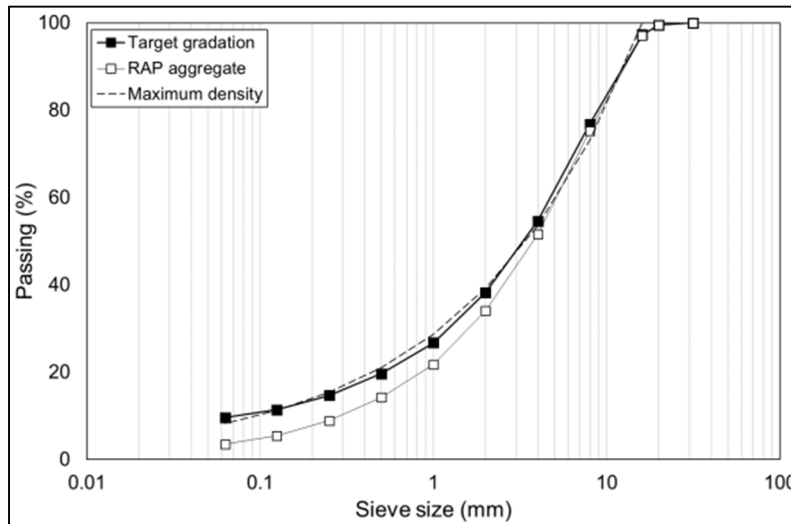


Figure 6.1 Gradation of the studied granular material

The mixtures were produced initially blending the dry aggregates with the absorption water and letting the humid blend rest overnight. Afterwards, cement (when required), additional

water (when required) and bitumen emulsion were added in this order, manually mixing the mixture at each addition. The specimens were compacted with a Superpave Gyratory Compactor (SGC) by using an undrained mould with $D = 100$ mm, 600 kPa of constant pressure, gyration rate of 30 rpm and external inclination angle of 1.25° .

The volumetric properties during and after compaction were analyzed through two parameters, the Voids in the mixture (V_m) and the Voids Filled with Liquids (VFL) (Grilli et al., 2016):

$$V_m = \frac{V_{V,A} + V_{W,I}}{V} \cdot 100 = \frac{V - (V_S + V_C + V_{B,R})}{V} \cdot 100 \quad (6.1)$$

$$VFL = \frac{V_{B,R} + V_{W,I}}{V_{B,R} + V_{W,I} + V_{V,A}} \cdot 100 = \frac{V_{B,R} + V_{W,I}}{V - V_S - V_C} \cdot 100 \quad (6.2)$$

where V is the total volume of the specimen, V_S is the bulk volume of aggregates, V_C is the volume of cement, $V_{B,R}$ is the volume of residual bitumen from emulsion, $V_{W,I}$ is the volume of intergranular water and $V_{V,A}$ is the volume of air. In order to have specimens with same value of V_m , at first, mixes 0C_2W and 15C_2W were compacted at 200 gyrations and the final value of V_m was recorded. Afterwards, mixes 0C_4W and 15C_4W were compacted at fixed height to reach almost the same V_m value. The volumetric properties of the studied mixes are listed in Table 6.3. After compaction, the specimens were stored in a chamber at fixed temperature of 40 ± 2 °C and relative humidity of $55 \pm 5\%$.

The experimental program was developed performing Indirect Tensile Strength (ITS) test in dry and wet conditions, Indirect Tensile Stiffness Modulus (ITSM) test, dynamic modulus measurements with wave propagation at different curing ages, and image analysis through a Scanning Electron Microscope (SEM) (García et al., 2013; Godenzoni, 2017; Richardson, 1999; Rutherford et al., 2014). The ITS test was performed on three dry specimens at 25 °C, in accordance to ASTM D6931. The ITS value was calculated as:

$$ITS = \frac{2000 \cdot P}{D \cdot t \cdot \pi} \quad (6.3)$$

where P is the maximum load (N), D is the specimen's diameter (mm) and t is the specimen's thickness (mm).

Table 6.3 Volumetric composition of the studied mixtures

Components (%)	0C_2W	0C_4W	15C_2W	15C_4W
RAP aggregate	80.4	79.2	80.3	78.8
Filler	5.0	5.0	4.2	4.1
Unhydrated cement	0.0	0.0	1.0	1.0
Residual bitumen	6.1	6.0	6.0	5.9
Emulsion water	4.1	4.1	4.1	4.0
Additional water	0.0	4.1	0.0	4.0
Air	4.4	1.6	4.4	2.2
Total	100	100	100	100
Gyrations	200	95	200	100
V _m	8.0	9.7	8.5	10.2
VFL	72.8	89.9	69.3	87.2

The ITS test in wet conditions was performed on three specimens which were previously submerged in water at 25 °C for 2 hours. The Indirect Tensile Ratio was calculated:

$$ITR = \frac{ITS_{wet}}{ITS_{dry}} \quad (6.4)$$

The ITSM test was performed on one specimen each mixture at three temperatures: -10 °C, 0 °C and 10 °C, in accordance to UNI EN 12697-26 (Annex C). The test was repeated on both diameters and the average ITSM value was calculated as:

$$ITSM = \frac{F \cdot (\nu + 0.27)}{z \cdot h} \quad (6.5)$$

where F is the maximum load (N), ν is the Poisson ratio, z is the horizontal deformation (mm) and h is the specimen's thickness (mm). Dynamic modulus measurements were performed by

means of a Portable Ultrasonic Non-destructive Digital Indicating Tester (PUNDIT), using compression and shear waves. Shear waves transducers were attached on both faces of the specimen, using a coupling gel. The two probes were properly aligned in the same plane to achieve maximum transmission. The test was carried out on one specimen for each mixture, and the average value of three measurements was recorded at 1, 3, 5, 7 and 14 days of curing. The testing temperature was 40 °C.

6.4 Results analysis

Figure 6.2 shows the results of ITS test in dry and wet conditions. It is highlighted that the ITR value is between 90% and 110%, indicating the low water susceptibility of all the studied mixtures. In terms of resistance, the mixtures with more intergranular water (0C_4W and 15C_4W) have in both cases less ITS than the respective mixtures with less water. Another important result is the slight effect of cement. In fact, mixtures 15C_2W and 15C_4W did not show a remarkable increase in the strength, as it was supposed to happen. However, mixes without cement showed very high ITS results, making less effective the addition of cement.

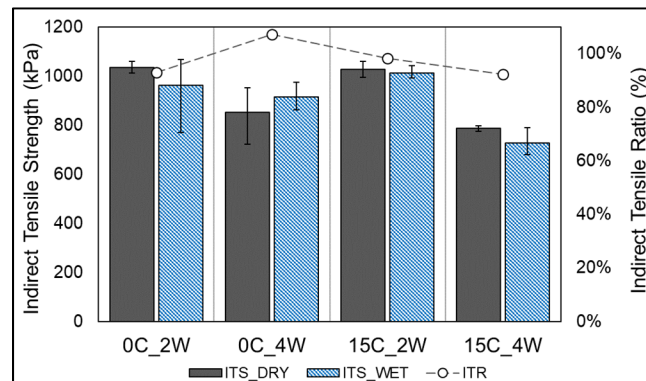


Figure 6.2 Indirect Tensile Strength test results in dry and wet conditions

Figure 6.3 shows the results of the ITSM test. It is possible to observe that for all mixtures, stiffness is temperature sensitive. It is important to highlight that the mixture without cement 0C_2W showed the lower tensile stiffness, whereas the mix which was characterized by the

highest stiffness is the 15C_2W. Mixtures 0C_4W and 15C_4W have similar ITSM values, which is unexpected since the presence of cement should improve stiffness. Hence, results for these two mixtures were probably influenced by the higher air voids. Furthermore, although the mixture 15C_4W contains cement and the mixture 0C_2W does not, their mechanical properties appear similar. Hence, the mixture 15C_4W showed ITSM values of a mixture without the effect of the emulsion, giving similar results to the mixture without cement (0C_4W). This evaluation can be confirmed also by the ITS results.

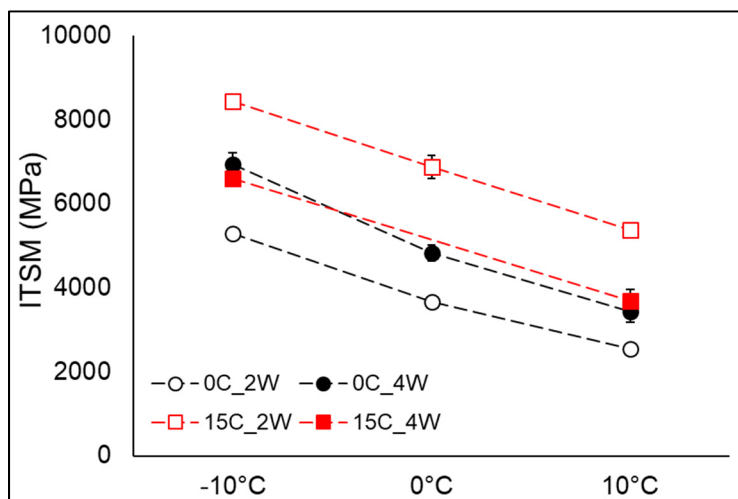


Figure 6.3 Indirect Tensile Stiffness Modulus test results

Figure 6.4 shows the dynamic modulus values at different curing ages. For all the studied mixes, it is possible to observe the effect of curing in the increase of the dynamic modulus. From those results, it can be highlighted that after 7 days of curing, no significant increase in the modulus value occurred. In general, mixes with cement (15C_2W and 15C_4W) always had higher modulus than the mixes without cement. The mixture 15C_4W showed a slower increase, probably due to the higher amount of water in the mixture. Nevertheless, at the end of curing, the mixture 15C_4W has lower dynamic modulus, justified by the higher voids. Along the curing time, mixtures without cement 0C_2W and 0C_4W showed very close results, and values after 14 days lower than mixtures with cement.

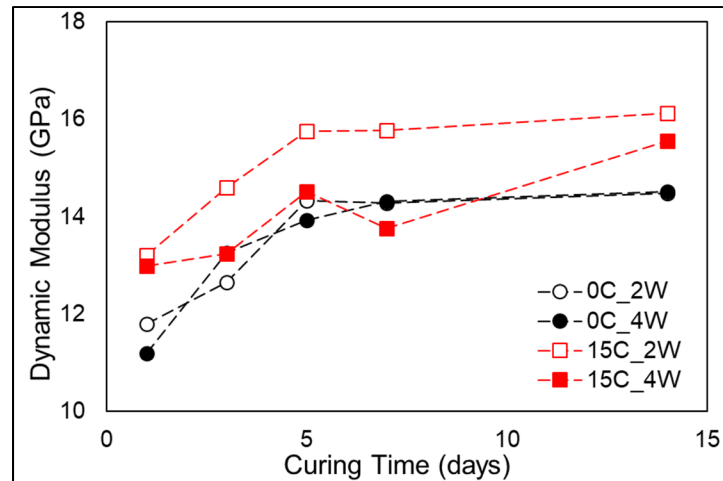


Figure 6.4 Dynamic Modulus test results
(PUNDIT at 40°C)

Figure 6.5 shows Scanning Electron Microscope images taken from broken samples after mechanical testing. The test was performed on the material without any particular surface treatment prior testing. Comparing the pictures of mixes 0C_2W and 0C_4W, it is highlighted the contribution brought by the higher amount of water in the bitumen dispersion. Analyzing the mixes with cement it can be seen that the hydrates product formation is lower in the mixture 15C_2W, in which it is concentrated only in few spots. On the contrary, the mixture 15C_4W clearly shows the cement hydration process, which at the same time makes difficult to recognize the bituminous phase.

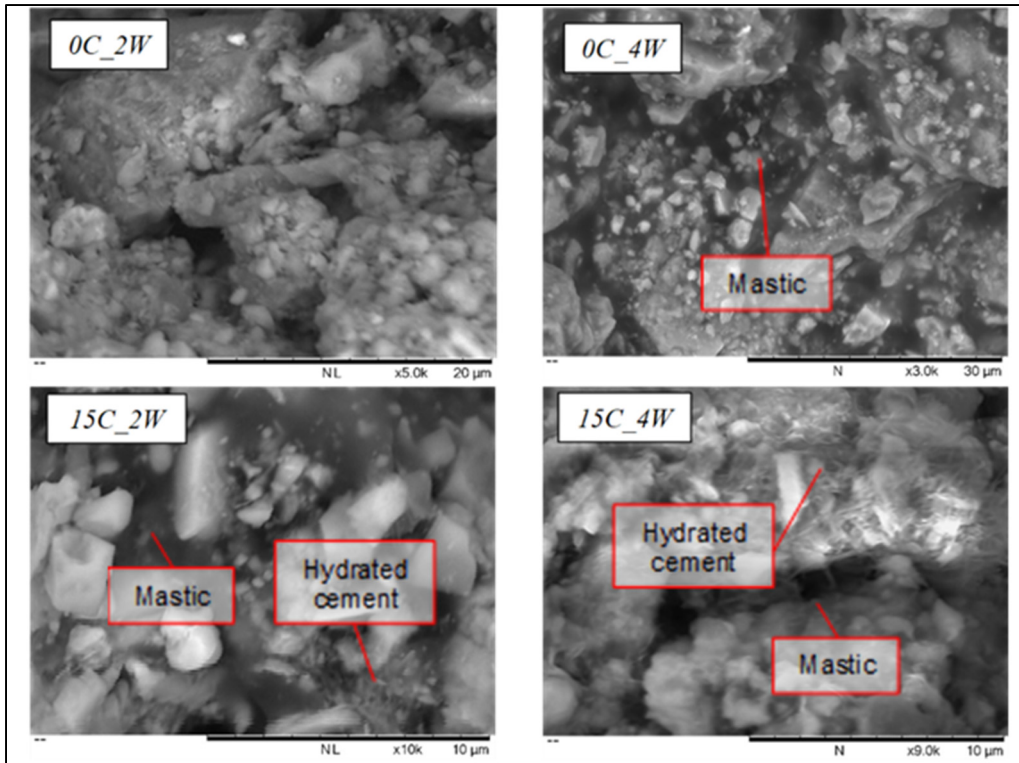


Figure 6.5 Scanning Electron Microscope images

6.5 Conclusions

This research aimed to understand the effect of water content and cement content in CRM materials with bitumen emulsion. Four mixes, characterized by two cement dosages and two water contents, were analyzed in terms of ITS test, ITSM, dynamic modulus and SEM image analysis after a curing period of 14 days. The following conclusions can be drawn:

- From ITS results, the higher water content generally decreased the strength of the mix, whereas the addition of cement did not lead to a significant increase in resistance. It must be noted that mixes with more water required less compaction energy, which could have led to a lower aggregate packing;
- From ITSM results, the temperature susceptibility of the mixes is highlighted. Mixes with cement did not always show higher stiffness; in fact, the cement hydration seemed to have

- damaged the effect of the emulsion when more water was used. This led to lower stiffness values. In mixes with no cement, more water allowed a better dispersion of the bitumen phase and gave higher stiffness;
- Dynamic modulus measurements along curing showed an increase of the dynamic modulus significant in the first 7 days for all the four mixes. After 14 days, mixes with cement had higher modulus than the mixtures without cement, which were not different regarding the water content;
 - From SEM image analysis, it was possible to capture important aspects of the mixes produced. In fact, the higher water content allowed a higher bitumen dispersion among the mixes 0C_2W and 0C_4W. In mixes with cement (15C_2W and 15C_4W), more water led to a higher cement hydration, which at the same time prevent a full contribution from the bitumen phase.

Further studies are needed in this perspective, especially at a microstructural level, to fully understand and estimate the collaboration between bitumen and hydraulic binders (such as cement). From the results, the contemporary presence of both did not lead to the most efficient mix.

CHAPTER 7

SUMMARY OF SECTION 1 AND INTRODUCTION OF SECTION 2: INFLUENCE OF RAP AGGREGATE ON CBTM PROPERTIES

The goal of this chapter is to summarize the results obtained in Section 1 and introduce the next topic of the thesis, i.e. the influence of RAP aggregate on CBTM properties.

7.1 Summary of Section 1

The results obtained in the previous two papers highlighted some important aspects related to the employment of cement and water in the mix design of CBTM mixtures. The dosage of both components is fundamental to avoid issues in terms of production process and mechanical properties. The main findings are listed below.

The combination of glass powder and hydrated lime improved strength and stiffness of each of the two components considered alone. However, it did not lead to the same properties conferred by ordinary Portland cement. Although the global stiffness of the material was related to the cement dosage, a balanced proportion between residual bitumen and cement (mass ratio 2:1, respectively) highlighted the contribution given by both binders. Furthermore, water dosage resulted to be important to address the effects of residual bitumen and cement. In fact, results showed that when a higher dosage of water was used, the degree of cement hydration was higher and had probably hidden the role of bitumen. On the other hand, when the dosage of water was smaller, the cement hydration reaction did not develop completely and its contribution was less significant than the bituminous phase.

Further studies are encouraged to improve knowledge on the results obtained and additional tests could be considered. The identification of chemical components in the cured mixture, as well as isothermal calorimetry tests, could both give more details regarding the role of cement in cold recycled mixtures. Moreover, water and compaction energy are aspects that need

balance in order to obtain a mixture with the desired volumetric properties without an excess of compaction effort. This balance is easier to reach in laboratory rather than for in-situ applications. For this reason, a volumetric mix design as described in CHAPTER 3 is highly recommended as a preliminary step for cold recycled mixtures projects. Such protocol should be improved by the correlation between compaction techniques (and energy) in the laboratory and the field compaction. It is also important to remark the high control that the volumetric approach confers on the dosage of constituents inside the CBTM mixture.

Another important aspect that was not treated in these chapters are the steps followed for the mixing procedure. In general, the addition of cement, additional water and bitumen emulsion were performed in this order, on the aggregate blend in SSD conditions. However, it is possible that changing the order of introduction of the components could affect the general properties of the mixtures, especially in terms of bitumen emulsion breaking and cement hydration. This aspect should also be considered for further studies.

7.2 Section 2: study of the RAP aggregate effect on CBTM properties

In Section 2, constituted by three journal papers, the study focuses on the influence of RAP source in CBTM mixtures properties, evaluating different aspects. A first step was needed to study the influence of the RAP aggregate distribution on the properties of the produced mixtures (CHAPTER 8). The production of CBTM mixtures with different RAP aggregate distribution was investigated in two laboratories: ÉTS – LCMB (Canada) and UNIVPM (Italy). The effect of the aggregate gradation on the compactability and mechanical properties is important mainly because it can be responsible for the air voids dimensions and distribution inside the mixture, as well as the degree of dispersion of the mastic and aggregate coating. Such aspects are considered fundamental because the amount of binder used in CBTM is generally low, and it does not allow a uniform aggregate coverage.

As a second step, two RAP sources were selected according to the fragmentation test (Perraton, Tebaldi, et al., 2016). The two sources selected, RAP1 coming from Italy and RAP2 from

USA, are characterized by different fragmentation indexes. Hence, the goal of the second paper is to evaluate how the two RAP sources are affecting physical and mechanical properties of the CBTM mixtures (CHAPTER 9). Results obtained left some questions open and some aspects needed to be clarified. In fact, some findings could have been limited by the tests chosen, as well as by the different filler contents (5.2% and 8.3% for RAP1 and RAP2, respectively). For these reasons, in CHAPTER 10, gradation of both RAP sources have been slightly modified and cement was not added to strictly evaluate the RAP source effect. Compactability and fundamental rheological properties were investigated to have a wider view on the effect of the RAP aggregate source.

CHAPTER 8

EFFECT OF GRADATION ON VOLUMETRIC AND MECHANICAL PROPERTIES OF COLD RECYCLED MIXTURES (CRM)

Simone Raschia^a, Chiara Mignini^b, Andrea Graziani^b, Alan Carter^a, Daniel Perraton^a, Michel Vaillancourt^a

^a Construction Engineering department, École de technologie supérieure (ÉTS) 1100, Notre-Dame Street West, Montreal, Canada

^b Department of Civil and Building Engineering, and Architecture, Università Politecnica delle Marche, Via Brecce Bianche, 60131 Ancona, Italy

Paper published in the journal Road Materials and Pavement Design, Taylor & Francis, July 2019

8.1 Abstract

In recent times, recycling using cold bituminous mixtures has become one of the most interesting techniques in pavement engineering from sustainability aspect. This study focuses on the clarification of the steps concerned with the cold mixture mix design to determine the initial aggregate gradation of the mixture. The study has been developed involving procedures followed in Canada and Italy. In both the cases, three different gradations, normally employed in the production of traditional bituminous mixtures, were compared. The effect conferred by the gradation type has been studied in terms of workability, compactability and mechanical properties. Results show that in both the procedures the gradation influenced the workability and the compaction behaviour of the mixtures studied. At the same time, in terms of mechanical properties, the gradation influenced the strength of the final mixture in only one of the procedures applied.

8.2 Introduction

Cold recycling as a technology is developing more interest in the framework of road maintenance and rehabilitation. This is a process to obtain new materials normally used for base or binder courses with impressive advantages in terms of economic and environmental sustainability, as well as mechanical properties (ARRA, 2001; Kuleshov, 2018). The possibility of using a high amount of reclaimed asphalt pavement (RAP) aggregate directly means a continuous availability of the solid phase of the mixtures, which can reduce the dependency on virgin aggregates.

The main binder in cold recycled mixtures (CRM) is bitumen, which can be used in form of bitumen emulsion or foam. Both techniques allow reducing the viscosity of the bitumen in order to produce and compact mixtures at ambient temperature. In this paper, only bitumen emulsion is considered (ARRA, 2001; Asphalt Academy, 2009; Xiao et al., 2018). As an additional binder, Portland cement, lime, fly ash, etc. can be employed in small amounts to increase the short and long-term resistance and stiffness of the material. Normally, water is added to the mixture, which reduces the internal friction and enhances the workability and compactability (Brown et al., 2000; Cross, 1999; Du, 2014; Oruc et al., 2007; Raschia et al., 2018).

In the literature, the terms workability and compactability are often used as synonyms, to indicate the specific characteristic of the material to be easily laid in place and compacted with a reduced amount of energy (Dessouky et al., 2012; Gudimettla et al., 2003). In hot mix asphalts (HMA), workability is normally controlled in terms of production temperature, whereas the aggregate gradation, which is also very important, is often considered as a secondary aspect (Bennert et al., 2010). As a standard practice, it is usual to assume a dense-graded distribution to have a workable mix, evaluating the maximum density line as the best to be compacted (Fuller & Thompson, 1907). The Bailey method (Bailey, 2002) considers that an aggregate blend can be divided in stone, interceptor, coarse sand and fine sand particles, each of them with a specific role in the final structure of the bituminous mixture. With this

method it is possible to evaluate the aggregate packing ability, which can affect the HMA mechanical properties, especially in terms of rutting resistance (Kim et al., 2008).

Furthermore, Olard and Perraton (2010) showed that by optimizing the proportions of coarse and fine fractions in an aggregate blend, it is possible to produce high performance asphalt concrete (HPAC), i.e. materials with improved compactability, strength and stiffness. Such optimization leads to fill the free volume of air among coarse particles with the remaining fine fraction. It is highlighted that an excessive amount of medium-sized aggregate can induce the “wall effect”, that is the contact loss in the coarse fraction.

Francken and Vanelstraete (1998) and Van de Ven, Voskuilen and Tolman (2003) tried to develop a mix-design procedure based on the packing theory by comparing different approaches. General results showed that no exact correlation could be found between the packing simulation of multi-size gradation and the mix design process.

From a realistic point of view, a CRM mixture can show a double behaviour in terms of ability to be mixed and laid (workability), and in terms of energy consumption for compaction (compactability). It can happen that the two properties are not directly linked, meaning that a loose mixture that shows good workability can require unexpectedly a high compaction energy (Raschia, Graziani, et al., 2019a). These two different aspects of the compaction ability of a mixture are not simple to optimize, if not normally acting on the water content of the mixture. However, water content should respect a maximum value, that will prevent water loss together with fine particles and bitumen droplets during compaction (Grilli et al., 2016). When CRM specimens are compacted in the laboratory using a gyratory compactor, it is possible to evaluate the workability and compactability of the mixture by using two parameters linked to the compaction curve (Grilli et al., Graziani et al., & Bocci et al., 2012; Raschia et al., 2019). The workability, intended as the self-compaction ability of the mix, is represented by the value of voids in the mixture at the beginning of compaction, whereas the compactability can be related to the slope of the linear part of the compaction curve in a semi-logarithmic plane.

Results from Xu, Wang and Wang (2017) are related to the effect of gradation on CRM, where the mechanical properties are linked to two parameters representing the gradation: the fineness modulus, which is an empirical value describing how coarse or fine is the gradation, and the fractal dimension, which estimates the slope of the gradation in a bi-logarithmic plot. The results highlight that a balance between the fractal dimension value, the density and adhesion was the key to improve mechanical properties of CRM, rather than bitumen emulsion content and cement content.

In concrete mix design, the workability aspect has been improved with the introduction of Self-Compacting Concretes (SCC). In these particular mixtures, the achievement of high levels of workability is ensured by two main aspects: the high deformability of the paste (or mortar), and the segregation resistance between coarse and fine aggregates. Both aspects can be obtained by using high amount of filler aggregate which increases the viscosity of the paste and reduces the internal stress between coarse aggregates (Brouwers, 2004; Brouwers & Radix, 2005; Ouchi & Okamura, 1999).

The main objective of this research is to investigate the effect that the aggregate gradation of CRM has on their workability and compactability. In order to give an exhaustive answer, mixtures characterized by different gradations were prepared in the laboratory and compacted using the gyratory compactor. The experimental data were analysed using specific parameters obtained from the grading curves and from the compaction curves. The relation between aggregate gradation and mechanical properties of CRM was also investigated.

Similar experimental plans were carried out according to typical practices followed in North America and Europe. In the first case, the work was performed at École de technologie supérieure (ÉTS) in Montréal (Canada), studying the effect of three gradations that are more commonly used in Canada, whereas in the second case the study was developed at Università Politecnica delle Marche (UNIVPM) in Ancona (Italy), involving three aggregate gradations generally used in Italy. It must be highlighted that this study does not address to compare the two cases. On the contrary, the analysis will be focused separately on each laboratory in which

the experimental plan was carried out. In this way, the aggregate gradation effect can be analysed considering three different gradations employed in two different materials.

8.3 Materials and methods

8.3.1 Mixtures composition

The work developed at ÉTS involved the investigation of three aggregate gradations which are typical for the construction of base courses. The first refers to the Fuller-Thompson maximum density curve with a maximum aggregate size of 14 mm (CA_FT), the second represents a gap-graded gradation employed in the production of HPAC (CA_HPAC), while the third is designed to respect the grading envelope provided by the Ministère du Transport du Québec (MTQ) for base course (CA_MTQ) (Figure 8.1.a). It is highlighted that the three gradations are composed only of RAP aggregate with a small correction of filler (Table 8.1).

Table 8.1 Granular composition of the aggregate blends

Component	CA_FT	CA_HPAC	CA_MTQ
RAP 0/10 (%)	94.9	41.6	73.6
RAP 10/14 (%)	0	51.8	21.3
Filler (%)	5.1	6.6	5.1
Component	IT_FT	IT_SMA	IT_FINE
RAP 0/14 (%)	80.0	0	80.0
RAP 2/14 (%)	0	70.0	0
Sand 0/2 (%)	17.0	20.0	0
Filler (%)	3.0	10.0	20.0

Similarly, at UNIVPM, the experimental work was carried out on three different aggregate blends in the perspective of the production of a binder course. The first is close to the Fuller-Thompson curve with a maximum aggregate size of 14 mm (IT_FT), the second is a gap-

graded curve derived from specifications for stone mastic asphalts (IT_SMA), and the third is a maximum density curve with increased dosage of filler (IT_FINE) (Figure 8.1.b). To obtain these three aggregates gradations, RAP aggregates, virgin aggregates and filler were combined (Table 8.1). The main physical properties of aggregates used are reported in Table 8.2.

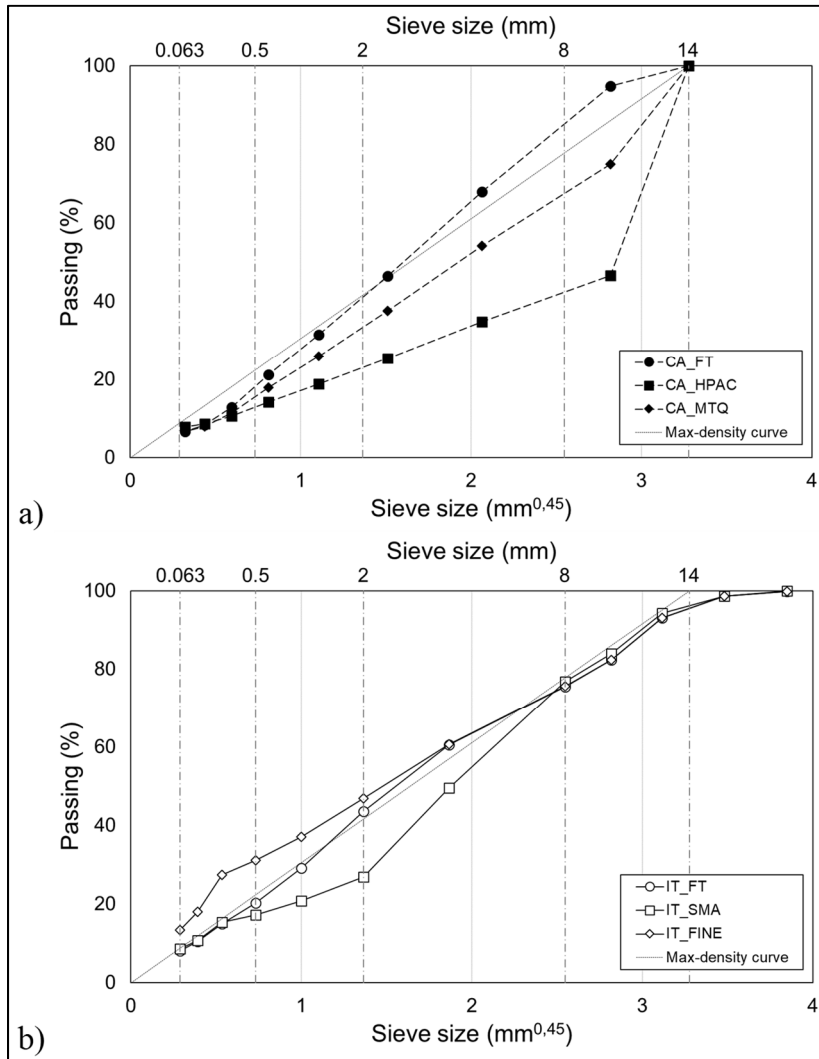


Figure 8.1 Aggregate blend gradations studied at:
a) ÉTS; b) UNIVPM

Mixtures composition in both laboratories was selected in accordance to local mix-design practices. Hence, the composition may vary in terms of cement, bitumen and water content,

whereas particular attention was paid to reproduce the same laboratory operational steps (mixing and compaction) in both cases.

Table 8.2 Main properties of aggregates used

ÉTS		
RAP0/10		
Property	Standard	Value
Bulk Specific Gravity of the aggregate	LC 26-045	2.537
Water absorption	LC 21-066	1.0%
Binder content (by aggregate mass)	LC 26-006	6.1%
RAP 10/14		
Property	Standard	Value
Bulk Specific Gravity of the aggregate	LC 26-045	2.550
Water absorption	LC 21-066	1.0%
Binder content (by aggregate mass)	LC 26-006	4.0%
UNIVPM		
RAP 0/14		
Property	Standard	Value
Apparent density	EN 1097-6	2.482 g/cm ³
Saturated Surface Dried density	EN 1097-6	2.441 g/cm ³
Water absorption	EN 1097-6	1.14%
Binder content (by aggregate mass)	EN 12697-1	5.7%
VA 0/2		
Property	Standard	Value
Apparent density	EN 1097-6	2.732 g/cm ³
Saturated Surface Dried density	EN 1097-6	2.685 g/cm ³
Water absorption	EN 1097-6	1.50%

Cationic slow-setting emulsions were used and their properties, together with the residual bitumen properties, are listed in Table 8.3. The residual bitumen content was fixed in both cases: 2% by aggregate mass at ÉTS and 3% by aggregate mass at UNIVPM. The cement used at ÉTS is a GU type (CSA A3000) with a compressive strength of 43.9 MPa after 28 days. At UNIVPM, a high-resistance cement was used, characterized by a compressive strength of 56.0 MPa after 28 days. The cement content was also fixed in both laboratories: 1.5% by aggregate mass at ÉTS and 2.5% by aggregate mass at UNIVPM.

Table 8.3 Main properties of bitumen emulsions and bitumen residue

ÉTS		
Property		
Bitumen emulsion	Standard	Value
Residual bitumen	ASTM D6997	62.8%
Viscosity Saybolt-Furol @ 25°C	ASTM D7496	28.1 s
Oversized particles	ASTM D6933	< 2%
Residual bitumen		
Pen @ 25°C	ASTM D5	170 mm/10
UNIVPM		
Property		
Bitumen emulsion	Standard	Value
Residual bitumen	EN 1428	60%
Viscosity @ 40°C	EN 13302	42.5 s
Breaking Index	EN 13075	2%
Residual bitumen		
Pen @ 25°C	EN 1426	100 mm/10
Softening point	EN 1427	43°C

8.3.2 Mixing and compaction

The mixing was carried out following the same steps at ÉTS and UNIVPM, even though it was performed manually in the first case and mechanically in the second case. The dry aggregate blend was preliminary mixed to obtain the target gradation, and the water amount corresponding to the absorption water was added and mixed. The mixture obtained was kept sealed in a plastic bag for at least 12 hours to allow moisture distribution and a good level of absorption by the aggregates. Then, cement, additional water and bitumen emulsion were added in this order and mixed at each addition until a good homogeneity was obtained. This second step normally required 5 to 10 minutes.

Compaction was started immediately after mixing. At ÉTS, the compaction was performed by a gyratory compactor with mould diameter of 100 mm, constant pressure of 600 kPa, gyration rate of 30 rpm, and at an external angle inclination of 1.25°. At UNIVPM, the same compaction parameters were used with a mould diameter of 150 mm.

Compaction by means of a gyratory compactor allows to measure the height of the specimen, and more specifically its volume. During the mixing process, the mass of each component in the mixture is known and its volume can be calculated. This means that during compaction, it is possible to relate the volume of the compacted specimen to the volume of the loose mixture (and maximum density) at each gyration. With the increasing compaction energy, the density of the specimen increases because the volume occupied by the air slowly fills with liquids (water and bitumen). In this way, it is possible to characterize CRM compaction properties by calculating the Voids in the mixture (V_m):

$$V_m(\%) = \frac{V_{V,A} + V_{W,I}}{V} \cdot 100 = \frac{V - (V_S + V_C + V_{B,R})}{V} \cdot 100 \quad (8.1)$$

where V is the total volume of the specimen, V_S is the bulk volume of aggregates (and hence includes the volume of absorbed water), V_C is the volume of unhydrated cement, $V_{B,R}$ is the volume of residual bitumen from emulsion, $V_{W,I}$ is the volume of intergranular water and $V_{V,A}$

is the volume of air. It is important to highlight that the residual bitumen from the emulsion is not absorbed by aggregate, and thus is considered totally effective. This can be assumed since the RAP aggregates are characterized by very low absorption values, and by the fact that aggregates surface voids are already saturated with water at the moment of mixing with bitumen emulsion. In the calculation of V_m only intergranular water is considered, which is the amount of water not absorbed by the aggregates.

At ÉTS a preliminary series of specimens were compacted to select a suitable intergranular water content to reach a V_m value of $10 \pm 1\%$ in the three mixtures, which was fixed at 2% by mass of aggregates.

At UNIVPM the compaction was performed at 100 gyrations and different water contents were tested to reach the lowest V_m value without having material loss during compaction (water and fine particles). The intergranular water was fixed at 3% by mass of aggregates for IT_FT and IT_FINE, and at 2.5% by mass of aggregates for IT_SMA.

8.3.3 Laboratory testing

Depending on the ambient conditions, such as temperature and relative humidity, the CRM needs a certain amount of time (curing period) to reach the cured state (Cardone et al., 2014; Godenzoni, Cardone, et al., 2016; Graziani, Iafelice, et al., 2018).

Compacted specimens were placed in an environmental chamber for curing at different conditions: at ÉTS the curing was 3 days at 38 ± 2 °C and 60% of relative humidity, while at UNIVPM the curing was performed for 7 days at 25 °C and 70% of relative humidity.

During the curing process the water evaporation takes place, together with cement hydration. A method to control the curing process is to monitor the evolution of the specimen mass, or more specifically, the final weight related to the cured state. In this way it is possible to have an idea of when the curing process is mostly occurred:

$$\Delta W^{(t)} = \frac{W^0 - W^{(t)}}{W_{TOT}} \cdot 100 \quad (8.2)$$

where $\Delta W^{(t)}$ is the water loss by evaporation (%) at the curing time t , W^0 is the initial mass of the specimen; $W^{(t)}$ is the mass of the specimen at the curing time t and W_{TOT} is the total amount of water in the specimen.

The experimental plan at ÉTS was carried out performing Indirect Tensile Strength (ITS) Test in dry and wet conditions, to evaluate the Indirect Tensile Strength Ratio (ITR). The test was performed in accordance to ASTM D6931 at 25 °C. This test measures the tensile resistance of the material along the vertical diametral plane subjected to a compressive load, with a loading rate of 50 mm/min. The ITR is calculated as the ratio between ITS in wet and dry conditions. Both values are an average of three replicates. To investigate the water susceptibility, the ITS_{wet} value was measured on specimens previously submerged in a water bath for 2 hours at 25 °C.

At UNIVPM, the ITS test in dry conditions and the Indirect Tensile Stiffness Modulus (ITSM) test were performed. The ITS test was performed in accordance to EN 12697-23 at 25 °C.

The ITSM test was carried out following the EN 12697-26 (Annex C) at 25 °C. The test measures the stiffness modulus in indirect tensile configuration by a series of 5 vertical load pulses with rise-time equal to 124 ± 4 ms. The ITSM is calculated as:

$$ITSM = \frac{F \cdot (\nu + 0.27)}{z \cdot h} \quad (8.3)$$

where F is the peak load of the applied repeated pulse, z is the amplitude of the horizontal deformation, h is the mean thickness of the specimen and ν is the Poisson's ratio (assumed as 0.30). The established horizontal deformation value was 2 μm . This value is lower to the horizontal deformation suggested by the standard for HMA and was selected to prevent premature failure of the samples due to the low bitumen content and cement addition. The test was repeated on three specimens for each mixture.

8.4 Results and discussion

8.4.1 Workability and compactability

Figure 8.2.a shows the compaction curves obtained at ÉTS, and each curve is an average of six specimens. The three mixtures are characterized by similar slope, and the number of gyrations required to reach the target V_m depends of the aggregate blend. The lowest energy was applied to the mixture CA_MTQ, 84 gyrations, whereas mixtures CA_FT and CA_HPAC needed 142 and 180 gyrations, respectively. The difference at the end of compaction is also visible at the beginning (at 1 gyration). In fact, the mixtures CA_MTQ, CA_FT and CA_HPAC were characterized by a V_m value of 22.7%, 24.0% and 26.4%, respectively. During the compaction process, the gap at 1 gyration did not change, since the three mixtures showed very similar slopes of the compaction curve.

Figure 8.2.b shows the compaction curves obtained at UNIVPM, which were obtained as an average of two specimens for each mix. In this case, the effect of gradation can be observed both in the initial value of V_m and in the value at 100 gyrations (hence, the slope of the curve). In fact, mixtures IT_FT and IT_SMA are characterized by the same V_m value at 1 gyration (24.0%), whereas the value at the end of compaction is quite different (9.3% and 7.3% for IT_SMA and IT_FT, respectively).

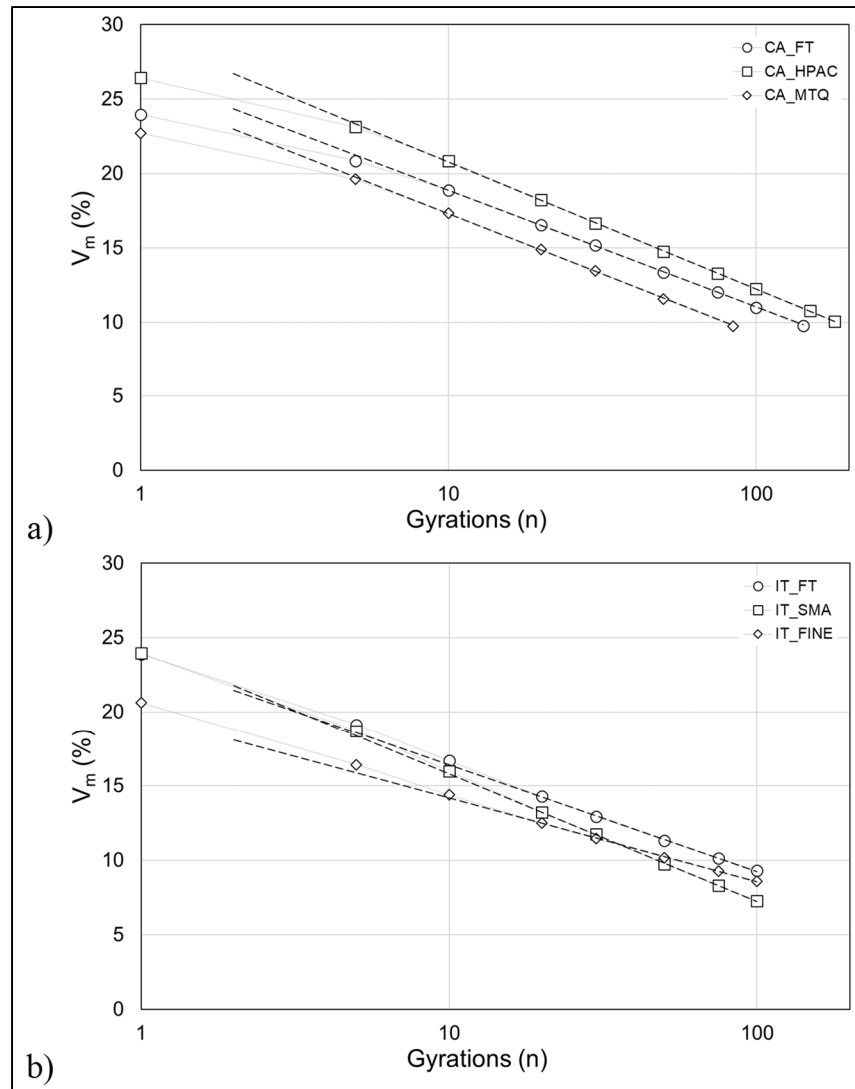


Figure 8.2 Compaction curves for the six mixtures at: a) ÉTS; b) UNIVPM

At the same time, the mixture IT_FINE is characterized by values of V_m at 1 and 100 gyrations of 20.6% and 8.6%, respectively, meaning that in this case the lowest V_m initial value did not lead to the lowest V_m value at 100 gyrations.

To further analyse the workability and compactability aspects using the gyratory compactor curves, it is useful to introduce two parameters: $V_m(10)$ and k :

$$V_m = V_m(10) + k \log N_g \quad (8.4)$$

where $V_m(10)$ are the voids in the mixture after 10 gyrations, k is the slope of the compaction curve after 10 gyrations and N_g is the number of gyrations (Grilli et al., 2012). The threshold at 10 gyrations was selected because it is the most accurate point after which the compaction curve can be approximated as linear in a semi-log representation. $V_m(10)$ can be used to represent the workability, since it indicates the amount of voids in the mixture when a very low compaction energy is applied, while k can describe the mixture compactability, since the slope of the linear part is associated to the compaction energy required to reach the required volumetric properties. Since k represents the compaction curve slope, the highest is its value, the better is the compactability. On the contrary, $V_m(10)$ is the percentage of voids in the low-compacted mixture, hence low values mean higher self-compaction ability (Table 8.4).

Table 8.4 Linear regression parameters: average value (standard error)

Mixtures	Workability $V_m(10)$	Compactability k	R^2
CA_FT	18.890 (0.013)	7.837 (0.015)	0.9996
CA_HPAC	20.757 (0.009)	8.507 (0.010)	0.9998
CA_MTQ	17.300 (0.016)	8.120 (0.024)	0.9994
IT_FT	16.419 (0.020)	7.193 (0.028)	0.9987
IT_SMA	15.797 (0.014)	8.560 (0.020)	0.9995
IT_FINE	14.177 (0.018)	5.610 (0.025)	0.9983

Figure 8.3 shows the results in terms of compactability k and workability $V_m(10)$. It is possible to observe that, both at ÉTS and UNIVPM, the mixtures characterized by the highest compactability k are the gap-graded type (8.51 and 8.56 for CA_HPAC and IT_SMA, respectively). At ÉTS, all the three mixtures had similar values of k (between 7.84 and 8.51), preventing a distinction in terms of compaction behaviour among the studied materials. At UNIVPM, the differences between the mixtures are more visible. The mixture IT_FINE shows the best workability $V_m(10)$ (14.18%), even though the compactability k was the lowest among

all the studied mixtures (5.61), meaning that the high viscosity of the mortar due to the high amount of filler influenced the energy necessary to reach the target air voids. In terms of workability $V_m(10)$, mixtures produced at UNIVPM are generally characterized by better results. In particular, it is highlighted that the mixtures CA_HPAC and IT_SMA, which showed similar compactability values, are characterized by different values of workability (20.76% and 15.80%, respectively). Moreover, both at ÉTS and UNIVPM, the maximum density curves (CA_FT and IT_FT) were not the optimal gradations in terms of workability and compactability.

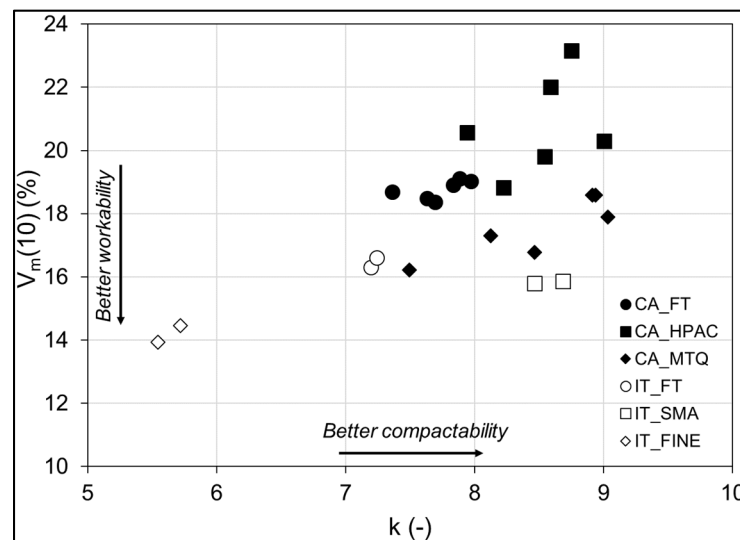


Figure 8.3 Results for k and $V_m(10)$ parameters

To describe the aggregate gradation two parameters are used (Ouchi et al., 1999). The first parameter G/G_{lim} is the ratio between the volume of the coarse aggregate fraction G and the total volume of aggregates G_{lim} . The lowest is this ratio, the lowest is the interaction and the friction between coarse particles. The second parameter S/S_{lim} is the ratio between the volume of the fine aggregate S (not including filler-sized particles) and the mortar volume S_{lim} (fine aggregate and filler-sized particles). This ratio represents the viscosity of the mortar. Values of both parameters can give an idea of the workability of the mixture, despite are characteristic of the aggregate blend. In this research, the threshold sieve to separate coarse from fine

aggregates was assumed as 2 mm, since it is the common sieve size to separate the mortar phase from the coarse fraction (Mignini et al., 2018a; Miljković & Radenberg, 2014; Underwood & Kim, 2013).

Figure 8.4 shows the values of G/G_{lim} and S/S_{lim} that characterize the six gradations studied. In addition, the characteristic values related to self-compacting concrete (SCC) and roller-compacted concrete (RCD) are reported (Ouchi et al., 1999). It must be highlighted that for SCC and RCD the values are related to a threshold sieve of 4.76 mm. As it can be seen, the studied mixtures are all situated in an intermediate region, since the mixtures do not contain enough filler to be comparable to SCC, but at the same time they still have a good percentage of mortar compared to the coarse fraction. As expected, the gap-graded gradations (CA_HPAC and IT_SMA) and the Fuller-Thompson curves (CA_FT and IT_FT) showed similar values. Moreover, the mixture closest to the SCC area, IT_FINE, is the mixture which was characterized by the better workability (lowest value of $V_m(10)$).

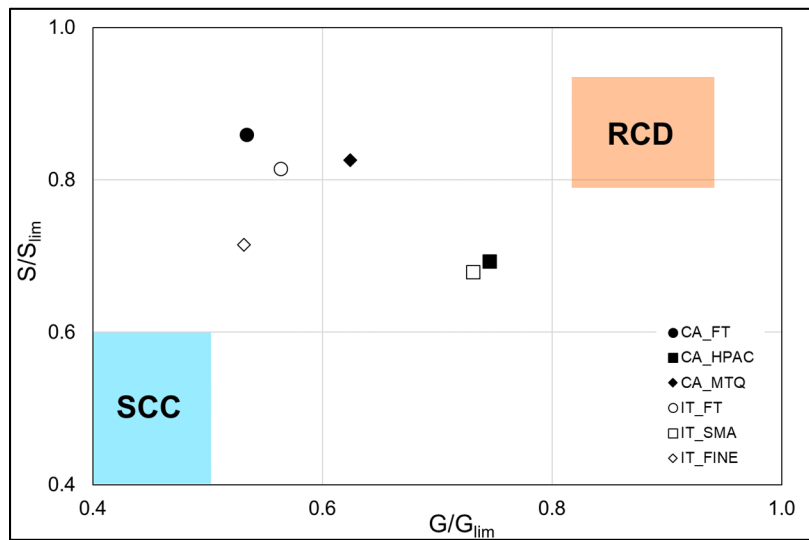


Figure 8.4 G/G_{lim} and S/S_{lim} values

Figure 8.5 shows the relation between the gradation parameters (S/S_{lim} , G/G_{lim}) and the mixture compaction parameters $V_m(10)$ and k . It can be seen that there is a clear distinction

between the gap-graded and the dense-graded mixtures. In fact, gap-graded mixtures are characterized by a value of S/S_{lim} below 0.7 and a G/G_{lim} value above 0.7 (shaded area of the plots). Furthermore, a relationship between the S/S_{lim} ratio and $V_m(10)$ and k in mixtures dense-graded (CA_FT, CA_MTQ, IT_FT and IT_FINE) seems to exist. More specifically, the higher the S/S_{lim} ratio, the lower is the workability and the higher is the compactability. This means that increasing the amount of filler-sized particles, the workability tends to increase.

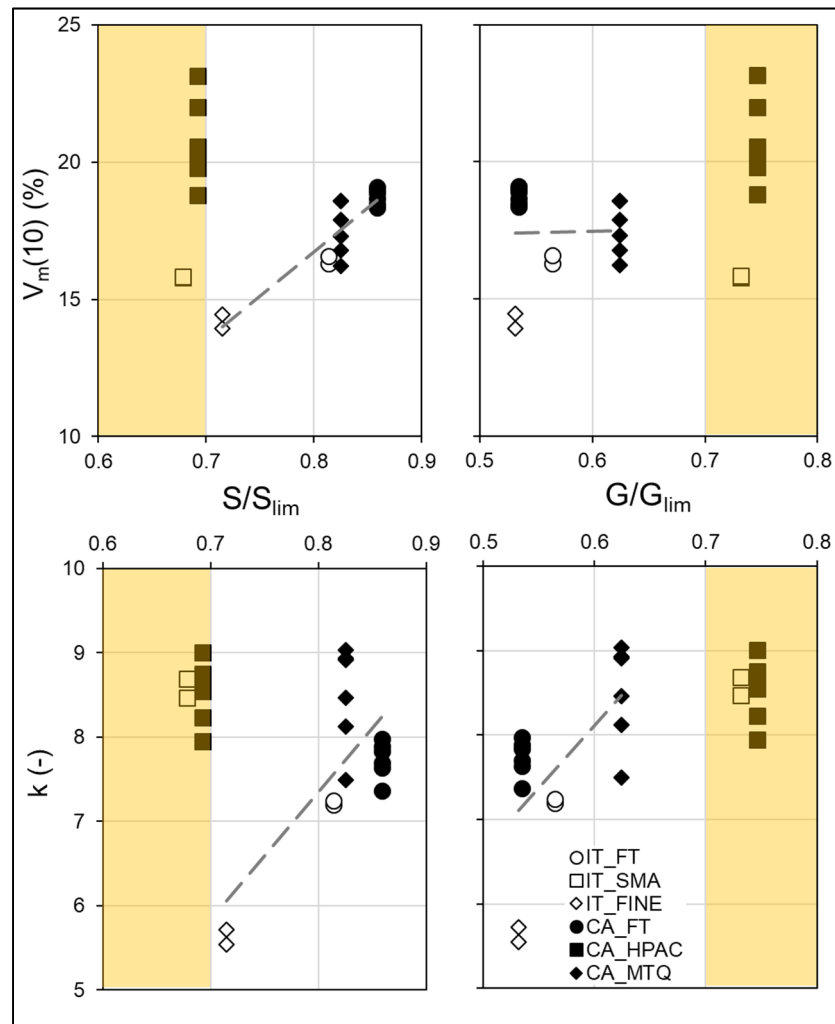


Figure 8.5 Correlation between gradation, workability and compactability parameters

Comparing the gap-graded mixtures CA_HPAC and IT_SMA, the workability is better in the mixture IT_SMA, due to the higher amount of filler compared to the mixture CA_HPAC (10.0% and 6.6%, respectively). The parameter S/S_{lim} is a pretty useful tool to preliminary predict the workability of the mix, which is mostly influence by the content of filler-sized particles in the mix. A clear relation between G/G_{lim} , $V_m(10)$ and k is difficult to be found. For dense-graded mixtures, high values of G/G_{lim} tends to decrease workability and it is linked to better compactability. On the other hand, gap-graded mixtures have comparable compactability but different workability, confirming that the coarse fraction does not have a clear effect.

In general, a good level of both workability and compactability can be reached with both dense-graded and gap-graded distribution (IT_FINE or IT_SMA), considering an adequate filler-sized particles content ($> 10\%$) in relation to the volume of coarse particles.

8.4.2 Mechanical properties and water loss

Figure 8.6 shows the results of the mechanical tests. For each mix, the water loss after curing is also reported. At ÉTS, ITS values highlighted a significant difference between the three mixtures. The reference mixture CA_FT is characterized by the highest resistance (714.4 kPa), whereas the mixtures CA_HPAC and CA_MTQ showed much lower strength (547.5 and 389.21 kPa, respectively). Considering that the volume of residual bitumen, water, cement and air is constant, this difference can be caused by an insufficient distribution of the binding phase in the specimen. Higher amount of water (which was fixed at 2%) could be needed to improve workability, compactability and tensile strength when the gradation is different from the maximum density distribution. On the other hand, the high ITR values demonstrate the very low water susceptibility of the studied mixtures.

At UNIVPM, ITS values do not highlight a real difference among the three gradations, which show a resistance between 499.1 kPa and 564.5 kPa. In terms of ITSM however, the effect of gradation is more visible, since the stiffness modulus is increasing with the filler content in the

mixture. This shows that ITSM is more sensitive to differences in mixtures behaviour than ITS.

Mixtures produced at ÉTS are characterized by water loss data close to 90-100%, despite the curing was performed only for 3 days. The small size of the specimen enhanced the water evaporation, whereas the aggregate gradation did not have a remarkable effect.

At UNIVPM, water loss was generally lower than what was observed at ÉTS, due to the bigger size of the specimens. As a consequence, the curing of 7 days at 25 °C was not enough to complete the development of the mechanical properties.

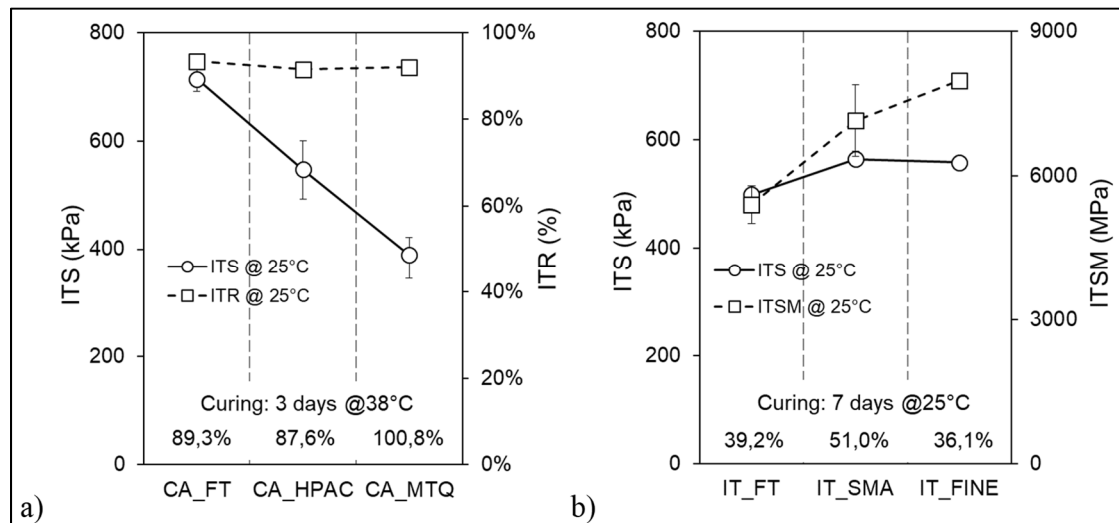


Figure 8.6 Mechanical tests results: a) ITS and ITR at ÉTS; b) ITS and ITSM at UNIVPM

8.5 Conclusions

This study focused on the influence of aggregate gradation on the workability and compactability of the CRM mixtures, as well as on the mechanical properties.

The work was extended to two laboratories, the École de technologie supérieure (ÉTS) in Canada and the Università Politecnica delle Marche in Italy, where similar mixtures were

prepared following the respective standard practices. However, this research did not compare the two laboratories procedures, due to the fact that many of the adopted parameters were different, such as cement content, bitumen content, voids in the mixture and curing period. From the results obtained, the following conclusions are listed:

- Analysing workability and compactability aspects, the six studied gradations were mostly influenced by the filler content, which enhanced the workability of the loose mixture. In fact, a higher percentage of filler generally caused an improvement of the workability, leading however to a lower compactability. At the same time, the coarse aggregate fraction did not seem to have a clear effect on the workability and compactability of the mixtures. Also, the parameters S/S_{lim} and G/G_{lim} , originally developed for SCC, may be useful parameters to analyse the workability and compactability of CRM.
- At ÉTS, the ITS test highlighted a difference between the three gradations studied, even though the binding phase volume (water, air, cement and residual bitumen) was constant. This means that when a gradation has a different composition compared to the maximum density curve, particular attention should be paid to the water content, which will not only improve the workability of the mix, but will also lead to a higher homogeneity inside the material.
- At UNIVPM, the high amount of water in the mixtures after curing made difficult to understand the effect of gradation in the mixtures studied. Nevertheless, a visible effect on stiffness modulus was brought by the filler content that led to higher stiffness values at higher dosages.

ITS and ITSM values may be affected by grading curves, however the effect of binders dosages is more important.

From the results obtained, it is possible to highlight the effect of gradation and the aggregates material on the properties of CRM. Further investigations are needed for a full understanding of the workability and compactability behaviour, especially in terms of effect of filler and

cement contents. At the same time, in such mixtures, bitumen is used in a solid state in form of dispersed particles and this could affect the compactability properties of the loose mixture.

CHAPTER 9

LABORATORY MECHANICAL CHARACTERISATION OF COLD RECYCLED MIXTURES PRODUCED WITH DIFFERENT RAP SOURCES

Simone Raschia^a, Andrea Graziani^b, Alan Carter^a, Daniel Perraton^a

^a Construction Engineering department, École de technologie supérieure (ÉTS) 1100, Notre-Dame Street West, Montreal, Canada

^b Department of Civil and Building Engineering, and Architecture, Università Politecnica delle Marche, Via Brecce Bianche, 60131 Ancona, Italy

Paper published in the journal Road Materials and Pavement Design, Taylor & Francis, March 2019

9.1 Abstract

Cold Recycled Mixtures (CRM) are composed of high amounts of Reclaimed Asphalt Pavement (RAP) together with bitumen emulsion. As additional binder, some ordinary cement is normally employed. Since RAP aggregates represents almost the entire solid structure, it is important to fully characterize Cement-Bitumen Treated Materials (CBTM) produced with different RAP materials.

This work focuses the characterization at small strain level, investigating the stiffness modulus at three testing temperatures; at the failure point, measuring the Indirect Tensile Strength; and studying the fracture behaviour, in Semi-Circular Bending Test configuration.

From the results, it is possible to confirm the influence of different RAP materials, also characterized by different aggregates Nominal Maximum Size. As a consequence, a reliable RAP classification can allow a better prediction of the final CBTM mechanical properties.

9.2 Introduction

In the perspective of new technologies recently studied in the road pavement framework, cold recycling brings high benefits in terms of economic, energetic and environmental sustainability (ARRA, 2001; Kuleshov, 2018). The most important aspect of these materials is the replacement of the purely bituminous phase of traditional hot mix asphalt (HMA) with bitumen emulsion, in which bitumen droplets are suspended in an aqueous phase. This characteristic allows to produce and compact these materials at ambient temperature (Stroup-Gardiner, 2011; Xiao et al., 2018). To confer additional resistance at short and long term, a small amount of hydraulic binders (between 1% and 3% by aggregates mass) is normally added to the mixture (Brown et al., 2000; Oruc et al., 2007).

Because of the presence of water, cement-bitumen treated materials (CBTM) show an evolutive behaviour of the mechanical properties, which are directly related to water evaporation, emulsion breaking and cement hydration. These aspects describe the curing phenomenon, which clearly depends on environmental conditions (Cardone et al., 2014; Graziani, Iafelice, et al., 2018; Ojum et al., 2014). In CBTM, most of the solid structure of the mix is normally composed of reclaimed asphalt pavement (RAP) aggregate, obtained from the milling and stockpiling of old pavements. RAP aggregate is commonly employed as a ‘black rock’, i.e. mineral aggregate coated by an aged bitumen film which does not contribute to the internal cohesion of the mixture.

When virgin aggregates are employed, the material is originally selected in accordance to the infrastructure importance and to the design traffic level; as a consequence, such aggregates have to respect both geometric and quality requirements. Hence, it is reasonable to suppose that, as quality levels exist for virgin aggregates, then it is possible to classify RAP aggregate with respect to its mechanical properties, in addition to the physical parameters normally studied. Perraton et al. (2016) proposed a procedure to characterize RAP materials using a Fragmentation Test, which links the RAP quality to the susceptibility to be fragmented under the dynamic action of the Proctor hammer. The material produced with this procedure which

results finer than a control sieve is used as an index to distinguish different classes of RAP aggregate (PCS index). This test campaign was performed at 3 temperatures and on 4 granular fractions; it was observed that the PCS index decreased as the testing temperature increased for all the fractions taken into account. Moreover, it has been shown that the value of PCS is mainly depending on the RAP binder content and aging; in fact, the PCS increases if the bitumen content increases and if the penetration decreases.

The objective of this research is to study the influence of different RAP sources on the mechanical properties of the CBTM mixtures produced. In order to give an exhaustive mechanical characterization, two RAP sources with different Nominal Maximum Size (NMS) were selected, and the experimental plan was developed at increasing deformation levels: in the elastic field, performing Indirect Tensile Stiffness Modulus (ITSM) test, at failure point, measuring the Indirect Tensile Strength (ITS), and characterizing the material according to the fracture behaviour, following the Semi-Circular Bending (SCB) test protocol.

9.3 Materials and methods

9.3.1 Materials

Several RAP sources were initially taken into account to select the more appropriate to be used to produce CBTM mixes. This selection was based on the fragmentation test (Perraton, Tebaldi, et al., 2016). The testing protocol consists in following the Modified Proctor procedure and measuring the percentage of fines produced. This amount corresponds to the passing to a control sieve (1.7 mm) and it is indicated as PCS index, which is used to discriminate different RAP sources. PCS indexes results for the RAP sources investigated are reported in Table 9.1. From the results obtained, RAP sources coming from Italy (from here on named RAP1) and NCAT-USA (RAP2) were chosen to be investigated, since they are characterized by the highest gap between PCS values. Table 9.2 summarizes the main properties of both materials.

Table 9.1 RAP sources classification (PCS index)

	Categories			
	B	C	D	E
PCS _{5/10} (%) @ 20°C	≤ 7	≤ 9	≤ 11	≤ 14
RAP sources investigated	RAP Italy	RAP Chambly RAP Bouval RAP St Isidore	RAP St Bruno RAP Sherbrooke	RAP NCAT

Table 9.2 Properties of RAP sources used

Property	Standard	Unit	RAP1	RAP2
Binder content	ASTM D6307	%	5.51	5.49
Nominal maximum particle dimension	ASTM D448-03	mm	16	10
Maximum specific gravity	ASTM C127-128	-	2.482	2.498
Water absorption	ASTM C127-128	%	1.10	1.08
Fragmentation @ 5 °C (fraction 5/10) – PCS	ASTM D1557	%	7.6	-
Fragmentation @ 20 °C (fraction 5/10) – PCS	ASTM D1557	%	6.7	13.9

Table 9.3 Bitumen emulsion properties

Emulsion properties	Standard	Unit	Value
Density	ASTM D6397-16	g/cm ³	1.0
Residue content	ASTM D6997-12	%	60.3
Storage stability @ 24 hours	ASTM D6930-10	%	0.6
Residual bitumen properties			
Needle penetration @ 25 °C	ASTM D5-13	mm	4.1
Softening point	ASTM D36-14	° C	48.6

The bitumen emulsion used in this work is a CSS-1 type (ASTM D2397) and the main properties are listed in Table 9.3. Following ASTM D6997 procedure, the bitumen residue was extracted and analysed too. The cement employed is a type GU (CSA A3000) with compressive strength at 28 days of 43.9 MPa (ASTM C109).

9.3.2 Mixtures

Three mixes were produced with RAP1 and RAP2: the first composed of RAP1 and aggregate NMS 16 mm (R1_16), the second produced with RAP2 and NMS 10 mm (R2_10), and the third mixture composed of RAP1 aggregate and NMS 10 mm (R1_10). The three granular compositions were corrected to follow the Fuller-Thompson curves related to NMS 10 and 16 (F/T D = 10 and F/T D = 16 respectively), hence limestone filler was added to the RAP material: 5.5%, 7.0% and 10% by mass of aggregates for R1_16, R1_10 and R2_10, respectively. The volume of cement, whose dosage was fixed at 1.5% by mass of dry aggregates, was also considered as part of the aggregate blend during mix design (Figure 9.1).

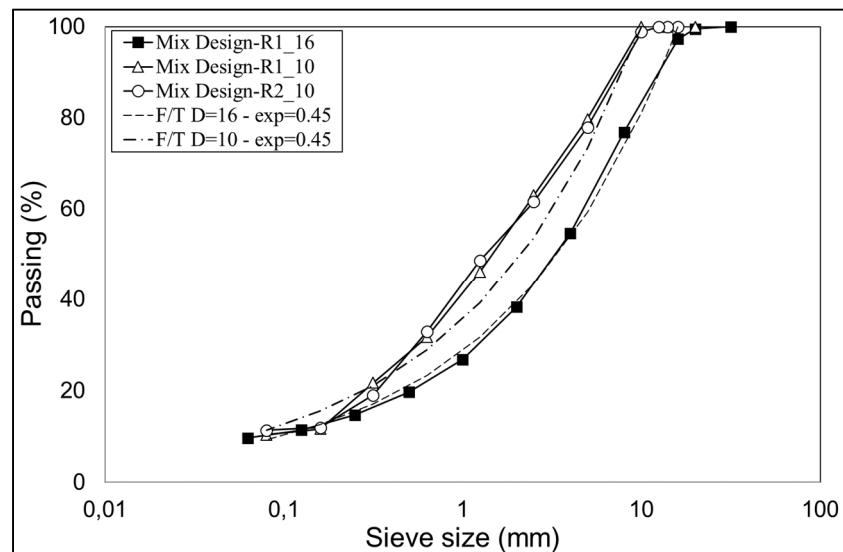


Figure 9.1 Aggregate blend gradations of the studied mixes

The residual bitumen content was fixed at 3% by mass of dry aggregates, which corresponds to 5% of bitumen emulsion dosage. The water content was adjusted through a mix-design procedure to optimize compaction and avoid voids saturation (Grilli et al., 2016). The quantity of total water in the mix, which was selected at 4.5%, includes the bitumen emulsion water and additional water. Dosages of water, residual bitumen and cement are the same for all the studied mixes.

The production of mixtures was carried out in two steps. In the first, RAP aggregates were oven-dried at 40°C until constant mass was reached. Afterwards, filler was added to RAP according to proportions, to obtain the target aggregate blend. Absorption water of RAP was then added to the material and mixed. The resulting humid blend was kept in a sealed plastic bag for at least 12 hours to allow moisture distribution. In the second step, the moist aggregates were placed into a bowl and cement, additional water and bitumen emulsion were added in this order. For each component addition, hand-mixing was performed until homogeneity was visually checked. The second step of mixture production normally required from 5 to 10 minutes.

9.3.3 Specimens compaction and curing

Compaction was performed immediately after mixing, by means of a gyratory compactor, using a mould with diameter of 150 mm, constant pressure of 600 kPa, gyration rate of 30 rpm and external inclination angle of 1.25°. The gyratory compactor allows to monitor the total volume of the mix at each gyration. In this way, two important volumetric parameters can be calculated: the Voids in the mixture (V_m), which is the volume percentage of the compacted mixture occupied by air and intergranular water, and the Voids Filled with Liquids (VFL), which represents the degree of voids in the mineral aggregate filled by the bitumen and water phases:

$$V_m(\%) = \frac{V_{V,A} + V_{W,I}}{V} \cdot 100 = \frac{V - (V_S + V_C + V_{B,R})}{V} \cdot 100 \quad (9.1)$$

$$\text{VFL (\%)} = \frac{V_{B,R} + V_{W,I}}{V_{V,A} + V_{W,I} + V_{B,R}} \cdot 100 = \frac{V_{W,I} + V_{B,R}}{V - V_S - V_C} \cdot 100 \quad (9.2)$$

where V is the total volume of the specimen, V_S is the bulk volume of aggregates (and hence includes the volume of absorbed water), V_C is the volume of unhydrated cement, $V_{B,R}$ is the volume of residual bitumen from emulsion, $V_{W,I}$ is the volume of intergranular water and $V_{V,A}$ is the volume of air. It is important to highlight that the residual bitumen from the emulsion is considered totally effective. During compaction, at increasing energy corresponds a decreasing value of V_m , whereas the value of VFL increases until the volume of air in the mixture approaches zero. If compaction continues, liquids are usually expelled out of the material, changing drastically its composition. Hence, it is important that no material loss occurs during this process.

In order to have specimens ready for testing, compaction was performed at fixed height (63.5 mm, 75 mm and 120 mm), and the mixture quantity was calculated to reach a V_m^0 value of $12 \pm 1\%$ and $73 \pm 1\%$ of VFL^0 (2420 g, 2850 g and 4560 g, respectively). V_m^0 and VFL^0 refer to values of both parameters at the end of compaction, when curing starts. The volumetric composition and compaction parameters of the compacted specimens for each mix are shown in Table 9.4, in which the RAP content refers to the saturated surface dry density. It can be observed that, at the end of compaction, the three mixtures are composed of the same volumetric proportions between aggregate blend, cement, residual bitumen, water and air voids. A total of 27 specimens were produced with the same procedure. Compactability aspects related to the same mixtures treated in this work are exhaustively investigated by Raschia, Graziani, Carter, & Perraton (2019). It was found that the RAP source affected the workability of the mix, since RAP2 required less energy than RAP1. In the same way, also the aggregate NMS affected the compaction of the mixtures. In fact, the CBTM with higher NMS globally showed a better workability and compactability. Furthermore, the specimens' height did not affect compactability of the material.

Table 9.4 Volumetric characterization of the compacted mixes

Element ^(a)		R1_16	R1_10	R2_10
RAP material	V_S^0	77.0	76.3	73.4
Filler		4.5	5.2	8.3
Unhydrated cement	V_C^0	1.0	1.0	1.0
Residual bitumen	$V_{B,R}^0$	5.9	5.9	5.9
Bitumen emulsion water	$V_{W,I}^0$	3.9	3.9	3.9
Additional water		3.0	3.0	3.0
Air	$V_{V,A}^0$	4.7	4.7	4.5
Total		100	100	100
V_m		11.6	11.6	11.4
VFL		73.1	73.1	74.0
Number of gyrations		55	125	53
⁽¹⁾ Percentages of each element are related to the total volume of the compacted specimen				

Compacted specimens were demoulded and weighted to check if any material loss occurred during compaction. After that, they were cured in an environmental chamber for 14 days at 40 ± 2 °C and $55 \pm 5\%$ of relative humidity. These parameters were decided in order to reach a good level of curing in a reasonable amount of time.

Throughout the curing process, the material is characterized by an evolution of the volumes related to some elements contained in the mixture. In the fresh state, the volumetric composition is well-known because based on the production phase, while the composition during curing and service life is related to the change of volumes (Grilli et al., 2016; Grilli et al., 2012) (Figure 9.2).

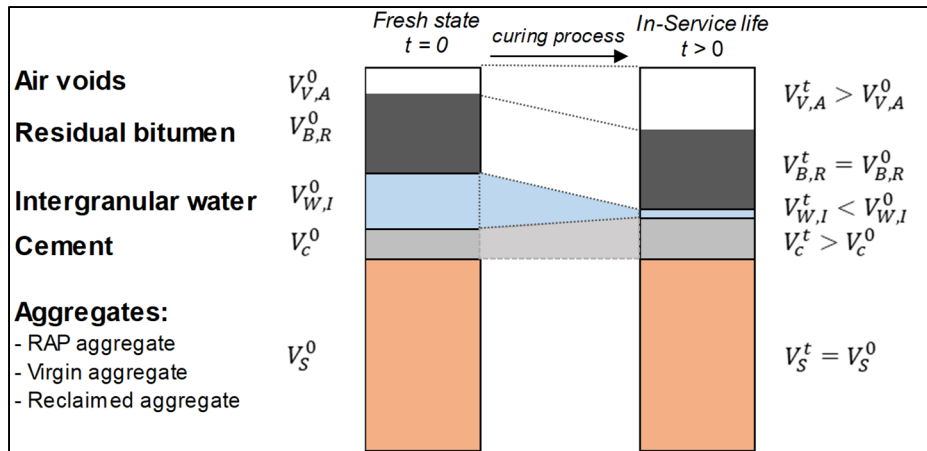


Figure 9.2 Volumetric characterization of CBTM mixtures

The volume of the aggregate phase (RAP, Virgin and Reclaimed aggregates) is not changing during curing ($V_S^0 = V_S^t$), as well as the volume occupied by the residual bitumen of the bitumen emulsion ($V_{B,R}^0 = V_{B,R}^t$). The volume of air voids increases with time ($V_{V,A}^0 < V_{V,A}^t$), whereas the volume of water decreases ($V_{W,I}^0 > V_{W,I}^t$) because of evaporation and cement hydration. In fact, cement volume increases ($V_C^0 < V_C^t$) and the value for V_C^t can be estimated as the amount of unhydrated cement V_C^0 plus the water chemically bonded (Brouwers, 2004). This approach requires a thorough dosage of the constituents at the moment of the mixture production, as well as a continuous monitoring of the water loss evolution along curing.

In order to relate the residual amount of water in the mixes to their mechanical properties, the water loss ΔW was measured after 1, 3, 5, 7 and 14 days:

$$\Delta W^{(t)} = \frac{W^0 - W^{(t)}}{W_{TOT}} \cdot 100 \quad (9.3)$$

where $\Delta W^{(t)}$ is the water loss (%) at the curing time t , W^0 is the initial mass of the specimen; $W^{(t)}$ is the mass of the specimen at the curing time t and W_{TOT} is the total amount of water in the specimen.

9.3.4 Testing

The experimental plan involved different testing procedures to give a wide mechanical characterization of the CBTM studied: Indirect Tensile Stiffness Modulus test (ITSM), Indirect Tensile Strength test (ITS) and Semi-Circular Bending test (SCB).

The ITSM test is performed following the standard EN 12697-26 (Annex C). The test measures the stiffness modulus by a series of 10 applications of vertical load pulses characterized by a rise-time of 124 ± 4 ms. The tests are performed in strain control mode with a repetition time of 3.0 s. For each pulse the stiffness modulus is obtained with Eq. (5.8):

$$\text{ITSM} = \frac{F \cdot (R + 0.27)}{L \cdot H} \quad (9.4)$$

where F is the peak value of the applied repeated vertical load, H is the amplitude of the horizontal deformation (fixed at 7 ± 2 microns), L is the mean thickness of the specimen and R is the Poisson's ratio (assumed as 0.35).

ITSM value for each mix was calculated as an average of three repetitions along both diameters on specimens 75 mm thick. The test was performed at three temperatures, -10 °C, 0 °C and 10 °C, after a conditioning time of 4 hours at each temperature.

The ITS was carried out following the standard ASTM D 6931. The test allows measuring the tensile strength developed along the vertical diameter plane of the specimen which undergoes a compressive load. The test was performed at a constant loading rate of 50 mm/min and the tensile strength is calculated as:

$$\text{ITS} = \frac{2 \cdot P}{\pi \cdot D \cdot t} \quad (9.5)$$

where ITS is the tensile strength, P is the maximum load, t is the specimen height and D is the specimen diameter. The ITS was measured on three specimens 63.5 mm thick for each studied mix at a testing temperature of 25 °C, after a conditioning time of 4 hours.

The SCB test was performed following the standard ASTM D 8044. SCB test allows measuring the strain energy necessary to start the crack propagation from a given notch. For each mix, three notch depths a are required: 25 mm, 32 mm and 38 mm. In this test, a semi-circular shaped specimen is placed in a three-points bending configuration and loaded with increasing force until failure.

Four repetitions are performed at each notch depth and for each test the Strain Energy to Failure U is measured as the area under the load-displacement curve, up to the maximum load. U normally decreases when the notch depth increases, and the slope of the linear regression line represents the critical value of J-Integral (J_c), which is determined using Eq. (5.10).

$$J_c = -\frac{1}{b} \left(\frac{dU}{da} \right) \quad (9.6)$$

where b is the specimen thickness and $\left(\frac{dU}{da} \right)$ is the slope of the linear regression line which represents the relation between the calculated Strain Energy U and the notch depth a .

J_c value is used by the elastic-plastic fracture mechanics (EPFM) theory to describe the global fracture behaviour of the material, represented as the variation of the total energy of the system with respect to the crack size variation (Anderson, 2017; Dongre et al., 1989). In other terms, J_c is the amount of energy spent to increase the crack size, and it decreases when the crack size increases.

Results of the SCB test can be analysed in terms of linear-elastic fracture mechanics (LEFM) calculating the critical stress intensity factor K_{IC} (or fracture toughness). K_{IC} represents the amplification rate that the remote stress applied to the material has at the proximity of a flaw, and which starts the crack propagation (Anderson, 2017).

For the SCB, an equation was obtained by a FEM analysis by Lim, Johnston, & Choi (1993) to calculate the K_{IC} value:

$$K_{IC} = \frac{F}{D \cdot t} \cdot \sqrt{(\pi a)} \cdot Y_I \left(\frac{a}{W} \right) \quad (9.7)$$

where F is the force, D is the specimen diameter, t is the specimen thickness and Y_I is a dimensionless function which depends on notch depth a and specimen height W .

Lim et al. (1993) provides a relationship between Y_I and $\left(\frac{a}{W}\right)$ for several s/D ratios (0.8, 0.67, 0.61, 0.5), where s is the space between the roller bearings of the testing configuration. This aspect of Lim's equation is of fundamental importance because in ASTM standard, which was followed in this work, the SCB configuration is characterized by a value of $s/D = 0.847$. By a simple linear regression, it was possible to extrapolate a value of Y_I for the testing conditions of the present study (Figure 9.3).

Specimens for testing were obtained by compacted specimens 120 mm thick, which were sawed at the end of curing in two circular specimens 57 ± 1 mm thick. The circular specimens were then divided in four semi-circular specimens to be tested at one notch depth. The procedure was repeated for the other two notch depths, for a total of 12 specimens for each of the studied mixes.

The testing temperature, for HMA mixes, should be selected based on the climatic intermediate performance grade temperature of the bitumen, $PG\ IT$. When bitumen emulsion is used for cold recycling, this approach is difficult to apply. However, for a common bitumen normally used in Canada for base courses with PG 58-28, the $PG\ IT$ is 19 °C. For this reason, SCB test was performed in an MTS device with controlled air temperature at 20 ± 2 °C.

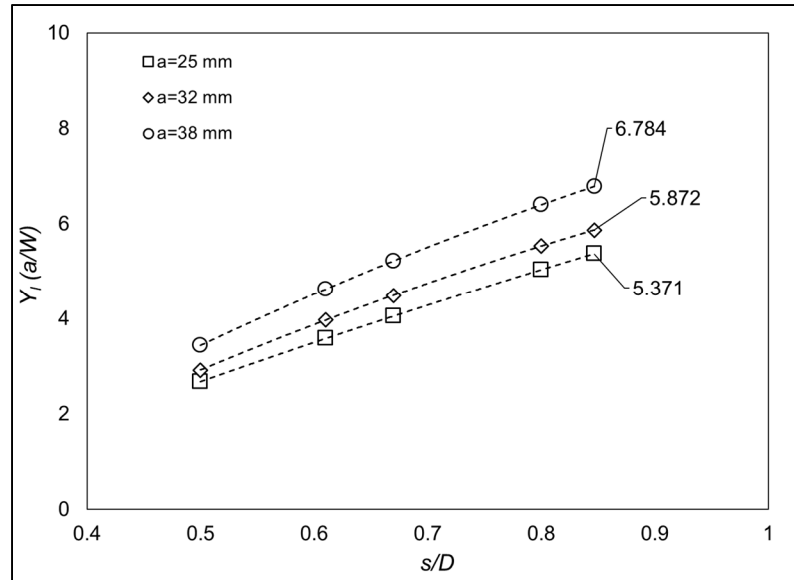


Figure 9.3 Determination of Y_1 factor for different notch depths (25 mm, 32 mm and 38 mm) for a $s/D = 0.847$

9.4 Results and discussion

9.4.1 Water Loss

Figure 9.4 illustrates the water loss evolution along curing time. The three graphs show the behaviour of the mixes R1_16, R1_10 and R2_10, respectively and the curves illustrated in each graph are related to different specimens height (i.e. 63.5, 75 and 120 mm, respectively). The $\Delta W^{(t)}$ measurements were modelled by means of a non-linear hyperbolic model similar to the Michaelis-Menten model (Michaelis et al., 2007):

$$y(t) = y_1 + \frac{(y_A - y_1) \cdot (t - 1)}{(t - 1) + (H - 1)} \quad (9.8)$$

where $y(t)$ is the material property under investigation (in this case, water loss), t is the curing time (days), y_A is the asymptotic value, y_1 is the value related to 1 day and H is the time (days) for $y(t)$ to reach half of the gap between y_A and y_1 .

In Figure 9.4 it is possible to observe the superposition of the model on the experimental data, together with a graphical description of the model parameters y_A , y_1 and H which are reported in Table 9.5.

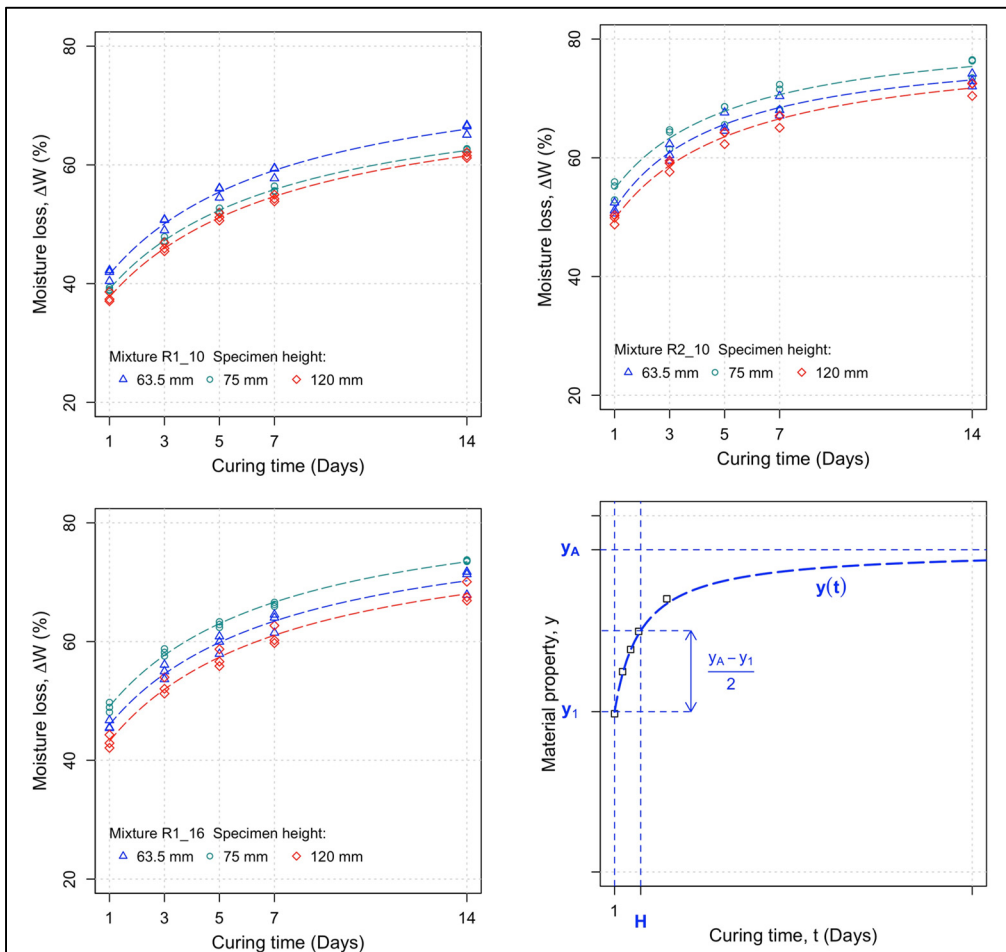


Figure 9.4 Water Loss model and results

Analysing in general the three parameters, it is possible to state that they are slightly sensitive to the specimens height. The mix R1_10 is characterized by the lowest value of the asymptotic water loss y_A (75.6%), which means that the mix loses less water than the other two mixes, which instead are comparable (82.8% and 80.6%).

Table 9.5 Fitting parameters of the water loss model

Mixture	R1_16			R1_10			R2_10		
Specimen type	ITSM	ITS	SCB	ITSM	ITS	SCB	ITSM	ITS	SCB
Specimen height (mm)	75	63.5	120	75	63.5	120	75	63.5	120
y_A (%)	85.6	82.4	80.5	74.2	78.6	74.1	82.5	79.7	79.7
y_1 (%)	49.1	46.0	43.2	39.1	41.6	37.7	54.7	51.4	49.7
H (days)	7.5	7.5	7.5	7.6	7.7	7.9	5.5	5.0	5.7
Std. error (%)	0.59	1.40	1.38	0.38	0.88	0.64	1.67	1.27	0.98

At the same time, in terms of water loss after one day, the mix R1_10 showed the lowest y_1 value, 39.5%. This is probably due to the higher compaction energy applied to the mix R1_10, which probably led to the fragmentation of some RAP aggregate particles. As a consequence, the internal structure of the specimen could be characterized by different voids distribution and smaller pores. However, it is important to highlight that a difference in water loss of 5% corresponds to a weight loss of 0.2% by aggregate mass.

Focusing on the H parameter, it is possible to highlight the influence of the RAP source only, whereas NMS of aggregates did not have an impact. In fact, the mixture R2_10 has a faster water loss at short term compared to the mixes produced with RAP1.

9.4.2 Indirect Tensile Strength Modulus

Figure 9.5 shows results from ITSM test. At -10 °C, the mix R1_16 shows a slightly higher ITSM value if compared to the other two, but at 0 °C and 10 °C all the three mixes are close enough to consider their stiffness independent from the type of aggregates used. The three mixes also have similar temperature sensitivity. In general, the test tends to evaluate the tensile stiffness, in which the binding phase should play the most important role. The three mixes are characterized by the same volume of residual bitumen and cement and the RAP binder

contribution to the resilient deformation is low in the studied temperature range, which is below 10 °C. These considerations justify why it is difficult to discriminate the mixtures studied in terms of stiffness.

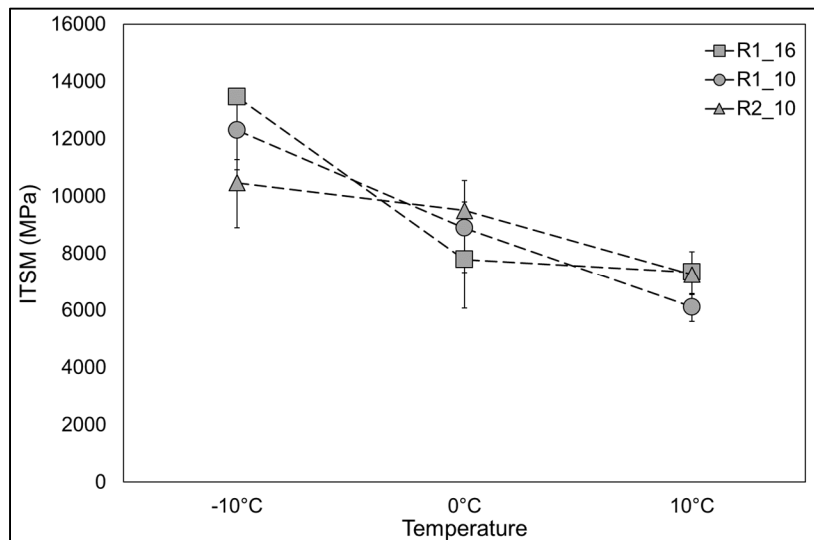


Figure 9.5 Indirect Tensile stiffness modulus results

9.4.3 Indirect Tensile Strength

Figure 9.6 shows the results related to the ITS test. The mixture with higher resistance is the one produced with RAP1 but with reduced NMS (R1_10). The difference with the same material, but higher NMS (R1_16), is probably due to the higher specific area characteristic of materials with smaller particles. The higher specific area of the aggregate blend lead to a better distribution of the bitumen emulsion which results in a better coating and in an increase of the strength.

The effect of the RAP source used to produce the CBTM mixes had a strong effect on ITS results. In fact, the mix R1_10 showed a significantly different strength if compared to the mix R2_10 (819 kPa and 525 kPa respectively). Since the filler amount in the aggregate blend is low compared to RAP, this gap must be related to the RAP source, which clearly plays an

important role on the global ITS resistance of the mix. Apparently, different RAP sources do have an influence on the cohesion between the aggregate and bituminous phases, and they should not be considered any further similar one to another.

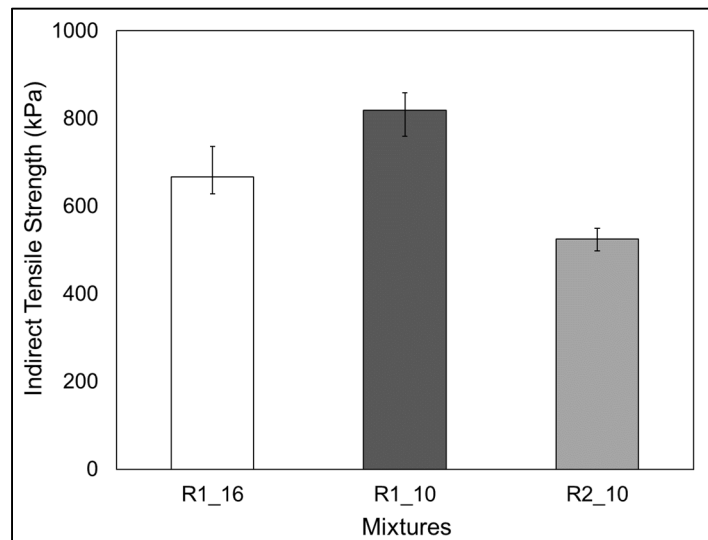


Figure 9.6 Indirect Tensile Strength results

9.4.4 Semi-Circular Bending Test

Figure 9.7 and Figure 9.8 show SCB test results in terms of Strain Energy to Failure U and critical Energy Release Rate J_c , respectively. In Figure 9.7 it is possible to observe the experimental results for U as a function of the measured notch depth. The points related to each mixture are interpolated by a regression line, whose slope is indicated with the J_c value.

It is highlighted that the Strain Energy U is decreasing with increasing of the notch depth in all the studied mixtures. The mixture R1_10 has globally higher values of U , which means that the mixture, in presence of flaws, is able to store more energy applied by external forces than the other two mixes, before that cracking occurs. Increasing the aggregates NMS, the influence of the notch depth is less evident (mix R1_16), since the slope of the linear regression is lower. The mix R2_10 is characterized by the lowest U values, expressing a global higher sensitivity

to crack propagation. What is evident is that the slopes of the curves related to mixes R1_10 and R2_10 are very similar. Figure 9.8 highlights that the J_c values are very close when mixtures with same NMS are considered (R1_10 and R2_10). J_c represents a global behaviour of the material in terms of fracture resistance, which is normally above 0.5 kJ/m^2 in traditional HMA mixes (Mohammad et al., 2004; Molenaar et al., 2003; Wu et al., 2005); for the studied mixes, values around 0.4 kJ/m^2 were obtained for mixes R1_10 and R2_10, whereas R1_16 showed the lowest value (0.23 kJ/m^2). Lower J_c values lead to flatter regression lines, which directly means that a small crack or a big crack can propagate with similar values of energy.

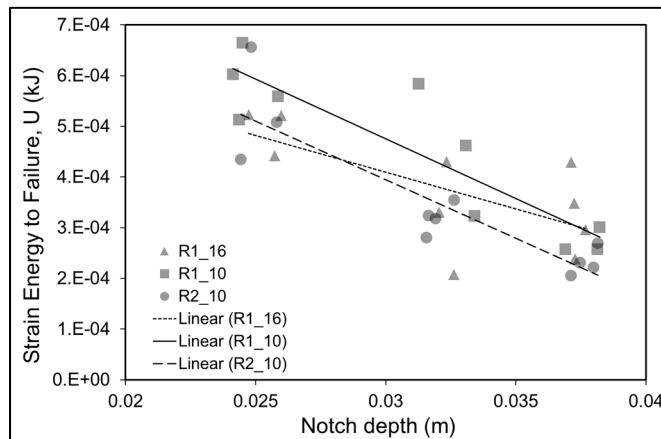


Figure 9.7 Strain Energy to Failure U results

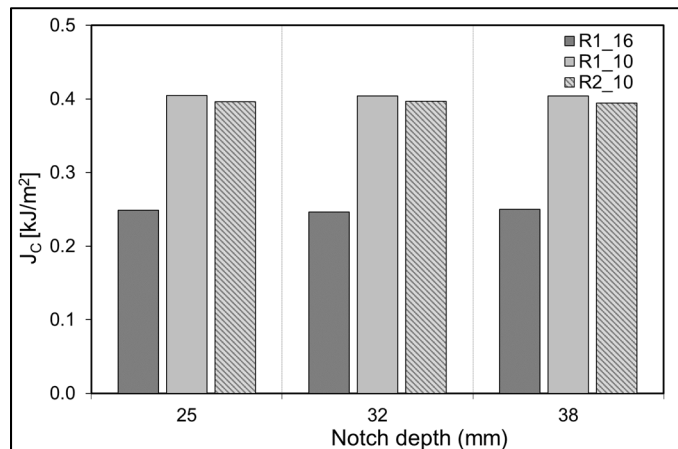


Figure 9.8 Critical Energy Release Rate J_c results

Figure 9.9 shows K_{IC} results. It is possible to observe a clear distinction among the three mixes at notch depths of 25 and 32 mm, whereas at a notch depth of 38 mm the three values are similar. This means that at a certain depth of the fracture the three materials have similar resistance. On the contrary, at smaller sizes of the notches, the mix R1_10 is characterized by the highest level of toughness (around $4 \text{ N/mm}^{3/2}$) while the two mixes R1_16 and R2_10 show values of K_{IC} close to $3 \text{ N/mm}^{3/2}$. K_{IC} directly describes the amplified stress at the crack tip, and its critical value indicates the beginning of the crack propagation. In other terms, it can be seen as the maximum resistance to fracture of the binding mastic, since the low level of cohesion due to the presence of dispersed emulsion should not cause the fracture of the aggregate components. As a consequence, a high value of K_{IC} corresponds to a better dispersion and coating of the bituminous phase, which in this case should depend on the aggregate composition and shape.

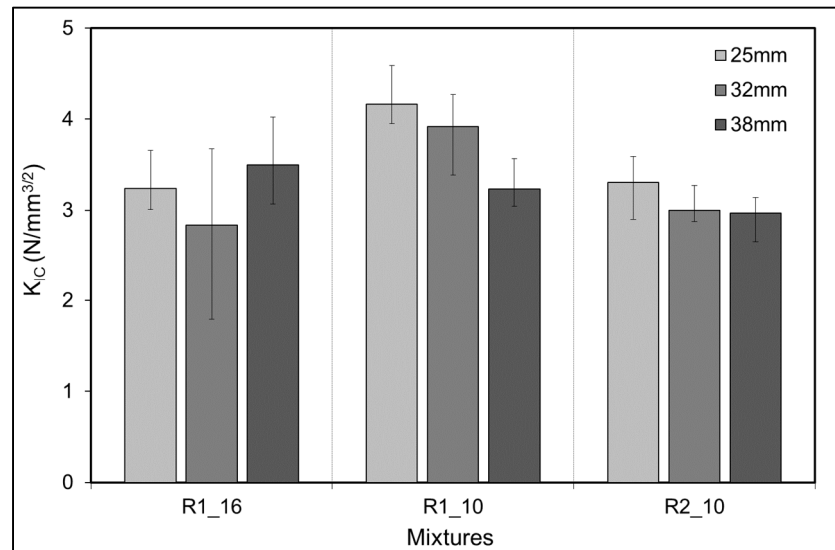


Figure 9.9 Critical Stress Intensity Factor K_{IC} results

9.5 Conclusions

This study aimed to mechanically characterize CBTM mixtures produced with two RAP sources and different NMS. To achieve that, a wide experimental program was carried out

producing three mixes with the same volumetric composition, in terms of aggregate blend, water content, bitumen emulsion content, cement content and air voids content. The water loss along curing, the stiffness (ITSM), the strength (ITS) and fracture parameters (U , J_c , K_{IC}) obtained with the SCB test, were measured.

The effect of nominal maximum size of the aggregate can be summarized as follows:

- The higher aggregate size led to a higher water loss, because of the different internal structure of the material caused by a different compaction effort;
- The stiffness of the mixtures is characterized by the composition of the binding phase (bitumen, cement, water and air), hence the aggregate size did not influence the modulus values and the temperature sensitivity;
- In terms of ITS and SCB results, a higher aggregate size gave lower values of strength and fracture toughness. A value of J_c close to the minimum standard requirement for HMA was obtained with the lowest aggregate size.

The effect of RAP source can be summarized as follows:

- The higher compaction effort required by one source of RAP probably led to fragmentation of aggregate particles and to different water evaporation trends if compared to the other source;
- The RAP source did not affect the ITSM stiffness values and temperature sensitivity, since both are parameters mainly dependant on binding phase composition, which was same;
- In terms of resistance, the RAP source with lower fragmentation index showed higher ITS and fracture toughness values. On the other hand, the J_c values were very similar; this means that the RAP source affects the crack initiation but does not influence the crack propagation mechanism.

Results globally showed that the interaction between the binding phase (bitumen and cement) and the aggregate surface is different if different RAP sources are used. This could be caused by the compatibility between the two bituminous components (RAP binder and residual

bitumen from the emulsion). Future works should focus on viscoelastic properties of such mixes and to investigations directly related to job field applications.

CHAPTER 10

EFFECT OF RAP SOURCE ON COMPACTABILITY AND BEHAVIOUR OF CRM MIXTURES IN THE SMALL STRAIN DOMAIN

Simone Raschia^a, Taher Baghaee Moghaddam^b, Daniel Perraton^a, Hassan Baaj^b, Alan Carter^a, Andrea Graziani^c

^a Construction Engineering department, École de technologie supérieure (ÉTS) 1100, Notre-Dame Street West, Montreal, Canada

^b Centre for Pavement and Transportation Technology, Department of Civil and Environmental Engineering, Faculty of Engineering, University of Waterloo, Waterloo N2L 3G1, Canada

^c Department of Civil and Building Engineering, and Architecture, Università Politecnica delle Marche, Via Brecce Bianche, 60131 Ancona, Italy

Submitted and under review with the journal *Journal of Materials in Civil Engineering*, ASCE, May 2020

10.1 Abstract

Cold recycled materials (CRM) belong to modern recycling techniques employed in maintenance and rehabilitation of pavement structures with significant economical and environmental benefits. CRM mixes are produced at ambient temperature with the contribution of bitumen emulsion or foamed bitumen as binding agent, and the aggregate phase is composed mainly of reclaimed asphalt pavement (RAP). This paper investigates the compactability of two RAP sources and their effect on the behaviour of CRM mixtures tested in the small strain domain. The compactability was studied using experimental results and the compressible packing model (CPM). Thereafter, complex modulus tests of the CRM mixtures produced were conducted, and results were modelled using the DBN model. Findings showed that, despite the same gradation and formulation of CRM mixes, one RAP source required almost half of the compaction energy than the second source to reach the design air voids content. Furthermore,

the rheological analysis results highlighted the impact of the RAP source on the behaviour of the CRM mixes in the small strain domain.

10.2 Introduction

Due to environmental and economic measures, the last decade has witnessed the development of new techniques in road pavement construction. One of these techniques employs cold recycled materials (CRM) which was developed for the pavement structural layers (binder, base and sub-base layers) (Gandi et al., 2017; Grilli et al., 2019). The main advantage of CRM is the possibility to produce them at the ambient temperature (generally higher than 10°C). This is much lower than the temperature needed for conventional hot mix asphalt (HMA) (Gandi et al., 2019; Raschia et al., 2020). The temperature reduction is possible due to the use of bitumen emulsion or foam with lower viscosities than traditional bitumen, which also allow the CRM mixture to be placed and compacted at lower temperatures. In addition, the workability and compactability of the mixes are ensured by addition of water (Cross, 2003; Grilli et al., 2016; Wendling et al., 2014). Due to the presence of water in the mix, the early-life mechanical properties of CRM mixtures are usually low, and therefore hydraulic binders, such as cement, are added to act as co-binder with the bitumen. In this case, the material is called cement-bitumen treated material (CBTM) (Bocci et al., 2011; Brown et al., 2000; Fang et al., 2016; Mignini et al., 2018b; Miljković et al., 2019). The curing process of the material is an important aspect that requires time in order to let the water inside the mixture to evaporate, and to allow the reaction with hydraulic binders, when used. In this regard, the ambient conditions such as temperature and humidity play major roles in the determination of the curing rate and the properties development of cold mixtures (Cardone et al., 2014; Gandi et al., 2019; Graziani, Iafelice, et al., 2018; Kim et al., 2011; Serfass et al., 2004).

Generally, bitumen emulsions used in cold recycling projects are the cationic slow-setting type. Such characteristics are conferred by the chemical composition of the emulsion, in particular by the pH, the type and dosage of emulsifier, etc. Cationic slow-setting emulsions do not break immediately, and they ensure a certain degree of stability in order to have a compactable

mixture (Needham, 1996; Salomon, 2006). However, the breaking of the emulsion is fundamental to create a binding structure in the aggregate blend. The affinity (and adhesion) between bitumen emulsion and aggregate surface is an important parameter in mix durability and needs to be evaluated preliminarily when designing a cold mixture (Cardone et al., 2018; Miller et al., 2010). Nonetheless, bitumen emulsions are often provided by industrial producers, and it is not possible to know the exact components and formulation followed for the production.

In cold in-place recycling projects, the aggregate blend is mainly composed of reclaimed asphalt pavement (RAP). Identification of the RAP is generally difficult, since no specific procedure has been developed so far, and standards related to virgin aggregates are applied to RAP aggregate (Asphalt Academy, 2009; Perraton, Tebaldi, et al., 2016; Tebaldi et al., 2018; Tebaldi et al., 2014). However, since RAP is employed at the ambient temperature, it is reasonable to consider it as a “black rock”, which means that the aged binder in the RAP does not reactivate and blend with the emulsion’s bitumen. A finite element method (FEM) simulation demonstrated that the presence of RAP in cold mixtures can improve mechanical properties, due to the fact that the aged binder acts as a cushion between the aggregate phase and the residual bitumen, reducing stress and strain at the interface (Yan et al., 2014).

In the literature, Raschia et al. (2019) showed that the RAP gradation can influence the workability and mechanical properties of the CRM mixtures. In particular, mixtures with higher filler-sized particles content were characterized by a better workability, computed as the voids in the loose mixture at the beginning of compaction. One way to optimize the aggregate gradation is to use the compressible packing model (CPM), introduced by de Larrard (1999) for high-performance Portland cement concrete (PCC). It predicts the packing density of aggregate blends, cements and cementitious materials, defined as the ability of the mixture to fill the volume of voids available. The CPM is a mathematical model and considers contemporarily the effects of shape, texture and particles’ gradations. Moghaddam et al. (2018) used the model for optimization of asphalt concrete mix design and showed that using the CPM

model as an optimization tool resulted in aggregate distributions close to the maximum density curve.

The objective of this study is evaluating the effect of the RAP source on the compactability and rheological properties of CRM mixtures. The first aspect was investigated on fresh mixtures by means of the CPM model and by the evaluation of morphological parameters of the RAP aggregate particles. The second objective was achieved on cured mixtures, performing complex modulus tests and by applying the DBN model to describe the rheological properties.

10.3 Analytical models

The effects of the RAP source on the compactability and the viscoelastic properties of CRM materials was investigated by the application of two models in relation to the experimental results. The CPM model was used to evaluate compactability and the DBN model to analyze viscoelastic properties.

10.3.1 Compressible Packing Model (CPM)

An important aspect when evaluating the compactability of a HMA or CRM mixture is the porosity of the aggregate blend, which can be defined as follows:

$$\text{Porosity} = \left(1 - \frac{V_S}{V_T}\right) \cdot 100\% \quad (10.1)$$

where V_S is the solid volume of the aggregate blend calculated as the ratio between the mass and the bulk specific gravity of the aggregate particles, and V_T is the total bulk volume of the aggregate blend, considering the volumes of aggregates and the voids. The ratio between the solid volume and the total volume is called packing density, β . As expected, when the packing density increases, the porosity of the aggregate blend decreases. This is possible when fine and coarse particles are well proportioned, and the smaller particles can fill the voids in the coarse

particles skeleton. Particles' shape, texture and grading distribution determine the degree of aggregate interlock and as a consequence of the porosity, since voids will always remain unfilled.

The compressible packing model (CPM) allows optimizing the packing ability of aggregate blends combining mathematically the effects of shape, texture and grading of particles. This is possible if the packing density β_i of each aggregate fraction i , the size distribution of aggregates and the compaction energy used are known. The packing density of each fraction β_i is measured experimentally and such value collects both physical and morphological properties. The CPM model provides a virtual packing density which is the maximum density that can be obtained considering the particles' original shapes. In fact, it was developed to quantify the volumetric percentage of several aggregate fractions to obtain the minimum voids content in the aggregate blend. This model has been developed and used for concrete proportioning using crushed aggregates (De Larrard, 1999; Moghaddam et al., 2018; Tierrie et al., 2016). The virtual packing density Y_i for an aggregate blend (when class i is dominant) is calculated using the following equation:

$$Y_i = \frac{\beta_i}{1 - \sum_{j=1}^{i-1} \left[1 - \beta_i + b_{ij} \beta_i \left(1 - \frac{1}{\beta_j} \right) \right] y_j - \sum_{j=i+1}^n \left[1 - a_{ij} \beta_i / \beta_j \right] y_j} \quad (10.2)$$

Where n is the total number of classes, β_j is the packing density of each class, y_j is the volume fraction of each class in the aggregate blend, and a_{ij} and b_{ij} are parameters related to "loosening effect" and "wall effect", respectively. The term "class" indicates either a specific aggregate fraction (d/D) or a full aggregate gradation ($0/D$). According to Eq. (10.2), Y_i can vary between β_i (if only one class is used) and 1 (no air voids in the aggregate blend). The "wall effect" is the interaction between the particle and any type of wall, such as a mould, but it can also occur between particles belonging to different classes. The "loosening effect" is caused by an excessive amount of fines that will push away the coarse particles. They are determined as:

$$\text{Loosening effect: } a_{ij} = \sqrt{1 - \left(1 - \frac{d_j}{d_i}\right)^{1.02}} \quad \text{when } d_j \leq d_i \quad (10.3)$$

$$\text{Wall effect: } b_{ij} = 1 - \left(1 - \frac{d_i}{d_j}\right)^{1.50} \quad \text{when } d_i \leq d_j \quad (10.4)$$

where d_i and d_j are the mean sieve size of the granular classes i and j , respectively.

Equation (10.2) must be applied as many times as are the classes considered in the optimization of the aggregate blend. For each application, a certain class is considered dominant (i^{th}), and the volume fractions of the other classes y_j are optimized to obtain the highest value of Y_i .

For example, assuming that in Figure 10.1 the dominant class in the aggregate blend is fraction B, the model is applied considering $i = B$:

$$Y_B = \frac{\beta_B}{1 - \left[1 - \beta_B + b_{BA}\beta_B \left(1 - \frac{1}{\beta_A}\right)\right] y_A - \left[1 - \frac{a_{BC}\beta_B}{\beta_C}\right] y_C} \quad (10.5)$$

The highest Y_i is the virtual packing density and identifies the dominant class i .

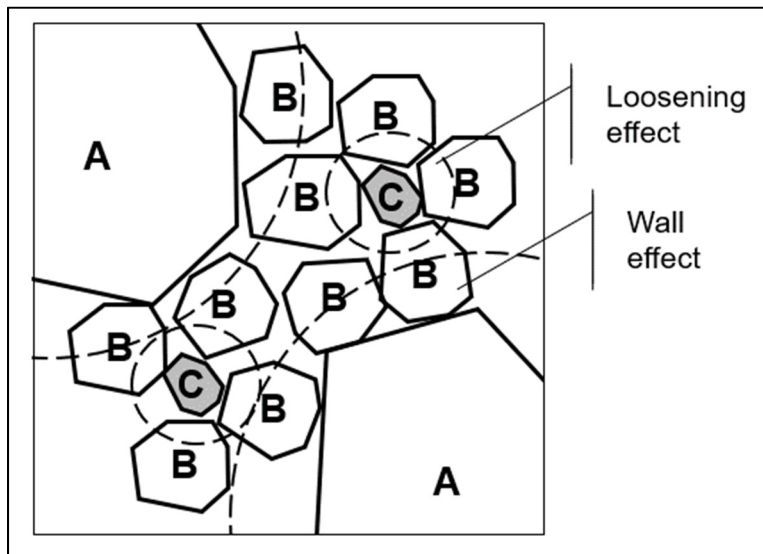


Figure 10.1 Effect of finer and coarser fractions on an intermediate fraction (readapted from (De Larrard, 1999))

In this paper, the volume fractions of the different classes are fixed. Hence, the CPM model is not applied to optimize the aggregate blend composition, but to determine its virtual packing density and evaluate compactability. In this paper the aggregate blend is fixed and the volume fractions of the different classes are already known. Hence, the CPM model is not applied for optimization but for the estimation of the maximum virtual packing density of the aggregate blend considered.

10.3.2 Di Benedetto-Neifar (DBN) model

Di Benedetto and Neifar (DBN) model for bituminous mixtures considers thermo-viscoplastic phenomena in the material behaviour (Di Benedetto, Delaporte, et al., 2007; Di Benedetto, Mondher, et al., 2007). Viscoplastic behaviour is related to large strain levels and small number of cycles for temperatures not too low, leading to ductile failure (Neifar & Di Benedetto, 2001). Non-linearities are represented in the model by elasto-plastic bodies (EP) placed in series with viscous dashpots (Figure 10.2). The EP bodies are characteristic of non cohesive granular materials, which can show a non-viscous dissipation. For instance, plastic dissipation is typical in sands for cyclic loadings at small strain amplitude and it is represented by a hysteretic stabilized behaviour (Sauzeat, 2003).

Increasing the number of elements increases the model precision and when it tends to the infinite, the representation passes from a discrete spectrum to a continuous spectrum. When only viscous dissipation is present, the EP bodies are replaced by linear springs and the DBN model takes its asymptotic form as a Generalized Kelvin-Voigt (GKV) (Neifar et al., 2001).

Given this background, it can be assumed that non-viscous dissipation occurs independently from temperature and frequency. CRM mixtures can be considered as intermediate between bituminous (viscous) and granular (non-viscous) mixtures. In case of a small number of cycles and small strain, the DBN model with some simplifications (Attia, 2020) can be used to simulate their rheological behaviour.

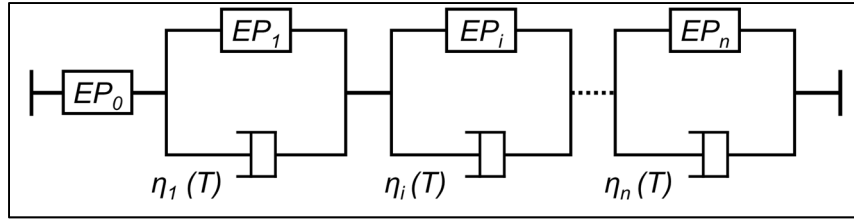


Figure 10.2 DBN model for bituminous mixtures

The dissipation behavior of construction materials (metals, concrete, soils, etc.) can be characterized using the specific damping capacity ψ , which is defined as the ratio between the energy dissipated in a loading cycle and the elastic energy stored in the system in the condition of maximum deformation (Genta, 2009). For Kelvin-Voigt bodies, under sinusoidal excitation, it is computed as:

$$\psi = \frac{\Delta W_{LVE}}{W_E} = \frac{\pi \varepsilon_0 \sigma_0 \sin \phi}{1/2 \varepsilon_0 \sigma_0} = 2\pi \sin \phi \quad (10.6)$$

where ΔW_{LVE} is the area of the linear viscoelastic (LVE) hysteresis loop, W_E is the energy stored by the spring, ε_0 is the amplitude of the strain, σ_0 is the amplitude of the stress and ϕ is the frequency-dependent phase angle describing the lag between stress and strain.

EP bodies are characterized by elastic energy storage and time-temperature independent dissipation. For low-dissipation materials, the energy dissipated ΔW_{EP} is calculated as:

$$\Delta W_{EP} = W_{EP} \psi = 1/2 \varepsilon_0 \sigma_0 \psi = 2\pi D \varepsilon_0 \sigma_0 \quad (10.7)$$

where $D = \psi/4\pi$ is an adimensional time-temperature independent damping ratio.

In case the number of cycles applied and the deformation are small, the plastic energy dissipation ΔW_{EP} can be expressed as an equivalent linear viscoelastic dissipation ΔW_{LVE} through the definition of an equivalent phase angle, by fixing $\Delta W_{EP} = \Delta W_{LVE}$:

$$\sin(\phi_{EP}) = 2D \quad (10.8)$$

As a consequence, the version of the DBN used for the modelling of CRM materials consists of viscous and temperature-dependent dissipation through the dashpots ($\eta_i(T)$) and non-viscous dissipation through the EP bodies (E_i, D_i). The first unit does not have a dashpot and all the elements are characterized by the same damping ratio ($D_i = D$) (Figure 10.3).

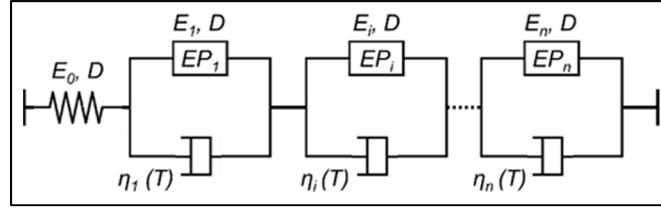


Figure 10.3 Schematic representation of the DBN model for small strain and small cycles

The total phase angle ϕ_{DBN} for the given configuration is composed of both viscous and non-viscous dissipations:

$$\begin{aligned} \sin(\phi_{\text{DBN}}) &= \sin(\phi_{\text{LVE}} + \phi_{\text{EP}}) = \frac{\Delta W_{\text{DBN}}}{\pi \epsilon_0 \sigma_0} = \frac{\Delta W_{\text{LVE}} + \Delta W_{\text{EP}}}{\pi \epsilon_0 \sigma_0} \quad (10.9) \\ &= \sum_{i=0}^n \left(\frac{\omega \eta_i}{E_i^2 + (\omega \eta_i)^2} + \frac{2 \cdot D \cdot E_i}{E_i^2 + (\omega \eta_i)^2} \right) \cdot |E^*| \end{aligned}$$

where ΔW_{DBN} is the total dissipation in a cycle (viscous and non-viscous), ω is the pulsation defined as $\omega = 2\pi f$, where f is the frequency, E_i and η_i are the Young's modulus and the Newtonian viscosity of the i^{th} element, respectively, ϕ_{LVE} is the phase angle of the viscous dashpot and ϕ_{EP} is the phase angle of the non-viscous damping.

The presence of non-viscous energy dissipation does not influence the norm of the complex modulus $|E^*|$, which is calculated as for the GKV model:

$$E_{\text{GKV}}^*(i\omega, T) = \left(\frac{1}{E_0} + \sum_{i=1}^n \frac{1}{E_i + j\omega \eta_i(T)} \right)^{-1} \quad (10.10)$$

where j is the complex number ($j^2 = -1$), T is the temperature and E_0 is the Young's modulus of the first element. The number of elements defines the precision of the model, which is selected in function of the 2S2P1D model (Olard et al., 2003):

$$E_{2S2P1D}^*(i\omega\tau) = E_{00} + \frac{E_0 - E_{00}}{1 + \delta(j\omega\tau)^{-k} + (j\omega\tau)^{-h} + (j\omega\beta\tau)^{-1}} \quad (10.11)$$

where k and h are constant exponents ($0 < k < h < 1$), δ is a constant, E_{00} is the static modulus for $\omega \rightarrow 0$, E_0 is the glassy modulus when $\omega \rightarrow \infty$, and τ_E is the characteristic time, which is the only parameter depending on the temperature:

$$\tau_E(T) = a_T(T) \cdot \tau_{0E} \quad (10.12)$$

where $a_T(T)$ is the shift factor at a temperature T , $\tau_E(T) = \tau_{0E}$ at the reference temperature T_S and $\tau_E(T)$ is determined at each isotherm by minimizing the error between the measured and modelled norm of the complex modulus. In this study, the number of elements was fixed at 40.

The calibration process is performed by initially determining the shift factors according to the master curve of the norm of complex modulus at the chosen reference temperature. This is allowed if the material is thermo-rheologically simple and the Time-Temperature Superposition Principle (TTSP) is valid. The experimental shift factors obtained can be analytically modelled by the Williams-Landel-Ferry (WLF) model (Ferry, 1980):

$$\log(a_T) = -\frac{C_1(T - T_S)}{C_2 + T - T_S} \quad (10.13)$$

where C_1 and C_2 are constants.

The following step consists in calibrating 2S2P1D model according to the master curve of the norm of the complex modulus, minimizing the error between the experimental points and the model curve. At this point, the number of GKV elements is chosen and the values of E_i and η_i for each element are calculated. Afterwards, the value of Φ_{EP} is assessed on the master curve of the phase angle in order to minimize the error between the experimental points and the model curve. So, with seven constants defined by the 2S2P1D and one constant defined by the

DBN model, it is possible to fully describe the material behaviour in the small strain domain, considering both viscous and non-viscous dissipations.

10.4 Mixtures and methods

This section contains information about the materials selected, the production and curing protocol followed, as well as the device and tools used to develop this study.

10.4.1 Materials and mixtures

Two RAP sources were selected from stockpiles in Italy and Alabama (USA) and coded as RAP1 and RAP2, respectively. These materials already showed to have different effects on the mechanical properties of the CBTM mixtures produced (Raschia, Graziani, et al., 2019b), in particular in terms of tensile strength and fracture resistance. Table 10.1 lists the properties of the RAP aggregates. The residual RAP binders were extracted by centrifuge extraction and recovered by rotary evaporation. The recovered binders were analysed in terms of complex shear modulus using a dynamic shear rheometer (DSR) (Figure 10.4). It is observed that the high stiffness of the RAP binders caused a low precision of the data. However, in the range of frequencies and temperature analyzed, the RAP1 binder showed higher phase angle compared to RAP2, suggesting a higher viscous dissipation ability.

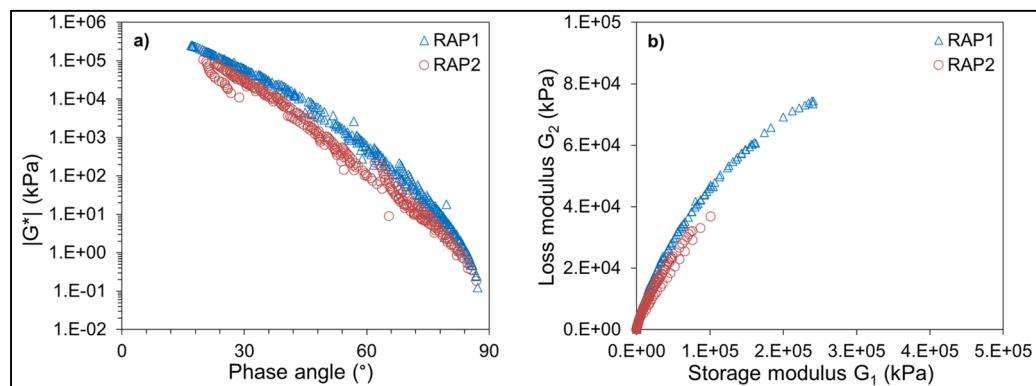


Figure 10.4 Complex shear modulus results on the RAP residual binder: a) Black space; b) Cole-Cole plan

The CRM mixtures were produced using a bitumen emulsion type CSS-1 (ASTM D2397), for which the main properties are summarized in Table 10.2. The residual bitumen properties, obtained after extraction (ASTM D6997), are listed too. In order to precisely investigate the effect of RAP sources, two mixtures were produced with the same aggregate size distribution as shown in Figure 10.5 which refers to the Fuller-Thompson maximum density curve with exponent 0.45.

Table 10.1 Properties of RAP sources used

Property	Standard	Unit	RAP1	RAP2
Binder content	ASTM D6307	%	5.51	5.49
Maximum specific gravity of the blend	ASTM C127-128	-	2.482	2.498
Bulk specific gravity – Fraction 0/2.5	LC 21-065	-	2.170	2.373
Bulk specific gravity – Fraction 2.5/5	LC 21-066	-	2.380	2.462
Bulk specific gravity – Fraction 5/10	LC 21-067	-	2.437	2.427
Fragmentation @ 5 °C (fraction 5/10) – PCS	ASTM D1557	%	7.6	n.a.*
Fragmentation @ 20 °C (fraction 5/10) – PCS	ASTM D1557	%	6.7	13.9
* n.a., not available				

The RAP aggregates were initially sieved and divided in three fractions: 0/2.5, 2.5/5 and 5/10. Such fractions were subsequently combined to obtain the same curve for RAP1 and RAP2 mixtures in the following percentages: 40% of 0/2.5, 20% of 2.5/5 and 30% of 5/10. The remaining 10% was composed of limestone filler in both mixtures. The residual bitumen dosage was fixed at 3.0% (corresponding to 5.0% of bitumen emulsion) by mass of dry aggregates. The total water dosage (water from the emulsion and added water) was fixed at 5.4% by mass of dry aggregates.

Table 10.2 Bitumen emulsion properties

Emulsion properties	Standard	Unit	Value
Density	ASTM D6397-16	g/cm ³	1.016
Residue content	ASTM D6997-12	%	60.3
Storage stability @ 24 hours	ASTM D6930-10	%	0.6
Residual bitumen properties			
Needle penetration @ 25 °C	ASTM D5-13	dmm	41
Softening point	ASTM D36-14	° C	48.6

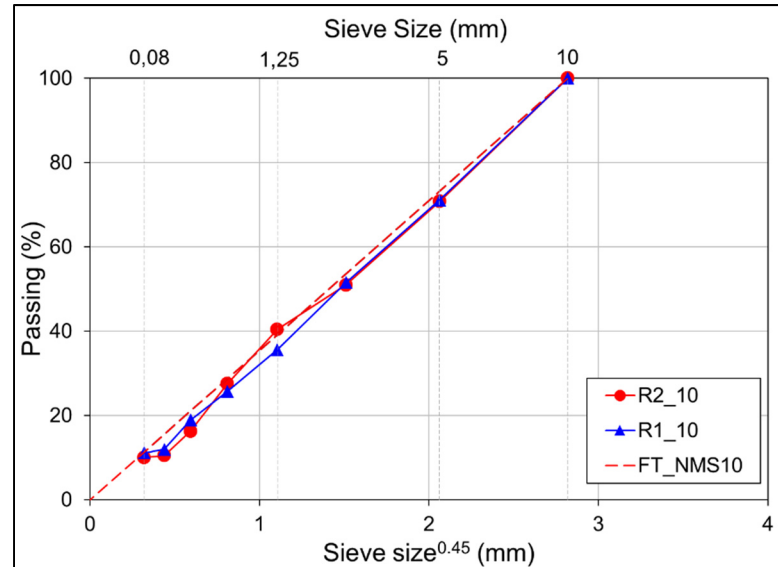


Figure 10.5 Aggregate distribution of the mixtures studied

10.4.2 Mixing, compaction and curing

In the first mixing step, the dried aggregate blend (RAP and filler) was mixed with only absorption water to better represent field condition (Grilli et al., 2016). The moist aggregate blends were sealed in plastic bags for at least 12 hours. In the second step, additional water is added to confer better compactability, and the material is mixed mechanically for about 60

seconds. Afterwards, the bitumen emulsion is added, and the mixture is mechanically mixed for an additional 60 seconds. Compaction was performed immediately after mixing using a gyratory compactor with mould diameter of 150 mm, constant pressure of 600 kPa, internal angle of 1.16° and gyration rate of 30 rpm. During compaction it is possible to monitor three important volumetric parameters: the voids in the mixture (V_m), the voids in the mineral aggregate (VMA) and the voids filled with liquids (VFL):

$$V_m = \frac{V_{AIR} + V_{W,I}}{V} \cdot 100 = \frac{V - (V_S + V_{B,R})}{V} \cdot 100 \quad (10.14)$$

$$VMA = \frac{V_{AIR} + V_{W,I} + V_{B,R}}{V} \cdot 100 = \frac{V - V_S}{V} \cdot 100 \quad (10.15)$$

$$VFL = \frac{V_{W,I} + V_{B,R}}{V_{AIR} + V_{W,I} + V_{B,R}} \cdot 100 \quad (10.16)$$

where V_{AIR} is the volume of air, $V_{W,I}$ is the volume of intergranular water, V is the total volume of the specimen, V_S is the volume of aggregates (in SSD condition) and $V_{B,R}$ is the volume of residual bitumen from emulsion. The fixed V_m value was $10 \pm 1\%$ with a VFL value of $90 \pm 1\%$. The VFL close to 100% theoretically means a complete saturation of the VMA and values higher than 90% could lead to the expulsion of water and fine particles during compaction (Grilli et al., 2016). Two specimens for each RAP source were compacted at the fixed V_m , that were reached with 63 ± 5 and 30 ± 2 gyrations for RAP1 and RAP2 mixtures, respectively. The volumetric compositions of the specimens after compaction, as well as the average compaction energy expressed in gyrations, are reported in Table 10.3. The volumes of air and intergranular water represent the obtained value of V_m .

The specimens were cured in two steps: 14 days at 25 °C plus additional 14 days at 40°C (with $55 \pm 5\%$ RH), in order to reach a stable condition of the physical and mechanical properties (Raschia et al., 2020). After the total curing time of 28 days, specimens were cored and saw cut to have $\varnothing 75 \times 130H$ mm specimens (Figure 10.6).

Table 10.3 Volumetric composition of the mixtures after compaction to reach $V_m = 10.8\%$

Component	RAP1 (%)	RAP2 (%)
RAP aggregate ⁽¹⁾	75.6	75.4
Limestone filler	7.6	7.7
Residual bitumen ⁽²⁾	6.0	6.1
Intergranular water	9.2	9.2
Air	1.6	1.6
Total	100.0	100.0
Number of gyrations	63 ± 5	30 ± 2
⁽¹⁾ The percentage is referred to the SSD condition		
⁽²⁾ The residual bitumen is calculated as 60% by bitumen emulsion mass		



Figure 10.6 Specimens employed for testing

10.4.3 Experimental program

In order to apply the CPM model, the packing density of each fraction used in the RAP aggregates blend was measured under compaction employing the gyratory compactor in

accordance with a method introduced by Perraton et al. (2007). In the present study, the energy imposed by the compaction was fixed at 20 gyrations, to limit attrition, segregation and abrasion under compaction (Olard, 2012). For each fraction, 0/2.5, 2.5/5 and 5/10 in this study, a fixed amount of dry RAP aggregate (1000 g) was compacted at room temperature and the final volume of two samples was recorded. So, the average packing density β_i of each fraction i was measured for both RAP sources, and such values were employed to calculate the virtual packing density Y_i of the three combined fractions. In fact, the CPM model was applied only to the RAP aggregate, without considering the volume of filler which was the same between the two mixtures. In this study, Y_i calculated by the CPM model represents the volume fraction occupied by the RAP aggregate phase in a fixed volume, and the value $1 - Y_i$ is the porosity of the system. Hence, it can be assumed that such porosity has the same physical meaning as the voids in the RAP mineral aggregate, VMA_{RAP} . VMA_{RAP} was calculated using Eq. (1) and replacing V_S with the bulk volume of the RAP aggregate and V_T with the total volume of the SGC compacted specimen.

To contribute to the analytical part of the packing density evaluation, morphological parameters such as elongation, roundness, concavity and shape factor were obtained using OCCHIO belt aggregates image analyzer. The elongation is represented by a minimum ratio of two diameters of a 2D ellipse having the same area as the particle. The roundness parameter is the average curvature of asperities located on the aggregate perimeter at regular points. A roundness value of 100% is associated to a perfectly circular particle, whereas values below 50% generally belong to very irregular surfaces. High values of roundness and shape factors normally improve compactability, whereas low values of elongation and concavity negatively affect compactability.

The rheological properties of the CRM mixes were evaluated by complex modulus tests using a MTS press. The sinusoidal compressive loading (haversine loading) was applied on the top of the specimen, and the bottom was glued to an aluminum cap with a thermo-resistant epoxy. The applied loading frequencies were 0.1, 0.3, 1, 3 and 10 Hz.

The axial strain was measured by placing three extensometers in the middle part of the specimen and 120° apart (measuring base of 50 mm). The target axial strain was 40 $\mu\text{m}/\text{m}$. The test was conducted at seven temperatures: -20, -10, 0, 10, 20, 30 and 40 °C.

10.5 Results and discussion

CPM model (equation 10.2) was used to calculate the virtual packing densities of the RAP aggregate blends. Table 10.4 lists the results according to the application of the CPM model on the RAP sources. The fractions' volumes in the full gradation y_i is reported without considering the limestone filler content, which was constant between the two RAPs. It can be observed that comparing the same fraction between the two RAPs, the values of β_i are similar except for the fraction 5/10. The fragmentation test used to characterize the RAP source was performed on the fraction 5/10, highlighting a higher fine content produced after fragmentation of RAP2. This could explain the difference in porosity of this specific fraction, which is higher for RAP2 probably because of partial fragmentation during the packing test. In both RAP sources, the assumed dominant fraction class is 0/2.5, since it is the one occupying the highest volume. It has to be noted that being the class with the lowest dimension, it is only subjected to the “wall effect” due to coarser fractions. Consequently, the residual two fractions can be considered as a dispersion in the fine matrix. Considering this, the virtual packing $Y_{0/2.5}$ is calculated and results are shown in Table 10.4. The CPM model results show that both RAP sources have potentially the same ability to compact, predicting a virtual packing density of 83% for RAP1 aggregate and 82% for RAP2 aggregate after 20 gyrations (virtual porosity of 17% and 18% for RAP1 and RAP2, respectively). This was in some way expected, since the values of β_i are similar between RAP1 and RAP2, as well as the same gradations were chosen. The voids in the RAP aggregate skeleton reached after compaction, VMA_{RAP} (24% and 25% for RAP1 and RAP2, respectively), can be compared to the values of virtual porosity obtained with the CPM model. It is observed that the virtual porosity is lower than the value of VMA_{RAP} for both RAP aggregates, meaning that the maximum packing of the aggregates was not reached, and this was needed to leave volume for water and bitumen. Despite these results

belong to only the RAP aggregate particles, a difference in compaction energy between the two CRM mixtures produced was observed in terms of compaction energy (63 and 30 gyrations for RAP1 and RAP2, respectively). For this reason, shape and texture of the aggregate particles were studied.

Table 10.4 CPM model results

	RAP1			RAP2		
	0/2.5	2.5/5	5/10	0/2.5	2.5/5	5/10
Volume fraction y_i	0.45	0.22	0.33	0.45	0.22	0.33
Packing density β_i (20 gyr)	0.74	0.67	0.66	0.71	0.68	0.70
Porosity ($= 1 - \beta_i$)	27%	33%	35%	29%	33%	30%
Mean diameter (mm)	0.45	3.54	7.07	0.45	3.54	7.07
Virtual packing density $Y_{0/2.5}$	0.83			0.82		
Virtual packing porosity ($= 1 - Y_{0/2.5}$)	17%			18%		
VMA_{RAP}^*	24%			25%		
* $VMA_{RAP} = \left(1 - \frac{V_{RAP}}{V}\right)$, where V_{RAP} is the bulk volume of RAP aggregate						

Shape parameters were evaluated by the OCCHIO belt aggregates image analyzer (Moghaddam et al., 2018) and are listed in Table 10.5. From this analysis, it is observed that, in general, the parameters obtained are not significantly different between the two RAP sources. It is remarked that higher roundness and shape factor lead to better compactability. The attention is focused on the fraction 0/2.5, being the dominant class and because the difference is more marked. For this fraction, RAP2 aggregate had lower roundness and shape factor, and higher concavity and elongation compared to RAP1. This would suggest lower compactability for RAP2 than RAP1, which is the opposite of what happened in practice with the CRM mixtures, i.e. a higher compactability of the mixture produced with RAP2.

Another important factor that can affect the compactability of the CRM mixtures is bitumen emulsion. Both RAP aggregates showed similar virtual packing densities, but when mixed with

bitumen emulsion, the compactability was different among the two mixtures. In this study, the emulsion used was a slow-setting emulsion type, but probably the RAP binder played a major role for compactability, in terms of affinity. The degree of bitumen coating and breaking process of the emulsion strongly depend on the chemical reactions between RAP binder and emulsion (Needham, 1996). If the breaking process occurs rapidly, the bitumen droplets suspended in the liquid phase do not have the time to evenly spread in the system, which results in poor compactability.

Table 10.5 Morphological parameters of RAP sources fractions

Fraction class	Roundness*		Concavity		Elongation		Shape factor	
	RAP1	RAP2	RAP1	RAP2	RAP1	RAP2	RAP1	RAP2
0/2.5	48.21	37.24	13.96	24.03	35.30	37.63	76.47	56.54
2.5/5	10.48	11.40	5.51	3.45	32.10	29.87	70.50	73.90
5/10	41.46	42.75	4.64	3.78	27.96	24.91	98.12	100.00
* 100% for perfectly circular particles, lower than 50% for very irregular surfaces								

Figure 10.7 shows the complex modulus test results. The repeatability between the two tests is very good and this confirms the quality of the results. In both representations (Cole-Cole plan and Black space), the measured data are disposed along a continuous line, meaning that the TTSP is valid and the material is thermo-rheologically simple. RAP1 mixture is characterized by a lower phase angle, showing a lower ability to dissipate energy compared to RAP2 mixture. It is highlighted that these results have an opposite trend compared to the RAP binder characteristics (Figure 10.4), hence the mixture rheological properties cannot be directly linked to the RAP binder properties. Moreover, it is clear how the RAP source has an impact on the modulus.

The isothermal curves of the norm of the complex modulus and phase angle can be shifted at a reference temperature (20 °C). This procedure is performed by the closed-form shifting

(CFS) algorithm that minimizes the area between two successive curves and gives an operator-independent estimation for the shift factors (Gergesova et al., 2011; Graziani et al., 2020).

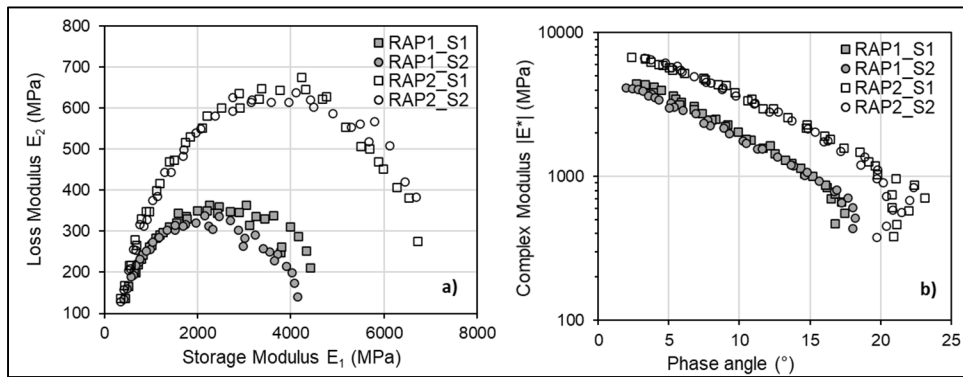


Figure 10.7 Experimental results: a) Cole-Cole plan and, b) Black space

Figure 10.8 shows the master curves of the tested specimens (2 RAP sources and 2 replicates, S1 and S2). The RAP2 mixture is characterized by higher stiffness at high frequencies (low temperatures) and lower stiffness at low frequencies (high temperature) compared to RAP1 mixture, which on the contrary shows a lower dependency on frequency (and temperature). This is confirmed by the phase angle master curve, where RAP1 mixture showed lower values of phase angle at all temperatures investigated. Since the phase angle is an energy dissipation parameter, it can be affected by many variables, such as air voids content, bitumen type and content.

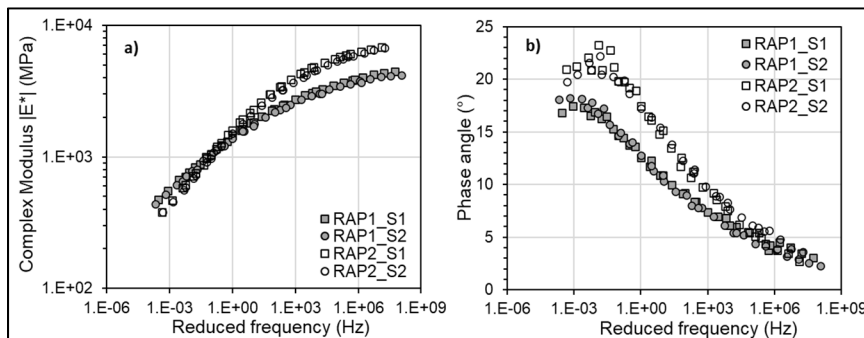


Figure 10.8 Master curves at $T_s = 20^\circ\text{C}$: a) Norm of the complex modulus and, b) Phase angle

In this study, where all these aspects are not variable, the only parameter that could affect the phase angle is the RAP source and the interaction with the bitumen emulsion. The higher effect of frequency and temperature on RAP2 mixture, as well as the higher values of the phase angle, could be related to either the effect of RAP binder or a better affinity between RAP and bitumen emulsion. Figure 10.9 shows the experimental shift factors (a_T) of the four tested specimens modelled by the WLF analytical model. It is observed that mixtures with RAP1 are characterized by a slightly higher slope, and highly temperature sensitivity, compared to mixtures with RAP2.

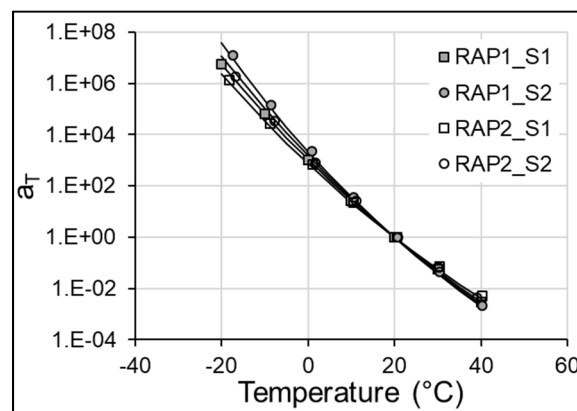


Figure 10.9 Shift factors and WLF model for the studied mixtures

Figure 10.10 shows the experimental results modelled by DBN model. The model parameters for the tested mixes are listed in Table 10.6. It is worth mentioning that the average values of glassy modulus (E_0) at low temperatures (high frequencies) for RAP1 and RAP2 mixtures are 4700 MPa and 7950 MPa, respectively. This parameter can be related to the aggregate skeleton and voids content. Since the only variable is the RAP aggregate source, the higher value for RAP2 mixture could be obtained due to a better dispersion and bonding with the aggregate particles. On the contrary, the static modulus (E_{00}) values for both mixtures at high temperatures (low frequencies) are quite similar (225 and 210 MPa for RAP1 and RAP2, respectively). In this case, the bituminous phase is considered as fluid and the stiffness is

mostly influenced by the aggregate phase. Since the two gradations and the RAP bitumen properties are similar, it is expected to have similar values for E_{00} .

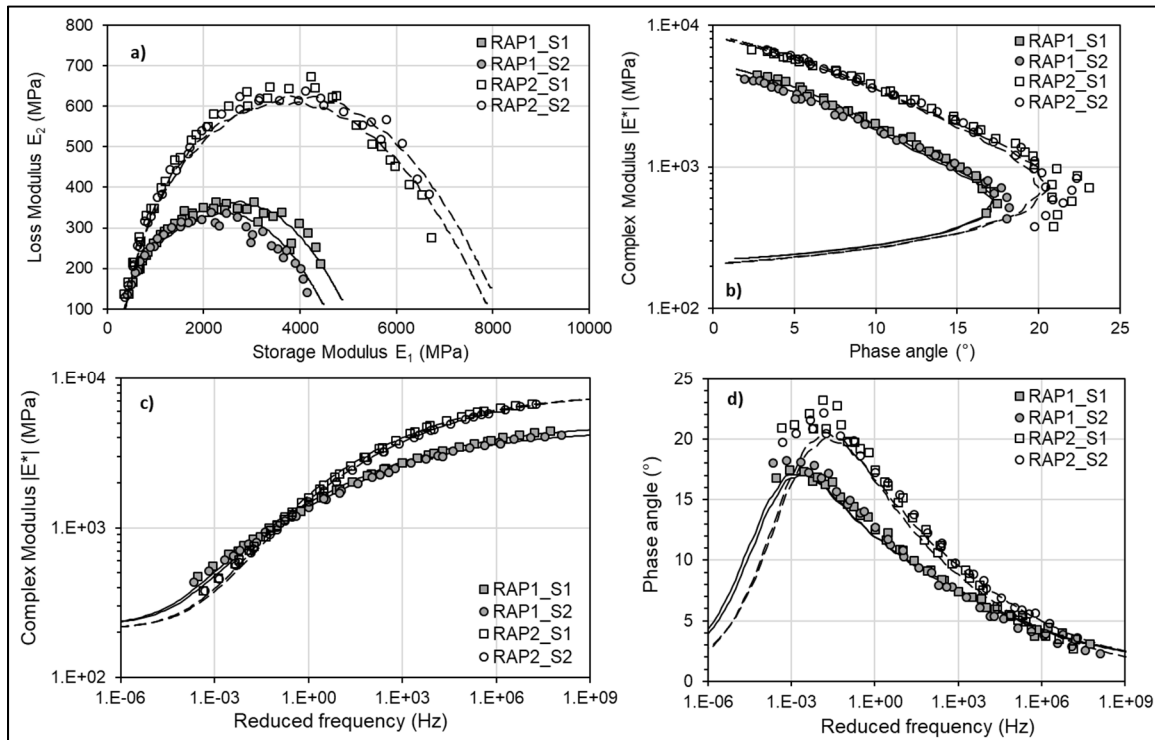


Figure 10.10 Experimental results modelled with the DBN model ($n = 40$): a) Cole-Cole plan, b) Black space, c) Master curve of the norm of the complex modulus at $T_s = 20^\circ\text{C}$ and, d) Master curve of the phase angle at $T_s = 20^\circ\text{C}$

The LVE dissipation parameters h , k , δ and β are similar for both RAP mixtures since the bitumen emulsion used was the same. This would also confirm that the RAP used in the CRM is a “black rock”. The characteristic time (τ_E) can be linked to the bitumen phase consistency and it is higher for harder bitumen (Mangiafico et al., 2014). However, the residual bitumen used is coming from the same emulsion. Hence, the different τ_E obtained depends on the RAP binder or the relation between the RAP binder and the residual bitumen. Analyzing the non-viscous equivalent phase angle (φ_{EP}), the average values obtained are 1.35° and 0.88° for RAP1 and RAP2, respectively. The value of φ_{EP} could be linked to non-viscous dissipation caused by frictional and plastic phenomena (Graziani et al., 2020), and the results showed that

the RAP source has a small effect. It could be suggested that non-viscous dissipation can occur at the interface between emulsion and RAP aggregate and/or at the interface between aggregate and RAP binder, whereas LVE dissipation is only attributed to the virgin binder. In this regard, RAP2 mixture had lower non-viscous component in the energy dissipation, meaning that it is closer to the pure LVE field compared to RAP1 mixture.

Table 10.6 DBN model parameters

	E_{00} (MPa)	E_0 (MPa)	h	k	δ	$\tau_E(20^\circ\text{C})$ (s)	β	φ_{EP} ($^\circ$)	C_1	C_2
RAP1_S1	225	4900	0.50	0.16	4.05	3.5	5000	1.35	31.0	215.4
RAP1_S2	225	4500	0.50	0.16	3.80	3.0	5000	1.35	27.9	187.3
RAP2_S1	210	7900	0.47	0.17	3.10	0.2	5000	0.75	28.0	215.7
RAP2_S2	210	8000	0.47	0.17	3.50	0.1	5000	1.00	29.6	214.8

10.6 Conclusions

The objective of this research was to evaluate the effects of two RAP sources (RAP1 and RAP2) on the compactability and LVE properties of the CRM materials produced.

Compactability of the RAP sources was analyzed in two steps: evaluating the packing density of the dry RAP aggregate, and considering the compaction energy necessary to reach the target volumetric properties of the CRM mixtures. The first step showed that both RAP aggregates, characterized by the same gradation, had the same packing density. This was observed from two approaches: compacting RAP aggregate samples with a gyratory compactor, and by predicting the maximum packing density of the full blend with compressible packing model (CPM). On the other hand, image analysis of the shape parameters for both RAP1 and RAP2 aggregates suggested that RAP2 aggregate was characterized by a lower compactability. Nonetheless, when mixtures were produced, an opposite trend was observed and the mixture with RAP2 required half of the compaction energy required by the RAP1 mixture. Hence, the

compactability of the CRM mixture was not linked to the physical and morphological properties of the RAP aggregate used. With high probability, CRM mixtures compactability was influenced by the chemical interaction between bitumen emulsion and RAP aggregate and the difference in RAP binders' properties.

The influence of RAP binders' properties was confirmed by complex modulus tests results. The test was performed on two specimens for each mixture, showing an excellent repeatability. RAP2 mixture showed a higher temperature dependency compared to RAP1 mixture. In order to understand the mixtures properties, the DBN model presented in the literature was selected as the most reliable for cold mixtures applications. The model parameters considered both LVE and elasto-plastic phenomena, considering both viscous and non-viscous dissipations under cyclic loading. Based on the results, LVE dissipation parameters did not change for the two RAP sources. However, RAP2 mixture was characterized by a lower non-viscous dissipation, as well as higher phase angle values. This confirms the fact that the residual bitumen in the RAP aggregate is more important for non-viscous dissipation rather than for viscous dissipation.

In conclusion, the compactability and the properties of CRM mixtures in the small strain domain are affected by the RAP source, even when considered as a "black rock". In particular, the affinity between the RAP aggregate and bitumen emulsion is an important parameter that needs to be considered when evaluating the CRM properties. Further studies are strongly encouraged in order to implement an analysis of the RAP-emulsion relationship as a fundamental point of a mix design.

CHAPTER 11

SUMMARY OF SECTION 2 AND INTRODUCTION OF SECTION 3: INFLUENCE OF LOW PRODUCTION TEMPERATURES ON CBTM PROPERTIES

In this chapter the main findings obtained in Section 2 are summarized, and the next topic of the thesis is introduced, i.e. the influence of low production temperatures on CBTM properties.

11.1 Summary of Section 2

CHAPTERS 8, 9 and 10 showed interesting results related to the RAP aggregate used in CBTM mixtures. The analysis performed involved a wide range of investigation fields, such as workability and compactability, evolution of the mechanical properties along curing, and mechanical tests at different levels of deformation. The work was divided in two specific aspects: the study of the RAP aggregate distribution (CHAPTER 8) and the study of the RAP aggregate source (CHAPTERS 9 and 10).

The analysis of the aggregate distribution was based on shape parameters of the distribution curve normally employed for cement concrete applications. These parameters allowed to consider the fine fraction and the coarse fraction of the aggregate gradation separately, which were consequently linked to the workability and compactability of the mixtures. An increase in the filler content corresponded to an improvement of the mixture workability, penalizing at the same time the compactability. In terms of mechanical properties, the most important parameter resulted to be the bitumen and cement dosages. The aggregate distribution affected resistance and stiffness of CBTM mixtures, in particular changing the nominal maximum aggregate size. In fact, it was observed that passing from 16 mm to 10 mm the mechanical properties were globally improved, even though compactability was penalized.

In terms of effect of the RAP source, the CBTM mixture produced with RAP2 required lower compaction energy compared to RAP1, even though the two RAP aggregate blends were

characterized by similar morphology and theoretical maximum packing density. In addition, thanks to rheological modelling, it was possible to observe the influence of the RAP binder on the thermal response of the material. In terms of tensile strength and fracture resistance, the RAP1 mixtures showed higher values, being more performant than RAP2. Concluding, it was not possible to rank a RAP source as globally better than the other, since their properties are different according to the field of investigation. Fundamental properties of both RAP sources are collected in Annex I.

Additional studies are needed to confirm these findings. The maximum density line as described by Fuller-Thompson is often chosen as the optimal distribution, even though gap-graded distributions (HPAC or SMA) could be equally valid if thoroughly designed. The formulation of an optimal aggregate distribution for CBTM projects is needed, since nowadays technical specifications often allow a wide range of acceptance leading to high variability. Moreover, the fragmentation test was not enough to link the properties of the RAP source to the mechanical properties of the CBTM mixture produced. However, it is believed that the properties of the aged RAP binder affect the mechanical properties of the CBTM mixture, even if considered as a black rock and more research is encouraged in this direction.

11.2 Section 3: study of the effect of low production temperatures on CBTM properties

The next three chapters deal with the effect of production temperatures on mixtures produced with RAP1 and two emulsion sources, focusing the attention on temperatures which are lower than the ones commonly recommended (below 10 °C) (ARRA, 2016; Asphalt Academy, 2009; Jacobson, 2002; Shoenberger, 1992).

In cold central-plant recycling (CCPR), projects the plant where the CBTM production is performed can be placed several kilometers from the construction site. In such case, the ambient temperature and the operating times during the mixtures production can play a crucial role when air temperature is low (< 10 °C). At first, a distinction needs to be made between the

different steps followed. Initially, the RAP aggregate that was milled from the pavement and stockpiled in plant is blended with the rest of the components, cement, water and bitumen emulsions (mixing process). In many cases, only the temperature of the bitumen emulsion is known and carefully maintained for an adequate storage. When the truck is loaded, the mixture is hauled to the construction site for laydown. The time employed for the transportation, combined with the ambient conditions (humidity and temperature), can be critical for the moisture content and the stability of the bitumen emulsion, which could break prematurely. At this point, the mixture is laid and compacted to the target density (transportation and compaction process). The following step consists in waiting for the water evaporation and the development of enough resistance to carry the traffic load. This period is highly arbitrary and it can vary between 24 hours and several days. When this step is considered completed (generally moisture content in the mixture less than 1% according to Kim et al., 2011), the upper HMA layer can be placed and compacted. It is important to notice that even if an optimum mix-design for the CBTM layer is carried out, the production of such mixtures at critical temperatures could permanently prevent the development of mechanical properties.

Starting from these considerations, the experimental program followed in this chapter is shown in Figure 11.1. In this figure, it is reported an example for a mixture mixed at 25 °C, transported and compacted at 5 °C, and cured for 14 days of the first curing at 5 °C. In particular, the entire simulation of the production process in laboratory consisted of:

- Mixing process at 5 °C or 25 °C for 5 minutes: the two mixing temperatures can represent the aggregate's temperature during cold or warm seasons;
- Transportation and compaction at 5 °C or 25 °C for 2 hours plus 30 minutes: the two temperatures can represent the hauling process during cold or warm seasons;
- 14 days of curing at the same temperature of transportation and compaction: it is assumed that the first 14 days of life of the mixture are at around the same temperature at which it was laid and compacted;
- 14 days of curing at 40 °C to represent 1-3 years of pavement life in the field;

- Additional 11 months (330 days) curing at room temperature to evaluate the mechanical properties of the material after 1 year in sealed and unsealed conditions.

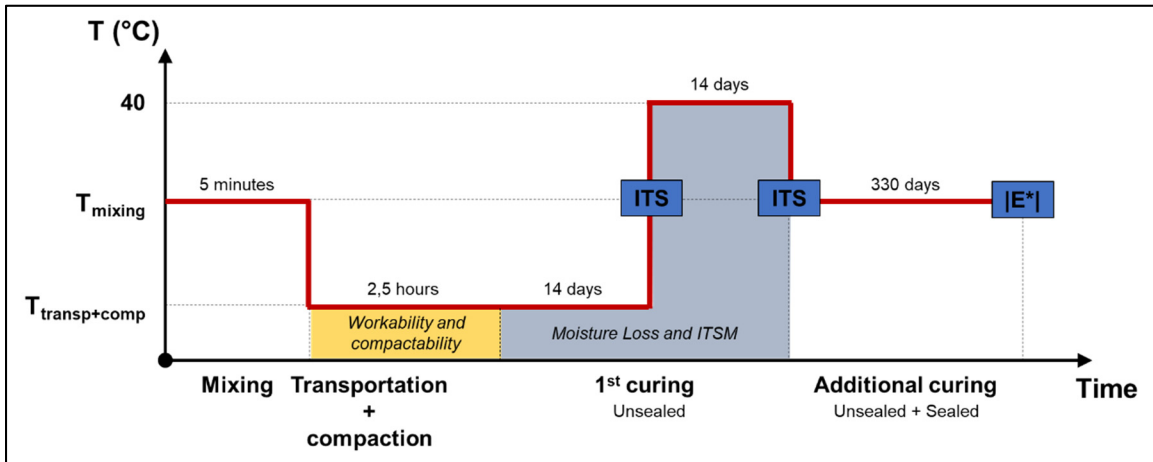


Figure 11.1 Laboratory production simulation and experimental program

In the research program developed, among all the others, two particular cases were evaluated: a) mixing at 5 °C and transportation and compaction at 25 °C and, b) mixing at 25 °C and transportation and compaction at 5 °C. The first one was tested to evaluate the effect of only low mixing temperature, and considering the possibility that warming up the mixture during transportation would preserve the material properties. In the second case it is the opposite, and it was hypothesized that if only the mixing is carried out at 25 °C, perhaps the low transportation and compaction temperature are not negatively affecting the material properties.

The results obtained are mainly divided in two parts: the material properties after the first curing (14 days + 14 days), and the properties after the additional curing at 1 year. The first part is developed in CHAPTER 12. In particular, properties such as workability, compactability and evolution of the mechanical properties in the first month of the material life were evaluated. Workability and compactability were analyzed by means of the SGC, whereas the properties development was monitored by moisture loss, ITS and ITSM tests. This allows to clarify if the low production temperatures are crucial in the first days of service of

the material. However, since the knowledge of such materials is still poor in terms of long term properties, it is not demonstrated that acceptable performance in the short-term are linked to good properties in the long term also.

The second part of the experimental program is treated in CHAPTERS 13 and 14 where the rheological properties of the same mixtures treated in CHAPTER 12 after one year of curing are investigated with the help of the DBN model, already introduced in the literature. The additional curing was performed in two different conditions: sealed and unsealed. In the first case the confinement allowed to represent the field conditions, where the CBTM layer is covered with an upper layer. In the second case ageing and full exposure to environmental factors (humidity and light) were promoted.

CHAPTER 12

INFLUENCE OF LOW PRODUCTION TEMPERATURE ON COMPACTABILITY AND MECHANICAL PROPERTIES OF COLD RECYCLED MIXTURES

Simone Raschia^a, Daniel Perraton^a, Andrea Graziani^b, Alan Carter^a

^a Construction Engineering department, École de technologie supérieure (ÉTS) 1100, Notre-Dame Street West, Montreal, Canada

^b Department of Civil and Building Engineering, and Architecture, Università Politecnica delle Marche, Via Brecce Bianche, 60131 Ancona, Italy

Paper published in the journal *Construction & Building Materials*, Elsevier, October 2019

12.1 Abstract

In cold regions, the production of Cement-Bitumen Treated Materials (CBTM) represents an issue in terms of annual time available for production. The objective of this research is to study the influence of different combinations of production temperatures for mixing, compacting and curing (developed in two steps) on the mechanical properties of CBTM produced with two sources of bitumen emulsion. Workability, compactability, indirect strength and other additional tests were involved in the analysis. Findings highlighted the critical effect of transportation and compaction temperatures on CBTM workability. Moreover, the emulsion source significantly affects the mixture strength when produced at low temperatures.

12.2 Introduction

Production of traditional hot mix asphalts (HMA) in road industry, intended as mixing, transportation and compaction, is normally performed at a range of temperatures between 150 °C and 170 °C (Cominsky et al., 1994; Stimilli et al., 2016). The reasons that lead to the

definition of such temperatures is the necessity to reduce the bitumen viscosity in order to well coat aggregates, to provide a workable mixture and to be properly compacted in the field.

The economical and environmental crisis that characterized the last decades brought to the introduction of new techniques to obtain materials addressed to the production of the pavement structure: warm mix asphalts (WMA) (Frigio & Canestrari, 2018; Stimilli et al., 2017) and cold asphalt mixtures (CAMs) (Stroup-Gardiner, 2011; Tebaldi et al., 2014; Xiao et al., 2018). In the first case, production temperatures can be decreased by around 30 °C thanks to the use of additives able to reduce the bitumen viscosity (Frigio et al., 2016). In the second case, the entire production process can be performed at ambient temperature employing the bitumen in form of foam or emulsion. The use of water in these mixtures ensures workability and compactability, allowing at the same time the use of wet aggregates. For such reasons, this technique brings high environmental and energy-saving benefits if compared to standard HMA or WMA mixtures (AIPCR-PIARC, 2002; Bowering & Martin, 1976; Chandra et al., 2013; Yan et al., 2010).

A further improvement in terms of sustainability is obtained when reclaimed asphalt pavement (RAP) is used as aggregate material (Chandra et al., 2013; Dal Ben & Jenkins, 2014; Giani et al., 2015; Godenzoni, Graziani, et al., 2016; Thenoux et al., 2007). The re-use of RAP instead of virgin aggregates in Cold Recycled Mixtures (CRMs) leads to the possibility to have performant mixtures for base or binder layers with a material that is normally available in high quantities (Gandi et al., 2017; Godenzoni, Graziani, et al., 2016).

To improve short-term and long-term mechanical properties, a small amount of Ordinary Portland Cement is added to CRMs obtaining cement-bitumen treated materials (CBTM) (Oruc et al., 2007). The quantity of cement used is usually lower than the bitumen content in order to have materials that are considered having a bituminous behaviour (Cardone et al., 2014). For this reason, the balance between the two binding agents is an important parameter to control. As mentioned previously, bitumen can be added in the form of foam or emulsion in CRMs. In this paper, we concentrate on emulsion treated materials. Bitumen emulsions are obtained by

sheering the bitumen in a colloidal mill, which is then suspended in a watery phase in form of droplets. The suspension of bitumen droplets is ensured by the presence of an emulsifier in the system, that is responsible for the repulsive effect (Circular, 2006). This phenomenon allows storing the emulsion for a certain period (2–3 months) and to have a good breaking on the RAP material. The nature of bitumen emulsion makes it extremely sensitive to temperatures, from the storage to the long-term performance of the final mixture (Needham, 1996).

At present, no specific standard establishes the minimum temperature required to produce a CBTM mixture, but many manuals recommend different temperatures based on their experience, without distinguish the three different processes: mixing, transportation and laydown and compaction. For example, in some cases, the minimum temperature for laydown must be above 5 °C, whereas in other cases a temperature of at least 10 °C is required to carry out a cold recycled project (Asphalt Academy, 2009; Jacobson, 2002; Shoenberger, 1992). An AASHTO report (1998) establishes that for projects using bitumen emulsions, a minimum ambient temperature range between 10 and 16 °C should be respected during production. If cement or fly ash are used as additional binders in CBTM, the minimum ambient temperature can be 4 °C (No., 1998). The Asphalt Recycling & Reclaiming Association (ARRA) also provided construction guidelines for cold in-place recycling (CIR) using bitumen emulsion, specifying that operating temperatures are extremely variable depending on the emulsion used and/or RAP temperature, requiring in some cases ambient temperatures higher than 16 °C (ARRA, 2016). Many other studies report the production temperature in the laboratory equal to room temperature, or able to represent as close as possible the field conditions (Du, 2014; García et al., 2013; Gaudefroy et al., 2008; Graziani, Iafelice, et al., 2018; Lesueur et al., 2004; Martínez-Echevarría et al., 2012). This aspect of CBTM mixtures is of fundamental importance when construction projects are carried out in cold regions such as Canada, North-East USA or North-Europe. In fact, average climate conditions throughout the year do not allow a wide time span for CBTM production and laydown.

Not only production's temperatures are important for the CBTM mechanical properties, but also the conditions characterising the curing process. During this time, the water present in the mixture evaporates, accelerating the emulsion breaking process and improving the mechanical properties. When cement is used in addition to bitumen emulsion, a certain amount of water is used for the hydration process. Therefore, the amount of time to allow a complete curing is highly dependent on environmental conditions, such as temperature, relative humidity and wind (Cardone et al., 2014; Godenzoni, Cardone, et al., 2016; Grilli et al., 2019; Kim et al., 2011; Olard et al., 2003; Serfass et al., 2004). Because of this high variability, it is impossible to establish a single laboratory procedure to represent field curing. At the same time, the evolution of curing in the field is difficult to follow, because of the distortion brought by performing cores (Tebaldi et al., 2014).

However, Bocci et al. (2011) showed that changing the curing temperature in the laboratory from 40 °C to 20 °C, it is possible to reach the same level of stiffness, although the curing time required is very different (10 days and 50 days, respectively). On the other hand, a curing temperature of 5 °C for 60 days did not allow to increase the stiffness enough; but, when an additional curing of 14 days at 40 °C was carried out, the tested mixture reached the same stiffness as the ones of the other curing conditions. In that research, the double step curing can be seen as a simulation of a material cured during the cold season first, and with a long-term curing afterwards. It is highlighted that in that case, mixtures were mixed and compacted at room temperature, and only the curing temperature effect was studied (Bocci et al., 2011).

The objective of this research is to understand how the low production temperatures (mixing, transportation and compaction, and curing) are affecting the long-term mechanical properties of CBTM treated with bitumen emulsion, changing the emulsion source. For this purpose, different combinations of temperatures for the three processes were reproduced in the laboratory, focusing the work towards low temperatures.

12.3 Experimental approach

Cold in-plant recycling (CIPR) projects are characterized by the presence of a production plant (fixed or mobile) located several kilometres from the construction site. In such cases, the entire process is developed in different steps. At first, the existing pavement is milled at a specified depth according to the thickness of the damaged layer or layers. During this operation, the RAP material is obtained and collected, in order to be moved to the production plant. At this point, the CBTM mixture is prepared, adding to the RAP aggregate cement, bitumen emulsion, and water. If required, the RAP aggregate gradation can be corrected to respect local gradation specifications. At the moment of mixing, only the temperature of the emulsion is known, since it is stocked at a precise temperature. On the other hand, all the other raw materials characterizing the CBTM mixture are kept at ambient temperature. The obtained mixture is then transported to the construction site, in order to be laid and compacted. During transportation and compaction, ambient temperature and time are very important, to avoid a premature breaking of the emulsion (in case of low temperatures) or rapid water evaporation (in case of high temperatures). In both cases, laydown and compaction characteristics of the material could be changed. When the required density is reached, the compaction stops and a certain amount of time is often required before that the upper layer is placed. This time is necessary to allow the water to evaporate, in order to let strength and stiffness of the mixture to increase. Normally, this process is considered finished when around 1% of residual water is present in the mixture (Tebaldi et al., 2014).

In the present study, the entire process is simulated in the laboratory, in order to investigate the effect of temperature on each step of the production process. In fact: a) mixing, b) transportation and compaction and c) curing, are considered separately, with a specific assigned time and temperature.

12.4 Materials and methodology

12.4.1 Materials and mixtures

The mixes were produced using a single RAP source sampled from a stockpile in Italy. The main characteristics of the RAP aggregate are listed in Table 12.1. The gradation of the RAP material was modified to obtain a distribution close to the maximum density curve with exponent 0.45. For this reason, the aggregate blend was composed of 94% of RAP and 6% of crushed limestone filler (Figure 12.1). The cement used was a GU type (CSA A3000) with compressive strength at 28 days of 43.9 MPa (ASTM C109). The cement content was fixed at 1.5% by mass of aggregates.

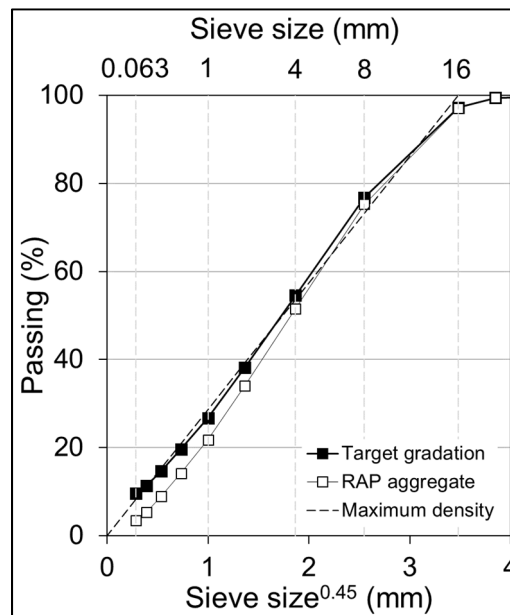


Figure 12.1 Target aggregate blend

Two bitumen emulsions were used for this study: one is a slow-setting cationic emulsion produced in United Kingdom classified as CSS-1 (ASTM D2397), whereas the other is a slow-setting cationic emulsion produced in Italy and classified as C60B10 (EN 13808). The main

properties of both emulsions are listed in Table 12.2, where for simplicity are named from now on as Emulsion A and Emulsion B, respectively.

Table 12.1 RAP aggregate properties

Property	Standard	Unit	Value
Binder content	ASTM D6307	%	5.51
Nominal maximum particle dimension	ASTM D448-03	mm	16
Maximum specific gravity	ASTM C127-128	-	2.482
Average bulk density	LC 21-065-066-067	-	2.323
Water absorption	ASTM C127-128	%	1.10

Table 12.2 Bitumen emulsions properties

Emulsion A			
Bitumen emulsion properties	Standard	Unit	Value
Density	ASTM D6397-16	g/cm ³	1.0
Residue content (bitumen)	ASTM D6997-12	%	60.3
Storage stability @ 24 hours	ASTM D6930-10	%	0.6
Residual bitumen properties			
Penetration @ 25 °C	ASTM D5-13	mm	4.1
Softening point	ASTM D36-14	°C	48.6
Emulsion B			
Bitumen emulsion properties	Standard	Unit	Value
Residual bitumen	EN 1428	%	60.0
Viscosity @ 40 °C	EN 13302	s	42.5
Breaking Index	EN 13075	%	2
Residual bitumen properties			
Penetration @ 25 °C	EN 1426	mm	10.0
Softening point	EN 1427	°C	43.0

It is possible to observe that the main difference between the emulsions regards the residual bitumen penetration value. In fact, Emulsion B is characterized by a softer residual bitumen. Moreover, this is confirmed by the lower softening temperature. In both cases, the bitumen emulsion dosage was kept constant at 5% (3% of residual bitumen) by mass of aggregates for the mixes. A mix design protocol was performed to fix the amount of total water, characterized by the water absorbed by the aggregates, the water from bitumen emulsion and the added water to improve compactability. Such amount was fixed at 4.0% by mass of aggregate, in order to reach the target air voids (15%) without employing high compaction energy and avoiding any material loss (water, bitumen and/or fine particles) during compaction.

12.4.2 Mixtures production

In order to investigate the effect of production temperature, loose mixes and specimens were obtained dividing the entire process in four steps: mixing, transportation and compaction, first period of curing and finally the second period of curing. Table 12.3 summarizes the details regarding the production process.

The mixing protocol required from 5 to 10 minutes and was performed by adding to the humid aggregate blend cement, water for compaction and bitumen emulsion, in this order. The mixing was carried out after conditioning materials and mixing tools (except for bitumen emulsion) at the target temperature for more than 12 hours. At the same time, the two bitumen emulsion sources were stored at room temperature (Emulsion A) and at 40 °C (Emulsion B) (Institute & Association, 1979).

A rest period was planned to simulate the transportation process for in-situ applications. In the laboratory, the mixture was poured in a plastic bag and sealed carefully to avoid any water loss by evaporation. The material was then placed in an environmental chamber at the target temperature for 2 hours. After the simulated transportation time, the compaction process was carried out by means of a Superpave Gyrotory Compactor (SGC) in a 100 mm undrained mould, with a constant pressure of 600 kPa, gyrations rate of 30 rpm and internal angle of

1.25 °. Prior to compaction, the mould and all the tools employed were placed in the environmental chamber for conditioning at the target temperature for at least 12 hours. The compaction was performed at fixed height, to obtain the same amount of voids in the mixture (V_m):

$$V_m = \frac{V_{V,A} + V_{W,I}}{V} \cdot 100 = \frac{V - (V_S + V_C + V_{B,R})}{V} \cdot 100 \quad (12.1)$$

where V is the total volume of the specimen, V_S is the bulk volume of aggregates, V_C is the volume of cement, $V_{B,R}$ is the volume of residual bitumen from emulsion, $V_{W,I}$ is the volume of intergranular water and $V_{V,A}$ is the volume of air. The specimens' volume, V , was fixed to obtain a V_m of $15 \pm 1\%$.

Table 12.3 Mixtures naming and production process

Processes		Production		Curing	
Steps		Mixing	Transportation + compaction	1 st period	2 nd period
Allowable time		5–10min	2 hours + 30 min	14 days	14 days
Emulsion A	A_25_25	25 °C	25 °C	25 °C	40 °C ⁽²⁾
	A_25_5	25 °C	5 °C	5 °C ⁽²⁾	
	A_5_25	5 °C	25 °C	25 °C	
	A_5_5	5 °C	5 °C	5 °C ⁽²⁾	
	A_5_5_0C ⁽¹⁾	5 °C	5 °C	5 °C ⁽²⁾	
Emulsion B	B_25_25	25 °C	25 °C	25 °C	40 °C
	B_5_5	5 °C	5 °C	5 °C	
⁽¹⁾ The mixture does not contain cement. The volume of cement was replaced by filler.					
⁽²⁾ The curing was performed with controlled relative humidity at $55 \pm 5\%$					

After compaction, the specimens started a first period of curing of 14 days in the environmental chamber, after which a first series of test was performed. In this first part, two temperatures were chosen: 5° C and 25 °C. The first represents the minimum temperature that several manuals recommend to produce cold mixtures, whereas the second represents the typical

environmental temperature, often used in literature as reference temperature for the study of such materials (Gandi et al., 2019; Karray et al., 2019). All the specimens not tested were cured for an additional period of 14 days at 40 °C, regardless of the mixture, and another series of test was performed afterwards. This step was necessary to have specimens representing a long-term curing, in order to understand the effect of the initial production and curing temperatures.

It is important to remark that all the temperatures reported in Table 12.3 had a variability of ± 2 °C. As it can be seen, not all the mixtures produced with Emulsion A were repeated with Emulsion B. In fact, Emulsion A was chosen to investigate the different phases of the production process in different temperature conditions, whereas Emulsion B was used only for production at standard temperature and low temperature. It must be highlighted that both emulsions are designed for cold recycling purposes, even though they are employed in two different climates and markets. The letter at the beginning of the mixes names represents the emulsion, the first number is the mixing temperature, and the second number represents transportation, compaction and first cure temperature.

12.4.3 Testing program

12.4.3.1 Workability and compactability

SGC compaction curves can be described using several parameters. In this specific study the Compaction Energy Index (CEI), voids in the mixture after 10 gyrations $V_m(10)$ and the compaction curve slope k were chosen to analyse the mixtures in terms of compaction behaviour. In case of HMA, the CEI indicates the area under the compaction curve from the 8th gyration to the number of gyrations related to 92% of the mixture maximum density. Eight gyrations are selected to simulate the process of laydown performed by the paver in the field. In this case, the CEI is calculated between gyration number 10 and the number of gyrations required to reach the target V_m of $15 \pm 1\%$. Mixtures with low values of CEI are preferable because of improved constructability (Mahmoud & Bahia, 2004). Nevertheless, other authors

have elaborated several compaction indexes based on the relationship between maximum density and air voids ratio (Bayomy et al., 2002; Butcher, 1998; Dessouky et al., 2004).

Starting from 10 gyrations, the SGC compaction curve can be represented in a semi-logarithmic plot as a straight line having slope k . Parameters $V_m(10)$ and k are obtained by experimental data by means of a linear regression:

$$V_m(n) = V_m(10) - k \log n \quad (12.2)$$

where $V_m(n)$ are the voids in the mixture at the gyration number n .

In order to describe the mixture workability, i.e. the ease to be mixed and the laydown effort, the value of V_m at 10 gyrations, $V_m(10)$, is selected as the workability parameter. Low values of $V_m(10)$ characterise mixtures with improved workability. On the other hand, the slope is selected as a compactability parameter, and it is directly related to the mixture densification (Gandi et al., 2019; Karray et al., 2019). High k values represent better compactability.

As mentioned before, all the mixtures studied were compacted at fixed height to reach the same amount of voids in the mixture. Hence, in order to compare the CEI index results, it is not useful to consider the compaction area below the target value of V_m . Consequently, the area of the triangle is considered and named CEI_T^+ , as shown in Figure 12.2.

Normally the CEI_T^+ is calculated as the area under the graph according to the trapezoidal rule. However, an alternative way to calculate the CEI_T^+ is proposed in this research, as the area of the triangle characterized by the parameters $V_m(10)$ and k :

$$CEI_T^+ = \frac{(V_m(10) - V_{m,t})^2}{2 \cdot |k|} \quad (12.3)$$

where $V_{m,t}$ is the target voids in the mixture (15% in this case).

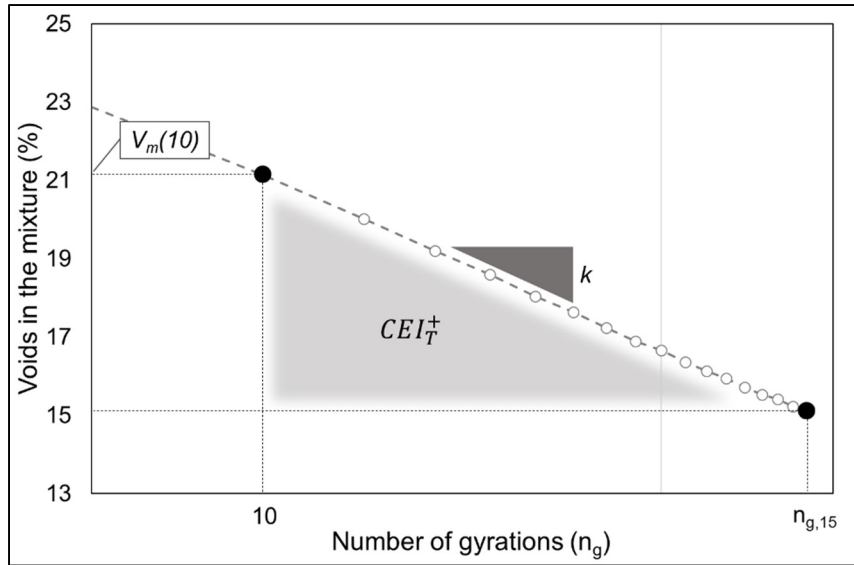


Figure 12.2 Graphic meaning of CEI_T^+ , $V_m(10)$ and k parameters

12.4.3.2 Water loss

Water loss was monitored along curing, measuring the specimens' mass after 1, 3, 5, 7, 14, 21 and 28 days for mixes produced with Emulsion A and after 1, 3, 7, 14, 15, 17, 21 and 28 days for mixes produced with Emulsion B. The water loss was calculated as:

$$\Delta W(t) = \frac{W_0 - W(t)}{W_{TOT}} \cdot 100 \quad (12.4)$$

where $\Delta W(t)$ is the water loss (%) at the curing time t , W_0 is the initial mass of the specimen; $W(t)$ is the mass of the specimen at the curing time t and W_{TOT} is the total amount of water in the specimen, constituted by absorbed water, bitumen emulsion water and added water for compaction.

12.4.3.3 Indirect Tensile Strength (ITS)

The Indirect Tensile Strength (ITS) test is used to investigate both the effect of the production temperature and of the emulsion source, as the resistance of the binding phase is assessed (Du, 2018). The test was performed according to ASTM D6931, at a testing temperature of 25 °C and on three replicates for each mixture produced. The test measures the tensile strength along the vertical diametral plane of the specimen as:

$$\text{ITS(kPa)} = \frac{2000 \cdot P(\text{N})}{\pi \cdot D(\text{mm}) \cdot l(\text{mm})} \quad (12.5)$$

where ITS is the tensile strength, P is the maximum compressive load, l is the specimen height and D is the specimen diameter.

The ITS test was performed on all mixes after the first period of curing (14 days) and after the second period of curing (14 days), to investigate the evolution of strength due to the additional curing period.

Indirect Tensile Stiffness Modulus (ITSM)

The Indirect Tensile Stiffness Modulus (ITSM) test, together with the water loss monitoring, can be carried out during the curing process to evaluate the mechanical properties evolution (Fang et al., 2016; Serfass et al., 2004). The test was performed according to EN 12697-26 (Annex C), at a testing temperature of 25 °C and on three replicates for each mixture produced with only Emulsion B. The test measures the average stiffness modulus after the application of 5 pulses with a rise time of 124 ± 4 ms. For each pulse, the stiffness modulus is obtained as:

$$\text{ITSM (MPa)} = \frac{F(\text{N}) \cdot (R + 0.27)}{l(\text{mm}) \cdot H(\text{mm})} \quad (12.6)$$

where F is the peak value of the applied repeated vertical load, H is the amplitude of the horizontal deformation, l is the mean thickness of the specimen and R is the Poisson's ratio (assumed as 0.35).

The test was performed to study the development of stiffness along curing, hence the measurements were taken after 1, 3, 7, 14, 15, 17, 21 and 28 days.

Scanning Electron Microscope (SEM)

The Scanning Electron Microscope (SEM) was performed on samples obtained from the broken specimens produced with only Emulsion A, after 14 and 28 days to verify if changes in the microstructure are seen with different production temperatures. The equipment employed allowed to have pictures of samples with an average dimension of 20 mm. Although organic elements are recommended to be treated on the surface before processing with SEM, no pretreatment was applied in this case, so as not to modify the nature of the material. In other works, researchers performed SEM analysis to evaluate the microstructure in cold bituminous mortars containing cement or other additives (Godenzoni, 2017; Richardson, 1999; Rutherford et al., 2014).

12.5 Results analysis

12.5.1 Workability and compactability

Figure 12.3 shows the compaction curves for the studied mixes. For simplicity, one reference curve for each mixture was chosen. The experimental points collected start from 1 gyration although the part after 10 gyrations is highlighted. In fact, points at 10 gyrations represent the $V_m(10)$ values, whereas the remaining part of the curves is described with the slope parameter k (Eq. (6.2)). It can be observed that between 1 and 10 gyrations, mixtures are placed in the same order. This means that the parameter $V_m(10)$ is consistent with the value after 1 gyration. Among the studied mixtures, the difference in workability $V_m(10)$ is more visible than the difference in compactability k . As already explained, it is also possible to use these two parameters to evaluate the area of the triangle CEI_T^+ . CEI_T^+ values for all the specimens produced were calculated following the trapezoidal rule and by Eq. (6.3). It was observed that the values obtained with both calculations are perfectly superposing. Such results confirm that the

approximation of the compaction curve in the semi-logarithmic plane as a straight line after 10 gyrations is valid. As a consequence, CEI_T^+ can be described using two parameters, workability $V_m(10)$ and compactability k , and used to evaluate the effect of production temperatures and of the emulsion source.

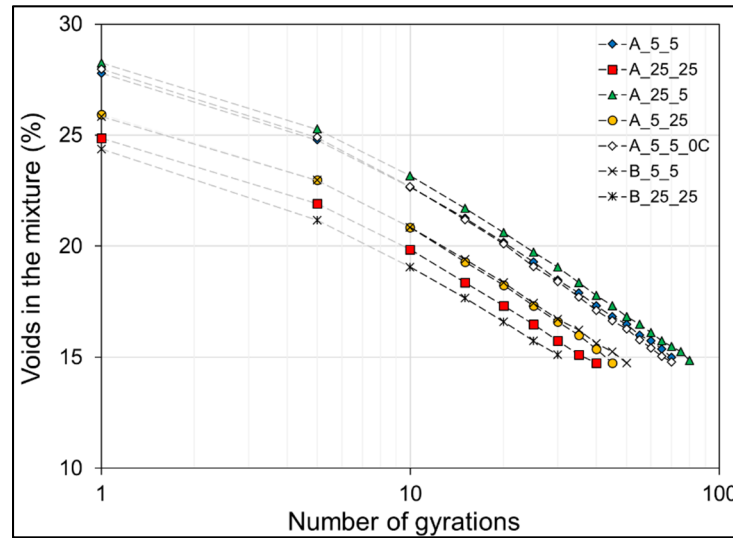


Figure 12.3 Compaction curves

12.5.1.1 Correlation between $V_m(10)$, k and CEI_T^+

Regarding the parameters just described, it is interesting to study the respective relationship that could exist among them ($V_m(10)$, k and CEI_T^+). Figure 12.4 shows the correlation between $V_m(10)$ and k , between CEI_T^+ and k , and between CEI_T^+ and $V_m(10)$. In Figure 12.4, both mixtures produced with Emulsion A and B are reported.

Figure 12.4 a) globally shows that for both emulsions used, $V_m(10)$ decreases when k decreases. According to this trend, a gain in workability is related to a loss in compactability (Raschia, Mignini, et al., 2019). However, experimental points related to Emulsion A show that workability significantly improves when transportation and compaction temperature increases from 5 °C to 25 °C (average $V_m(10)$ values of 23% and 19%, respectively). At the

same time, average values of compactability decrease from 9.5 to 8.0. An exponential trend line with quite a good R^2 value can describe all the points in the picture (for both emulsions used).

Figure 12.4 b) shows the influence of the compactability parameter k on the CEI_T^+ value. Also in this case, all the experimental points can be represented with an exponential trend line. It can be observed that if the value of k increases, i.e., the slope of the compaction line is higher, the compaction effort increases. In particular this happens for mixes transported and compacted at 5 °C. In fact, such mixes are characterized on one side by higher compactability, but at the same time they showed higher values of $V_m(10)$, which directly affected the compaction effort required to reach the target voids in the mixture. A very good correlation between the compaction effort CEI_T^+ and the workability $V_m(10)$ is shown in Figure 12.4c). The experimental points are described by an exponential trend line with R^2 value of 0.971. In particular, points with higher $V_m(10)$ and CEI_T^+ values are related to mixtures with transportation and compaction temperatures of 5 °C. When such temperature is increased to 25 °C, mixtures with increased workability and lower CEI_T^+ are obtained. This trend is observed for both emulsions used, even though the Emulsion B gave globally lower values of $V_m(10)$ and CEI_T^+ than Emulsion A.

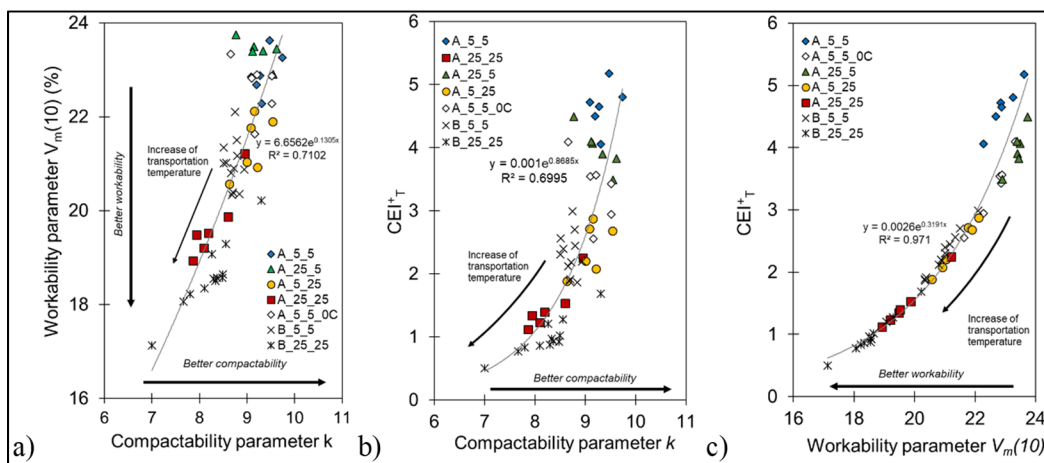


Figure 12.4 a) Relationship between $V_m(10)$ and k ; b) Relationship between CEI_T^+ and k ; c) Relationship between CEI_T^+ and $V_m(10)$

The softer residual bitumen contained in Emulsion B probably caused a better workability and less compaction effort for the mixtures produced. According to the results, the reduced transportation and compaction temperature (5 °C) lead to an increase of the compaction effort required by the mixture, acting more clearly on the initial workability (laydown process) rather than on the compactability (densification process). Because of the good correlation that exists between the CEI_T^+ and both parameters k and $V_m(10)$ (Figure 12.4b) and c), respectively), CEI_T^+ can be considered a reliable parameter that can be used to have an idea of the global compaction effort required by the studied mixes.

12.5.1.2 Effect of mixing and transportation temperatures on CEI_T^+

Figure 12.5 shows the effect of production temperatures (mixing, transportation and compaction) on the CEI_T^+ values of the mixes produced with Emulsion A. Mixtures produced with Emulsion B are not reported because no distinction was made between mixing and transportation temperatures. In the graphs, each point represents a compacted specimen, which were 6 for each mixture. A low mixing temperature (5 °C) did not result critical to the compaction effort required by the mixture to reach the target voids. In fact, values of CEI_T^+ are ranging between 1.1 and 5.2 regardless the mixing temperature.

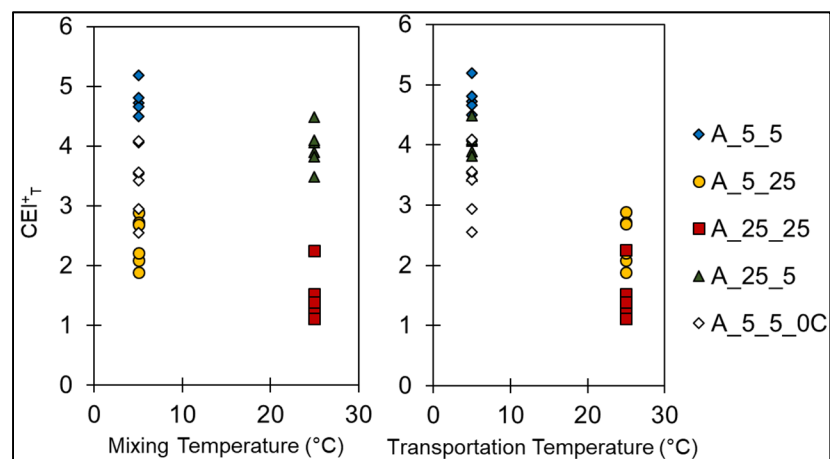


Figure 12.5 Relationship between CEI_T^+ , mixing temperature and transportation temperature

On the other hand, the influence of transportation (and compaction) temperature is more visible. When the mixture is transported and compacted at 5 °C, the lowest CEI_T^+ obtained is around 2.6. Increasing the transportation temperature from 5 °C to 25 °C, a CEI_T^+ of 1.1 can be reached. Such results show that, during the production process of CBTM mixtures, the mixing temperature is not critically affecting the effort required for the mixtures compaction, which is instead more influenced by the transportation and compaction temperature. This also highlights that the emulsion did not prematurely break in case of low mixing temperatures (5 °C), because it is reasonable to assume that this would lead to an increase of the CEI_T^+ .

In order to prove the above-mentioned statements, an analysis of variance (ANOVA) was also performed considering only the mixtures with added cement and with a level of significance $\alpha = 0.05$ (Table 12.4). It can be observed that both mixing and compaction temperatures statistically affect CEI_T^+ , since the F statistic is higher than the critical value. Among the two temperatures studied, the transportation and compaction temperature influences more the CEI_T^+ value than the mixing temperature. Furthermore, there is no connection between the two variables.

Table 12.4 Results of two-way ANOVA for CEI_T^+

Source of variance	SS	df	MS	F	p-value	F crit
Transportation and compaction temperature	33.798	1	33.7978	235.8242	1.56E-12	4.3512
Mixing temperature	3.842	1	3.8419	26.8068	4.58E-05	4.3512
Interaction	0.099	1	0.0986	0.6881	0.4166	4.3512
Error	2.866	20	0.1433			
Total	40.605	23				

12.5.2 Water Loss

Figure 12.6 shows water loss evolution along curing time for all the mixes studied. It is possible to observe, for both emulsions, the increasing trend of the experimental points, which are characterized by a step in proximity of the additional curing after the first 14 days. Experimental data for each mix were modelled thanks to a modified version of the Michaelis-Menten model (Graziani, Iafelice, et al., 2018; Michaelis et al., 2007; Raschia, Graziani, et al., 2019b), which is a non-linear hyperbolic function characterized by three parameters and valid starting from 1 day:

$$y(t) = y_1 + \frac{(y_A - y_1) \cdot (t - 1)}{(t - 1) + (H - 1)} \quad (12.7)$$

where $y(t)$ is the material property under investigation (in this case, water loss), t is the curing time (days), y_A is the asymptotic value, y_1 is the value related to 1 day and H is the time (days) for $y(t)$ to reach half of the gap between y_A and y_1 . It is important to highlight that terms $(t - 1)$ and $(H - 1)$ are used to describe the function after the first day, since what happens in the first hours of curing is dominated by a different and faster mechanism. In order to employ the model also in the second curing, the terms in Eq. (6.7) become $(t - 14)$ and $(H - 14)$, respectively. In Figure 12.6 the model related to each mix is superposed to the average experimental points and standard deviation, whereas the model parameters are reported in Table 12.5. Figure 12.6 a) shows results of mixtures produced with Emulsion A. In the second part of the curing at 40 °C, water loss was measured only at 21 and 28 days, so the model is not reported in the period between 14 and 21 days, as well as the parameter H is not listed in Table 12.5 for the second curing.

It can be observed that in mixtures produced with Emulsion A, lowest values for $y_{A,14}$ are related to a first curing temperature of 5 °C, which are also characterized by a slower evaporation rate H_{14} . In those two mixes (A_5_5 and A_25_5) only the mixing temperature is different, and it seems to have affected the water loss after 14 days. This can be due to the

cement that immediately trapped some water when mixed at 25 °C, leading to a lower water loss (72.9% instead of 77.9%). However, after a long-term curing of 28 days, all the four mixes with cement tend to similar values (comprised between 88.8% and 91.2%), whereas the mixture without cement reached 97.4%, since no water was used for the cement hydration.

Regarding mixtures produced with Emulsion B, mixture B_5_5 lost more water than mixture B_25_25 after 14 days, which is comparable to the same mixes produced with Emulsion A. This basically shows that the water evaporation mechanism does not strictly depend on temperature, but mostly on relative humidity. At the end of curing, at 28 days, the mixture B_5_5 lost 97.1% of the total water, which is very close to the value obtained for the mix A_5_5_0C, with no cement. In this case, it could mean that the cement hydration was eventually prevented in mixture B_5_5. At the same time, comparing mixes A_25_25 and B_25_25, it is highlighted that the water loss after 28 days was 91.2% and 91.5%, respectively; hence, at standard production temperatures, the emulsion did not really have an effect on the water evaporation of the mixture.

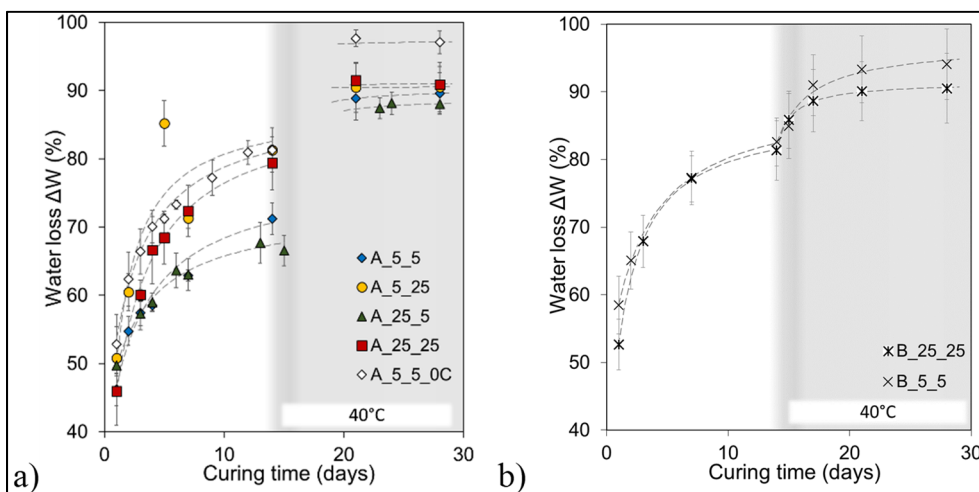


Figure 12.6 Water loss experimental data and superposed model for mixtures with: a) Emulsion A and b) Emulsion B

Table 12.5 Water loss model fitting parameters

Mixtures	1 st curing			2 nd curing	
	y_1 (%)	$y_{A,14}$ (%)	H_{14} (days)	y_{14} (%)	$y_{A,28}$ (%)
A_5_5	46.7	77.9	5.0	70.6	90.4
A_5_25	50.2	87.8	3.1	82.6	90.6
A_25_5	49.7	72.9	5.0	67.7	88.8
A_25_25	45.9	88.2	4.5	79.3	91.2
A_5_5_0C	53.6	88.3	4.4	81.1	97.4
B_25_25	52.6	86.9	3.4	81.5	91.5
B_5_5	58.6	89.7	4.9	82.5	97.1

12.5.3 Indirect Tensile Strength (ITS)

Figure 12.7 shows the influence of the mixing and compaction temperatures on the ITS results at 28 days. In the picture, all the mixes produced in this study are reported. It can be seen that for mixtures produced with Emulsion A at different temperatures, both mixing and transportation temperatures do not affect the ITS. In fact, at the end of curing, all the mixes show similar strength if compared to the mixture produced at room temperature (A_25_25). As expected, a drop in the ITS values is observed in the mix without cement (A_5_5_0C).

On the other hand, the Emulsion B used to produce mixes B_5_5 and B_25_25 gives different results. On one side, the mixture produced at room temperature (B_25_25) shows a remarkable lower strength compared to the same mixture produced with Emulsion A (A_25_25). This can be caused by the softer bitumen contained in Emulsion B, which caused a lower ITS resistance (Komacka et al., 2014). Moreover, Emulsion B results to be more sensitive to low production temperatures. In fact, at 28 days, the mixture B_25_25 is characterized by an ITS value 24% higher than the mixture B_5_5.

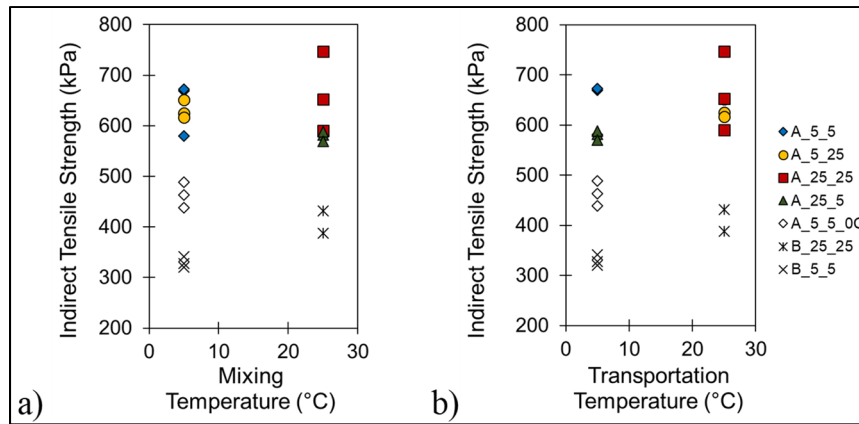


Figure 12.7 Effect of mixing and transportation temperatures on Indirect Tensile Strength (28 days)

Also in this case, a two-way ANOVA analysis was performed with the level of significance $\alpha = 0.05$ (Table 12.6). For mixtures with emulsion A, the F statistic is lower than the critical value, hence it is possible to conclude that both factors (mixing and transportation and compaction temperatures) do not affect the ITS results and there is no interaction between them. On the other hand, low production temperatures affect the strength of the samples produced with Emulsion B. In fact, the t-test confirms that the ITS of mixture B_5_5 is significantly lower than the ITS of mixture B_25_25 (p-value = 0.0217).

Table 12.6 Results of two-way ANOVA for ITS results (Emulsion A)

Source of variance	SS	df	MS	F	p-value	F crit
Transportation and compaction temperature	4073.2	1	4073.2	1.7391	0.2237	5.3177
Mixing temperature	621.7	1	621.7	0.2655	0.6203	5.3177
Interaction	6490.5	1	6490.5	2.7712	0.1345	5.3177
Error	18736.8	8	2342.1			
Total	29922.3	11				

Concluding, the emulsion source resulted to be critical for the final strength level at 28 days, as well as in terms of production temperature sensitivity. Figure 12.8 shows the relationship between the ITS results and the residual water in the mixtures, measured at 14 and 28 days of curing.

The residual water is simply calculated as the difference between the total water and the water loss at the moment of testing (Graziani, Iafelice, et al., 2018). The non-evaporable water, i.e. the amount of water required by the cement hydration, is estimated and reported in the graph (around 0.4% of the mixture mass). The points related to the mixtures produced with Emulsion A (only mixtures with cement) and Emulsion B are modelled separately with the original version of the Michaelis-Menten model:

$$ITS = \frac{a \cdot \Delta W}{b + \Delta W} \quad (12.8)$$

where a and b are regression parameters obtained through a least square minimisation.

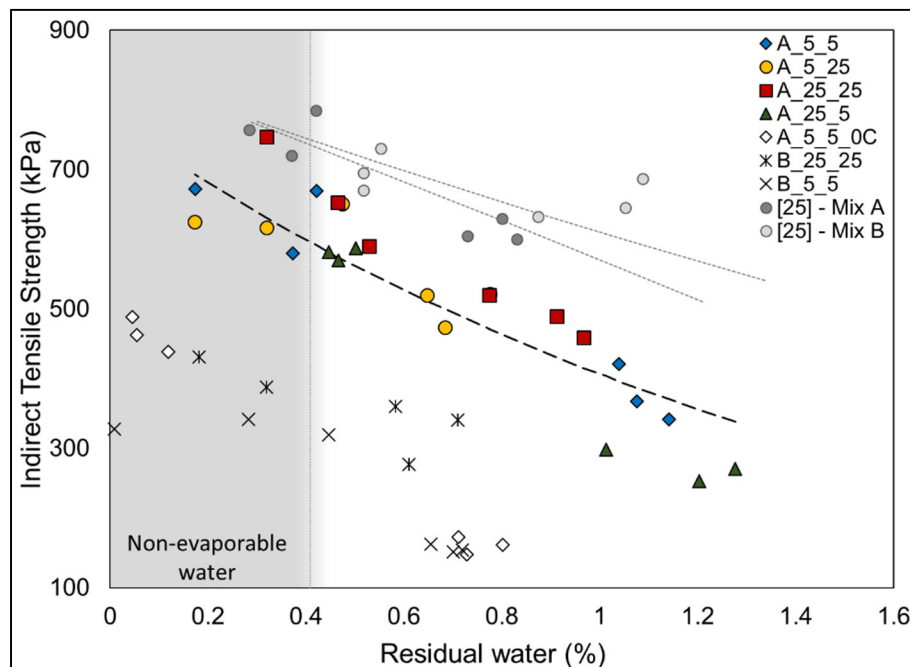


Figure 12.8 Correlation between residual water and Indirect Tensile Strength (at 14 and 28 days of curing)

After defining the parameters a and b , the same model is valid for the representation of the ITS results in terms of residual water. The points related to the mixtures produced with Emulsion A at different temperatures show a typical trend which links the increase of ITS with the decrease of residual water in the mixture, regardless of the mixing and transportation temperatures. This confirms that for mixes with Emulsion A, the ITS strength is strictly related to the curing conditions (i.e. residual water), rather than the production temperatures, as also shown in Figure 12.7. The mixture without cement, A_5_5_0C, is in fact characterized by a residual water content close to 0% at the end of curing. Hence, for mixtures with Emulsion A, the production temperatures did not permanently affect the mechanical properties, and the effect of low curing temperatures is recoverable. Mixtures produced with Emulsion B show more scattered results than Emulsion A mixes, meaning that the ITS strength is sensitive to both residual water and production temperatures.

In order to have a broader view on the results obtained, experimental points from (Task, 1998) are added to the same graph, and modelled in the same way by Eq. (6.8). Such results are related to two different CBTM mixtures produced in different laboratories and with different properties (cement, bitumen and water contents, as well as volumetric properties). Nevertheless, even though everything related to mixture's production is different, the two mixtures reach the same level of strength after 28 days of curing, close to 800 kPa. In the present research, mixtures produced at different temperatures with Emulsion A showed a similar trend, as well as close values of ITS after 28 days.

12.5.4 Indirect Tensile Stiffness Modulus

Figure 12.9 shows results from ITSM development along curing for mixes produced with Emulsion B. The mixture produced at room temperature, B_25_25, shows a typical increasing trend of the modulus (also shown by the Michaelis-Menten model), due to the contemporary presence of cement hydration, emulsion breaking and water evaporation. After 28 days of curing, the stiffness modulus does not seem to have reached an asymptotic condition, meaning

that the curing is still occurring and requires more time, even though the water evaporation is completed (residual water close to 0%).

Regarding mixtures produced at 5 °C, three specimens were tested in the initial 14 days (same three specimens tested at 3, 7 and 14 days), whereas three additional specimens were tested in the second curing period, for a total of six measurements. This was done because in the initial 14 days, the testing temperature (25 °C) could have affected the curing process at 5 °C, leading to unreliable results. The stiffness of the specimens were very low after one day of curing. Because of this, two specimens were slightly damaged during testing, which did affect the results for those specimens in the first 14 days. Between 14 and 28 days, the three not-tested specimens gave reliable results reaching a maximum final value of 2322 MPa. Results between 14 and 28 days of the two damaged specimens were not reported in Figure 12.9. ITSM results confirmed the temperature sensitivity of Emulsion B also in terms of stiffness. After one day of curing, it was also impossible to run a test in the small deformation field.

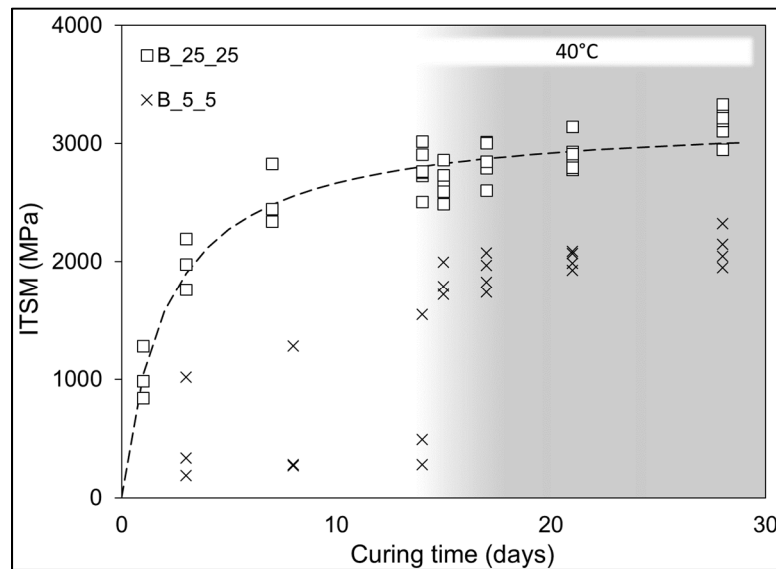


Figure 12.9 ITSM results

12.5.5 Scanning Electron Microscope (SEM)

Figure 12.10 shows images from SEM taken on samples of mixes produced with Emulsion A.

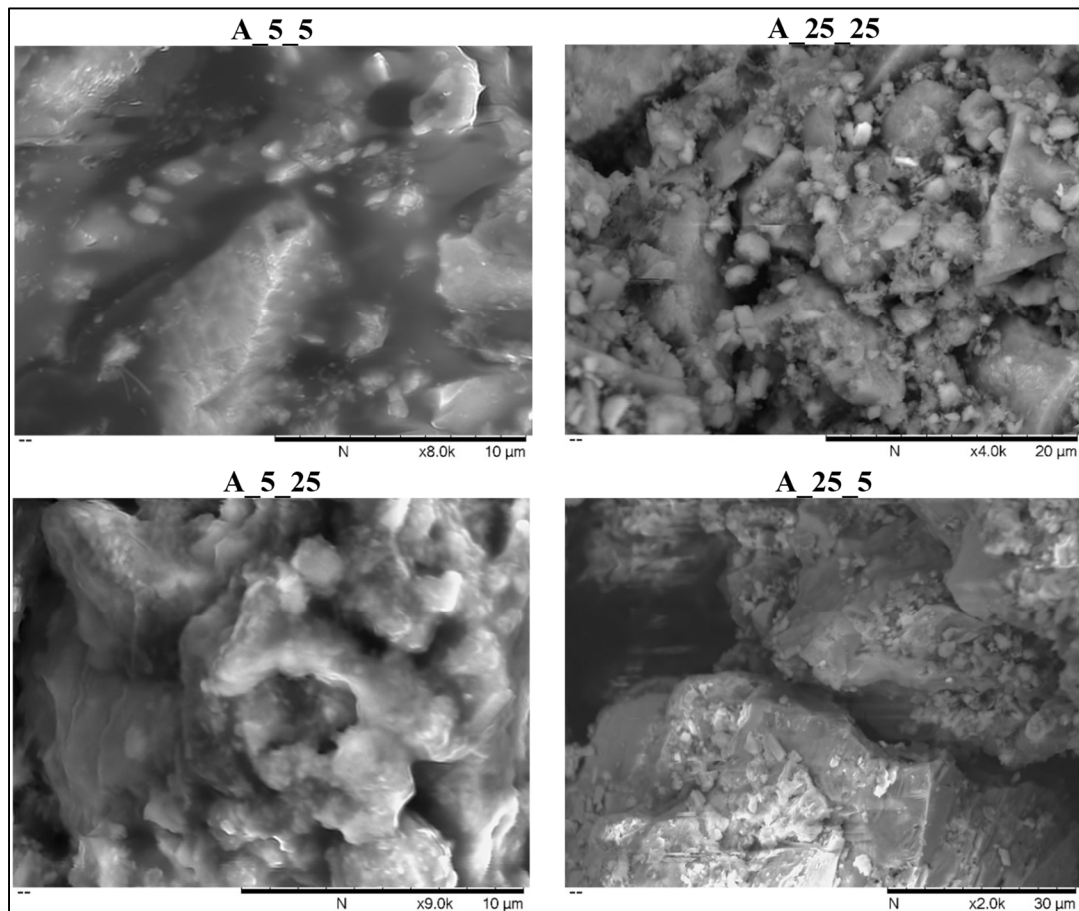


Figure 12.10 SEM images captured for mixes produced with Emulsion A after 28 days of curing

Pictures reported are only relative to samples cured for 28 days. It is possible to observe that in mixes A_5_5 and A_5_25, the mastic is visible and the bitumen film looks uniformly spread on the aggregate faces. On the other hand, it is difficult to recognize the hydration products from cement reaction, if not for some little spots. Mixtures mixed at 25 °C (A_25_25 and A_25_5) show similar microstructure, characterized by a bitumen film less dispersed. At the

same time, particles of cement seem to have reacted sufficiently to observe points in which the hydration products are visible. These images suggest that both bitumen and cement are sensitive to mixing temperature. The slow-setting nature of the emulsion particularly suitable for low temperatures allowed a more uniform dispersion at 5 °C without affecting the mechanical properties. When the mixture is mixed at 25 °C, the cement hydration is probably favored, whereas the bitumen assumes a spotted dispersion. However, as ITS results confirm, the final mechanical properties were not influenced.

12.6 Conclusions

This study focused on the effect of production temperatures on the mechanical properties of CBTM mixtures produced with two different bitumen emulsions.

In terms of workability and compactability, the compaction energy index CEI_T^+ was selected to link both material characteristics. CEI_T^+ is affected by the low transportation temperature rather than low mixing temperature. In fact, results showed that mixes transported and compacted at 5 °C required more energy to reach the target volumetric properties. Analysing the relationship between CEI_T^+ and the workability parameter $V_m(10)$, this energy increase can be related to the workability of the mixture, i.e. the amount of voids after 10 gyrations. This evaluation was valid for both emulsion sources used, even if the emulsion produced with a softer bitumen was characterized by a better workability and required less compaction energy.

After both 1 day and 14 days of curing, water loss was lower when curing temperature was 5 °C if compared to 25 °C. However, after the long-term curing (28 days), all mixes lost almost the same amount of water, which means that it was not negatively affected by the production temperatures or the emulsion source.

In terms of ITS and ITSM results, the production at 5 °C did not affect long-term strength and stiffness of mixtures with Emulsion A. This suggests that no premature breaking of the emulsion has occurred during the production process at 5 °C, even though the compaction

energy required was higher. On the other hand, mixtures produced with Emulsion B showed globally low values for ITS and ITSM, as well as a higher production temperature sensitivity. In general, the CBTM mixtures studied resulted highly affected by the emulsion used, both at standard (25 °C) and low (5 °C) production temperatures. This means that particular attention should be paid to the emulsion used for the production of CBTM. Results highlighted that two similar emulsion sources (both cationic slow-setting emulsions) significantly affected the final product mechanical properties.

Improved analysis and researches are recommended and strongly encouraged to clarify the effect of production temperatures on cold mixes, aspect still not standardized. More temperature and temperature combinations should be analyzed. Furthermore, attention should be paid to the bitumen emulsion composition and characteristics at the moment of production, such as storage and application temperatures.

CHAPTER 13

THERMO-RHEOLOGICAL MODELLING IN THE SMALL STRAIN DOMAIN OF CEMENT-BITUMEN TREATED MATERIALS

Simone Raschia^a, Hervé Di Benedetto^b, Sébastien Lamothe^a, Alan Carter^a, Andrea Graziani^c,
Daniel Perraton^a

^a Construction Engineering department, École de technologie supérieure (ÉTS) 1100, Notre-Dame Street West, Montreal, Canada

^b Université de Lyon, École Nationale des TPE, LTDS (CNRS UMR 5513), Vaulx-en-Velin, CEDEX, Lyon, France

^c Department of Civil and Building Engineering, and Architecture, Università Politecnica delle Marche, Via Brecce Bianche, 60131 Ancona, Italy

Submitted and under review with the journal *Transportation Geotechnics*, Elsevier,
March 2020

13.1 Abstract

Cold recycled mixtures (CRM) have been introduced as structural materials in road pavement structures thanks to their significant economical and environmental benefits. Among them, cement-bitumen treated materials (CBTM) are often employed because of both contributions given by bitumen (in form of emulsion) and cement. The first confers a bituminous behaviour, whereas the second ensures good short-term performance otherwise penalized by the presence of water. Water plays a fundamental role in providing workability of the mixture at the ambient production temperatures. Due to such peculiarities, CBTM mixtures require attention when rheological modelling is performed in the small strain domain. This paper provides an overview on the most common rheological model applied to bituminous mixtures (2S2P1D) and the main issues related to the application to CBTM mixtures are highlighted. Afterwards, another model is proposed from the literature, the DBN model, and applied to three mixtures. The mixtures were prepared to assess the effect of the bitumen emulsion used, as well as the

type of curing conditions. Results showed that the DBN model seems to be an excellent tool for not only CBTM rheological modelling in the small strain domain and it is recommended for applications in wider experimental programs.

13.2 Introduction

The increasing costs related to the road industry to face the necessity of frequent maintenance and rehabilitation projects have led to the promotion of sustainable technologies characterized by substantial environmental and economic benefits. Among them, cold recycled mixtures (CRM) are the most promising materials for structural layers (base or subbase), due to the possibility of reusing high quantity of reclaimed asphalt and performing the production process at ambient temperature (ARRA, 2001, 2016; Giani et al., 2015; Lauter & Corbett, 1998; Stroup-Gardiner, 2011). In fact, the bitumen is used in form of bitumen emulsion or foamed bitumen, whereas the workability of the mixtures is ensured by the addition of water (Asphalt Academy, 2009). A specific type of CRM materials is the cement-bitumen treated materials (CBTM), where the short and long-term properties are improved by the addition of ordinary Portland cement. Such materials show a dual behaviour (asphalt-like and cement-like) when bitumen and cement are employed at almost the same dosages (between 1 and 3%) (Bocci et al., 2011; Cardone et al., 2014; Grilli et al., 2012). In addition to the low amount of bituminous binder and the presence of cement, an important difference between CBTM and the traditional hot mix asphalts (HMA) is the use of reclaimed asphalt pavement (RAP) as a black rock (Raschia, Graziani, et al., 2019b). The RAP is generally employed in high amount in the CBTM aggregate gradation and it is reasonable to assume that, at ambient temperature, the aged binder coating the aggregate particles does not blend with the added virgin binder (emulsion or foam).

In the literature, mechanical characterization of CBTM mixtures is commonly performed by means of traditional tests, often empirical, determining the resistance at high deformations (failure) (Dal Ben et al., 2014; Graziani, Iafelice, et al., 2018; Hodgkinson et al., 2004; Kim et al., 2011). Only few feedbacks can be found on CBTM (or CRM) mixtures characterization in the small strain domain (Gandi et al., 2017; Godenzoni et al., 2015; Godenzoni, Graziani, et

al., 2016; Saleh, 2007), even though in many cases sigmoidal functions characterized by experimental parameters are preferred instead of rheological models composed by specific elements (springs and/or dashpots) (Graziani et al., 2020). In particular, the determination and modelling of rheological properties, such as complex modulus and phase angle, allow a better understanding of the material behaviour by means of the application of a valid rheological model. In case of bituminous mixtures, the Huet-Sayegh model was widely used in the past, even though it does not allow to well represent the material behaviour at very low frequencies (or very high temperatures) (Olard et al., 2003; Pronk, 2006). For this reason, the 2S2P1D was introduced to obtain a complete rheological description of bituminous mixtures and binders in the linear viscoelastic field (Olard et al., 2003). Of course, the application of this model is valid in any case where the loading conditions (number of cycles, strain amplitude, temperature) keep the material in the linear domain. When non-linearities are present, a more versatile model can be used, like the DBN model (Di Benedetto, Mondher, et al., 2007). In fact, the DBN model can be applied depending on the strain level and the formulation can be quite simple (in case of linear viscoelasticity) or more complex (permanent deformation or fatigue).

It is assumed that the 2S2P1D model could not perfectly describe the behaviour of CBTM mixtures, being a LVE model normally used for bituminous mixtures. In fact, CBTM mixtures have peculiar characteristics that do not allow the assumption of an only-viscous response to cyclic loading. Hence, the objective of this paper is to introduce a suitable rheological model to investigate the properties of CBTM mixtures in the small strain domain. The most common models proposed by the literature are applied, describing the main issues observed. Moreover, the analysis of the models' parameters will assess the influence of the type of bitumen emulsion used and the type of curing condition adopted.

13.3 Thermo-rheological modelling of HMA and CBTM

The main characteristic of CBTM mixtures is the contemporary presence of bitumen and cement. The contribution of both binding agents makes the thermo-mechanical and rheological description of such materials different from the traditional approaches followed for HMAs. In

fact, CBTM mixtures could be considered as an intermediate material between unbound granular mixtures, cement treated mixtures and bituminous mixtures. Rheological models developed so far are suitable for systems where the dissipation at small strain level can be explained when considering LVE behaviour. This assumption is considered valid probably because HMA are characterized by higher effective bitumen content and lower voids when compared to CBTM mixtures. For these mixtures, the aggregates are not completely coated by the bitumen film, which is instead dispersed irregularly, and the use of RAP as a black rock implies the presence of the aged binder in addition to the virgin binder (Asphalt Academy, 2009). Such considerations can explain, at a local scale, the observed behaviour during rheological testing and must be taken into account for the rheological modelling of CBTM mixtures.

The linear viscoelastic Huet-Sayegh model is a rather good tool to represent the rheological properties of bituminous mixtures but not binders, especially at low frequencies (or high temperatures). The analytical expression of the Huet-Sayegh complex modulus is described in Eq. (6.9):

$$E_{HS}^*(i\omega\tau_E) = E_{00} + \frac{E_0 - E_{00}}{1 + \delta(i\omega\tau_E)^{-k} + (i\omega\tau_E)^{-h}} \quad (13.1)$$

where i is the complex number defined as $i^2 = -1$, ω is the pulsation defined as $\omega = 2\pi f$, f is the frequency, k and h are constant exponents ($0 < k < h < 1$), δ is a constant, E_{00} is the static modulus for $\omega \rightarrow 0$, E_0 is the glassy modulus when $\omega \rightarrow \infty$, and τ_E is the characteristic time, which is the only parameter depending on the temperature:

$$\tau_E(T) = a_T(T) \cdot \tau_{0E} \quad (13.2)$$

where $a_T(T)$ is the shift factor at a temperature T , $\tau_E(T) = \tau_{0E}$ at the reference temperature T_0 and $\tau_E(T)$ is determined at each isotherm by minimizing the error between the measured and modelled norm of the complex modulus, $|E^*|$.

It was recently observed that applying the Huet-Sayegh model to CBTM and focusing the fitting on the $|E^*|$ led to a systematic error in the modelling of the phase angle (φ), parameter characterizing the viscous energy dissipation (Graziani et al., 2020). In particular, a constant phase lag independent of temperature and frequency was observed between the modelled and experimental values, stressing the fact that the model underestimates the total energy dissipation considering only the viscous component. As a result, it seemed that CBTM mixtures are characterized by a total energy dissipation composed of a viscous component and non-linear phenomena (non-viscous). The authors described this aspect as energy dissipation probably due to the aggregate-to-aggregate contact and friction. As a solution, they proposed an analytical modification to the Huet-Sayegh equation, which consists in the addition of a constant phase angle and expressed by Eq. (6.11).

$$E_{HSq}^*(i\omega\tau_E) = E_{HS}^*(i\omega\tau_E) \cdot \exp\left(iq\frac{\pi}{2}\right) \quad (13.3)$$

where $E_{HS}^*(i\omega\tau_E)$ is the Huet-Sayegh model (Eq. (6.9)) and the term $\exp\left(iq\frac{\pi}{2}\right)$ represents an additional dissipation element with an angle, φ_{AEP} , equal to $q\frac{\pi}{2}$ without affecting the absolute value of the complex modulus.

Such correction led to a better fitting of the experimental data obtained for CBTM mixtures, but in this form, the model is only suitable for sinusoidal loading and cannot be used to extend the material representation in the time domain for another loading path. This drawback does not exist for the DBN model presented below. In the literature, the 2S2P1D model is extensively used to describe the rheological behaviour of bituminous mixtures in the LVE field with good approximation. In addition, the parameters that define the 2S2P1D model are used in the calibration process of the DBN model.

13.3.1 2S2P1D model

The 2S2P1D model is a linear viscoelastic rheological model composed of 2 springs, 2 parabolic elements and 1 dashpot. In particular, one spring is placed in parallel with a series of the remaining elements (Figure 13.1). Thanks to its nature, this model is largely employed to model unidimensional or tridimensional behaviour of bituminous materials (binders, mastics and mixtures) (Di Benedetto, Delaporte, et al., 2007; Di Benedetto et al., 2004; Tiouajni et al., 2011). The analytical expression of the complex modulus in the 2S2P1D model is given in Eq. (6.12) for a fixed reference temperature:

$$E_{2S2P1D}^*(i\omega\tau_E) = E_{00} + \frac{E_0 - E_{00}}{1 + \delta(i\omega\tau_E)^{-k} + (i\omega\tau_E)^{-h} + (i\omega\beta\tau_E)^{-1}} \quad (13.4)$$

where some parameters are already explained, and β is a parameter linked to the dashpot viscosity $\eta = (E_0 - E_{00})\beta\tau$ when $\omega \rightarrow 0$.

As already mentioned, this model is particularly suitable for bituminous mixtures or materials with almost only viscous dissipation and with seven constants can fully describe the rheological behaviour of HMA mixtures. However, it is possible that, in case of CBTM mixtures, the 2S2P1D is not able to well represent the material behaviour.

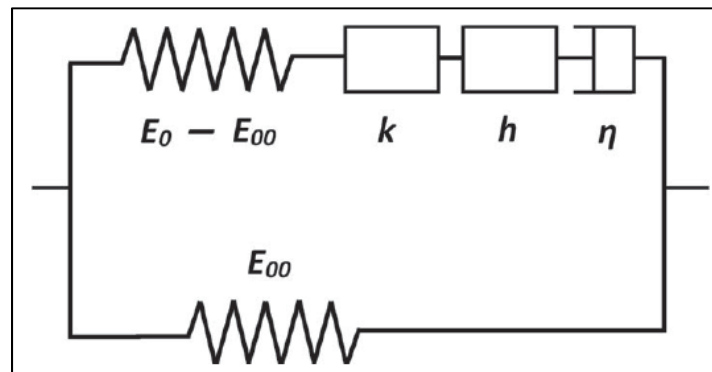


Figure 13.1 2S2P1D analogical representation (taken from Gayte et al., 2016)

Analyzing the model parameters in the literature, it is observed that E_0 and E_{00} are significantly different between HMA and CBTM mixtures (Carret et al., 2018; Gandi et al., 2017; Lamothe et al., 2017). In fact, springs stiffness depends mainly on the aggregate skeleton and the air voids content. In general, E_0 in CBTM mixtures is lower than in HMA due to the higher air voids and the lower bitumen dosage. On the other hand, the value of E_{00} in CBTM mixtures is usually higher than in HMA due to the presence of cement, which constitutes a stiffening phase also at very high temperatures (or very low frequencies), when the bitumen phase is considered as fluid. Moreover, the dashpot viscosity and the related parameter β is around 10 times higher in CBTM than in HMA, indicating the small role played by the dashpot when cement is used with bitumen.

13.3.2 DBN model

The DBN model (named after the authors Di Benedetto and Neifar) was specifically proposed to introduce non-linearity phenomena and to describe large-strain plastic behaviour of granular soils (Blanc et al., 2011; Di Benedetto et al., 2014). Later, its application was extended to analyze plastic dissipation phenomena in bituminous mixtures (Di Benedetto, Mondher, et al., 2007; Gayte, 2016; Neifar et al., 2001). In the model, the non-linearity is represented by means of elasto-plastic (EP) bodies in series with viscous dashpots, the latter representing the time-temperature dependency. The combination is then repeated n times (n elements) in order to increase the model precision (Figure 13.2a). When the strain level tends to 0, the DBN model takes its asymptotic form as a Generalized Kelvin-Voigt (GKV), and the EP bodies are replaced by springs (Figure 13.2b). When the number of elements tends to the infinite, the representation passes from a discrete spectrum to a continuous spectrum. Thanks to the high versatility, this model is able to describe behaviour for a wide range of solicitations, temperatures and cycle numbers.

The EP bodies, that represent a non-viscous behaviour, are generally adopted for non-cohesive (or elastoplastic) granular materials (Ashmawy et al., 1995; Blanc et al., 2011; Di Benedetto

et al., 2014; Tatsuoka et al., 2008). Plastic dissipation can be observed in sands for cycles at small strain amplitude, characterized by a hysteretic stabilized behaviour. Considering materials composed of aggregates and bituminous binder, the non-viscous behaviour should be attributed to aggregates (or RAP in this case), whereas the viscous contribution to the binder. With such considerations, it can be assessed that the non-viscous behaviour is independent from temperature (and frequency, if the Time-Temperature Superposition Principle stands), which is instead affecting the purely viscous part. In case the DBN model is applied to represent plasticity phenomena at small cycles number (and small strain domain), it can take a simplified form (Attia, 2020).

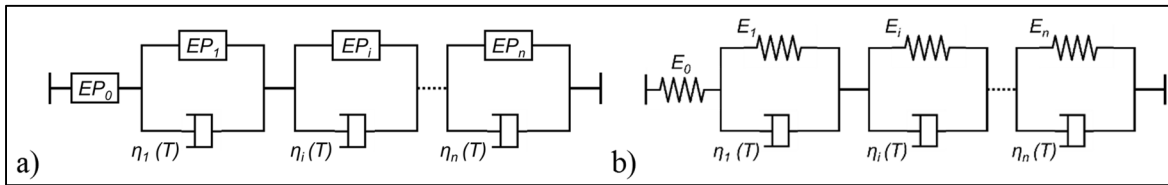


Figure 13.2 a) DBN model for bituminous mixtures, b) Generalized Kelvin-Voigt model, which gives an asymptotic representation of the DBN model when strain tends to 0

The cyclic response of EP bodies is characterized by a function linking the strain and the stress, called “virgin curve” (Figure 13.3). One property of this function is that the unloading (or loading) curve joins tangentially the virgin unloading (or loading) curve at the inverse value of the reversal stress (Di Benedetto, Mondher, et al., 2007).

For many construction materials, including metals, concrete and soils, the dissipation behavior may be expressed by the specific damping capacity ψ , which, for the KV body and small dissipation energy, is calculated as follows (Genta, 2009):

$$\psi = \frac{\Delta W_{LVE}}{W_E} = \frac{\pi \varepsilon_0 \sigma_0 \sin \phi}{1/2 \varepsilon_0 \sigma_0} = 2\pi \sin \phi \quad (13.5)$$

where ΔW_{LVE} is the area of the hysteresis loop with elliptical shape (energy dissipated at each cycle), W_E is the energy stored by the spring at each cycle, ε_0 is the amplitude of the sinusoidal

strain, σ_0 is the amplitude of the sinusoidal stress and φ is the frequency-dependent phase angle describing the lag between stress and strain in the linear viscoelastic response.

The EP bodies store elastic energy and dissipate through time-temperature independent mechanisms. As a result, a sinusoidal loading is represented by an hysteresis loop as in Figure 13.3. The energy ΔW_{EP} dissipated by the EP body is computed as:

$$\Delta W_{EP} = W_{EP}\psi = 1/2 \varepsilon_0 \sigma_0 \psi = 2\pi D \varepsilon_0 \sigma_0 \tag{13.6}$$

where $D = \psi/4\pi$ is an adimensional time-temperature independent damping ratio.

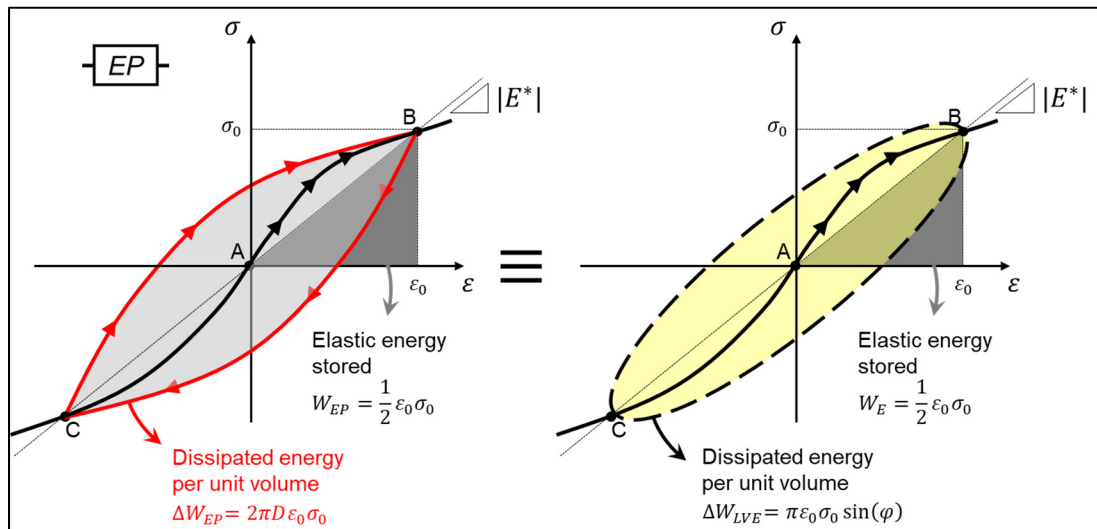


Figure 13.3 Cyclic loading behaviour of elasto-plastic element for small number of cycles (path ABCB)

In case the number of cycles applied and the deformation are small, the plastic energy dissipation ΔW_{EP} can be expressed as an equivalent linear viscoelastic dissipation ΔW_{LVE} through the definition of an equivalent phase angle, by fixing $\Delta W_{EP} = \Delta W_{LVE}$ (Figure 13.3):

$$\sin(\varphi_{EP}) = 2D \tag{13.7}$$

The version of the DBN model presented in this paper is obtained by the series arrangement of units consisting of a viscous and temperature-dependent dashpot $\eta_i(T)$ in parallel with a EP_i

body (E_i, D_i). Moreover, the dashpot is not present in the first unit ($\eta_0 = 0$) and all units are characterized by the same dissipation parameter ($D_i = D$) (Figure 13.4).

As a consequence, the DBN model phase angle φ_{DBN} is expressed as the total contribution by the viscous and non-viscous components (Figure 13.5):

$$\begin{aligned} \sin(\varphi_{\text{DBN}}) &= \sin(\varphi_{\text{LVE}} + \varphi_{\text{EP}}) = \frac{\Delta W_{\text{DBN}}}{\pi \varepsilon_0 \sigma_0} = \frac{\Delta W_{\text{LVE}} + \Delta W_{\text{EP}}}{\pi \varepsilon_0 \sigma_0} \quad (13.8) \\ &= \sum_{i=0}^n \left(\frac{\omega \eta_i}{E_i^2 + (\omega \eta_i)^2} + \frac{2 \cdot D \cdot E_i}{E_i^2 + (\omega \eta_i)^2} \right) \cdot |E^*| \end{aligned}$$

where ΔW_{DBN} is the total cycle dissipation (viscous and non-viscous), E_i and η_i are the Young's modulus and the Newtonian viscosity of the i^{th} element, respectively, ω is the pulsation, φ_{LVE} is the phase angle of the viscous dashpot, φ_{EP} is the phase angle of the non-viscous damping, and D is the damping ratio (Ashmawy et al., 1995).

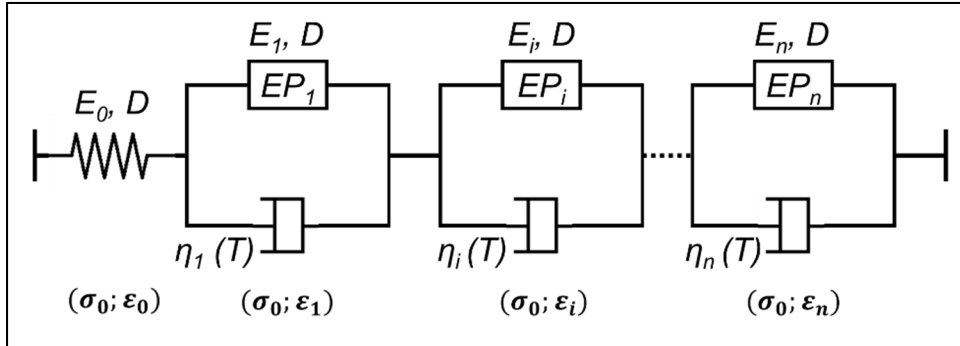


Figure 13.4 Representation of the DBN model applied in the small strain domain, EP are represented by a spring (modulus, E) and a non-viscous dissipation (D)

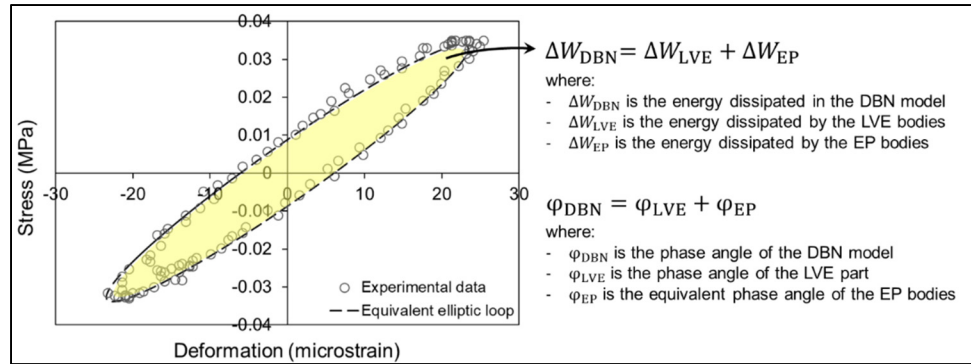


Figure 13.5 Energy dissipation during cyclic loading in the small strain domain (experimental data superposed to an equivalent sinusoidal loading)

It is assumed that the addition of non-viscous dissipation does not influence the value of the complex modulus, which can be expressed from the GKV configuration:

$$E_{GKV}^*(i\omega, T) = \left(\frac{1}{E_0} + \sum_{i=1}^n \frac{1}{E_i + i\omega\eta_i(T)} \right)^{-1} \quad (13.9)$$

where i , ω and T were previously explained, E_0 is the Young's modulus of the first element, E_i and η_i were previously explained. The number of elements n can be chosen arbitrarily to reduce the distance between the discrete GKV configuration and the 2S2P1D. In particular, the 2S2P1D model should be initially fitted on the norm of the complex modulus of the material, and then the GKV model is calibrated according to the 2S2P1D (Figure 13.6).

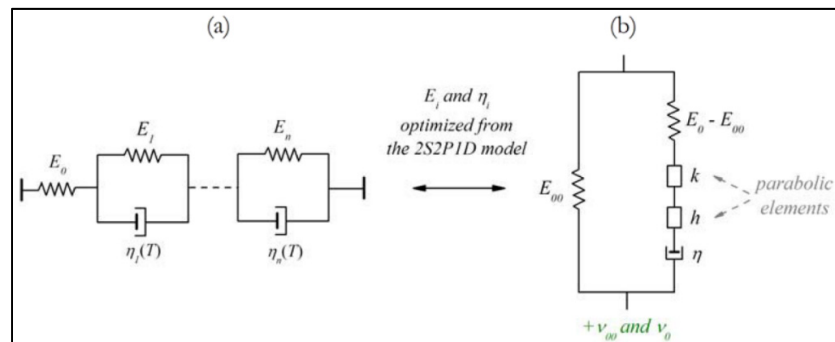


Figure 13.6 Correlation between: a) GKV model, and b) 2S2P1D model (taken from Di Benedetto, Delaporte et al., 2007)

Consequently for any chosen number of elements (n), the DBN model only needs seven constants from 2S2P1D plus an additional parameter (ϕ_{EP}) to take into account plasticity at small strain levels.

13.4 Materials and methodology

13.4.1 Materials and mixtures

The CBTM mixtures produced for this study are characterized by an aggregate distribution composed of 94% of RAP and 6% of limestone filler. The correction with filler allows having a gradation close to the maximum density curve (Figure 13.7). The properties of the RAP aggregate are listed in Table 13.1. The ordinary Portland cement dosage was fixed at 1.5% by mass of dry aggregates. The cement was a GU type (standard CSA A3000) with compressive strength at 28 days of 43.9 MPa (standard ASTM C109).

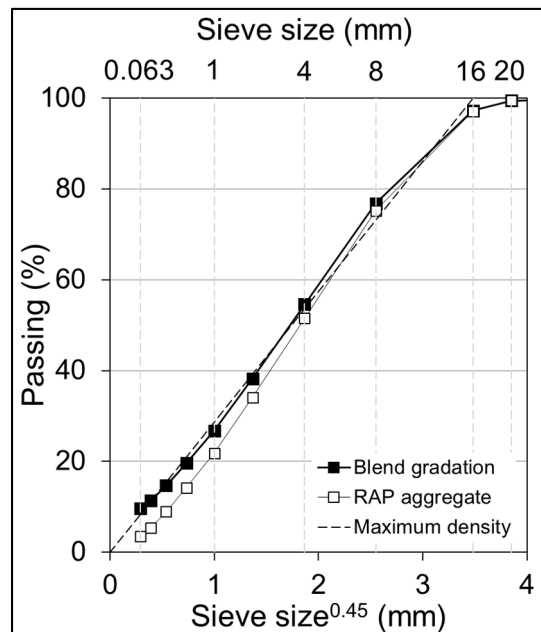


Figure 13.7 Maximum density curve, RAP and blend gradations

Mixtures were produced with two bitumen emulsions. The main properties of both emulsions are listed in Table 13.2, and they are named from now on as Emulsion A and Emulsion B. In both cases, the bitumen emulsion dosage was fixed at 5% (3% of residual bitumen) by mass of aggregates. The total water dosage was fixed at 4.0% by mass of aggregate, in order to reach the target air voids of 15% without employing high compaction energy and to avoid any material loss (water, bitumen and/or fine particles) during compaction.

Table 13.1 RAP aggregate properties

Property	Standard	Unit	Value
Binder content	ASTM D6307	%	5.5
Nominal maximum particle dimension	ASTM D448-03	mm	16
Maximum specific gravity	ASTM C127-128	-	2.482
Average bulk density	LC 21-065, -066 and -067	-	2.323
Water absorption	ASTM C127 and C128	%	1.1

Table 13.2 Bitumen emulsions properties

Bitumen emulsion properties	Standard	Unit	Emu. A	Emu. B
Density	ASTM D6397-16	g/cm ³	1.0	N/A
Viscosity @ 40 °C	EN 13302	s	N/A	42.5
Residual bitumen content	EN 1428 or ASTM D6997-12	%	60.3	60.0
Storage stability @ 24 hours	ASTM D6930-10	%	0.6	N/A
Breaking Index	EN 13075	%	N/A	2
Residual bitumen properties				
Penetration @ 25 °C	EN 1426 or ASTM D5-13	mm	4.1	10.0
Softening point	EN 1427 or ASTM D36-14	°C	48.6	43.0

13.4.2 Mixtures production

After mixing, the specimens were compacted by means of a gyratory compactor (GC) with mould diameter of 100 mm, constant pressure of 600 kPa, gyrations rate of 30 rpm and internal angle of 1.16°. The volumetric composition of the specimen is monitored with compaction, which is performed at fixed height to obtain the target value of voids in the mixture (V_m) of $15\% \pm 1\%$ (Grilli et al., 2016):

$$V_m = \frac{V_{V,A} + V_{W,I}}{V} \cdot 100 = \frac{V - (V_S + V_C + V_{B,R})}{V} \cdot 100 \quad (13.10)$$

where V is the total volume of the specimen, V_S is the bulk volume of aggregates (in saturated surface dried condition), V_C is the volume of cement, $V_{B,R}$ is the volume of residual bitumen from emulsion, $V_{W,I}$ is the volume of intergranular water and $V_{V,A}$ is the volume of air. A total of nineteen (19) specimens were produced, but only three (3) are considered in this study.

After compaction, the specimens followed a curing process as shown in Table 13.3 (Raschia et al., 2020). The period lasted 1 year, simulating a long-term curing to reach a quite stable condition of the physical and mechanical properties. The first and second curing periods, for a total of 28 days, was same for the three specimens. After that, two specimens were kept in unsealed conditions for the third curing period, whereas one specimen was wrapped in plastic foil and sealed with several layers of wax for a final coating thickness of around 5 mm.

The sealed condition after 28 days was chosen to stop the curing and/or ageing of the material, which instead were promoted in the unsealed specimens. At the end of the third curing period, the three specimens were cored at a diameter of 75 mm and prepared for complex modulus testing (Figure 13.8).

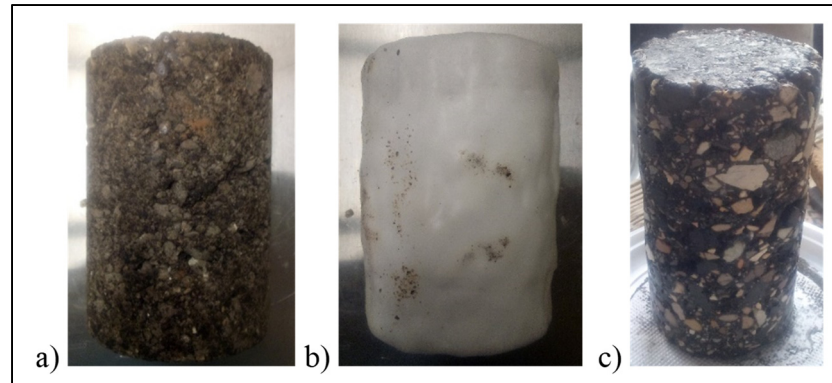


Figure 13.8 SGC specimen of Ø100 mm x 140mm: a) un-sealed condition, b) sealed condition and, c) coring and sawing to obtain the testing specimens of Ø75 x 120mm

Table 13.3 Mixtures naming and curing process

Emulsion	Mixture	Curing types		
		1 st	2 nd	3 rd
		14 days	14 days	11 months
A	A_Unsealed	25 °C	40 °C ⁽¹⁾	Room temperature (Unsealed)
	A_Sealed			Room temperature (Sealed)
B	B_Unsealed		40 °C	Room temperature (Unsealed)

⁽¹⁾ The curing was performed with controlled relative humidity at $55 \pm 5\%$

13.4.3 Experimental devices

The experimental program was carried out in two laboratories, and for this reason, with two different apparatus. In case of mixtures with Emulsion A, specimens were tested with an MTS press, whereas specimens with Emulsion B were tested with an asphalt mixture performance tester pro (AMPT PRO) servo-hydraulic press. However, complex modulus tests were performed in both cases in only compression configuration (haversine loading) and the axial strain was measured by placing three extensometers in the middle part of the specimen and

120° apart (Figure 13.9). The target axial strain was 50 and 30 microstrain for Emulsion A and Emulsion B mixtures, respectively. Specimens with Emulsion A were tested at a temperature range between -20 °C and 40 °C with 10 °C steps, while frequencies ranged between 0.1 Hz and 10 Hz. In case of Emulsion B, temperature ranged between 0 °C and 40 °C with 10°C steps, and frequencies varied between 0.1 Hz and 10 Hz.

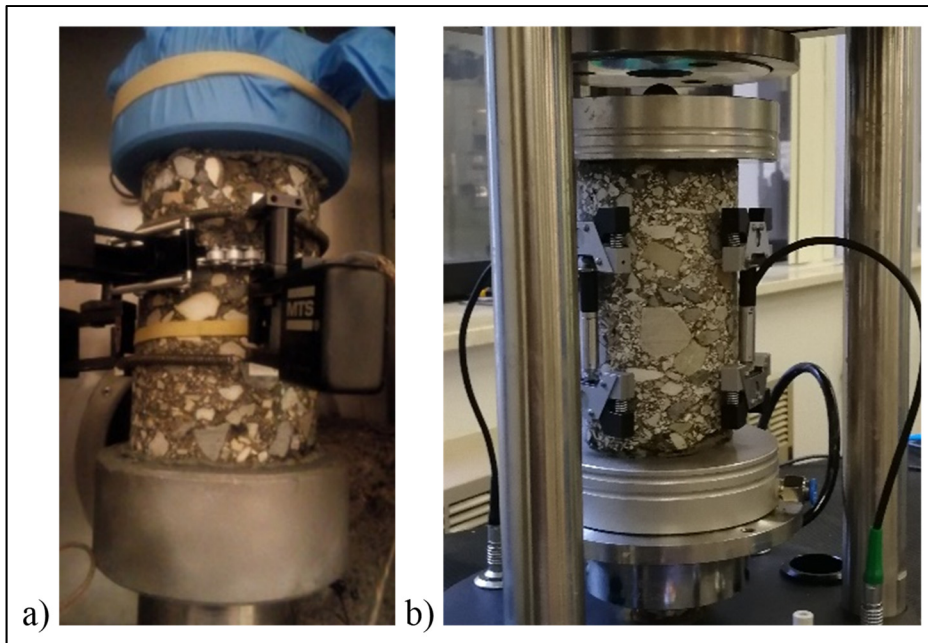


Figure 13.9 View of a specimen with measurement system in: a) MTS press and, b) AMPT PRO press

13.5 Results analysis

Figure 13.10 shows results from the tested mixtures in the Cole-Cole plan and Black space. It can be observed that in all the cases the experimental points follow a continuous line, indicating that the Time-Temperature Superposition Principle (TTSP) is respected and the rheological models described above can be applied. The range of $|E^*|$ values is quite the same for the three mixtures studied indicating that the emulsion type and the type of curing did not significantly affect the stiffness of the mixtures (Figure 13.10b). On the contrary, it can be observed that

mixture B_Unsealed is characterized by a different trend of the phase angle when compared to both mixtures with Emulsion A (Figure 13.10b). It is reasonable to expect that changing the emulsion, and hence the residual binder, the viscous properties could have been affected. Moreover, comparing the two mixtures, A_Unsealed and A_Sealed, it is noted that the experimental points are superposed and a distinction is not possible. Therefore, the sealing condition during the third stage of curing had a clear effect on mixtures produced with Emulsion A, since the material properties did not change as expected (no further curing and apparently no ageing).

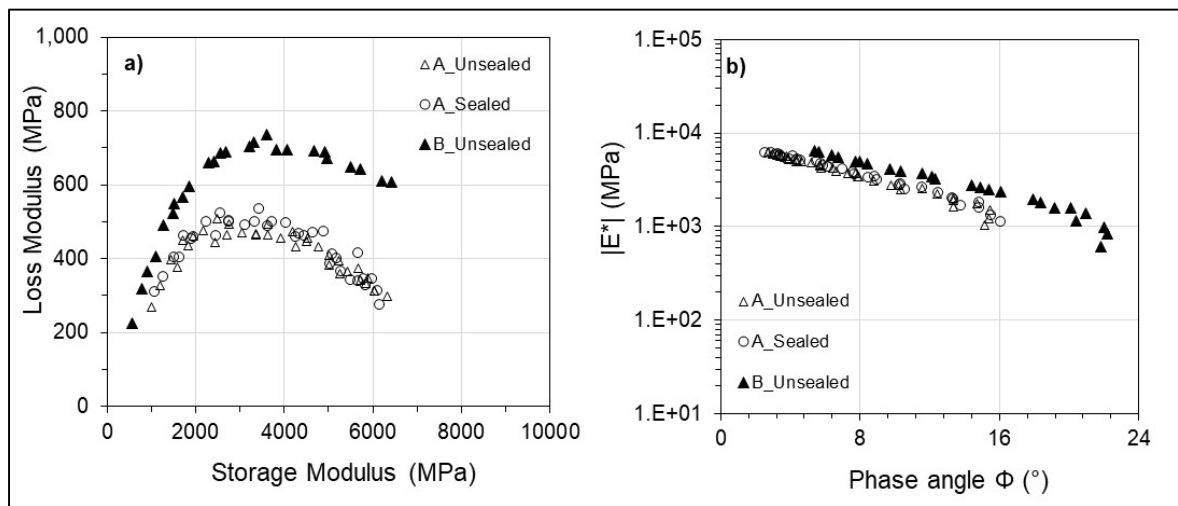


Figure 13.10 Experimental results showed in: a) Cole-Cole plan and, b) Black space

13.5.1 Time-Temperature Superposition Principle (TTSP)

The experimental data show that the TTSP is applicable to CBTM mixtures. As a consequence, the isothermal curves of the norm of the complex modulus, $|E^*|$, and of the phase angle, ϕ , can be shifted in order to obtain the respective master curves (Figure 13.11).

Figure 13.11 shows the master curves of the norm of the complex modulus and phase angle at a reference temperature $T_{ref} = 20$ °C. As in the previous representation, the effect of the

emulsion is highlighted on the mechanical properties of mixtures studied. In particular, mixture B_Unsealed showed lower modulus at low frequencies (or high temperatures) and higher modulus at high frequencies (or low temperatures), confirming the crucial role of the bituminous binder used in the thermal sensitivity of the mixture. Such effect is also visible in the master curve of the phase angle, which is globally higher for mixture with Emulsion B compared to mixtures with Emulsion A (Figure 13.11b). Considering that the dosage of residual bitumen is the same, this difference could be explained by the fact that the bitumen from Emulsion B is more time-temperature dependant than bitumen from Emulsion A.

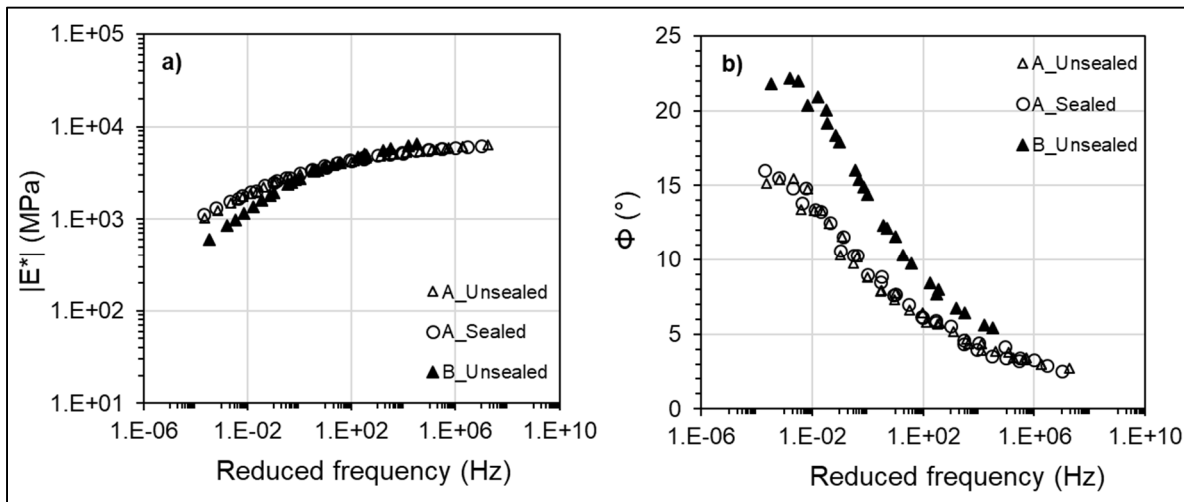


Figure 13.11 At $T_{ref} = 20^\circ\text{C}$, master curves of: a) The norm of the complex modulus $|E^*|$ and, b) The phase angle ϕ

Figure 13.12 shows the shift factors in function of the temperature. The experimental points are modelled by the Williams–Landel–Ferry (WLF) model, mathematically expressed as:

$$\log(a_T) = -\frac{C_1(T - T_S)}{C_2 + T - T_S} \quad (13.11)$$

where a_T is the shift factor, C_1 and C_2 are constants, T is the temperature and T_S is the reference temperature (Ferry, 1980). It is observed that the shift factors of the three mixtures are significantly close at all the temperatures tested. The obtained values of a_T can be compared

to the ones obtained for HMA mixtures in the literature, tested in the same range of temperatures (Di Benedetto et al., 2004). Moreover, such dependency on temperature highlights the thermo-mechanical response of CBTM mixtures. It has been shown that in HMA the a_T coefficients are very close between the binder and the related mixture (Di Benedetto et al., 2004). Hence, assuming this is also valid for CBTM, it would be possible to have the same shift factors for both residual bitumen of the emulsions used.

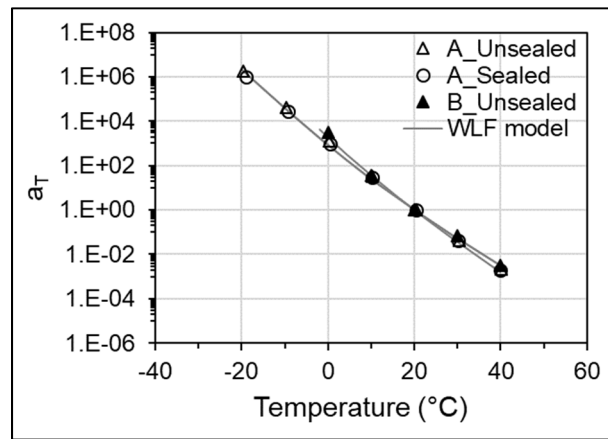


Figure 13.12 Shift factors, a_T , and WLF model related to the studied mixtures

Table 13.4 WLF parameters

Parameters	A_Unsealed	A_Sealed	B_Unsealed
C_1	34.7	34.7	38.7
C_2	258.5	258.5	258.2

13.5.2 The 2S2P1D model

Figure 13.13 shows the experimental data obtained for one mixture (B_Unsealed) modelled with the 2S2P1D model. According to the LVE theory for bituminous materials, if the TTSP is respected, the rheological model should be unique and valid in all the representations: master

curves, Black space and Cole-Cole plan. In Figure 13.13, three calibrations of the 2S2P1D model are presented:

- optimization from the data in the Cole-Cole and Black spaces, minimizing the error as in Eq. (6.20) (named: 2S2P1D_CC+BS);
- optimization from the data plotted in the master curve of the $|E^*|$, minimizing the error as in Eq. (6.21) (named: 2S2P1D_ $|E^*|$);
- optimization from the master curve of ϕ minimizing the error as in Eq. (6.22) (named: 2S2P1D_ ϕ).

$$|\Delta E^*| = \sqrt{(E_{1,\text{exp}} - E_{1,2S2P1D})^2 + (E_{2,\text{exp}} - E_{2,2S2P1D})^2} \quad (13.12)$$

$$\text{dev } |E^*| = \frac{|E^*|_{\text{exp}} - |E^*|_{2S2P1D}}{|E^*|_{\text{exp}}} \cdot 100 \quad (13.13)$$

$$\Delta\phi = \phi_{\text{exp}} - \phi_{2S2P1D} \quad (13.14)$$

In Figure 13.13, it is observed that none of the three optimizations superpose among them and with the experimental data in all the four representations. The calibration 2S2P1D_CC+BS does not well represent the master curves trend at both low and high reduced frequencies (high and low temperatures, Figure 13.13c-d). Furthermore, the optimization 2S2P1D_ Φ done on the phase angle master curve significantly underestimates the norm of the complex modulus, $|E^*|$, visible in the three other representations (Figure 13.13a-b-d). However, the model 2S2P1D_ $|E^*|$ calibrated on the master curve of the $|E^*|$ underestimates the ϕ of a constant value on the full frequencies range (around 2° , Figure 13.13c). This result can be justified by the presence of a non-viscous dissipation which cannot be taken into account with a LVE rheological model such as 2S2P1D.

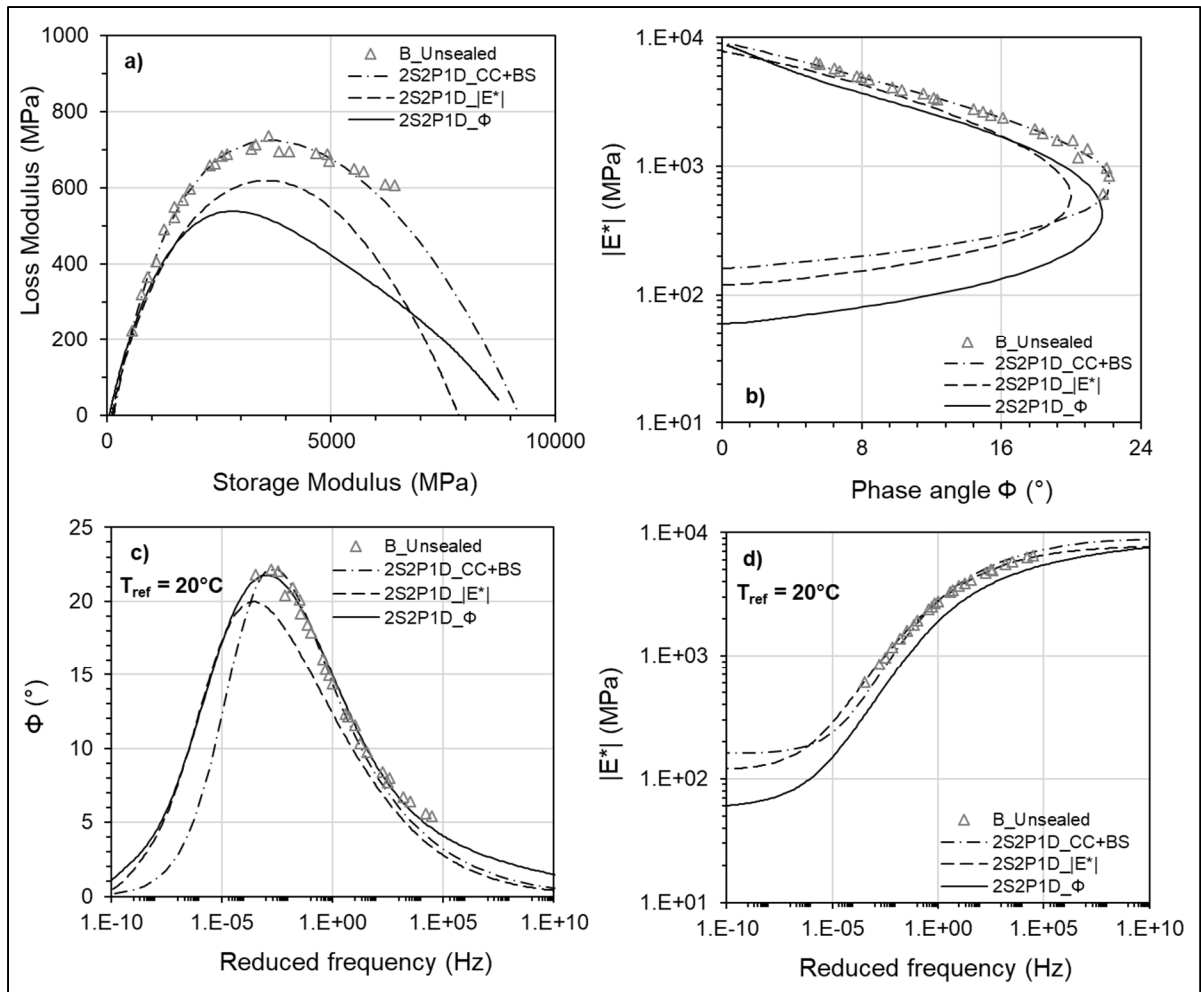


Figure 13.13 Optimization of the 2S2P1D model for B_Unsealed mixture according to: a) Cole-Cole plan, b) Black space, c) phase angle master curve and, d) complex modulus master curve ($T_{ref} = 20^{\circ}\text{C}$)

As a consequence, the results from the three mixtures studied are modelled fitting the 2S2P1D on the norm of the complex modulus (calibration : 2S2P1D_|E*|) (Figure 13.14). It is observed that the phase angle master curve is not well represented for all the mixtures and this is visible also in Black space and Cole-Cole plan (Figure 13.14a-b). For this reason, the DBN model should be applied to consider also the non-viscous contribution in the complex behaviour. The shifting was done by means of a closed-form shifting (CFS) algorithm which minimizes the

area between two successive isothermal curves of $|E^*|$ and estimates the shift factors (Gergesova et al., 2011).

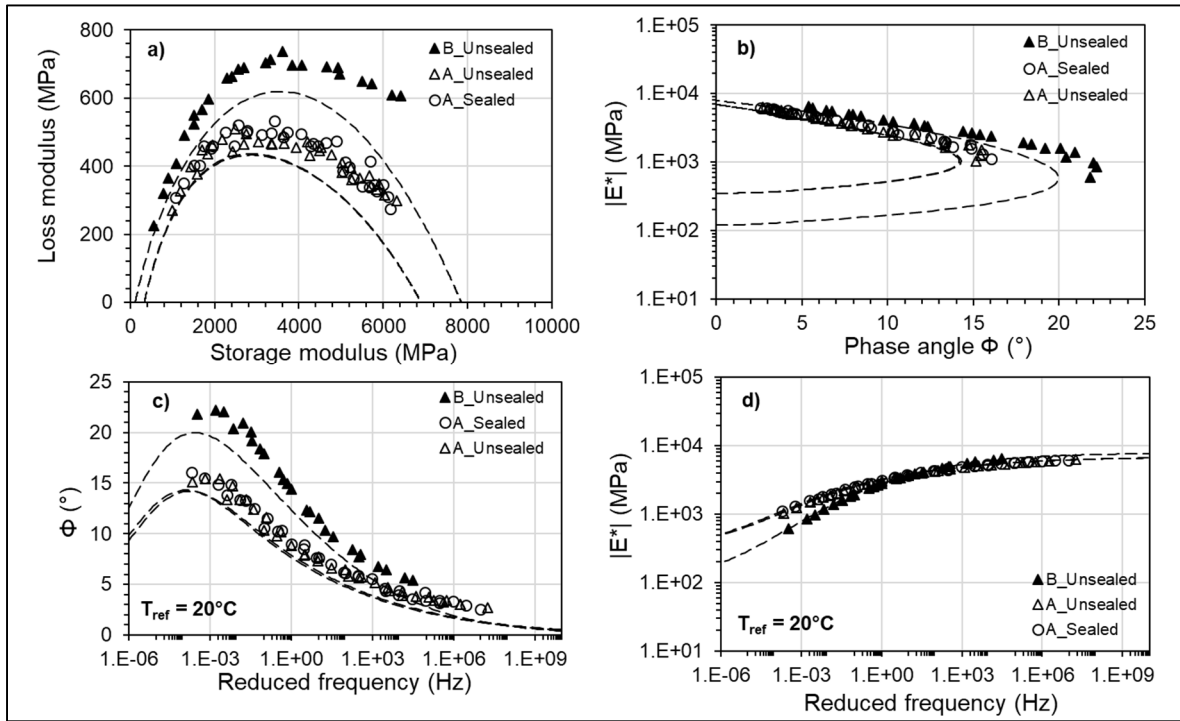


Figure 13.14 Application of 2S2P1D model fitted on the master curve of the norm of the complex modulus (calibration : 2S2P1D_ $|E^*|$) for: a) Cole-Cole plan, b) Black space, c) phase angle master curve and, d) complex modulus master curve ($T_{ref} = 20^\circ\text{C}$)

13.5.3 The DBN model

Figure 13.15 shows the experimental results of the three studied mixtures modelled with the 2S2P1D and DBN models. In order to obtain a good level of precision and correlation with the 2S2P1D, the number of elements in the GKV model was fixed at 40. The values of E_i and η_i for each element of the model are listed in the appendix (Annex VI). It can be observed that the two models are superposed in the plan of the norm of the complex modulus (Figure 13.15a), whereas in the other plans the difference between the two models is due to the introduction of an equivalent phase angle representing the non-viscous dissipation, φ_{EP} . This additional

parameter is visible as a shifting of the model in the Black space and phase angle master curve, and as a rotation in the Cole-Cole plan (Figure 13.15a-b-c).

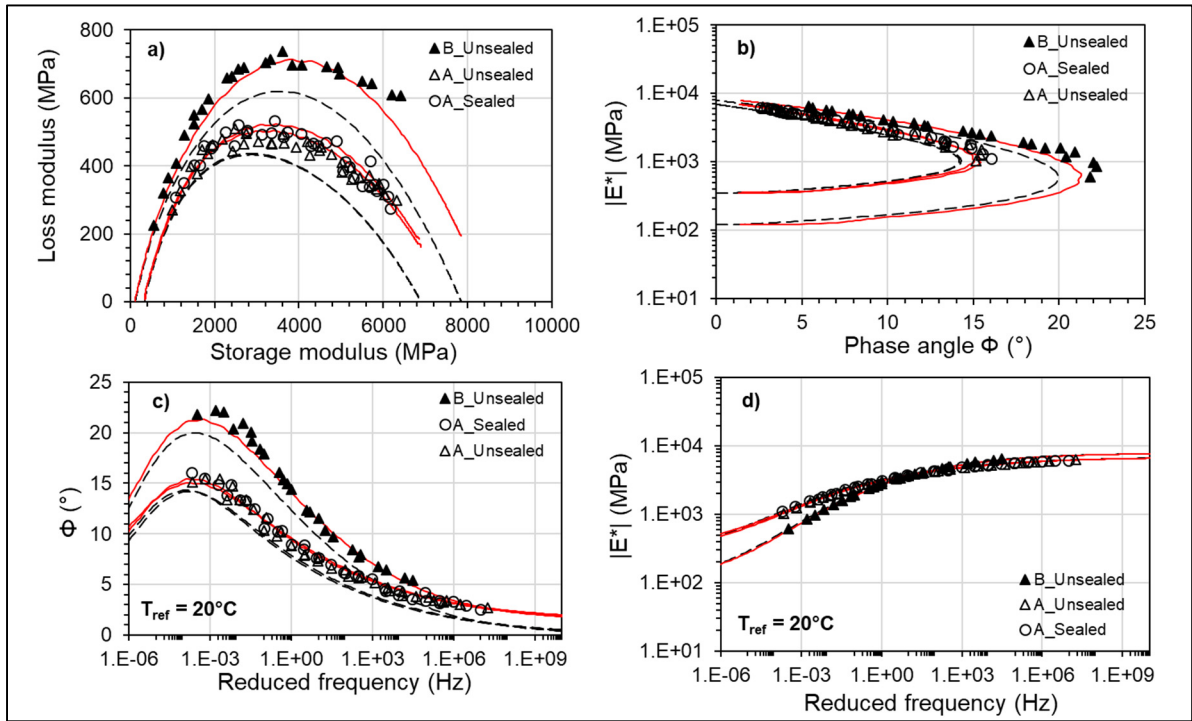


Figure 13.15 Application of the 2S2P1D (dashed line) and DBN (continuous line) models to the studied mixtures (n = 40): a) Cole-Cole plan, b) Black space, c) phase angle master curve and, d) complex modulus master curve ($T_{ref} = 20^{\circ}\text{C}$)

13.6 Discussion

Figure 13.16 shows the accuracy of the DBN model according to the experimental data on the whole frequency and temperature ranges. It is highlighted the good fitting in both plans: norm of the complex modulus ($\pm 5\%$) and phase angle ($\pm 2^{\circ}$).

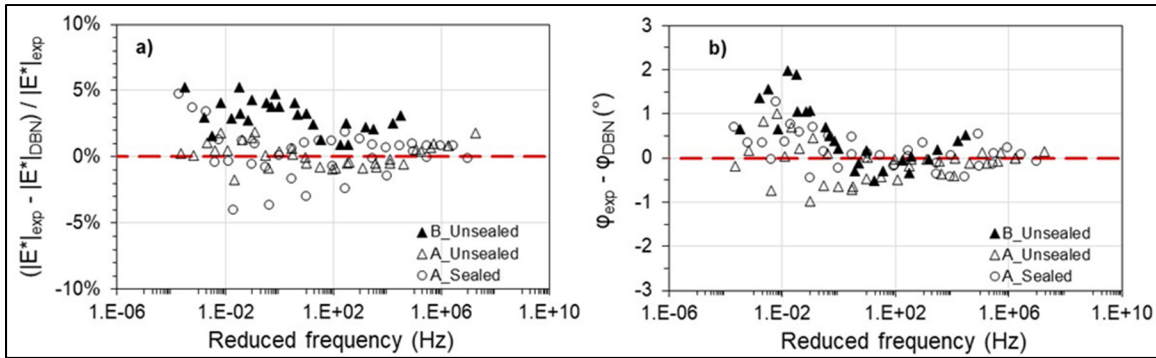


Figure 13.16 Accuracy of the DBN model for: a) norm of complex modulus and, b) phase angle

Table 13.5 lists the model parameters related to the DBN model and the modified version of the Huet-Sayegh model (Eq. 6.11). It is highlighted that the same values can be used by both approaches, even if the parameter β needs to be defined in case of DBN model. However, such high values make the contribution given by the dashpot almost negligible. This shows that the two approaches are able to fit the experimental data adopting the same parameters, but only in the case of DBN the material is represented by a rheological model which can be fully applied in the time domain and for higher strain rate (out of the LVE field).

Table 13.5 Rheological modelling parameters for the studied mixtures

Mixture	Model	E_{00} (MPa)	E_0 (MPa)	k (-)	h (-)	δ (-)	β (-)	τ_E (20°C) (-)	φ_{EP} (°)	φ_{AEP} (°)
A_Unsealed	DBN	350	6,900	0.14	0.37	2.25	10E+10	15.0	1.3	-
	HS _q	350	6,900	0.14	0.37	2.25	-	15.0	-	1.3
A_Sealed	DBN	350	6,900	0.14	0.37	2.25	10E+10	20.0	1.3	-
	HS _q	350	6,900	0.14	0.37	2.25	-	20.0	-	1.3
B_Unsealed	DBN	120	7,850	0.18	0.39	2.65	10E+05	2.5	1.4	-
	HS _q	120	7,850	0.18	0.39	2.65	-	2.5	-	1.4

Comparing parameters for mixes A_Unsealed and A_Sealed it is observed that the same are adopted, meaning that the sealed curing prevented further curing and ageing of the mixtures. The first two curing periods for a total of 28 days (14 days at 25 °C and 14 days at 40 °C) were enough to reach a stable condition of the material properties, which were not affected by ageing as much.

The most important factor that affected the rheology of CBTM mixtures was the different emulsion (i.e. different residual bitumen) used to produce the mixtures. In particular, important differences could be highlighted comparing model parameters for mixes A_Unsealed and B_Unsealed. Bitumen from Emulsion B conferred to the CBTM mixture a higher modulus value at high frequencies (or low temperatures) and lower modulus at low frequencies (or high temperatures), which means a global higher temperature dependency. Moreover, the parameters related to the viscous part of the model k , h , δ are lower for mixture A_Unsealed, highlighting the fact that bitumen from Emulsion A gives a less viscous response compared to Emulsion B. The same conclusion can be confirmed by the values of the characteristic time τ_E . Generally, the higher the value of τ_E , the lower is the viscous contribution given by the binder. From these results, the difference between Emulsion A and B is one order of magnitude.

The non-viscous parameter φ_{EP} is almost the same for curing confinement and emulsion used, meaning that it does not depend on the residual bitumen and confirming that the curing confinement did not change the rheological response of mixtures. Being a parameter used to represent frictional or slightly plastic phenomena it is reasonable to assume that it could depend on the air voids content, bitumen dosage and/or the type of aggregates used. Since these aspects were not analyzed in this study, further work is needed to clarify the role of the non-viscous component in CBTM mixtures.

13.7 Conclusions

This paper deals with the thermo-rheological modelling of CBTM mixtures in the small strain domain. An innovative approach is proposed employing the visco-plastic model DBN

proposed in the literature. After having validated the good representation of the material properties, the model parameters are analyzed to study the effects of curing confinement type and emulsion source in the long-term properties of the CBTM mixtures studied. The following conclusions can be drawn:

- DBN is a suitable rheological model to well represent the thermo-rheological behaviour of cement-bitumen treated materials (CBTM) in the small strain domain. With 8 parameters it is possible to include in the same model both viscous and non-viscous responses obtaining an optimal fitting of the experimental results. The equivalent phase angle, φ_{EP} , represents a non-viscous dissipation parameter typically observed at higher levels of deformation, but useful in this study to consider frictional and/or plastic phenomena for the CBTM mixtures. From the results obtained, the φ_{EP} does not seem to depend on binder type and curing procedure. Additional work is needed to improve the knowledge with regards to such new aspects in cold materials;
- Mixtures were cured for 14 days at 25 °C and 14 days at 40 °C in unsealed conditions. After that, a curing process of 11 months in sealed and unsealed conditions was followed, after which rheological properties were measured. Results showed that in both conditions the same stiffness was reached, meaning that the evolution of properties was not influenced by sealed or unsealed curing. It was assumed that in sealed condition stiffness evolution was slowed down or stopped. As a consequence, the initial 28 days proposed as curing protocol were probably enough to reach a quasi-stable condition of the CBTM mixtures stiffness;
- The same mixture composition was employed to produce CBTM mixtures with two different emulsion sources, hence different residual binder. The emulsions chosen are present in the market as specific for cold recycling projects and they have the same raw characteristics: cationic, slow-setting emulsions with unmodified binder. Nonetheless, results obtained are significantly affected by the type of residual bitumen, meaning that it is not an aspect that should be neglected in the mix design.

Future studies should focus on improving the application of the DBN model for cold materials to enhance the currently missing scientific knowledge of the material.

CHAPTER 14

VISCO-ELASTO-PLASTIC CHARACTERIZATION IN THE SMALL STRAIN DOMAIN OF CEMENT-BITUMEN TREATED MATERIALS PRODUCED AT LOW TEMPERATURES

Simone Raschia^a, Daniel Perraton^a, Hervé Di Benedetto^b, Sébastien Lamothe^a, Andrea Graziani^c, Alan Carter^a

^a Construction Engineering department, École de technologie supérieure (ÉTS) 1100, Notre-Dame Street West, Montreal, Canada

^b Université de Lyon, École Nationale des TPE, LTDS (CNRS UMR 5513), Vaulx-en-Velin, CEDEX, Lyon, France

^c Department of Civil and Building Engineering, and Architecture, Università Politecnica delle Marche, Via Brecce Bianche, 60131 Ancona, Italy

Submitted and under review with the journal *Journal of Materials in Civil Engineering*, ASCE, May 2020

14.1 Abstract

In the framework of recycling techniques employed in maintenance and rehabilitation projects for the road industry, cement-bitumen treated materials (CBTM) provide good performance as well as economic and environmental benefits. Being produced with bitumen emulsion at ambient temperature, the environmental factors during production are extremely important to guarantee the quality of the final product. This paper focuses on the stiffness of CBTM produced and conditioned at low temperatures, and cured in two different conditions (sealed and unsealed). The mixtures were evaluated in terms of rheological properties using complex modulus (E^*) tests performed one year after production. Results were modelled with an adapted version of the DBN (Di Benedetto-Neifar) model called DBNPDSC (Plastic Dissipation for Small Cycles). Results showed that the curing conditions, as well as the low production temperatures, significantly changed the rheological properties of the material. In

fact, mixing or compacting the mixtures at 5 °C, compared at 25 °C, resulted in a loss in stiffness of around 30 % in the small strain domain. This model is a good tool to describe, in the small strain domain, such material behaviour, which shows plastic non-viscous phenomena.

14.2 Introduction

Cold recycling is an innovative technology introduced in the construction materials framework to face the economical and environmental crisis related to the road pavement industry (Čížková et al., 2014; Jacobson, 2002; Kim & Lee, 2006; Sebaaly et al., 2004; Timm et al., 2018). The possibility to produce cold recycled materials (CRM) at ambient temperature means significant advantages in terms of energy consumption (Xiao et al., 2018). This is possible thanks to the use of bitumen in form of emulsion or foam. In addition, the major part of the aggregate phase consists of reclaimed asphalt pavement (RAP), available in large quantities and suitable to obtain good performance (Gandi et al., 2017; Godenzoni et al., 2015). Cement-bitumen treated materials (CBTM) are a particular type of CRM, in which short-term and long-term mechanical properties are enhanced by the addition of a co-binder, in particular Portland cement (Du, 2018; Mignini et al., 2018b; Miljković et al., 2019; Ouyang et al., 2018). In order to fully develop their properties, cement and bitumen emulsion (or foamed bitumen if used) require a certain curing time during which the emulsion breaking process, cement hydration and evaporation of the water employed to improve workability occur (Godenzoni, Cardone, et al., 2016; Graziani, Iafelice, et al., 2018; Ojum et al., 2014). Because of this, properties of CBTM materials are characterized by an evolutive behaviour (Graziani et al., 2017).

Bitumen emulsion is a component highly sensitive to temperature. In particular, it is usually stored at temperatures ranging between 20 °C and 40 °C, in order to maintain an acceptable level of stability of the suspended bitumen droplets (Needham, 1996). At the same time, the other materials used in CBTM mixtures, such as RAP, aggregates, cement and water, are generally stored at ambient temperature. In case where the CBTM are produced at low temperatures (below 10 °C), the bitumen emulsion can experience a thermal shock in contact

with the other cold components, especially aggregates. A study has shown that a compaction temperature of 5 °C increased significantly the energy required to reach the target volumetric properties (Raschia et al., 2020).

With years, pavements can experience different factors affecting the remaining service life compared to the initial design. In particular, the high uncertainty related to the long-term properties of CBTM mixtures limited the use of such material to low-volume pavements (Chesner et al., 2011). However it was shown that with the right awareness, a CBTM rehabilitated pavement can have a service life increased up to 12 years (Chesner et al., 2011). In the latest years, CRM and CBTM mixtures have been also applied to high-volume traffic roads, and several trial sections have not shown specific criticalities throughout the service life (Gu et al., 2019; Guatimosim et al., 2019; Sangiorgi et al., 2017). One fundamental step to have a performant CBTM layer is at the moment of production, in particular the curing time allowed before the upper layer is laid and compacted. If the CBTM mixture still contains water and the curing process did not develop sufficiently before being covered with HMA, it is possible that the combination of traffic and environmental factors compromise permanently its properties. In fact, when a mixture produced with bitumen emulsion is submerged with water to simulate a raining condition, the mechanical properties significantly decrease (Kim et al., 2011). In particular, it was found that the rigidity of mixtures is inversely proportional to the amount of water present (Du, 2018; García et al., 2013). In the field, the curing process mainly depends on construction (CBTM layer thickness, drainage condition of the underlying layer) and environmental factors that are variable according to season and site. Grilli et al. (2019) observed that cores taken from a CBTM field test section (cured for 2 days before the upper layer was laid) were characterized by an increase of stiffness during curing time. However such increase was slower if compared to the same specimens additionally cured at 40 °C in a laboratory after extraction. So, it was clear how the boundary conditions caused by the upper layer (in terms of temperature, drainage and oxidation) significantly slowed down the development of mechanical properties.

In the literature, the simulation of long curing times of CBTM in the laboratory is performed by a constant monitoring of properties (water loss, resistance and/or stiffness) and it generally shows that after 28 days of curing the material has reached quite a stable condition (Dolzycki et al., 2017; Yan et al., 2017). However, the conditions of curing are not always representative of the field conditions, and no reference is found on the effect of low production temperatures on the CBTM mechanical properties after a long curing period. Both the production (mixing, transportation and compaction) temperatures and the curing conditions could influence properties such as stiffness and ageing.

The objective of this paper is to evaluate the effect of low production temperatures on the visco-plastic properties of CBTM mixtures cured for one year. Moreover, two different types of curing, sealed (S) and unsealed (U), are evaluated as field limit conditions, since the real curing probably occurs in between. A visco-plastic rheological model, the DBN model, is chosen from the literature and applied to the results obtained for the CBTM mixtures tested (Di Benedetto, Mondher, et al., 2007). The description of the model, as well as the reasons why it was adopted, are provided in the document.

14.3 Materials and methodology

In order to reach the goal of this study, a single cold recycled mix treated with bituminous emulsion was produced and cured at different temperature. Complex modulus tests were performed on the laboratory produced mixes before modelling.

14.3.1 Materials and mixtures

Mixtures grading were composed mainly of RAP aggregate, for which the main characteristics are listed in Table 14.1. To respect the target grading (maximum density curve with exponent 0.45), the aggregate blend was composed of 94 % of RAP and 6 % of limestone filler (Figure 14.1). A GU type cement (CSA A3000) with compressive strength at 28 days of 43.9 MPa

(ASTM C109) was used as mineral additive, which dosage was fixed at 1.5 % by mass of aggregates.

A cationic slow-setting bitumen emulsion, classified as CSS-1 (ASTM D2397), was produced in the United Kingdom and provided by an industrial supplier generally involved in cold recycling projects. The main properties of the emulsion are listed in Table 14.2. The residual bitumen dosage of the CBTM mixtures was fixed at 3 % by aggregate mass in accordance to a previous mix design process, which corresponds to 5 % of emulsion dosage. As for the water, the total content was also fixed preliminarily at 4 %. This amount is composed of the bitumen emulsion water and the water added manually, which is in part absorbed by the RAP aggregate. On the contrary, the residual bitumen of the emulsion is considered totally effective. The water dosage was chosen in order to reach the fixed voids in the mixture avoiding high compaction effort and material loss during compaction.

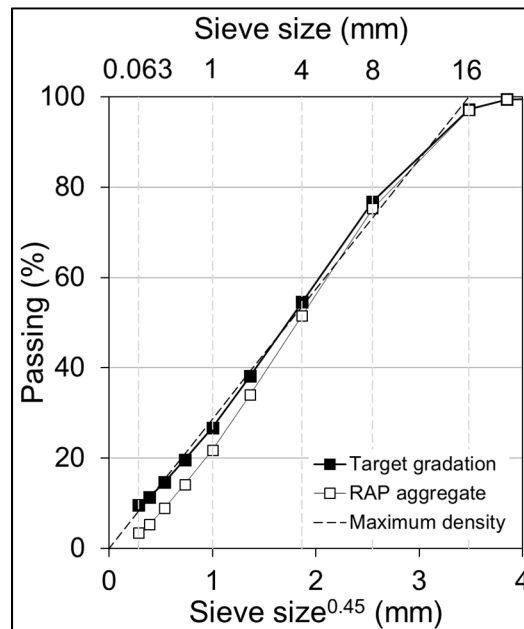


Figure 14.1 Gradation of RAP and aggregate blend

Table 14.1 RAP aggregate properties

Property	Standard	Unit	Value
Binder content	ASTM D6307	%	5.51
Nominal maximum dimension	ASTM D448-03	mm	16
Maximum specific gravity	ASTM C127-128	-	2.482
Average bulk density	LC 21-065-066-067	-	2.323
Water absorption	ASTM C127-128	%	1.1

Table 14.2 Bitumen emulsion properties

Bitumen emulsion properties	Standard	Unit	Value
Density	ASTM D6937-16	g/cm ³	1.019
Residue content	ASTM D6997-12	%	60.3
Storage stability @ 24 hours	ASTM D6930-10	%	0.6
Residual bitumen properties			
Penetration @ 25 °C	ASTM D5-13	mm/10	41
Softening point	ASTM D36-14	°C	48.6

14.3.2 Mixing, compaction and curing

The production process was divided in three (3) main steps: mixing, transportation and compaction, and curing (Figure 14.2). Each of these steps was characterized by a specific temperature. The mixing process was carried out adding to the humid blend (RAP, filler and absorption water), cement, additional water and emulsion, in this order. After mixing, the loose mixture was sealed in a plastic bag and placed in an environmental chamber for two (2) hours to simulate the transportation process in the field. Compaction was performed right after at 5 °C or 25 °C by means of a Shear Gyrotory Compactor (SGC). A mould diameter of 100 mm, constant pressure of 600 kPa, internal angle of 1.16 °, revolution speed of 30 rpm and fixed height of 140 mm were adopted for compaction. This height allowed to reach a content of voids in the mixture (air and intergranular water) of 15 ± 1 %.

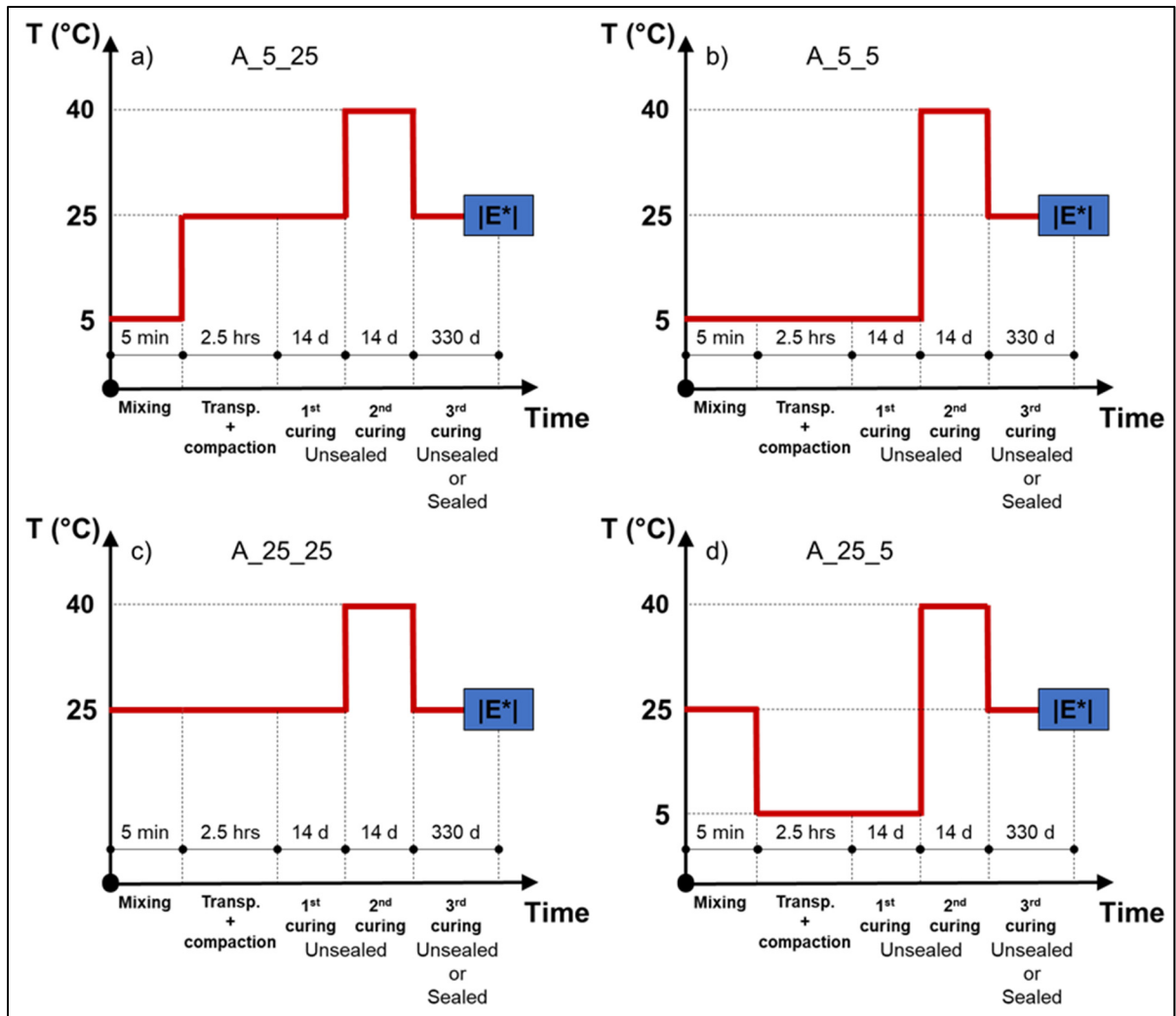


Figure 14.2 Laboratory production and experimental program: a) mixture A_5_25, b) mixture A_5_5, c) mixture A_25_25 and, d) mixture A_25_5

During mixing and compaction processes, all the tools and materials used were conditioned previously for at least 12 hours at the target temperature (5 $^{\circ}\text{C}$ and/or 25 $^{\circ}\text{C}$), except for the emulsion which was stored at 25 $^{\circ}\text{C}$ in all cases. Transportation, compaction and first curing (initial 14 days) were performed at the same temperature, since it is assumed that in field the three processes are exposed to similar temperatures. After this, an additional curing period of 14 days at 40 $^{\circ}\text{C}$ and 55% of relative humidity (RH) was applied to all mixtures to accelerate

the development of the material properties (Figure 14.2). After the first 28 days, specimens were stored for additional 11 months at room temperature in sealed (S) and unsealed (U) conditions to evaluate the influence of production temperatures (mixing, transportation and compaction) and curing conditions on the rheological properties. The complete organization of the experimental program is shown in Figure 14.2.

Table 14.3 Mixtures code, production steps (laboratory time), conditioning temperatures and number of specimens

Mixtures code ⁽¹⁾	Mixing (5 min)	Transportation + SGC compaction (2 hrs + 30 min)	Curing			Specimens (number)
			1 st (14d)	2 nd (14d)	3 rd (330d ⁽³⁾)	
A_25_25_1.5C_U	25°C	25°C	25°C	40°C	25°C (U)	1
A_25_25_1.5C_S	25°C	25°C	25°C		25°C (S)	1
A_25_5_1.5C_U	25°C	5°C	5°C		25°C (U)	1
A_25_5_1.5C_S	25°C	5°C	5°C		25°C (S)	1
A_5_25_1.5C_U	5°C	25°C	25°C		25°C (U)	1
A_5_25_1.5C_S	5°C	25°C	25°C		25°C (S)	1
A_5_5_1.5C_U	5°C	5°C	5°C		25°C (U)	1
A_5_5_1.5C_S	5°C	5°C	5°C		25°C (S)	1
A_5_5_0C_U ⁽²⁾	5°C	5°C	5°C		25°C (U)	1
A_5_5_0C_S ⁽²⁾	5°C	5°C	5°C		25°C (S)	1
⁽¹⁾ Emulsion source_T _{mixing} _T _{transportation+compaction} _Cement dosage by dry aggregate mass_Unsealed or Sealed condition ⁽²⁾ Cement dosage of 0%. The volume of cement is replaced by limestone filler ⁽³⁾ Sealed (S) and Unsealed (U) conditions						

Table 14.3 shows the conditioning process applied to each mixture and the corresponding nomenclature coding. It can be observed that more combination of mixing/transportation and compaction temperatures were evaluated. Ten specimens were produced, half of which was

stored in unsealed (U) conditions (Figure 14.3a) and half in sealed (S) conditions (Figure 14.3b). The sealing was realized by wrapping the specimen with plastic foil and sealing it with several layers of wax for a final coating thickness of around 5.0 mm (Figure 14.3b). The sealed condition after 28 days was chosen to stop the curing and/or ageing of the material, which instead was promoted in the unsealed specimens. Moreover, the sealed material is more representative of the field condition, where the cold layer is compacted and sealed by the upper layer(s). At the end of the additional curing period, all 10 specimens produced were cored at a diameter of 75 mm and prepared for complex modulus testing (Figure 14.3c).

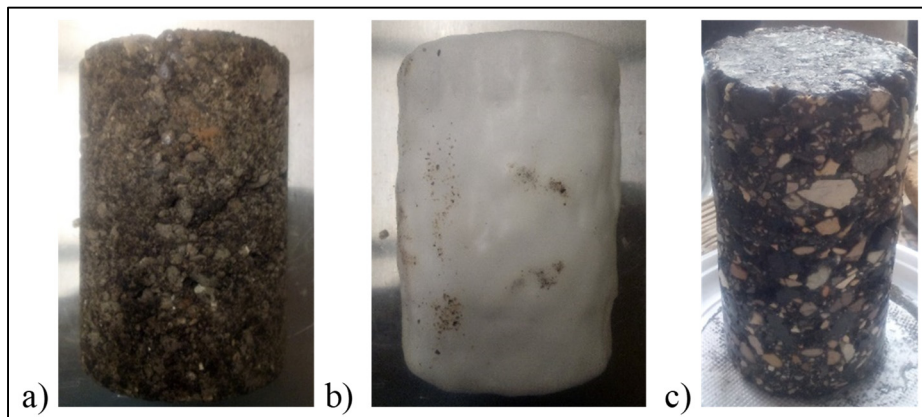


Figure 14.3 SGC specimen of $\text{Ø}100\text{mm} \times 140\text{mm}$: a) unsealed condition, b) sealed condition and, c) coring and sawing for testing specimens of $\text{Ø}75 \times 120\text{mm}$

14.3.3 Complex modulus test

The complex modulus tests were carried out with an MTS press under sinusoidal strain-controlled loading in compression only (haversine loading). The loading was applied on the top face of the specimen through an aluminum cap (not glued), whereas the bottom face was glued to an aluminum cap with a thermo-resistant epoxy. The axial strain of $50 \mu\text{m}/\text{m}$ (measuring base of 50 mm) was measured by placing three extensometers in the middle part

of the specimen and 120° apart. Specimens were tested at a temperature range between -20 °C and 40 °C with 10 °C steps, while frequencies ranged between 0.1 Hz and 10 Hz.

The sinusoidal strain, $\varepsilon(t)$, and stress, $\sigma(t)$, curves were fitted to the experimental data and used to calculate the norm $|E^*|$, and phase angle, ϕ_E , of the complex modulus E^* based on Equations 14.1 to 14.3:

$$\varepsilon(t) = \varepsilon_0 \sin(\omega t) \quad (14.1)$$

$$\sigma(t) = \sigma_0 \sin(\omega t + \phi_E) \quad (14.2)$$

$$E^* = \frac{\sigma_0}{\varepsilon_0} e^{j\phi_E} = |E^*| e^{j\phi_E} \quad (14.3)$$

where $\varepsilon(t)$ is the strain function, ε_0 is the strain amplitude, ω is pulsation, t is time, $\sigma(t)$ is the stress function, σ_0 is the stress amplitude, ϕ_E is the phase angle and represents the time delay Δt between strain (ε) and stress (σ) under cyclic conditions, $\phi_E = 2\pi f \Delta t$, and j is the imaginary unit defined as $j^2 = -1$.

14.3.4 Rheological modelling

Graziani et al. (2020) pointed out for the first time that CBTM mixtures show dissipation mechanisms that are irreversible and time-temperature independent. A modified version of the Huet-Sayegh model was proposed for the rheological modelling, but in this research a further improvement is proposed. The DBN model is considered particularly suitable for the purpose, since it introduces non-linearity and/or plastic phenomena which are not considered with the linear viscoelastic law (Di Benedetto, Mondher, et al., 2007; Gayte, 2016; Neifar et al., 2001). Such model takes into account non-viscous dissipation represented by means of elasto-plastic (“EP”) bodies in series with viscous dashpots (Figure 14.4). The number of elements selected in the model increases the precision and when only viscous dissipation is present, springs are used instead of the EP bodies obtaining a Generalized Kelvin-Vöigt (GKV) model.

Considering the nature of CBTM materials, they can be characterized by an intermediate behaviour between bituminous mixtures, cement bounded materials and granular materials. In the first case, the material response is highly linear visco-elastic and dependent on frequency and temperature (Perraton, Di Benedetto, et al., 2016). In the second case, the material shows time-temperature independent behaviour (stiffness and dissipation ability), whereas in the third case the material presents plastic dissipation and is basically slightly viscous and the response is few dependent on frequency and temperature (Di Benedetto et al., 2002; Enomoto et al., 2009). For these reasons, the DBN model including EP bodies could be reliable tools to adequately represent CBTM materials. In fact, EP bodies are characteristic of non-cohesive granular materials. In case of small strain and a small number of cycles applied, its configuration is simplified (Attia, 2020) and it is called DBN_{PDSC} (for Plastic Dissipation for Small Cycles).

Specific damping capacity ψ for many materials can be computed for Kelvin-Vöigt (KV) elements and small dissipation energy as:

$$\psi = \frac{\Delta W_{LVE}}{W_E} = \frac{\pi \varepsilon_0 \sigma_0 \sin \phi_E}{1/2 \varepsilon_0 \sigma_0} = 2\pi \sin \phi_E \quad (14.4)$$

where ΔW_{LVE} is the area of the LVE hysteresis loop with elliptical shape (energy dissipated at each cycle), W_E is the energy given by $1/2 \varepsilon_0 \sigma_0$ and ϕ_E is the frequency-dependent phase angle describing the lag between stress (σ_0) and strain (ε_0). The energy dissipated by EP bodies, ΔW_{EP} , which are characterized by time-temperature independent dissipation, is calculated as:

$$\Delta W_{EP} = W_{EP} \psi = 1/2 \varepsilon_0 \sigma_0 \psi = 2\pi D \varepsilon_0 \sigma_0 \quad (14.5)$$

where $D = \psi/4\pi$ is an adimensional time-temperature independent damping ratio classically used in soils dynamic (Ashmawy et al., 1995).

When cycles number and strain are small, it can be assumed that ΔW_{EP} can be interpreted as an equivalent linear visco-elastic dissipation, meaning that the plastic energy dissipation can

be approximated as a linear viscoelastic dissipation by the definition of an equivalent elasto-plastic phase angle ϕ_{EP} (Equation 14.6).

$$\sin(\phi_{EP}) = 2D \quad (14.6)$$

As a consequence, the DBN model corresponds to a Generalized Kelvin-Vöigt (GKV) model with viscous dissipation ($\eta_i(T)$) and an additional non-viscous dissipation D_i in the springs with stiffness E_i (Figure 14.4). The first DBN_{PDSC} element does not have a dashpot and D_i is chosen to be the same (D) for all the elements considered in the model.

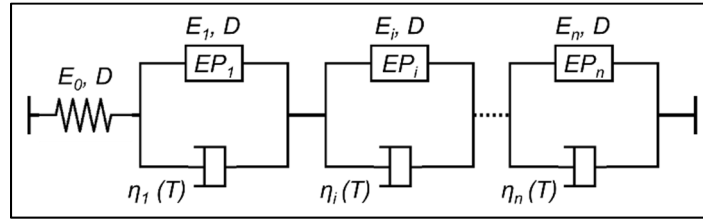


Figure 14.4 Representation of the DBN model applied in the small strain domain (few cycles)

The new coefficient D (or ϕ_{EP} from Equation 14.6) is considered in the calculation of the phase angle in the DBN model, which then considers viscous and non-viscous dissipations (Equation 14.7).

$$\begin{aligned} \sin(\phi_{DBN}) &= \sin(\phi_E) + \sin(\phi_{EP}) = \frac{\Delta W_{DBN}}{\pi \varepsilon_0 \sigma_0} = \frac{\Delta W_{LVE} + \Delta W_{EP}}{\pi \varepsilon_0 \sigma_0} \quad (14.7) \\ &= \sum_{i=0}^n \left(\frac{\omega \eta_i}{E_i^2 + (\omega \eta_i)^2} + \frac{2 \cdot D \cdot E_i}{E_i^2 + (\omega \eta_i)^2} \right) \cdot |E^*| \end{aligned}$$

where ΔW_{DBN} is the total dissipation (viscous and non-viscous), E_i and η_i are the Young's modulus and the Newtonian viscosity of the i^{th} element, respectively, ϕ_E is the phase angle of the viscous part, ϕ_{EP} is the phase angle conferred by the EP bodies, and D is the damping ratio.

The addition of non-viscous dissipation does not influence the absolute value of the complex modulus, which is indeed expressed from the GKV configuration (Equation 14.8).

$$|E_{GKV}^*(j\omega, T)| = \left| \left(\frac{1}{E_0} + \sum_{i=1}^n \frac{1}{E_i + j\omega\eta_i(T)} \right)^{-1} \right| \quad (14.8)$$

where T is the temperature and E_0 is the Young's modulus of the first element.

The calibration of the model is initially done by fixing the seven constants of the 2S2P1D model on the norm of the complex modulus $|E^*|$, and choosing the number of elements, n , to reduce the error between the discrete GKV configuration and the 2S2P1D. The complex modulus value computed by the 2S2P1D model is (Olard et al., 2003):

$$E_{2S2P1D}^*(j\omega\tau_E) = E_{00} + \frac{E_0 - E_{00}}{1 + \delta(j\omega\tau_E)^{-k} + (j\omega\tau_E)^{-h} + (j\omega\beta\tau_E)^{-1}} \quad (14.9)$$

where k and h are constant exponents ($0 < k < h < 1$), δ is a constant, E_{00} is the static modulus for $\omega \rightarrow 0$, E_0 is the glassy modulus when $\omega \rightarrow \infty$, β is a parameter linked to the dashpot viscosity $\eta = (E_0 - E_{00})\beta\tau$ when $\omega \rightarrow 0$, and τ_E is the characteristic time, which is the only parameter depending on the temperature:

$$\tau_E(T) = a_T(T) \cdot \tau_{0E} \quad (14.10)$$

where $a_T(T)$ is the shift factor at a temperature T , $\tau_E(T) = \tau_{0E}$ at the reference temperature T_0 and $\tau_E(T)$ is determined for each isotherm.

The shift factors of the isothermal curves can be estimated by a closed-form shifting (CFS) algorithm that minimizes the area between two successive curves (Gergesova et al., 2011). The values obtained are modelled by the Williams-Landel-Ferry (WLF) equation:

$$\log(a_T) = -\frac{C_1(T - T_0)}{C_2 + T - T_0} \quad (14.11)$$

where C_1 and C_2 are constants (Ferry, 1980).

After the calibration of the 2S2P1D model on the master curve of $|E^*|$, the additional parameter to consider non-viscous dissipation D is fitted. As a consequence, the DBN_{PDSC} model needs

seven constants from 2S2P1D (E_{00} , E_0 , k , h , δ , β and τ_E) and an additional constant D (or ϕ_{EP}) to represent CBTM behaviour in the small strain domain.

In this paper, the DBN model is applied and part of the analysis was performed considering the ratio between the experimental data (measurements) of each mixture and a reference mixture simulated by the DBN model:

$$\frac{|E^*|_{\text{meas}} - |E^*|_{\text{DBN,REF}_{\text{MIX}}}}{|E^*|_{\text{DBN,REF}_{\text{MIX}}}} \cdot 100 \quad (14.12)$$

$$\phi_{\text{meas}} - \phi_{\text{DBN,REF}_{\text{MIX}}} \quad (14.13)$$

This approach has been applied in other researches (Lachance-Tremblay et al., 2017; Lamothe et al., 2017), and it is a reliable analysis when different specimens are tested in similar (but not exactly the same) conditions (frequencies, temperature, type of loading, etc.). Furthermore, it is a useful tool to observe the difference between the different mixtures in the whole range of frequencies.

14.4 Results Analysis

The analysis of the results shows, at first, the DBN model applied to the experimental data obtained, and treats afterwards two specific parameters, the characteristic time (τ_{0E}) and the glassy modulus (E_0). The effect of curing conditions and low production temperatures is then evaluated in the tested frequency range.

14.4.1 Rheological Modelling

Figure 14.5 shows the experimental data in Cole-Cole plane (Figure 14.5a) and Black space (Figure 14.5b) representations for the mixtures tested. It can be observed that data from all mixtures are close and follow similar trends, however a part of the analysis will focus on the model parameters in order to evaluate differences not visible at this stage.

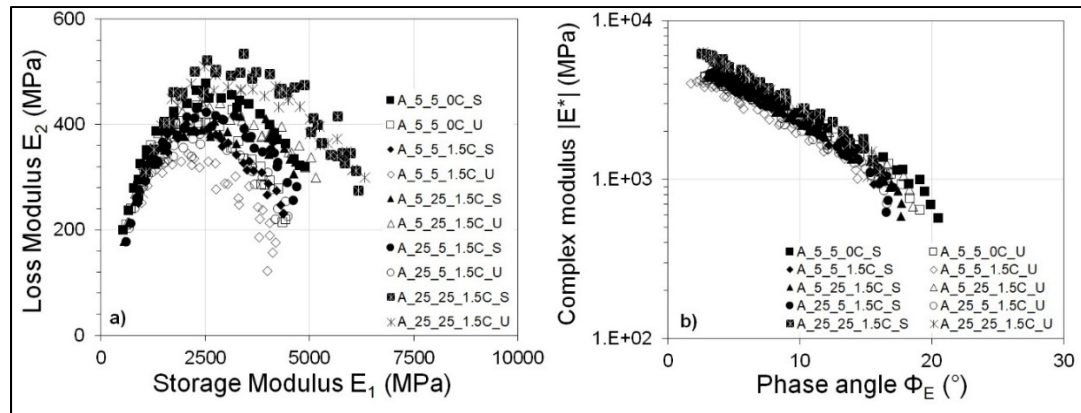


Figure 14.5 Experimental data from complex modulus tests: a) Cole-Cole plan and, b) Black space

Furthermore, the experimental data related to each mixture in both the Cole-Cole plane and Black space are disposed along a continuous curve (Figure 14.5). This is a fundamental aspect for the validation of the Time-Temperature Superposition Principle (TTSP). When this principle is valid, the isothermal curves of $|E^*|$ and ϕ_E can be shifted with the same value according to a reference temperature (T_0) to build master curves. CBTM being hybrid materials between granular, cementitious and viscoelastic bituminous mixtures, this is an important aspect that highlights the high impact of the residual binder employed. compared to the rest of the mixtures produced. This was expected, since the action of cement increases the material stiffness especially at high temperatures, when the bituminous phase is considered as fluid. However, a deeper analysis of the results is performed considering the effect of production temperatures (5 °C and 25 °C) and of the curing conditions (sealed and unsealed) separately. Table 14.4 contains the WLF model constants C_1 and C_2 . It is noted that values of C_1 and C_2 are similar for the same mixture, meaning that sealed and unsealed conditions did not affect the shift factors. Figure 14.6 shows the master curves of the studied mixtures shifted according to the shift factors estimated. It is possible to note that the mixtures without cement (A_5_5_0C), sealed and unsealed, show lower modulus (Figure 14.6a) and higher phase angle (ϕ_E) at low frequencies or high temperature (Figure 14.6b) compared to the rest of the mixtures produced. This was expected, since the action of cement increases the material stiffness

especially at high temperatures, when the bituminous phase is considered as fluid. However, a deeper analysis of the results is performed considering the effect of production temperatures (5 °C and 25 °C) and of the curing conditions (sealed and unsealed) separately.

Table 14.4 WLF shifting parameters ($T_0 = 20\text{ °C}$)

Mixture	C_1	C_2
A_25_25_1.5C_S	34.4	258.5
A_25_25_1.5C_U	35.0	258.4
A_25_5_1.5C_S	34.5	261.0
A_25_5_1.5C_U	38.2	259.6
A_5_25_1.5C_S	31.2	214.6
A_5_25_1.5C_U	28.5	215.6
A_5_5_1.5C_S	41.4	265.0
A_5_5_1.5C_U	37.4	214.9
A_5_5_0C_S	29.9	216.4
A_5_5_0C_U	30.0	216.5

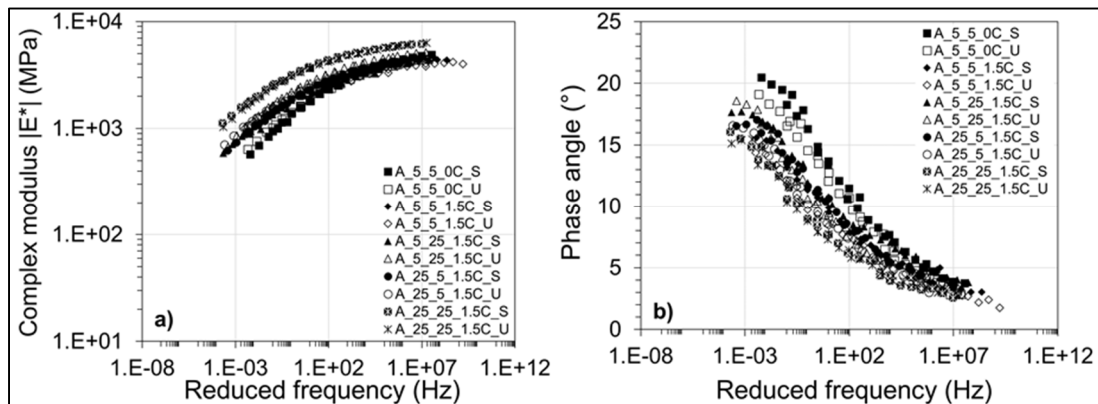


Figure 14.6 Master curves at reference temperature $T_0 = 20\text{ °C}$ of: a) norm of the complex modulus and, b) phase angle

To do so, the DBN model has been first optimized to obtain a good description of the mixtures analyzed (Figure 14.7). In Table 14.5, the model parameters k , h , δ and β were fixed for all the

mixtures, as such parameters depend on the viscous components, emulsion residual bitumen and RAP aged binder (Di Benedetto et al., 2004). In this case, both residual and aged binder were the same for all the mixtures investigated. On the other hand, the static modulus E_{00} depends on the aggregate skeleton structure and the presence of cement. E_{00} is quite difficult to determine with precision and an accurate distinction cannot be made based on this parameter.

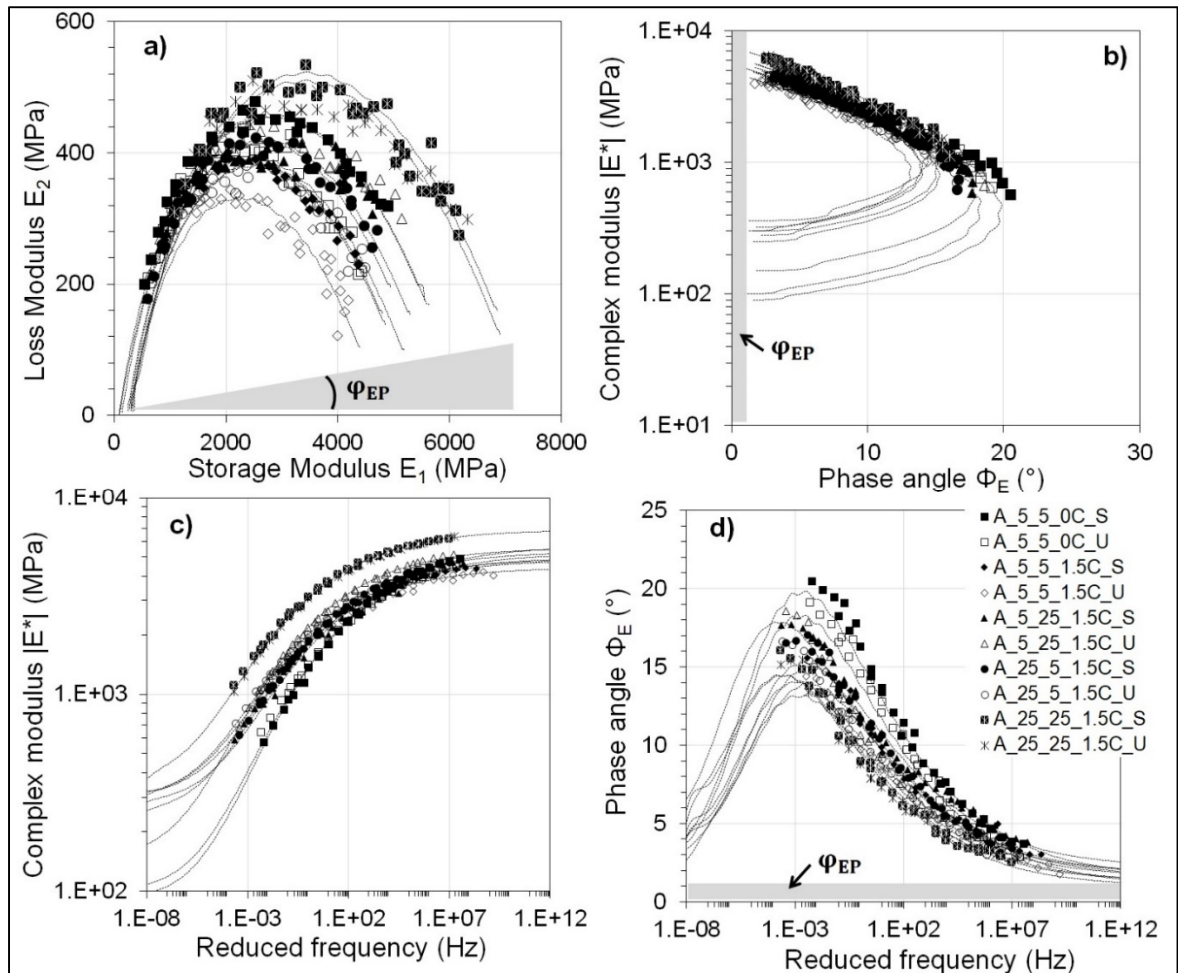


Figure 14.7 Experimental data and DBN model ($T_0 = 20^\circ\text{C}$) for $n = 40$: a) Cole-Cole plan, b) Black space, c) master curve of the norm of the complex modulus $|E^*|$ and, d) master curve of the phase angle φ_{EP} (φ_{EP} is shown and represents the elasto-plastic phase angle)

The elasto-plastic phase angle ϕ_{EP} is mainly dependent on the strain amplitude, which in this case was the same for all the studied mixtures. In fact, all the values for ϕ_{EP} were between 1.0° and 2.2° and were not affected by either the production temperatures or the curing conditions. However, some differences can be highlighted in terms of glassy modulus E_0 and characteristic time τ_{0E} . A part of our analysis particularly focuses on these properties. The glassy modulus E_0 is the asymptotic material stiffness at low temperatures (or high frequencies). The characteristic time τ_{0E} (considered at the reference temperature of 20°C) is affected by the binder stiffness.

Figure 14.8 shows the accuracy of the model in terms of norm of complex modulus $|E^*|$ and phase angle ϕ_E . It is remarked the good fitting of the model in both representations, showing less than $\pm 15\%$ difference for $|E^*|$ and $\pm 3^\circ$ difference for ϕ_E (Figure 14.8a-b). From other studies, a difference of 20% for $|E^*|$ is considered acceptable (Lachance-Tremblay et al., 2017; Lamothe et al., 2017).

Table 14.5 DBN model parameters for the studied mixtures ($T_0 = 20^\circ\text{C}$)

Mixtures (code)	E_{00} (MPa)	E_0 (MPa)	k (-)	h (-)	δ (-)	τ_{0E} (at 20°C) (s)	β (-)	ϕ_{EP} ($^\circ$)	T_{eq} ($\tau_{0E}=19\text{s}$) ($^\circ\text{C}$)
A_5_5_0C_S	90	5 650	0.15	0.35	2.42	0.2	1E+10	1.6	6.6
A_5_5_0C_U	100	5 200				0.4		1.0	8.2
A_5_5_1.5C_S	320	4 800				2.5		1.8	14.5
A_5_5_1.5C_U	300	4 400				7.5		1.3	17.7
A_5_25_1.5C_S	280	4 950				1.4		2.2	12.5
A_5_25_1.5C_U	150	5 550				7.5		1.8	17.0
A_25_5_1.5C_S	250	5 300				2.0		1.6	12.8
A_25_5_1.5C_U	300	4 850				7.5		1.6	17.3
A_25_25_1.5C_S	360	6 850				19.0		1.3	20.0
A_25_25_1.5C_U	340	6 900				19.0		1.0	20.0

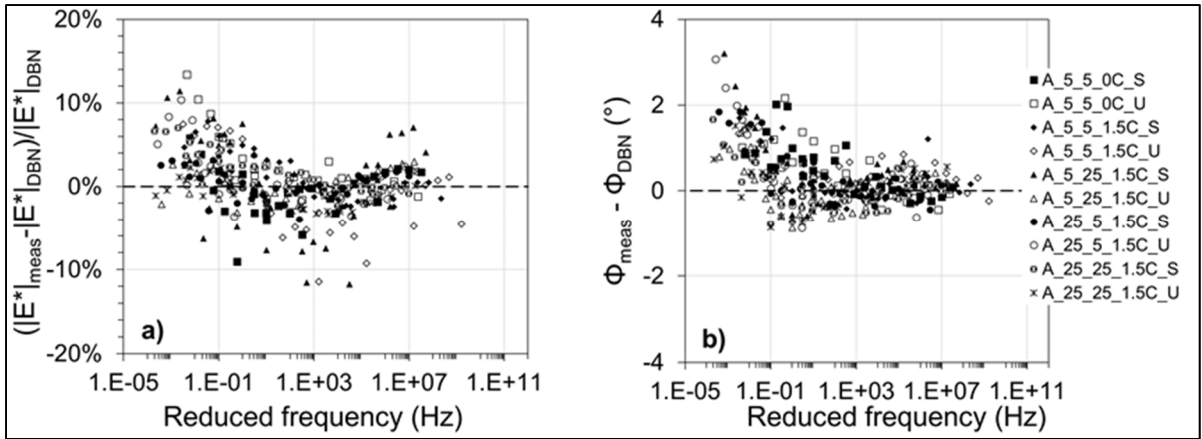


Figure 14.8 Accuracy of the DBN model according to experimental results ($T_0 = 20\text{ }^\circ\text{C}$): a) norm of the complex modulus and, b) phase angle

14.4.2 Characteristic Time τ_{0E}

In the master curves representations ($|E^*|$ and ϕ_E), a change in τ_{0E} value represents the shifting in the frequency domain. In Table 14.5, values of τ_{0E} refer to a reference temperature of $20\text{ }^\circ\text{C}$ and are different among the mixtures. However, if the TTSP principle is respected, a reference τ_{0E} can be fixed (τ_{0Eref}) and an equivalent temperature T_{eq} can be calculated. In this particular case, the reference τ_{0E} was assumed from both mixtures produced at room temperature (A_25_25_1.5C), i.e. 19.0 s. It is observed that for these two mixtures, $T_{eq} = T_0 = 20\text{ }^\circ\text{C}$. All other mixtures were characterized by lower values of τ_{0E} , which can be linked to softer bituminous phases (residual emulsion bitumen and RAP binder). In fact, τ_{0E} depends on bitumen consistency and it increases if the bitumen is harder, perhaps due to the effect of ageing or curing. Hence, it is assumed that if a mixture has a lower τ_{0E} compared to another one, the equivalent temperature to obtain the same stiffness should be lower. From the results obtained, this assumption is respected and all the mixtures produced at low temperatures are characterized by a lower equivalent temperature compared to the mixtures produced at standard temperature ($25\text{ }^\circ\text{C}$). With high probability the thermal shock conferred by low temperatures accelerates the emulsion breaking and alters the formation of bituminous bonds.

As a consequence, the micro-structure could have higher dissipative ability. Furthermore, the effect of cement has to be highlighted. In fact, the addition of cement caused an increase in τ_{0E} (and a decrease of T_{eq}), meaning an increase in the binding structure consistency. However, hydrated cement and bitumen do not form a unique material and they contribute to the stiffness as separate elements. The increase of τ_{0E} in HMA mixtures is observed in case that harder bitumen is used (Mangiafico et al., 2014). Figure 14.9 shows the effect of production temperatures on the characteristic time τ_{0E} and only on mixtures produced with cement. In both sealed and unsealed conditions, it is shown that when mixing and/or transportation temperatures are 5 °C (lower part of the pyramid), the values of τ_{0E} are quite similar, whereas there is a clear peak when considering the mixture produced at 25 °C. This aspect is also visible in Table 14.5, where all specimens cured in sealed conditions have a lower T_{eq} compared to unsealed specimens. This indicates that in sealed conditions the bituminous phases (residual bitumen and RAP binder) are globally softer. Such difference can be explained by a higher ageing or curing on the unsealed specimens compared to the sealed ones. As a consequence, the three values of τ_{0E} related to low production temperatures can be considered as three repetitions to run a single factor ANOVA analysis to evaluate the difference between sealed and unsealed conditions. Of course, this analysis involves only a limited number of specimens and for future studies more repetitions are needed. The analysis was performed assuming the null hypothesis $H_0: \alpha_i = 0$, meaning that all the samples' means are equal to the total mean. In this case, $i = 2$, i.e. sealed and unsealed conditions. The analysis was performed assuming a significance level $\alpha = 0.05$ and the results are shown in Table 14.6. It is remarked that $F > F_{crit}$ and that $p\text{-value} < 0.05$, meaning that the null hypothesis can be rejected and there is a significant difference between the characteristic times τ_{0E} obtained in sealed and unsealed conditions when mixtures are produced at low temperatures.

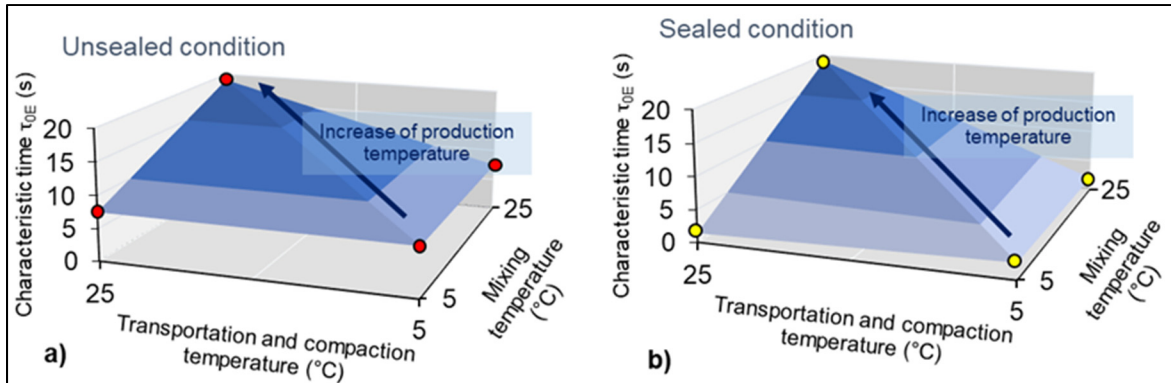


Figure 14.9 Effect of production temperatures on τ_{OE} : a) unsealed specimens and, b) sealed specimens

Table 14.6 Single Factor ANOVA analysis for τ_{OE} in mixtures produced at low temperatures

Source of Variation	SS ⁽¹⁾	df ⁽²⁾	MS ⁽³⁾	F	p-value	F _{crit}
Sealed vs Unsealed	45.9267	1	45.9267	302.8132	6.4018E-05	7.7086
Within Groups	0.6067	4	0.1517			
Total	46.5333	5				

⁽¹⁾ Sum of squares

⁽²⁾ Degrees of freedom

⁽³⁾ Mean square ($= \frac{SS}{df}$)

14.4.3 Glassy Modulus E_0

Figure 14.10 shows the effect of mixing, transportation and compaction temperature on the glassy modulus E_0 for the mixtures produced with cement. In general, all the mixtures characterized by mixing and/or transportation and compaction temperature of 5 °C showed a range of E_0 comprised between 4,400 and 5,550 MPa, regardless the curing conditions (sealed or unsealed). If the production process was performed entirely at 25 °C, E_0 was 6,850 and 6,900 MPa for sealed and unsealed conditions, respectively. As a consequence, low production

temperatures generally caused a decrease in E_0 . In other terms, by performing only one of the two processes (mixing or transportation and compaction) at 5 °C lead to lower values of E_0 compared to a full production process performed at 25 °C. As for the previous analysis of τ_{0E} , the thermal shock given to the bitumen emulsion altered the formation of continuous bituminous bonds. However, more repetitions are recommended for future analysis.

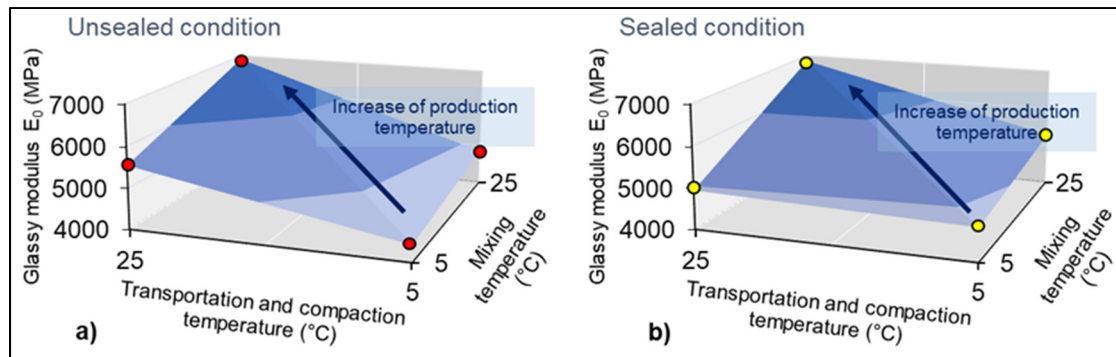


Figure 14.10 Effect of production temperatures on E_0 : a) unsealed specimens and, b) sealed specimens

Also in this case a single factor ANOVA analysis was performed to evaluate the difference between S and U conditions in mixtures produced at low temperatures. The same null hypothesis $H_0: \alpha_i = 0$ was adopted, meaning that all the samples' means are equal to the total mean. Also in this case a significance level $\alpha = 0.05$ was selected, and the results are shown in Table 14.7. It is noted that $F < F_{crit}$ and that $p\text{-value} > 0.05$, meaning that the null hypothesis cannot be rejected and there is no significant difference in E_0 between sealed and unsealed conditions. As a consequence, for the same mixture, E_0 values in sealed and unsealed conditions can be assumed as two replications to run a Two-Factor ANOVA analysis to evaluate the separate effect of mixing and transportation and compaction temperatures on the value of the glassy modulus. Results are shown in Table 14.8.

Table 14.7 Single Factor ANOVA analysis for E_0 in mixtures produced at low temperatures

Source of Variation	SS	df	MS	F	P-value	F_{crit}
Sealed vs Unsealed	10 416.6667	1	10 416.6667	0.0518	0.8310	7.7086
Within Groups	803 333.3333	4	200 833.3333			
Total	813 750	5				

Table 14.8 Two-Factor with replication ANOVA analysis for E_0 to evaluate production temperatures

Source of Variation	SS	df	MS	F	P-value	F_{crit}
Mixing temperature	2 205 000	1	2 205 000	24.3310	0.0079	7.7086
Transportation and compaction temperature	3 001 250	1	3 001 250	33.1172	0.0045	7.7086
Interaction	661 250	1	661 250	7.29655	0.0540	7.7086
Within	362 500	4	90 625			
Total	6 230 000	7				

In case of only mixing temperature is considered, the conditions for the rejection of the null hypothesis are respected, meaning that there is a significant difference in E_0 if the mixture is mixed at 5 °C or 25 °C. In the same way, in case of only transportation and compaction temperature is considered, results showed that transporting and compacting the mixtures at 5 °C or 25 °C led to a significant difference in E_0 . Analyzing the interaction between the two factors, $F < F_{crit}$ and $p\text{-value} > 0.05$, meaning that the two factors cannot be considered separately.

14.4.4 Analysis in the frequency range

Figure 14.11 shows the relative difference between mixtures cured in S and U conditions. In this case, Equations 14.12 and 14.13 were used assuming as a reference mixture the respective mixture that was cured in unsealed conditions. Regarding the ratio of $|E^*|$, it can be observed

that the cloud of points is mainly distributed around 0 % with the majority of points included in a range of ± 10 %. Even if this difference can be contained in the model precision, the trend seems to be lower than 0% at low frequencies (or high temperatures) and higher than 0% at high frequencies (or low temperatures). In terms of ϕ_E , the relative difference is small (between 0° and 4°) but results show that in general the S curing condition promoted the increase of the ϕ_E . In sealed condition, the specimens were not exposed to environmental factors, and this could have slowed down the ageing/curing process of the material, resulting in a higher dissipation ability.

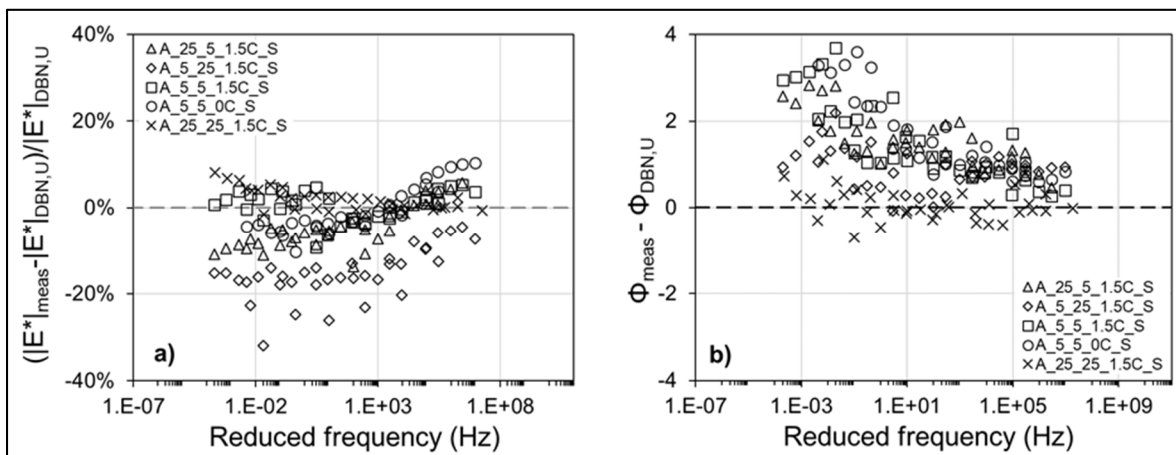


Figure 14.11 Relative difference values between mixtures cured in sealed conditions and unsealed conditions: a) norm of the complex modulus and, b) phase angle

Figure 14.12 shows the effect of production temperatures as relative difference between the mixtures produced at low temperatures and the reference mixture A_25_25_1.5C_U produced at room temperature. For simplicity, this analysis is performed only on specimens cured in unsealed conditions. In terms of difference on the $|E^*|$, all the mixtures that were mixed and/or compacted at 5°C show a global loss of stiffness of around 30% compared to the reference mixture. Such loss is quite constant for all the range of frequencies analysed, with exception for the mixture without cement (A_5_5_0C_U). As expected, the loss in stiffness is higher (up to 60%) at low frequencies, due to the lack of contribution of cement at high temperatures. In

terms of difference of the ϕ_E , all the mixtures with cement show quite similar values, and the range obtained can be considered in the variability due to testing conditions (between 0° and 2°). At the same time, the mixture without cement A_5_5_0C_U showed phase angle values higher than the reference mixture, due to the bigger viscous contribution given by the only presence of bitumen.

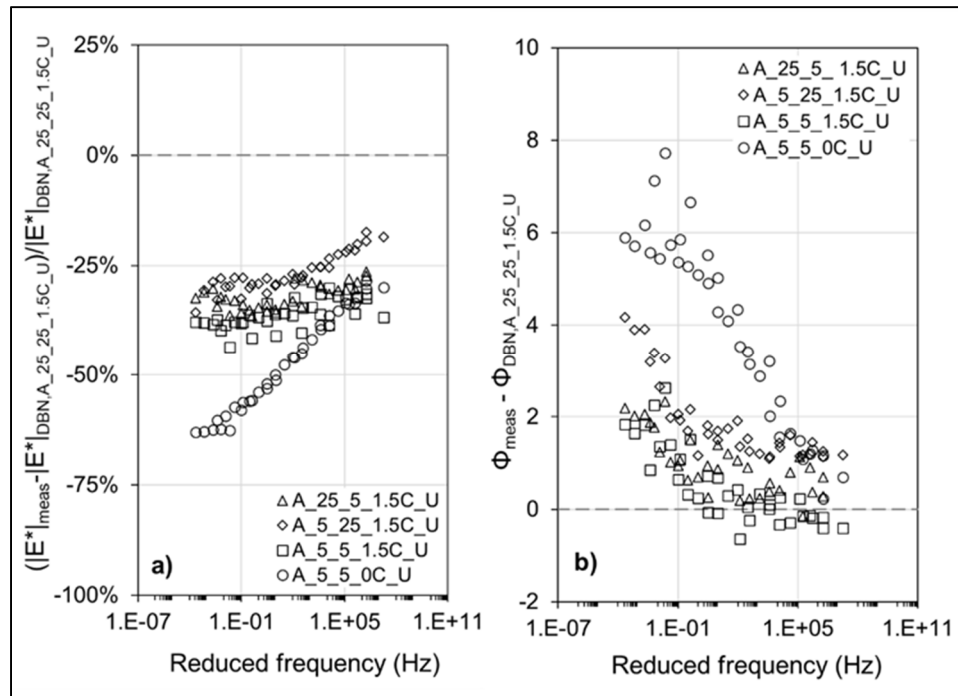


Figure 14.12 Relative difference values between mixtures produced at low and standard temperatures: a) norm of the complex modulus and, b) phase angle

14.5 Conclusions

This paper investigated the effect of low production temperatures and curing conditions (sealed and unsealed) in the properties of CBTM materials in the small strain domain. Experimental results from complex modulus test were analyzed by means of the DBN_{PDSC} model and the following conclusion can be drawn:

- The DBN model is a good tool that allows representing the material behaviour taking into account plastic non-viscous phenomena. Such aspect cannot be considered by LVE rheological models typically used for bituminous mixtures. The reliability of the rheological model is of extreme importance if the model is employed as a tool to compare different aspects, which in this case were curing conditions and production temperatures (Figure 14.8);
- Sealed and unsealed conditions were evaluated analyzing in particular the characteristic time τ_{0E} and the glassy modulus E_0 . It was observed that the glassy modulus E_0 was not significantly affected by the sealing conditions (Figure 14.10). On the other hand, the characteristic time was higher (Figure 14.9) and phase angle lower (Figure 14.11b) in case of unsealed conditions. Probably the hardened bitumen under the effect of ageing or curing affected the viscous dissipation ability. In terms of $|E^*|$ in the reduced frequencies range analyzed, it was not possible to observe a significant difference between the two curing conditions (Figure 14.11a);
- Low production temperatures (5 °C for mixing and/or compaction) globally penalized the stiffness of the mixtures produced after a year of curing, in particular affecting the characteristic time τ_{0E} and the glassy modulus E_0 . In fact, in the reduced frequencies range considered, a uniform stiffness loss of around 30% was observed (Figure 14.12a). If the mixture is produced at 5 °C and without cement, this additionally negatively influences its properties at low frequencies (high temperatures). In general, when producing CBTM mixtures at low temperatures (mixing and/or transportation and compaction at < 10 °C), performance are expected to decrease (Figure 14.10 and Figure 14.12a). Probably the thermal shock caused by the low production temperature negatively affects the bituminous structure (coating and bonding) inside the mixture.

The production of CBTM materials at low temperatures is still an open issue which needs further studies. However, it can be assumed that the key element is the bitumen emulsion, which needs a deep characterization prior the execution of recycling projects in cold climates.

Moreover, as bitumen emulsions are particularly sensitive to low temperatures, a similar study on foamed bitumen is recommended to overcome the issues highlighted.

CHAPTER 15

SUMMARY OF SECTION 3

In CHAPTERS 12, 13 and 14 the research focused on the effect of production temperatures on the properties of CBTM mixtures. The mixtures were produced following the same formulation with two emulsion sources and an attempt to simulate production (mixing, transportation, compaction and curing at 25 °C or 5 °C) was made. The two chosen emulsion sources are typical market products used for cold recycling projects. The mechanical properties of the mixtures were mainly investigated after 28 days of curing (14 days at 5 °C or 25 °C, plus 14 days at 40 °C) to simulate 1-3 years of service life, and after 1 year of curing/ageing at room temperature.

Results in CHAPTER 12 showed that, during compaction, low temperatures negatively affected the energy required to reach the target volumetric properties, probably because of a change in the bitumen viscosity. In terms of mechanical properties, the bitumen emulsion type (and the residual bitumen from the emulsion used) influenced the CBTM mixtures properties at standard production temperatures (25 °C). Furthermore, only one emulsion was negatively affected after 28 days of curing by low production temperatures. In fact, if the material produced with such emulsion was not cured for at least 3 days at 5 °C (elastic modulus > 1000 MPa), even a light load could cause a permanent loss in adhesion and performance.

Specimens not tested during the first 28 days were cured for additional 11 months (for a total of 1 year), after which visco-plastic properties were tested and an approach for rheological modelling was proposed. This additional curing was adopted to investigate the material's properties in the long-term, assuming that a stable condition was reached. Results in CHAPTER 13 showed that the response of the CBTM mixture in the small strain domain is related to the properties of the bitumen used to produce the bitumen emulsion. It was found that LVE theory does apply to CBTM mixtures, since their response to cyclic loading in the small strain domain can be approximated as intermediate between bituminous mixtures and

granular materials. For this reason, it was observed that the energy dissipation is mainly viscous, but also a small contribution given by non-viscous dissipation should be considered. To take that into account, a simplified version of the DBN model was applied introducing an equivalent phase angle additional to the viscous phase angle (Attia, 2020). It is assumed that such parameter can represent frictional or visco-plastic phenomena in the material, due to the low bitumen content and dispersion, the high air voids content or the aggregates used. Further studies are needed on this topic.

According to modelling parameters in CHAPTER 14, it was observed that the characteristic time τ_{0E} , linked to the bitumen consistency, was higher for specimens cured in unsealed conditions. This suggests that the ageing process of the virgin binder is not negligible. In the frequency range analyzed, low production temperatures (5 °C) lead to a loss in complex modulus of 30%, while the phase angle was not affected significantly. Probably the thermal shock caused by the low production temperature negatively affects the bituminous structure (coating and bonding) inside the mixture. The results and model related to each mixture studied in CHAPTER 14 are reported in Annex II.

Further research is recommended to better understand the behaviour of CBTM mixtures when tested in the small strain domain. In particular, the concept of “black rock” applied to the RAP aggregate needs more studies. If the assumption of RAP as a black rock is valid, a multi-scale approach from mixtures to mastics to virgin binder would be possible and will allow a better understanding of the material properties. Moreover, more effort should be addressed to the application of the DBN model to CBTM mixtures, which are subjected to non-viscous energy dissipation (Graziani et al., 2020).

CONCLUSION

This thesis aimed to improve the knowledge on aspects of cement-bitumen treated materials (CBTM) related to the production process. In the majority of the cases, several factors regarding the production of cold mixtures in general are provided by local guidelines or the past experience on the field, without having a solid scientific approach. At the same time, this technique is still considered quite new and more effort should be put in terms of research in order to avoid issues related to the service life. An adequate knowledge will positively influence the future spread of a correct know-how during production.

All the experimental work done in the thesis is based on the application of the volumetric approach for mix design. The application of volumetric parameters is extensively used in case of hot mix asphalt mixtures and it is believed that a better control on production can be achieved if applied to CBTM mixtures too. Of course, new parameters were adopted, as voids in the mixture and voids filled with liquids. The recommendation to use the volumetric mix design in cold mixtures is motivated by the possibility to optimize at the same time water dosage, bitumen dosage and energy of compaction for a target air voids content. It was also shown the change of air voids content of the mixture due to the effect of cement hydration. The experimental work carried out in this thesis was divided in three sections.

Section 1 investigated the effects of mineral additions and water in CBTM mixtures. Hydrated lime, which is often employed as mineral addition in the cold mixtures instead of cement, was combined with silica powder obtained from micronized glass. In this way, it would be possible to further improve the environmental footprint of such materials. This combination showed better properties than the hydrated lime itself, but it did not allow to reach the same mechanical properties conferred by ordinary Portland cement. The drawback of this concept is also represented by the lightness of both hydrated lime and micronized glass, which obviously represents a higher danger for operators during production. Cement is not replaceable yet, but its dosage can be kept low (maximum of 1.5%) by decreasing the air voids. For this, water is

often considered a key component for workability and compactability, but the effect on mechanical properties needed to be studied too. Mixtures with different water contents did not show significantly different mechanical properties, which were more influenced by the air voids content. However, a mix design for the optimum water content should not take into account only workability and compactability, but consider the balance between energy of compaction and degree of saturation of the voids in the aggregate skeleton. In fact, the VFL (voids filled with liquids) could be a useful tool to ensure a good level of coating, since the water drives the bitumen droplets of the emulsion in the mixture. To achieve this, the volumetric mix design is highly recommended. However, when CBTM are produced in plant, it is believed that the humidity of the RAP aggregate and the water contained in the emulsion is enough to ensure a workable mix.

Section 2 deals with the effect of RAP aggregate (gradation and source) on the mechanical properties of the cold mixture produced. In this thesis, different gradations were investigated and the results highlighted the maximum density curve as a good reference for mixture gradation to obtain good results. However, since RAP is often composed of clusters, the filler-sized particles fraction is missing and a correction with virgin filler is usually needed and recommended. In fact, it was observed that the increase in filler dosage improved both workability and mechanical properties. Assuming the maximum density curve as reference gradation, the influence of the nominal maximum aggregate size (NMAS) was also evaluated. For the same RAP source, a reduction in the NMAS from 16 mm to 10 mm lead to a better performant material in terms of different properties: stiffness, strength and fracture. Due to the finer gradation in case of NMAS = 10 mm, the mastic dispersed in the coarse aggregates skeleton probably improved the mechanical properties.

At this point, two RAP sources (RAP1 and RAP2) with a maximum diameter of 10 mm were compared. The two RAP sources were characterized by a fragmentation test, which evaluates the amount of clusters in the RAP aggregate and the change in gradation due to fragmentation. RAP2 was characterized by a higher fragmentation index than RAP1, i.e. it contained more

clusters and the change in gradation is significant when fragmented. The sensitivity to fragmentation can be linked to the RAP binder stiffness. Using the same RAP sources to produce CBTM mixtures, RAP2 mixture required less compaction energy than RAP1 to reach the target volumetric properties, despite the mix formulation and the shape parameters of both RAPs particles were the same. In terms of tensile strength and cracking resistance, RAP2 was less performant than RAP1. At the same, the analysis in the small strain domain highlighted a better affinity of the RAP2 with the bitumen emulsion used, showing a more viscous response under cyclic loading. As a consequence, the fragmentation index of a RAP source cannot be directly linked to the global properties of the CBTM mixtures produced, since an additional key parameter seems to be the affinity between RAP aggregate and bitumen emulsion. Concluding, to know the effect of the RAP source used in the CBTM mixture produced in a mixing plant, it is extremely important to monitor constantly the properties of the RAP aggregate and to produce the mixture with a stable bitumen emulsion.

In Section 3 the production process of CBTM was simulated at low temperatures, 5 °C. This step was needed in order to consider the possibility of cold mixtures application also in harsh climates as in Québec. In particular, the production process was divided in mixing, transportation, compaction and curing and one or more of these steps were performed at 5 °C, while the rest was performed at 25 °C and a part of curing at 40 °C. The transportation and compaction temperature affects the energy required for compaction, acting on the bitumen viscosity. However, resistance of mixtures was not penalized by this aspect. It was observed that a loss in stiffness modulus can be expected up to 30% (50% if no cement is used), even if only the mixing or compaction processes were done at 5 °C. This was observed after one year of curing, meaning that the material reached a quasi-stable condition. However, even though the material is less performant, this will expand the time gap during the year in which the production can be carried out (from 5 to 7 months). Moreover, when the material is produced and cured at 5 °C, it is recommended to wait at least around 3 days before applying any load. Another important step is to deeply characterize the bitumen emulsion and the residual bitumen, which can be more or less sensitive to low temperatures, as well as affecting the

material performance at standard production temperatures. In a production plant, it is possible to evaluate the properties of the bitumen emulsion at low temperatures by producing several specimens at the same time of when the CBTM layer is put in place. The curing of the specimens can be done externally (in the same conditions of the pavement), and the development of strength and stiffness can be evaluated. In this way, it is possible to monitor at the same time the curing of the pavement and figure out critical aspects.

In the thesis, a rheological model was proposed to describe the thermo-visco-plastic behaviour of CBTM mixtures in replacement of traditional linear visco-elastic models employed for bituminous mixtures. The DBN model takes into account non-viscous contribution in the computation of the energy dissipated in the small strain domain. This is a characteristic aspect of cold mixtures due to the presence of cement, low bitumen dosages, high air voids content and frictional phenomena between aggregates. It is believed that such new approach could give an indication of the affinity between bitumen emulsion and RAP aggregate, but more studies are strongly encouraged in this direction.

RECOMMENDATIONS

According to the results obtained in this thesis, the following points are recommended to be considered for future works:

- 1) The effect of aggregate gradation was investigated by mechanical tests addressed to measure the stiffness or strength of the material. However, it is recommended to investigate the effect of different aggregate distribution and/or RAP source on long-term performance of the mixtures, such as fatigue or permanent deformation;
- 2) Part of the work involved only two RAP sources, which had an impact on the short-term mechanical properties of CBTM mixtures (maximum of 28 days of curing). Due to the large availability and the several factors affecting the properties of a RAP source, more sources should be characterized and considered to evaluate the above-mentioned long-term properties. Being cold recycled mixtures a construction material oriented to improve the environmental and economic footprint of the pavement, much effort should be put during mix design to ensure a longer life service of the new pavement. As a consequence, it is important to understand to what extent the RAP source needs to be considered;
- 3) The fragmentation test is a useful test to quickly characterize the RAP source. However, the fragmentation index is not enough to assess the global behaviour of the mixtures produced. Hence, it is recommended to follow a step-by-step approach which links the fragmentation test (step 1) to the final properties of the material (step n), perhaps considering a multi-scale study (from binder to mixture);
- 4) The visco-elastic properties and the failure resistance can be highly affected by the affinity between bitumen emulsion and RAP source, as well as the cement content defines the initial and final strength. So, it is recommended to take into account a 3-parameters approach during mix design, i.e. cement content, bitumen emulsion type and dosage and RAP source, in addition to water, in order to ensure better performance both in terms of initial strength and viscous response. As first assumption, the DBN model and the non-

viscous dissipation could be used to define the affinity between RAP and emulsion sources, even though additional studies are required;

- 5) The production of CBTM mixtures at 5 °C is possible. However, in such case, longer curing periods than usual are strongly recommended before the laying of the upper layer. In addition, some characterization tests on the bitumen emulsion should be carried out at low temperatures. Standard tests like storage stability, viscosity and breaking index should be carried out to characterize the bitumen emulsion at low temperature and compared to the values obtained at room temperature. Furthermore, also in this case the affinity between bitumen emulsion and RAP source could be considered for further studies regarding low production temperature;
- 6) One big issue of bitumen emulsions at low temperatures is stability and demulsification. However, as an alternative, foamed bitumen could be studied and considered for production of CBTM mixtures at low temperature. Foamed bitumen does not require time for breaking, process which is highly dependant on temperature and humidity. Moreover, being the foam produced at high temperatures (> 150 °C), some of the heat would be transferred to the aggregates ideally conferring better bonding. In both cases (bitumen emulsion and foamed bitumen), when production processes are carried out at low temperatures, it is recommended to limit as much as possible transportation times and proceed with CIR techniques. Some results related to the production of CBTM mixtures with foamed bitumen at room temperature are presented in Annex III, IV and V;
- 7) The field production of CBTM is still limited and the major part of the investigative work is performed in the laboratory. As a consequence, it is essential to extend the interest and the research effort on trial sections realized on full-scale pavements. This would give a significant contribution to the comprehension of the material.

According to the results obtained in this thesis, the following list of recommendations are proposed for the control of CBTM materials during production:

- 1) Frequent control of the RAP aggregate present in the production plant, especially in terms of gradation and water content (humidity). If necessary, move the RAP stockpile in a protected area to partially or totally block the environmental conditions;
- 2) Preliminar study of the recipe in order to fix the optimum water content (according to the RAP humidity), the cement content and the residual bitumen content. If possible, it is recommended to carry out this step with more than one bitumen emulsion, and eventually choose the more suitable;
- 3) In case of instable weather conditions, consider to increase the cement content to accelerate the material resistance in the first days. The maximum cement content should be fixed on the material produced taking into account values of strength, stiffness and fatigue life;
- 4) In general, it is recommended to wait at least 24 hours before the laydown of the upper layer;
- 5) In case of critical conditions (production temperature lower than 10 °C), it is possible to evaluate the properties of the bitumen emulsion at low temperatures by producing several specimens at the same time of when the CBTM layer is put in place. The curing of the specimens can be done externally (in the same conditions of the pavement), and the development of strength and stiffness can be evaluated. In this way, it is possible to monitor at the same time the curing of the pavement and figure out critical aspects.

ANNEX I

PROPERTIES OF MATERIALS EMPLOYED IN THE THESIS

A-I.1 RAP Chambly (CA)

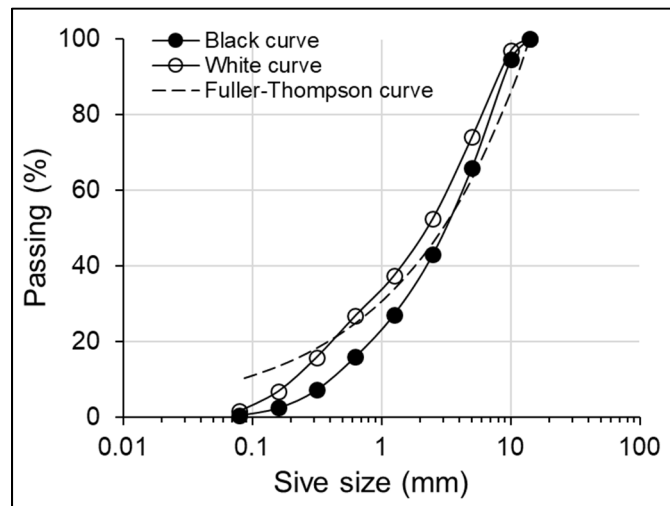


Figure-A I-1 Black curve, white curve and maximum density curve

Table-A I-1 RAP aggregate properties

Property	Standard	Unit	Value
Bitumen content	LC 26-006	%	6.10
PCS _{5/10} @20 °C	ASTM D1557-12	%	9.60
Apparent density of the aggregate blend	LC 26-045	g/cm ³	2.577
Absorption	EN 1097-06	%	1
Maximum aggregate size	ASTM D 448-03	mm	14

A-I.2 RAP St. Isidore (CA)

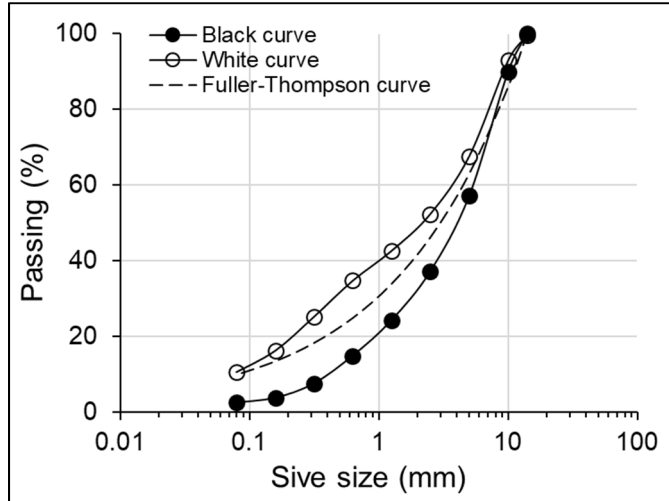


Figure-A I-2 Black curve, white curve and maximum density curve

Table-A I-2 RAP aggregate properties

Property	Standard	Unit	Value
Bitumen content	LC 26-006	%	5.02
PCS _{5/10} @20 °C	ASTM D1557-12	%	8.25
Apparent density of the aggregate blend	LC 26-045	g/cm ³	2.545
Maximum aggregate size	ASTM D 448-03	mm	14

Table-A I-3 RAP binder properties

Property	Standard	Unit	Value
Brookfield viscosity at 135 °C	ASTM D2196	Pa*s	1.727
Brookfield viscosity at 165 °C	ASTM D2196	Pa*s	0.391
Penetration @ 25 °C	ASTM D5	dmm	11
Softening point	ASTM D36	°C	69.7

A-I.3 RAP-CBR (IT)

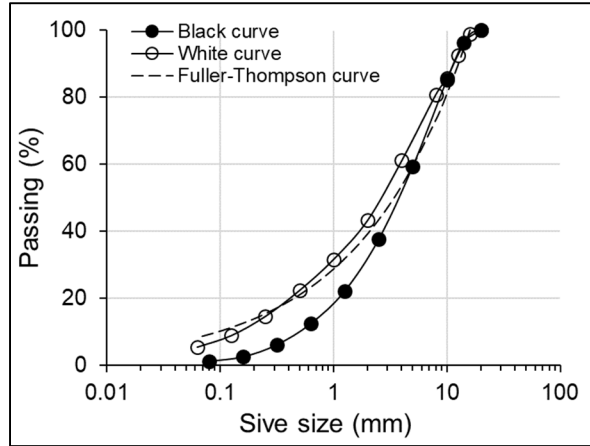


Figure-A I-3 Black curve, white curve and maximum density curve

Table-A I-4 RAP aggregate properties

Property	Standard	Unit	Value
Bitumen content	LC 26-006	%	5.51
PCS _{5/10} @20 °C	ASTM D1557-12	%	7.85
Apparent density of the aggregate blend	LC 26-045	g/cm ³	2.486
Absorption	EN 1097-06	%	1
Maximum aggregate size	ASTM D 448-03	mm	20

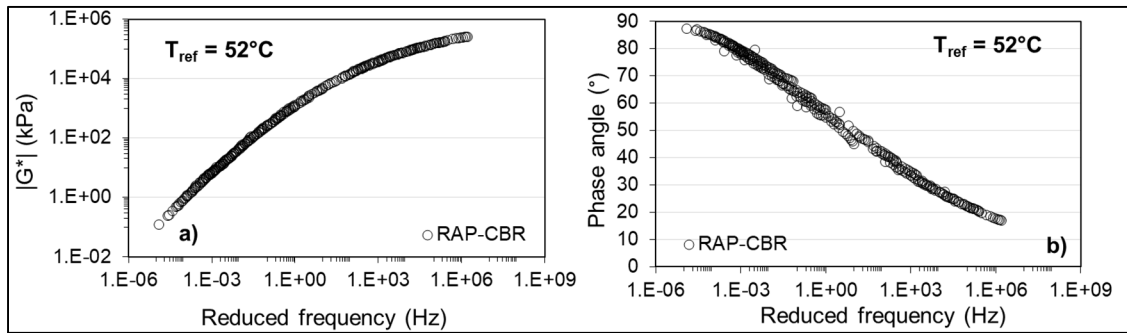


Figure-A I-4 Master curves of RAP binder: a) Complex modulus, b) phase angle

A-I.4 RAP-NCAT (USA)

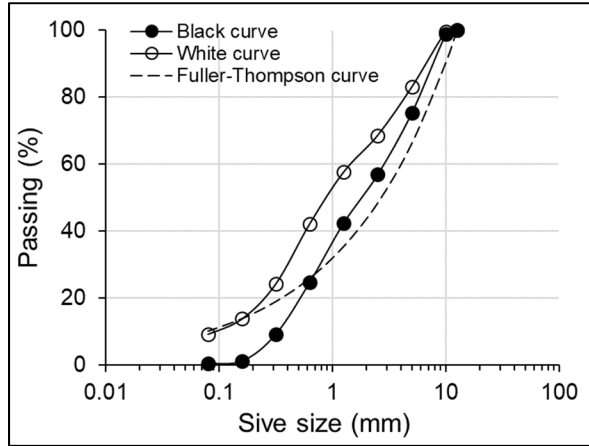


Figure-A I-5 Black curve, white curve and maximum density curve

Table-A I-5 RAP aggregate properties

Property	Standard	Unit	Value
Bitumen content	LC 26-006	%	5.49
PCS _{5/10} @20 °C	ASTM D1557-12	%	13.60
Apparent density of the aggregate blend	LC 26-045	g/cm ³	2.498
Absorption	EN 1097-06	%	1
Maximum aggregate size	ASTM D 448-03	mm	10

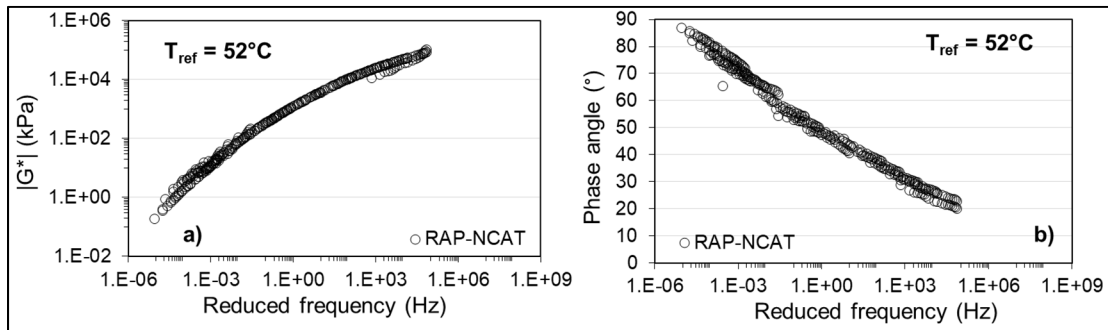


Figure-A I-6 Master curves of RAP binder: a) Complex modulus, b) phase angle

A-I.5 Limestone sand 0/2 (IT)

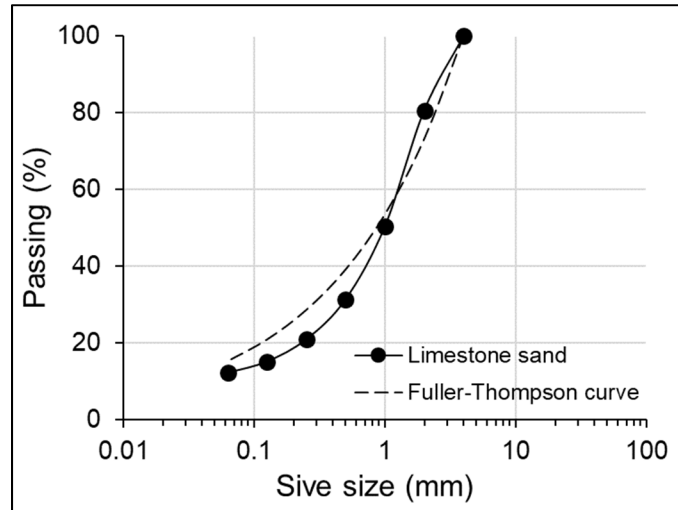


Figure-A I-7 Sand gradation and maximum density curve

Table-A I-6 Limestone sand properties

Property	Standard	Unit	Value
Absorption	EN 1097-06	%	1
Rigden voids	EN 1097-04	%	26.2

A-I.6 Fillers

Table-A I-7 Limestone fillers properties

Property	Standard	Unit	Limestone filler (CA)	Limestone filler (IT)
Particle density	EN 1097-06	g/cm ³	2.650	2.650
Rigden voids	EN 1097-04	%	50.1	23.8
Stiffening power	EN 13179-1	°C	11.5	N/A
Passing 80µm	EN 933-1	%	91.0	N/A

A-I.7 Cements

Table-A I-8 Cement properties

Property	Standard	Unit	Cement GU (CA)	Cement II/B-S (IT)
Density	ASTM C188	g/cm ³	3.150	3.090
Blaine fineness	ASTM C204	cm ² /g	4100	4090
Cumulative< 90 µm	ASTM C430	%	N/A	99.5
Cumulative< 45 µm	ASTM C430	%	95.5	N/A
Initial settling time	CSA A3004-B2	Min	180	180
Final settling time	CSA A3004-B2	Min	277	245
Compressive strength at 28 days	CSA A3004-C2	MPa	43.9	56

A-I.8 Bitumen emulsions

Table-A I-9 Bitumen emulsions properties

Property of bitumen emulsion	Standard	Unit	CSS-1 (CA)	CSS-1 (UK)	C60B10 (IT)
Storage stability at 24 hours	ASTM D6930	%	0.1	0.6	N/A
Viscosity saybolt furol at 25 °C	EN 13302	s	28.1	N/A	N/A
Viscosity saybolt furol at 40 °C	EN 13302	s	N/A	N/A	42.5
Residual bitumen content	ASTM D6997	%	62.8	60.3	60.0
Density	ASTM D6397	g/cm ³	N/A	1.0	N/A
Breaking index	EN 13075	%	N/A	N/A	2

Table-A I-10 Residual bitumen properties

Property of residual bitumen	Standard	Unit	CSS-1 (CA)	CSS-1 (UK)	C60B10 (IT)
Penetration @ 25 °C	ASTM D5	dmm	170	41	100
Softening point	ASTM D36	°C	N/A	48.6	43.0

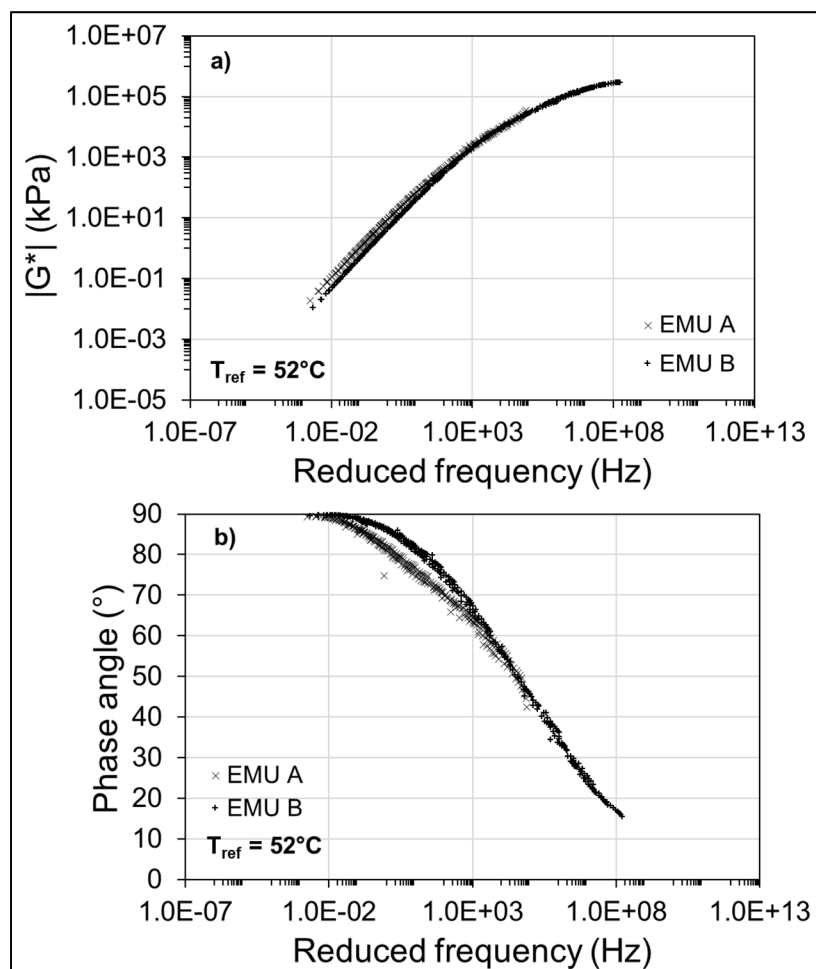


Figure-A I-8 Master curves of emulsion residual bitumen:
a) Complex modulus, b) phase angle

ANNEX II

GRAPHIC REPRESENTATION OF THE RESULTS FOR COMPLEX MODULUS TESTS TO EVALUATE THE EFFECT OF LOW PRODUCTION TEMPERATURES ON CBTM MECHANICAL PROPERTIES

CBTM MIXTURE MIXED AT 25 °C, TRANSPORTED AND COMPACTED AT 25 °C, CURED FOR THE FIRST 14 DAYS AT 25 °C AND KEPT SEALED FOR THE LONG TERM CURING (A_25_25_S)

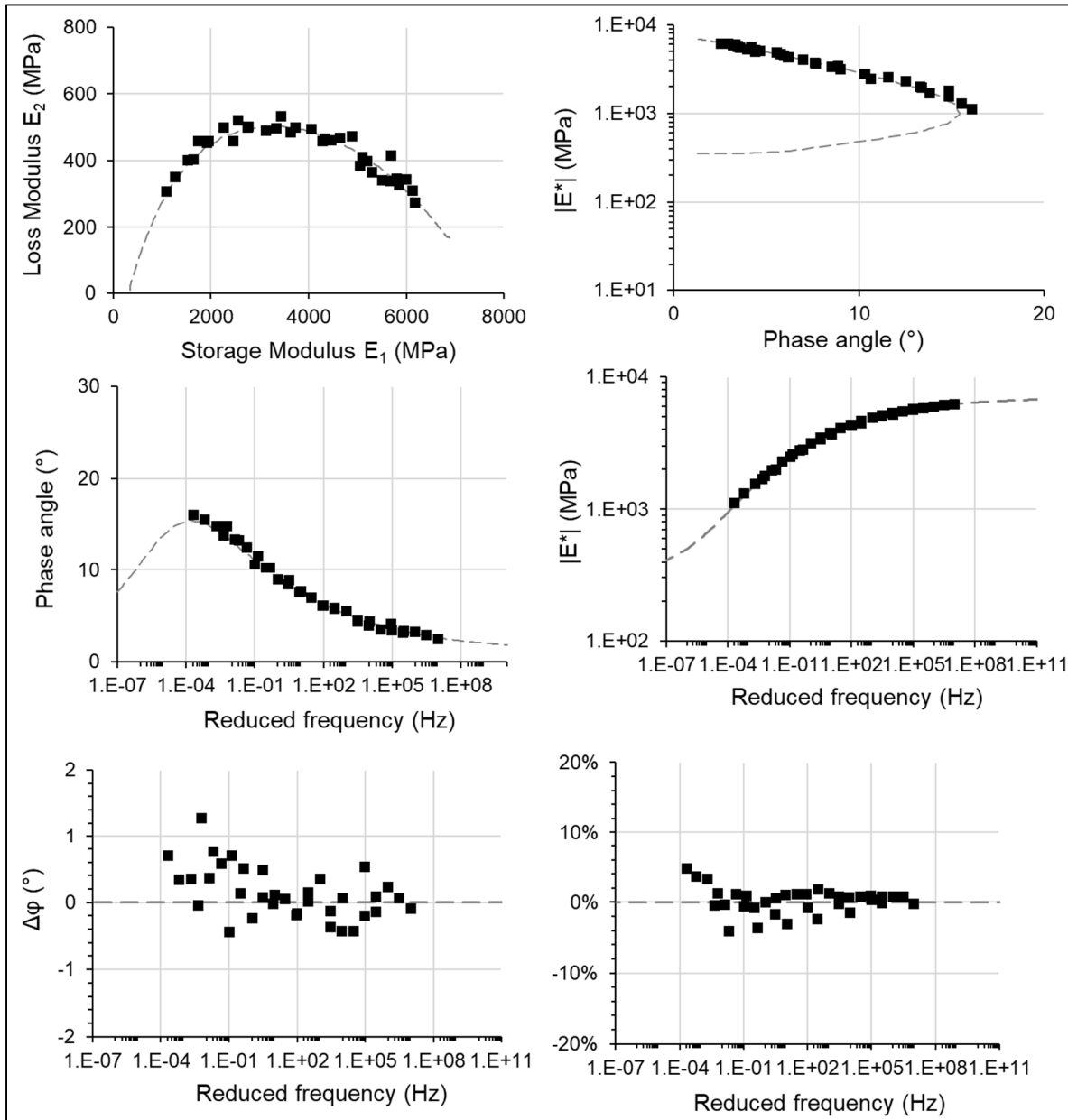


Figure-A II-1 Graphic representation of the complex modulus results for the mixture A_25_25_S ($T_0 = 20\text{ }^\circ\text{C}$)

CBTM MIXTURE MIXED AT 25 °C, TRANSPORTED AND COMPACTED AT 25 °C, CURED FOR THE FIRST 14 DAYS AT 25 °C AND KEPT UNSEALED FOR THE LONG TERM CURING (A_25_25_U)

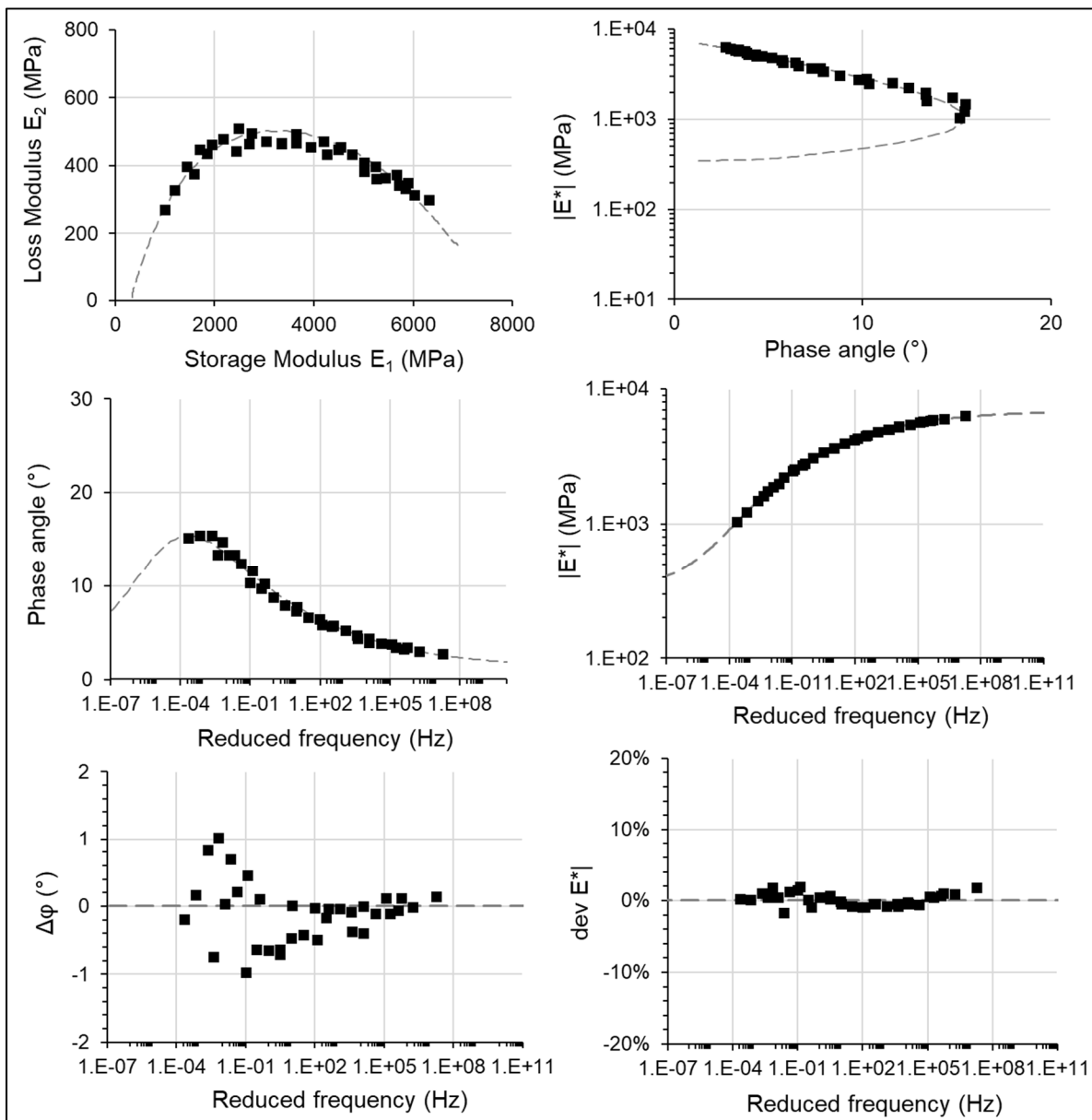


Figure-A II-2 Graphic representation of the complex modulus results for the mixture A_25_25_U ($T_0 = 20$ °C)

CBTM MIXTURE MIXED AT 5 °C, TRANSPORTED AND COMPACTED AT 5 °C, CURED FOR THE FIRST 14 DAYS AT 5 °C AND KEPT SEALED FOR THE LONG TERM CURING (A_5_5_S)

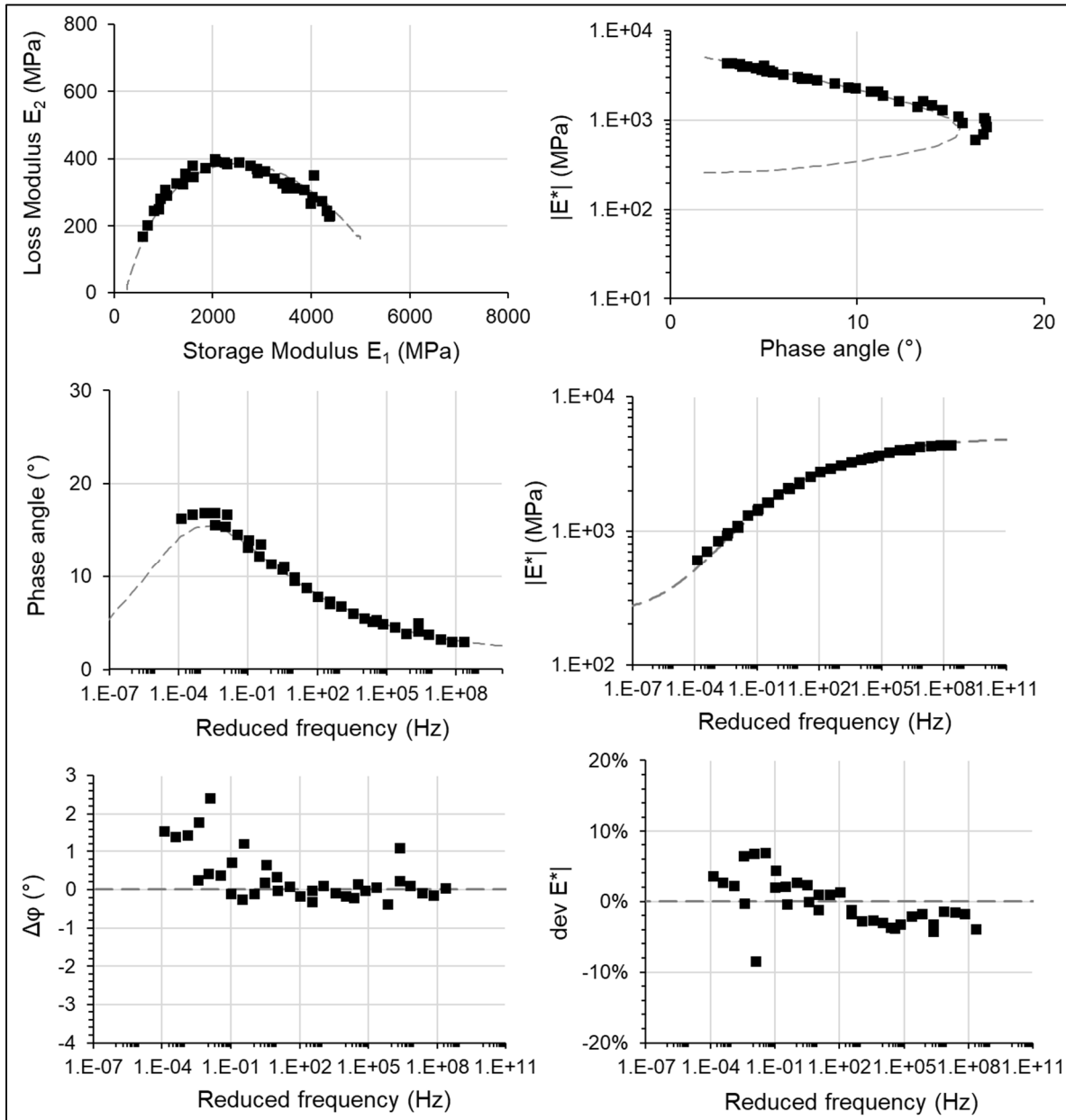


Figure-A II-I Graphic representation of the complex modulus results for the mixture A_5_5_S (T₀ = 20 °C)

**CBTM MIXTURE MIXED AT 5 °C, TRANSPORTED AND COMPACTED AT 5 °C,
CURED FOR THE FIRST 14 DAYS AT 5 °C AND KEPT UNSEALED FOR THE
LONG TERM CURING (A_5_5_U)**

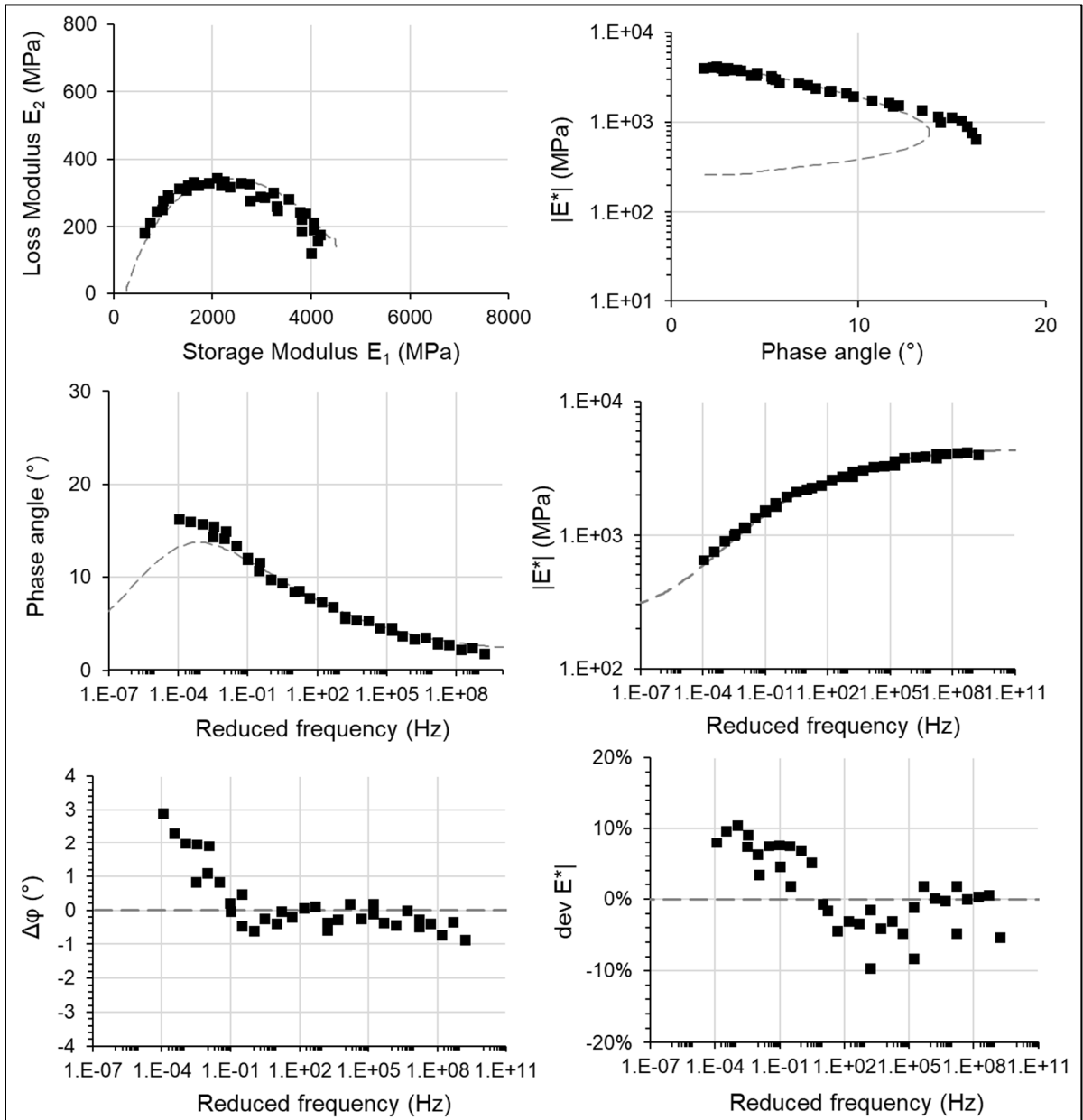


Figure-A II-4 Graphic representation of the complex modulus results for the mixture A_5_5_U ($T_0 = 20$ °C)

**CBTM MIXTURE MIXED AT 5 °C, TRANSPORTED AND COMPACTED AT 25 °C,
CURED FOR THE FIRST 14 DAYS AT 25 °C AND KEPT SEALED FOR THE
LONG TERM CURING (A_5_25_S)**

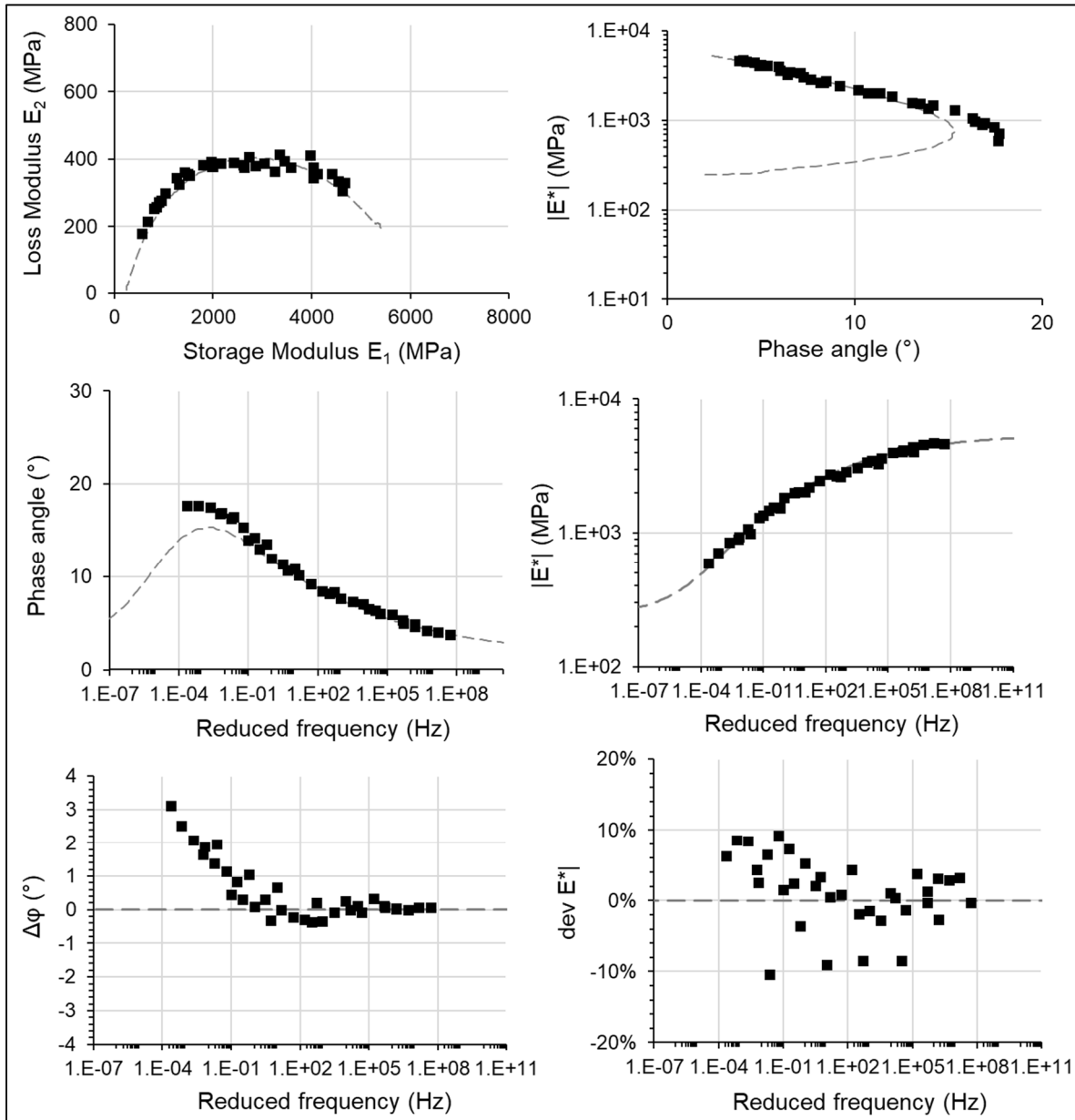


Figure-A II-5 Graphic representation of the complex modulus results for the mixture A_5_25_S ($T_0 = 20\text{ }^\circ\text{C}$)

**CBTM MIXTURE MIXED AT 5 °C, TRANSPORTED AND COMPACTED AT 25 °C,
CURED FOR THE FIRST 14 DAYS AT 25 °C AND KEPT UNSEALED FOR THE
LONG TERM CURING (A_5_25_U)**

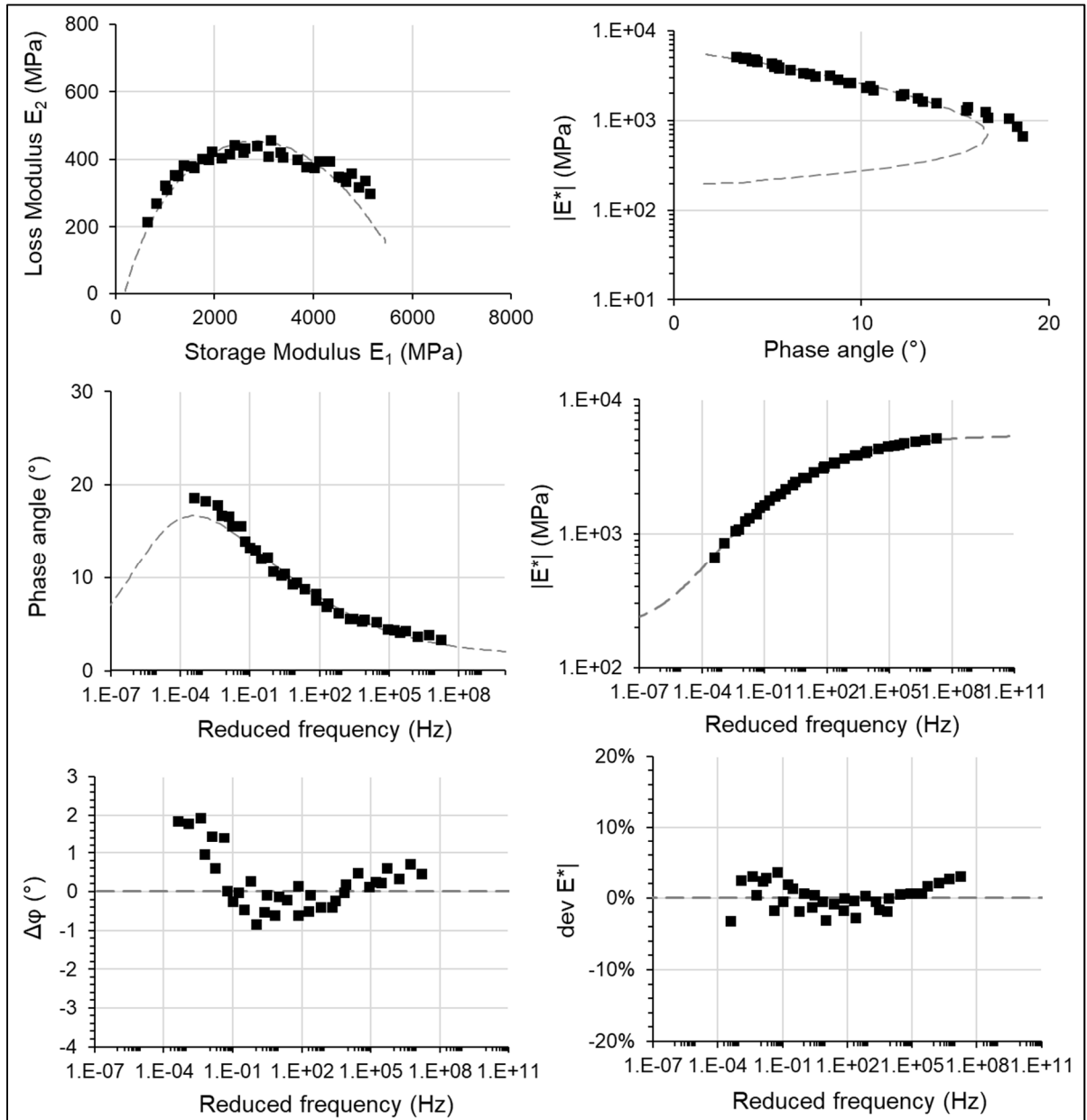


Figure-A II-6 Graphic representation of the complex modulus results for the mixture A_5_25_U ($T_0 = 20\text{ }^\circ\text{C}$)

**CBTM MIXTURE MIXED AT 25 °C, TRANSPORTED AND COMPACTED AT 5 °C,
CURED FOR THE FIRST 14 DAYS AT 5 °C AND KEPT SEALED FOR THE LONG
TERM CURING (A_25_5_S)**

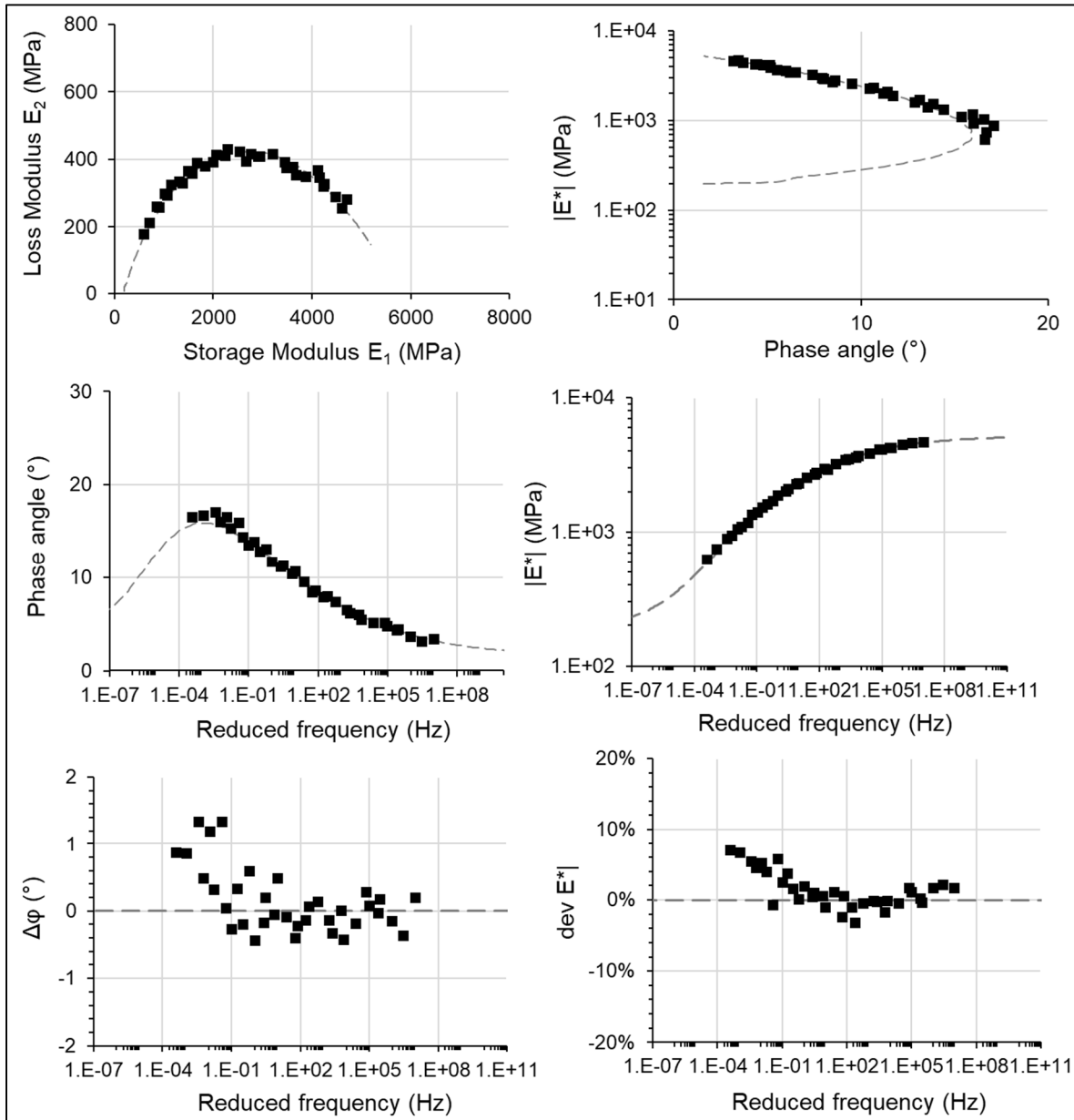


Figure-A II-7 Graphic representation of the complex modulus results for the mixture A_25_5_S ($T_0 = 20\text{ °C}$)

**CBTM MIXTURE MIXED AT 25 °C, TRANSPORTED AND COMPACTED AT 5 °C,
CURED FOR THE FIRST 14 DAYS AT 5 °C AND KEPT UNSEALED FOR THE
LONG TERM CURING (A_25_5_U)**

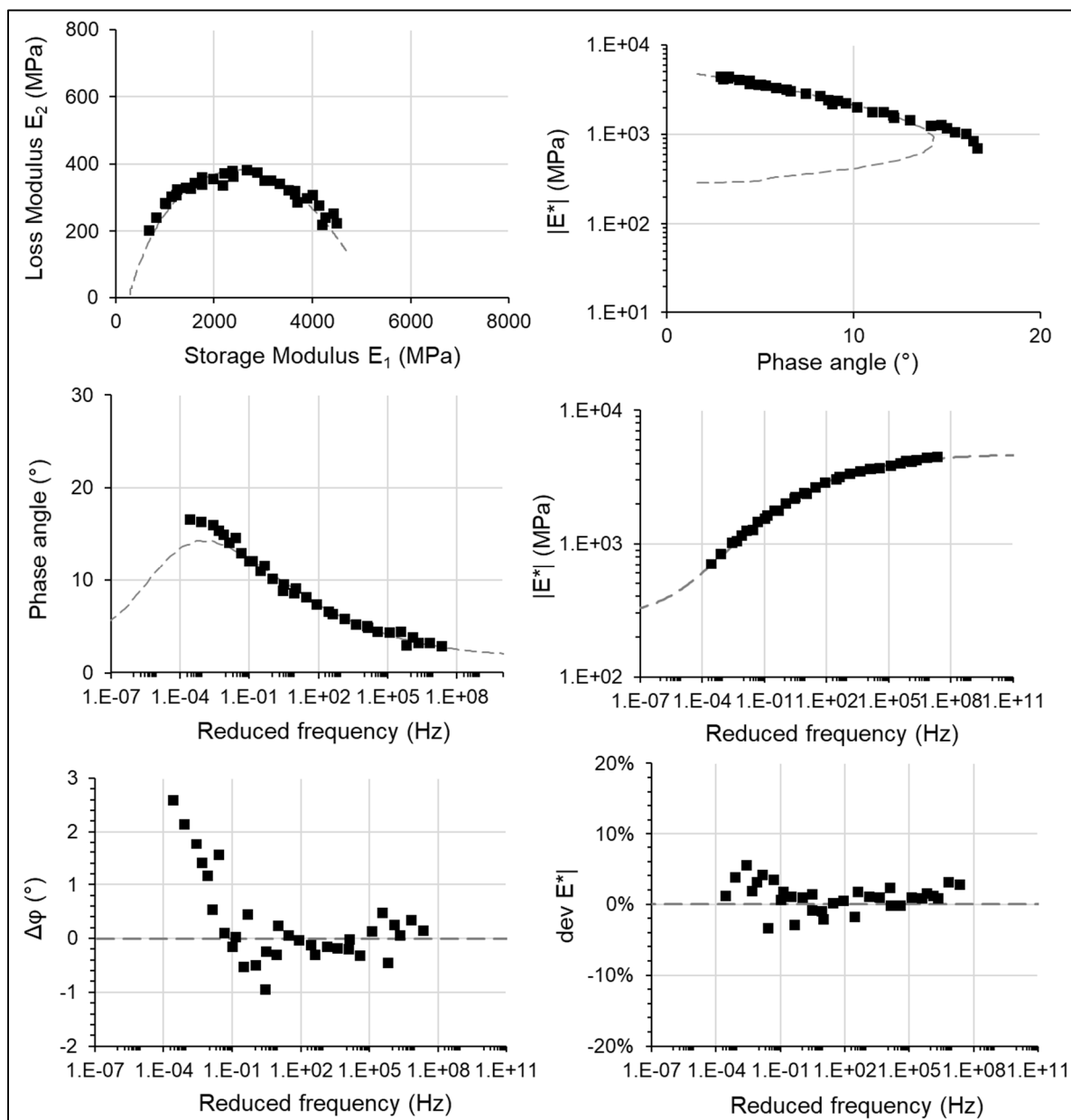


Figure-A II-8 Graphic representation of the complex modulus results for the mixture
A_25_5_U ($T_0 = 20$ °C)

CBTM MIXTURE WITHOUT CEMENT MIXED AT 5 °C, TRANSPORTED AND COMPACTED AT 5 °C, CURED FOR THE FIRST 14 DAYS AT 5 °C AND KEPT SEALED FOR THE LONG TERM CURING (A_5_5_0C_S)

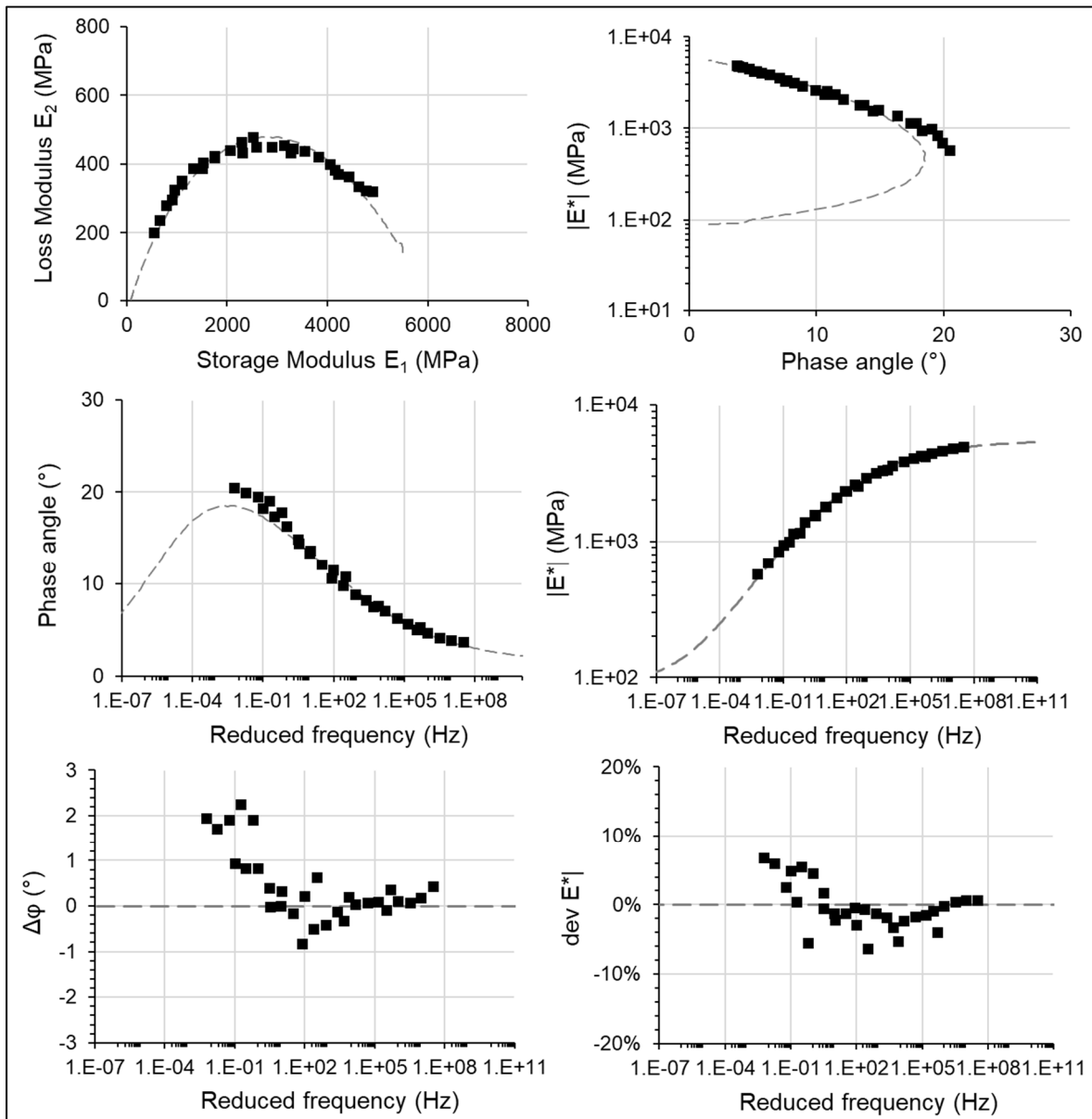


Figure-A II-9 Graphic representation of the complex modulus results for the mixture A_5_5_0C_S ($T_0 = 20\text{ }^\circ\text{C}$)

CBTM MIXTURE WITHOUT CEMENT MIXED AT 5 °C, TRANSPORTED AND COMPACTED AT 5 °C, CURED FOR THE FIRST 14 DAYS AT 5 °C AND KEPT UNSEALED FOR THE LONG TERM CURING (A_5_5_0C_U)

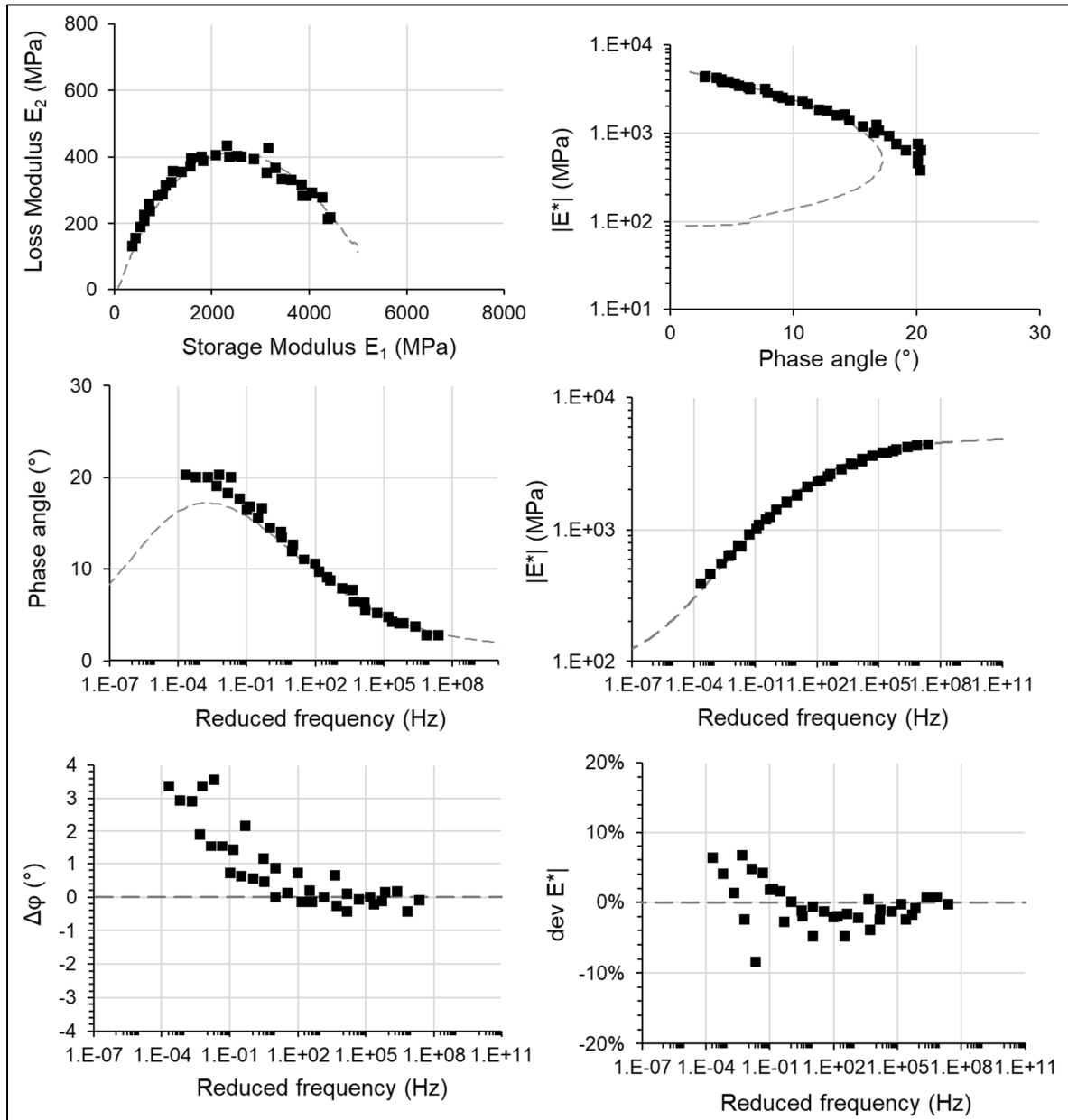


Figure-A II-10 Graphic representation of the complex modulus results for the mixture A_5_5_0C_U ($T_0 = 20\text{ }^\circ\text{C}$)

ANNEX III

REPEATABILITY STUDY ON THE LABORATORY PRODUCTION PROCESS OF CEMENT BITUMEN TREATED MATERIALS WITH FOAMED BITUMEN

Simone Raschia^a, Amir Rahmanbeiki^a, Daniel Perraton^a, Alan Carter^a, Andrea Graziani^b,
Andrea Grilli^c

^a Construction Engineering department, École de technologie supérieure (ÉTS) 1100, Notre-Dame Street West, Montreal, Canada

^b Department of Civil and Building Engineering, and Architecture, Università Politecnica delle Marche, Via Brecce Bianche, 60131 Ancona, Italy

^c Department of Economics, Science and Law, University of the Republic of San Marino, San Marino

Article accepted for presentation on July 2020 at the 9th International Conference on Maintenance and Rehabilitation of Pavements (MAIREPAV9), Zurich, Switzerland

A-III.1 Abstract

Cold recycled materials are mixes with high percentages of reclaimed asphalt (RA), while the binding phase is commonly composed of Portland cement and bitumen (emulsion or foam). The reproduction of such materials in the laboratory is an important issue for an accurate mix design, even more when applying a volumetric approach. Particularly, the lack of a specific control on the reliability of the foaming bitumen machine seems to hinder the potentiality of these mixtures. Hence, the goal of this study is to assess the composition variability of several batches produced in the laboratory starting from a specific cement-bitumen treated materials (CBTM) recipe and production procedure. An ignition oven was used to measure RA binder and the effective foamed bitumen amounts in produced specimens and a comparison between maximum dry density and theoretical maximum dry density was carried out.

The results have shown that the volumetric approach is a suitable tool to obtain the desired volumetric properties in CBTM produced with foamed bitumen. A certain variability between the theoretical maximum dry density and the measured value can be caused by the variability of bitumen content in the mixture.

A-III.2 Introduction

Cold recycling of bituminous pavements can be processed in-place or in-plant, and the reclaimed asphalt (RA), up to 100% of the granular mass, is usually treated with a bituminous binder in form of bituminous emulsion or foamed bitumen, and cement (Bowering, 1970; Jenkins, 2000a). Even if many successful sections using cement-bitumen treated materials (CBTM) have been built over the past 25 years (Bergeron, 2005; Kowalski & Starry, 2007), the use of cold recycling seems still limited to specific project and commonly not adopted as a design tool. The gaps among scientific knowledge and relationship between the laboratory procedures and field performances and the definition of a representative curing methodology are still open challenges (Cardone et al., 2014; Gandi, 2018).

A-III.3 Background and research objective

The intrinsic heterogeneity of the tested materials related to the sampling, preparation and testing methods cause a certain variability of the results. When using RA, the result variability is generally greater than when using virgin aggregates (Copeland, 2011; Zaumanis et al., 2018). Obviously, this discrepancy can be reduced when the RA storage and treatment processes are managed properly (Nady, 1997; West, 2009). For CBTM, there is limited information on the acceptable variability for the different characteristics and mix performance. For example, Carter et al. (2007) have shown a coefficient of variation (COV) of 11% on Marshall Stability measured on 106 specimens of the same field samples of cold recycled material. This is higher than the maximum 6% COV limit according to ASTM D6927-15 standard for asphalt mixtures. High variability has also been shown for laboratory measured rutting and fatigue resistance in the project “Characterization of Advanced Cold-Recycled Bitumen Stabilized Pavement

Solutions” (COREPASOL) project (Čížková et al., 2014) that was done specifically on cold recycled materials. According to the authors, the variability may be due to the variability of the RAP itself and also because of the different compaction method used. The variability in the maximum specific gravity was also evaluated in COREPASOL, and the highest standard variation measured was 0.288 (Batista et al., 2014) which is higher than the usual 0.016 limit used for asphalt mixtures for different laboratories according to ASTM D2041-19.

In most of the studies available in the literature, part of the variability measured can be linked to the different compaction methods, the variability of the RAP source and to the mix design methodology. Differently to hot mix asphalt (HMA), most CBTM mix design are not based on the volumetric properties. An accurate volumetric approach for CBTM in the fresh state can help in reducing the variability of the mix and results (Grilli et al., 2012). The aim of the study is to evaluate the composition variability of CBTM with foamed bitumen and cement following a volumetric mix design procedure.

A-III.4 Materials and methodology

A-III.4.1 Materials

Main properties of the RA aggregate employed in the CBTM produced are listed in Table-A III-1, whereas the characteristics of the bitumen used for foaming are collected in Table-A III-2. Foamed bitumen was produced by a laboratory unit at a temperature of 170 °C and a foaming water content of 1.9% by bitumen weight. The cement is a general use (GU) type (CSA A3000) with compressive strength at 28 days of 43.9 MPa (ASTM C109).

Table-A III-1 RA aggregate properties

Property	Standard	Unit	Value
Binder content	ASTM D6307	%	4.79
Nominal maximum particle dimension	ASTM D448-03	mm	16
Maximum specific gravity	ASTM C127-128	-	2.482

Table-A III-2 Basic properties of bitumen for foaming

Property	Standard	Unit	Value
Penetration	EN 1426	0.1 mm	64
Softening point	EN 1426	°C	52

A-III.4.2 Mixtures

Table-A III-3 shows the typical mix composition for a 30 000 g batch, containing 90% of RAP, 5.7% filler (virgin aggregate), 1.4% Portland cement and 2.9% of foamed bitumen. Six different 30 kg CBTM batches (Table-A III-4) were prepared in this study to limit the effect of the possible variability of the foam dosage.

Table-A III-3 CBTM mixes composition

	Components						
	RAP	Filler	Cement	Bitumen	Intergranular water	Absorbed water	Total
Mass (g)	M_{RAP}	M_{FILL}	M_{CEM}	M_{BIT}	M_{WI}	M_{WA}	
	26005.2	1659.9	415.0	830.0	830.0	260.1	30000.0
Density (g/cm ³)	2.486	2.650	3.015	1.015	1.000	1.000	
Volume (cm ³)	V_{RAP}	V_{FILL}	V_{CEM}	V_{BIT}	V_{WI}	V_{WA}	
	10486.0	626.4	137.4	817.7	830.0	260.1	482.4
Proportion (% by mass of mix)	86.7	5.5	1.4	2.8	2.8	0.9	100.0
Proportion (% by volume of mix)	79.7	4.8	1.0	6.2	6.3	2.0	100.0

In fact, the capacity of the pug mill is suitable for 30 kg batches and a reduced amount would probably mean a not uniform blending between the granular material and the foamed bitumen. Each batch produced was then compacted in laboratory with different techniques (Marshall hammer, Shear Gyratory Compaction (SGC) 100mm and 150mm, and Proctor rammer). After curing for 14 days at 40 ± 2 °C and RH of $55 \pm 5\%$ specimens were tested and the remaining material was crashed to conduct control tests on the mixtures, such as maximum dry density tests by pycnometer (G_{mm}) and bitumen content by ignition oven (3 repetitions of each test on each batch produced).

Table-A III-4 CBTM batches produced and experimental tests

Batch number	Compaction technique	Experimental tests
B1	Marshall	3 x G_{mm} (total of 18) 3 x Ignition oven (total of 18)
B2	SGC 100	
B3	SGC 150	
B4	SGC 150	
B7	Proctor 150	
B8	Proctor 150	

A-III.4.3 Methodology

A CBTM mixture was produced in the laboratory using fixed constituent materials and dosages. After checking the bitumen content by ignition testing, the theoretical maximum specific gravity was calculated and compared with the maximum specific gravity measured on laboratory samples.

Considering that replicate batches of a homogeneous mix have to show the same value of the maximum specific gravity, the variability of the mixes was assessed by monitoring the maximum specific gravity on the cured samples (after 14 days at 40 °C and 55% of RH) from each batch according to the ASTM D2041/D2041M – 19 standard.

The total bitumen content (bitumen in the RA and added foamed bitumen) was measured with the ignition oven. The theoretical maximum specific gravity can be calculated through Eq. (A III-1) and (A III-2). With Eq. (A III-1), the G_{mm} is calculated according to the total volume of the loose mix, with no voids, and with Eq. (A II-2) the G_{mm} only considers the solid particles, not the bitumen.

$$G_{mm} = \frac{M_{DRY}}{V_{DRY}} = \frac{M_{RAP} + M_{FILL} + M_{CEM} + M_{BIT}}{\frac{M_{RAP}}{\rho_{RAP}} + \frac{M_{FILL}}{\rho_{FILL}} + \frac{M_{CEM}}{\rho_{CEM}} + \frac{M_{BIT}}{\rho_{BIT}}} \quad (\text{A III-1})$$

Theoretical $G_{mm,s}$ (with respect to the solid phase: RAP, filler and cement)

$$G_{mm,s} = \frac{M_{SOLIDS}}{V_{SOLIDS}} = \frac{M_{RAP} + M_{FILL} + M_{CEM}}{\frac{M_{RAP}}{\rho_{RAP}} + \frac{M_{FILL}}{\rho_{FILL}} + \frac{M_{CEM}}{\rho_{CEM}}} \quad (\text{A III-2})$$

The theoretical percentage of foamed bitumen ($\%b^T$) content can be calculated with respect to the solids volume (RAP, filler and cement) by using both G_{mm} calculated from Eq. (A III-1) and (A III-2):

$$\%b^T = \frac{\rho_{BIT} \cdot (G_{mm,s} - G_{mm})}{G_{mm} \cdot (G_{mm,s} - \rho_{BIT})} \cdot 100 \quad (\text{A III-3})$$

The $\%b^T$ value obtained with Eq. (A III-3) represents the target value for mix design. Using equation (A III-3), it is possible to calculate the percentage of bitumen according to the measured G_{mm} ($\%b^{(1)}$) corresponding to each G_{mm} test, using the measured value of $G_{mm}^{(1)}$ instead of the theoretical one.

In addition to this, ignition oven test was also performed to assess the total bitumen content of the mixtures ($\%b^{(2)}$). From previous RAP characterization tests, the RAP binder is fixed at 4.79% by mass of the RAP aggregate (10 samples with standard deviation $s = 0.229$), which corresponds to 4.31% by dry mass (RAP, Filler, cement and foamed bitumen).

Using again Eq. (A III-3), it is possible to evaluate the values for $G_{mm}^{(2)}$ by calculation knowing the foamed bitumen by ignition test.

$$G_{mm}^{(2)} = \frac{G_{mm,s} \cdot \rho_{BIT}}{\rho_{BIT} \cdot (1 - \%b^{(2)}) + (G_{mm,s} \cdot \%b^{(2)})} \cdot 100 \quad (\text{A III-4})$$

A-III.5 Results and discussion

A-III.5.1 Laboratory tests

According to the considerations previously made, values related to Eq. (A III-1) and (A III-2) for this study are $G_{mm} = 2.396 \text{ kg/dm}^3$ and $G_{mm,s} = 2.496 \text{ kg/dm}^3$. As a consequence, by Eq. (A III-3), $\%b^T = 2.87\%$ by solids weight (RA, filler and cement). It is important to remark that these are theoretical (and target) values related to the mix design.

As already mentioned, G_{mm} values and the bitumen content by ignition oven were measured on eighteen samples. For both tests, average value \bar{X} , standard deviation s and confidence interval μ^\pm (Eq. (A III-5)) were calculated on a sample of 18 values, fixing a level of confidence $\alpha = 99.9\%$.

$$\mu^\pm = \bar{X} \pm t_{\frac{\alpha}{2}; n-1} \cdot \frac{s}{\sqrt{n}} \quad (\text{A III-5})$$

Figures A III-1 and A III-2 show the G_{mm} and bitumen content values in relationship with their confidence intervals, respectively.

The average value of bitumen content is 8.28% with a standard deviation of 0.783 while the average value of G_{mm} is 2.420 with a standard variation of 0.013. According to these results, the G_{mm} values are 67% reproducible (12 values on 18 are in the confidence interval). On the other hand, ignition oven tests were 83% reproducible (15 values on 18 are in the confidence interval).

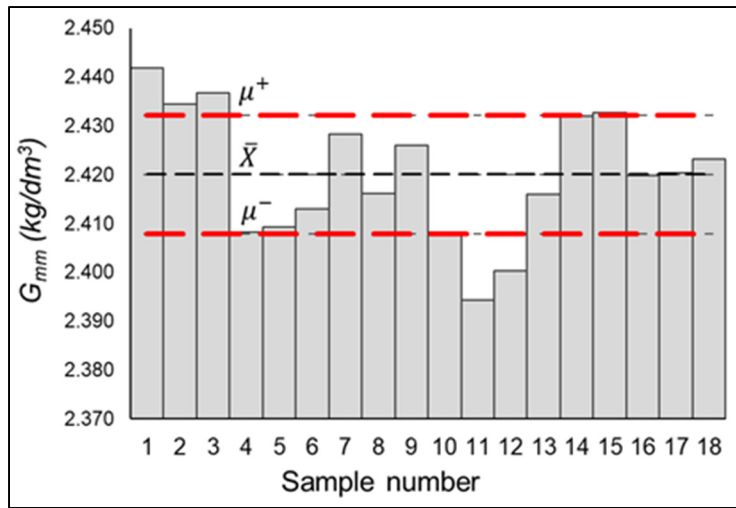


Figure-A III-1 Measured G_{mm} for all 18 specimens

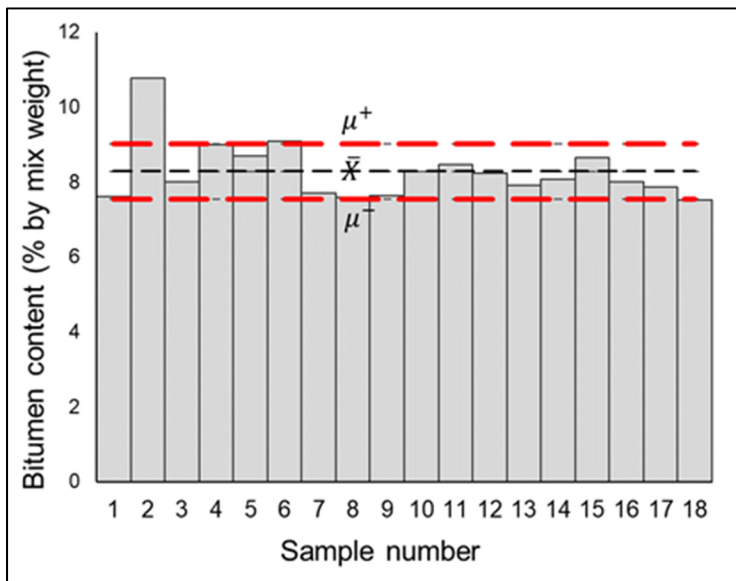


Figure-A III-2 Measured bitumen content in comparison with confidence interval

Moreover, the value $\%b^{(2)}$ is linearly related to $G_{mm}^{(2)}$, whereas the value $G_{mm}^{(1)}$ is linearly related to $\%b^{(1)}$, as shown in Figure-A III-3. It is important to remark that such calculations are valid

assuming that the solid phase composition (RAP, filler and cement), and then the $G_{mm,s}$, are consistent with the mix design.

From the results shown on Figure-A III-3, it can be observed that the ignition oven test overestimates the values of the added foamed bitumen in the mix, affecting in this manner the respective $G_{mm}^{(2)}$ values. This can be caused by an undesired material loss in the oven due to the high temperatures. According to Rodezno et al. (2017), using lower temperature with the ignition oven when RAP is present should reduce the variability.

At the same time, values obtained by the pycnometer test for the maximum specific gravity overestimate the $G_{mm}^{(1)}$, if compared to the theoretical value. Those higher values mean lower amount of foamed bitumen in the mix. This is, in some way realistic, because during the production and mixing of the foam mixture, it is clearly visible that not all the foamed bitumen is spread in the granular material. In fact, a significant amount tends to stick on the internal walls or the beaters of the pug mill. Moreover, a higher G_{mm} than the theoretical value (and a lower amount of foamed bitumen) can also be an indicator of bitumen absorption from the granular components. This would be unexpected in this case since the mix is made with RAP that should not absorb bitumen, and filler that also does not absorb bitumen.

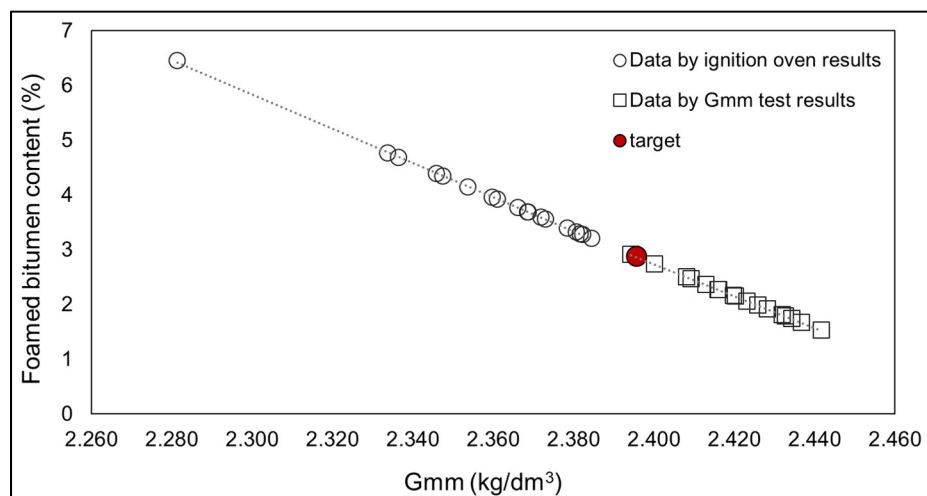


Figure-A III-3 Bitumen content according to G_{mm}

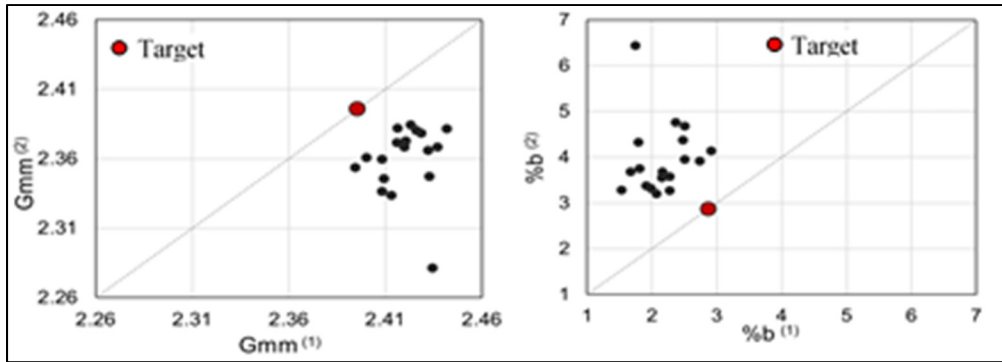


Figure-A III-4 Relationships between $G_{mm}^{(1)}$ and $G_{mm}^{(2)}$, and $\%b^{(1)}$ and $\%b^{(2)}$

The correspondence between $G_{mm}^{(1)}$ and $G_{mm}^{(2)}$, as well as between $\%b^{(1)}$ and $\%b^{(2)}$, can be observed in Figure-A III-4. Having found two different ranges of values for the G_{mm} , the evaluation of the air voids in the specimens should be carried out considering separately with $G_{mm}^{(1)}$ and $G_{mm}^{(2)}$. The density of the compacted specimens has been assessed by geometrical measurements and recording the weight at the end of curing (G_{sb}). For the volume measurements, three measures of diameter and three measures of the height of the specimens were used. The air voids are calculated using Eq. (A III-6).

$$\text{Air voids (\%)} = \frac{G_{mm} - G_{sb}}{G_{mm}} \cdot 100 \quad (\text{A III-6})$$

In the analysis, three different air voids content (Figure-A III-5) were calculated:

- $\%V_{th}$, which refers to the theoretical value of G_{mm} ;
- $\%V^{(1)}$, which refers to $G_{mm}^{(1)}$ (pycnometer test);
- $\%V^{(2)}$, which refers to $G_{mm}^{(2)}$ (calculated from ignition oven results).

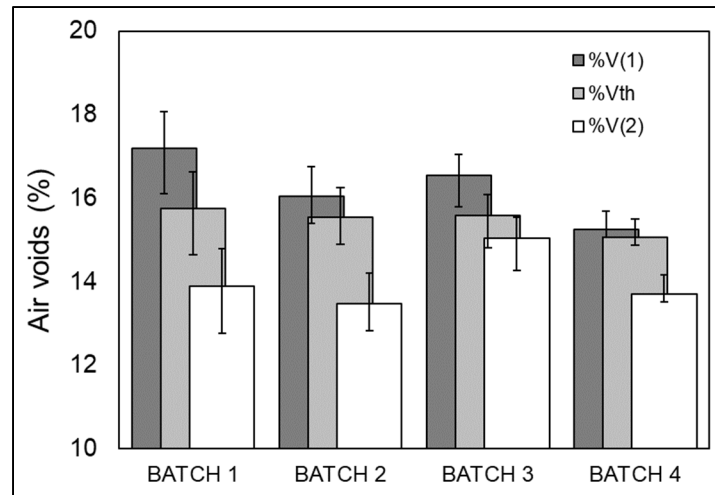


Figure-A III-5 The three different calculated air voids according to the different compaction methods

The air voids of the specimens made from the two batches compacted with the Proctor rammer were not measured because the height of the specimens were difficult to evaluate. The top surface of those specimens were uneven making an average height not representative. For all the compaction methods, the highest air voids is the one calculated according to the pycnometer test. It is interesting to note that even if the ranking of the different air voids remains the same for each compaction methods, the amplitude of the differences are quite different. Higher variability can be observed for batch 1, which are the specimens compacted with the Marshall hammer.

Figure-A III-6 shows that the air voids measured decrease with the decrease of the G_{mm} and the increase in the foamed bitumen content. The values related to the theoretical value of G_{mm} are placed in between the two calculations made using the pycnometer test and the ignition oven test.

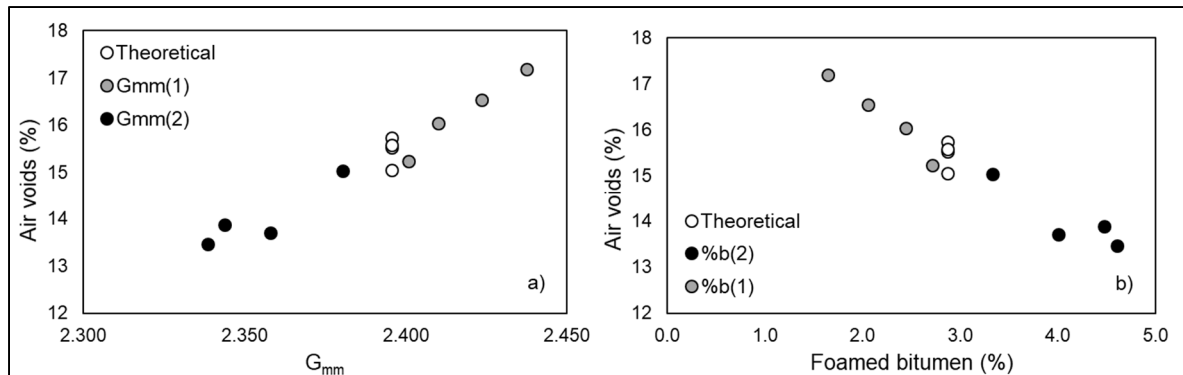


Figure-A III-6 Air voids vs G_{mm} and foamed bitumen content

A-III.4 Conclusion

In this study, the variability of a CBTM mix made with foamed bitumen was tested. The variability in the components was evaluated based on the maximum specific gravity, G_{mm} , and the bitumen content. The theoretical values based on volumetric calculations and the laboratory measured values were compared. The main conclusions are:

- The amount of bitumen measured with the ignition oven and the one calculated from the G_{mm} are different. The bitumen content from the ignition oven is higher than the target value. This is probably due to the loss of fine particles during the ignition test;
- The measure G_{mm} is higher than the theoretical value. This is normally explained by lower bitumen content which is not the case here according to the ignition oven results. However, as mentioned previously, we believe that the ignition results are too high.
- The volumetric approach can't be validated by the two chosen test, but it can be used as a tool to estimate real foam bitumen content.

The next step in this study is to test a greater number of specimens to have a better understanding of the variability. Different mix design should also be tested. The same exercise should also be carried out with mixes made with bituminous emulsion.

ANNEX IV

EXPERIMENTAL INVESTIGATION ON WATER LOSS AND STIFFNESS OF CBTM USING DIFFERENT RA SOURCES

Andrea Grilli^a, Simone Raschia^b, Daniel Perraton^b, Alan Carter^b, Amir Rahmanbeiki^b,
Patricia Kara De Maeijer^c, Davide Lo Presti^{d,e}, Gordon Airey^e, Chibuike Ogbo^f, Eshan V.
Dave^f and Gabriele Tebaldi^g

- ^a Department of Economics, Science and Law, University of the Republic of San Marino,
San Marino
- ^b Construction Engineering department, École de technologie supérieure (ÉTS) 1100, Notre-
Dame Street West, Montreal, Canada
- ^c Road Engineering Research Section, EMIB, Faculty of Applied Engineering, University of
Antwerp, Groenenborgerlaan 171, 2020, Antwerp, Belgium
- ^d Department of Engineering, University of Palermo, Viale Delle Scienze, 90128, Palermo,
Italy
- ^e Nottingham Transportation Engineering Centre, University of Nottingham, NG7 2RD,
Nottingham, UK
- ^f Department of Civil and Environmental Engineering, University of New Hampshire
33 Academic Way, Durham, NH 03824, United States
- ^g Department of Engineering and Architecture, University of Parma, Parco Area delle
Scienze 181/a, 43124, Parma, Italy

Article accepted for presentation on June 2020 at the RILEM International Symposium on
Bituminous Materials (ISBM), Lyon, France

A-IV.1 Abstract

Cold recycling of reclaimed asphalt (RA) is a promising technique to build or to maintain roads, combining performance and environmental advantages. Although this technique has been extensively used worldwide, there is no unique and internationally-shared method to characterize cold recycled mixtures. The previous work of the RILEM TC 237-SIB TG6 successfully attempted to characterize different RA sources with both traditional parameters (gradation, bitumen content and geometrical properties) and non-conventional properties

(fragmentation and strength testing). The current RILEM TC 264-RAP TG1 mainly focuses on the influence of different RA sources on physical and mechanical characteristics of cement-bitumen treated materials (CBTM) using foam or emulsified bitumen, taking into consideration compaction and curing methods. This paper presents results from the first step of the inter-laboratory project in which foamed bitumen and cement were used as binders. The influence of two RA sources, one from Alabama (USA) and one from San Marino, were investigated through the collaboration of several laboratories. Specimens were manufactured with the same diameter by means of both Marshall and gyratory compactors and then cured following two procedures: free surface drying (FSD) and partially-surface drying (PSD). A preliminary study allowed obtaining specimens with similar volumetric properties. Along with compactability and water loss, the indirect tensile stiffness modulus was measured and analyzed. The results have shown that the RA source and curing procedure influence the CBTM mechanical properties.

A-IV.2 Introduction

Cement-bitumen treated materials (CBTM) are produced with a significant amount of reclaimed asphalt (RA), bitumen emulsion or foamed bitumen, cement and water. CBTM is a hybrid material which inherits properties from both asphalt concrete (AC), since the bituminous component plays a significant role, and cement-treated materials (CTM), since the cement influences stiffness and curing of the mixture (Cardone et al., 2014; Grilli et al., 2012).

The RILEM TC 237-SIB TG6 on cold recycling worked in 2012-2018 on the characterization of reclaimed asphalt to be used for cold recycling (Tebaldi et al., 2019). This characterization differs from the commonly used RA characterization when used in hot recycling where the aged bitumen softens, and the aggregate gradation combines with the virgin materials that usually are the dominant component. In cold recycling, the RA behaves as it is and for instance black gradation, fragmentation resistance and geo-metric properties of particles have a significant influence on the performance of the final product. At the end of the TG6 mandate, the RILEM TC 264-RAP launched a new TG, so-called TG1, on cold recycling with the

purposes of sharing mix design and curing procedures that can better support the selection of the optimum mixture in relationship with RA characteristics and product performance. A new inter-laboratory testing program has been proposed to the TG1 members to evaluate the influence of different RA sources, appropriately selected and characterized, on strength and stiffness of cold recycled mixtures. The objectives of this paper were to assess both the influence of the RA source and curing conditions on properties of CBTM, such as water loss and stiffness.

A-IV.3 Materials

Two RA sources, one from the Republic of San Marino so-called RA1 and another one from NCAT-USA so-called RA2, were preliminary characterized by means of the fragmentation test which measures the amount of produced fines (passing material to 1.7 mm sieve size) after modified Proctor compaction (Perraton, Tebaldi, et al., 2016). The RA1 and RA2 properties are reported in Table-A IV-1. The two RA sources mainly differ each other by fragmentation resistance, gradation and maximum size. A mineral filler characterized by 91% of passing material at 0.080 mm sieve size, 50.1% voids of dry compacted filler measured by means of a Rigden apparatus (EN 1097-4) and a stiffening power $\Delta R\&B$ of 11.5 °C (EN 13179-1) was selected to adjust both RA gradations following the respective maximum density curves. A GU type cement (CSA A3000) with compressive strength at 28 days of 43.9 MPa (ASTM C109) and Blaine surface area of 410 cm²/g was chosen to improve the bituminous mastic consistency and short-term resistance. The bitumen has a penetration value of 64 mm · 10⁻¹ (EN 1426) and a softening point of 52 °C (EN 1427). A preliminary study established 1.9% of water by bitumen weight to achieve at 170 °C an expansion ratio of 10 and half-life of 6 s considered suitable for foam applications.

The two CBTM mixtures consisted of 4.0% of added water, 3.0% of bitumen, 1.5% of cement, 5.5% and 10.0% of filler and 93.0% and 88.5% of RA, for RA1 and RA2 respectively. Dosages refer to the total solid weight (RA, filler and cement). The dosages of water and bitumen were chosen according to common values typically used for cold recycled materials (Grilli et al.,

2016). Mixtures were coded as CBTM16RA1 and CBTM10RA2 using RA1 and RA2 respectively. CBTM16RA1 and CBTM10RA2 gradation follow the Fuller distribution with $D_{max} = 16$ mm and $D_{max} = 10$ mm, respectively.

Table-A IV-1 Properties of RA1 and RA2

Property	Standard	Unit	RA1	RA2
Bitumen content	ASTM D6307	%	5.51	5.49
Nominal maximum particle size	ASTM D448-03	mm	16	10
Maximum specific gravity	ASTM C127-128	-	2.482	2.498
Water absorption	ASTM C127-128	%	1.10	1.08
Fragmentation @ 5 °C	ASTM D1557	%	7.6	-
Fragmentation @ 20 °C	ASTM D1557	%	6.7	13.9
Flakiness index	EN 933-3	%	5	-
Shape index	EN 933-4	%	3	-

A-IV.4 Testing methods and procedure

According to a preliminary study, the two mixtures were compacted to get a representative air void content of $14.3\% \pm 1\%$ using both Marshall and Shear Gyratory Compactor (SGC). The compaction with Marshall was performed employing around 1100 g of mixture placed in the mould and compacted with 50 blows on each side. The same amount of material was used for specimens compacted with the SGC. In this case, the compaction was carried out at fixed specimen height, 67.7 mm, which was reached with an average of 40 gyrations for mixtures. Compacted specimens were demoulded and divided into two subseries following two protocols: free surface drying (FSD) and partially sealed drying (PSD). FSD required specimens to be cured in the air so they can dry from all sides, whereas PSD required to seal the cylinder sides of the specimen by a plastic film to allow drying only from the specimen top surface.

Specimens were cured in a climatic chamber for 14 days at 40 ± 2 °C and $55 \pm 5\%$ of relative humidity and weighted every day to monitor the water loss over time. Both mixtures were characterized in terms of the indirect tensile stiffness modulus (ITSM) test at 2, 10 and 20 °C (EN 12697-26). ITSM was measured after 3 hours conditioning at the testing temperature. At least 3 test repetitions for each series were performed.

A-IV.5 Results

A-IV.5.1 Water loss

Figure-A IV-1 shows the average values of water loss as a function of curing days at 40 °C for both CBTM16RA1 and CBTM10RA2. The results shown are related only to Lab.1 and each curve is an average of 10 specimens.

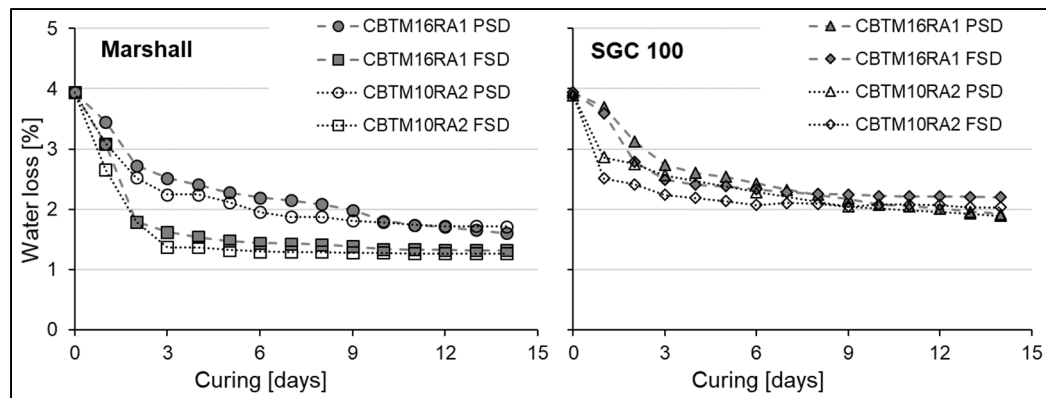


Figure-A IV-1 Experimental data of water loss for the studied mixtures

Water loss evolution appears to follow a bilinear trend changing rate significantly after 3-day curing period. As can be noticed in Figure-A IV-1, the general trend does not seem influenced by the compaction method and mix type, whereas the curing method influenced the water loss evolution, considerably. PSD method showed a lower water loss than FDS method. At the same time, Marshall compacted specimens showed higher water loss than SGC compacted specimens, probably caused by the different intergranular voids dispersion and size.

The experimental data were analyzed by a bilinear regression considering the inter-section point at a 3-day curing time and Table-A IV-2 shows the regression factors (s = slope; k = intercept value and R^2 = regression coefficient) for all series. FSD implied a fast decrease of water content until 3 days (phase 1) then a rather flat evolution (phase 2). This evolution was less remarkable for PSD series. FSD showed a higher rate difference between phase 1 and phase 2 than PSD. By extending the regression equation, PSD required more than 10 additional days to reach the FSD final water content.

Table-A IV-2 Properties of RA1 and RA2

Series	Regression factors 0-3d (Phase 1)			Regression factors 3-14d (Phase 2)			Phase1 vs Phase2	PSD vs FSD
	s_1	k_1	R^2	s_2	k_2	R^2	s_2/s_1 (%)	Δ days
CBTM16RA1 Marshall FSD	-0.823	3.845	0.934	-0.025	1.629	0.858	3.094	-
CBTM10RA2 Marshall FSD	-0.856	3.724	0.952	-0.010	1.381	0.779	1.116	-
CBTM16RA1 Marshall PSD	-0.499	3.909	0.962	-0.085	2.731	0.977	16.988	16
CBTM10RA2 Marshall PSD	-0.563	3.798	0.951	-0.051	2.341	0.871	9.027	21
CBTM16RA1 SGC 100 FSD	-0.516	3.977	0.956	-0.024	2.494	0.854	4.695	-
CBTM10RA2 SGC 100 FSD	-0.507	3.525	0.739	-0.016	2.222	0.692	3.119	-
CBTM16RA1 SGC 100 PSD	-0.417	4.001	0.973	-0.074	2.885	0.967	17.720	9
CBTM10RA2 SGC 100 PSD	-0.406	3.635	0.786	-0.058	2.684	0.944	14.264	11

A-IV.5.2 ITSM

Figure-A IV-2 depicts the ITSM values at 2, 10 and 20 °C for all series. It can be affirmed that PSD allows higher ITSM values than FSD. Moreover, CBTM10RA2 seems stiffer than CBTM16RA1 as well as SGC specimens seems to have higher stiffness than Marshall specimens. Slow water evaporation and a higher water content allows more effective cement hydration to be achieved with direct effect on stiffness values. However, the results from

different laboratories showed a notable scattering of values. Probably 3 repetitions for each series are not enough and the reproducibility of the testing method has to be improved.

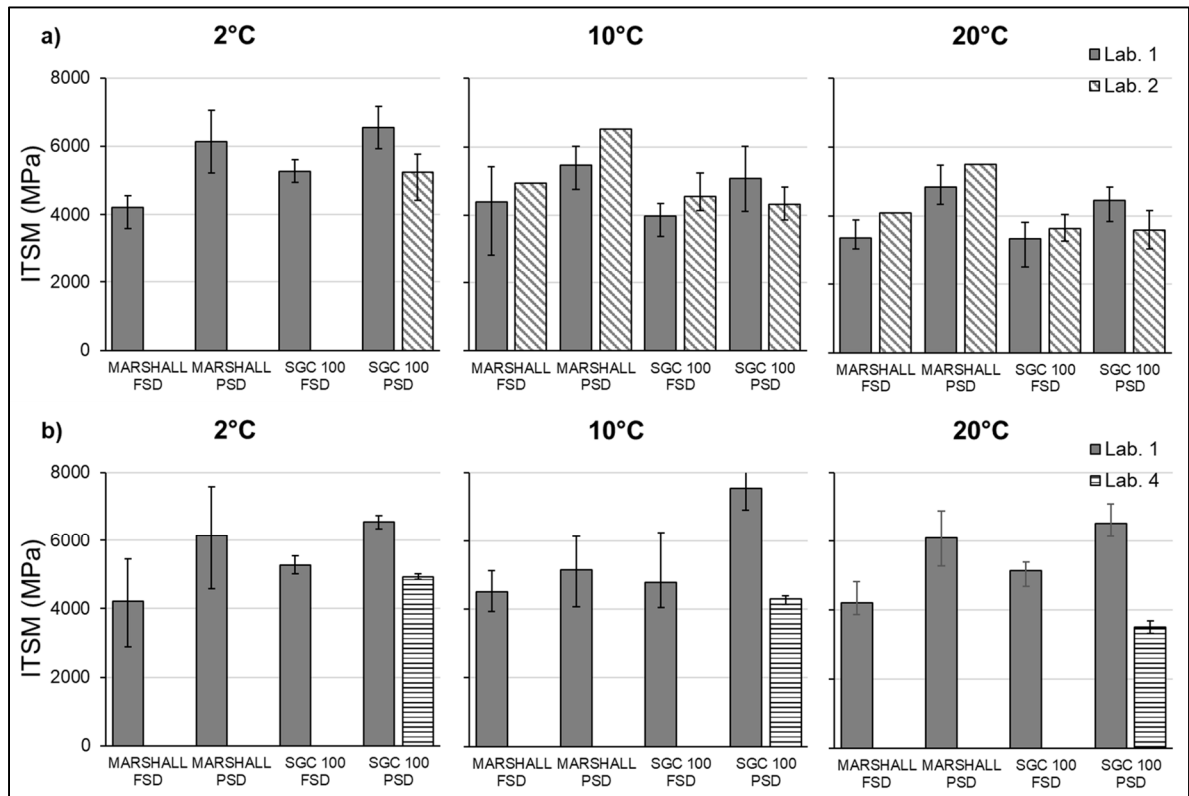


Figure-A IV-2 ITSM results for: a) CBTM16RA1, b) CBTM10RA2

A-IV.6 Conclusions

This paper shows the results from the first phase of the RILEM 264-RAP TG1 inter-laboratory project focused on cold recycling. Particularly, the influence of two RA sources in two mixtures using foamed bitumen and cement as binders were investigated. The results showed that even if RA2 has fragmentation value poorer than RA1, the correction of the gradation curve through mineral filler following the respective maximum density gradation (Fuller distribution) allows CBTM10RA2 to behave similarly to CBTM16RA1. Water loss evolution followed a bilinear trend changing rate after a 3-day curing period, significantly. FSD induced

a fast decrease of water content until 3 days (phase 1) then a rather flat evolution (phase 2) with the highest rate difference between phase 1 and phase 2. PSD prevented water evaporation and potentially required more than 10 additional days to reach the FSD final water content. The higher water content probably allows a more effective cement hydration in PSD entailing higher ITSM values than FSD. Moreover, SGC specimens seems to show higher stiffness values than Marshall specimens. However, the results from different laboratories showed a remarkable scattering of values and reproducibility of the testing method has to be improved.

ANNEX V

INFLUENCE OF CURING ON THE MECHANICAL PROPERTIES OF CEMENT-BITUMEN TREATED MATERIALS USING FOAMED BITUMEN: AN INTERLABORATORY TEST PROGRAM

Marco Pasetto^a, Emilano Pasquini^a, Andrea Baliello^a, Simone Raschia^b, Amir Rahmanbeiki^b, Alan Carter^b, Daniel Perraton^b, Francesco Preti^c, Beatriz Chagas Silva Gouveia^c, Gabriele Tebaldi^c, Andrea Grilli^d, Eshan V. Dave^e

^a Department of Civil, Environmental and Architectural Engineering, University of Padova, Via Marzolo 9, 35131, Padova, Italy

^b Construction Engineering department, École de technologie supérieure (ÉTS) 1100, Notre-Dame Street West, Montreal, Canada

^c Department of Engineering and Architecture, University of Parma, Parco Area delle Scienze 181/a, 43124, Parma, Italy

^d Department of Economics, Science and Law, University of the Republic of San Marino, San Marino

^e Department of Civil and Environmental Engineering, University of New Hampshire 33 Academic Way, Durham, NH 03824, United States

Article accepted for presentation on July 2020 at the 9th International Conference on Maintenance and Rehabilitation of Pavements (MAIREPAV9), Zurich, Switzerland

A-V.1 Abstract

The use of reclaimed asphalt (RA) in road pavements is continuously gaining interest thanks to the technical, economic and environmental advantages guaranteed by such sustainable practice. Cold recycling techniques compared to traditional asphalt mixes allows a significant reduction of energy, fume emissions, use of natural resources, etc. In this perspective, the Task Group 1 on “Cold Recycling” of the RILEM Technical Committee on “Asphalt Pavement Recycling” (TC 264-RAP) launched an interlaboratory test program (ITP) aimed at ensuring a better understanding for cold recycled mixtures. The paper presents the results collected by a restricted group of the participating laboratories testing cement-bitumen treated materials that

included a single RA source and prepared with foamed bitumen. Gyrotory compacted specimens were used to evaluate the influence of curing (free, partial or restricted-surface drying for 14 days at 40 °C at a relative humidity of 55±5%). Stiffness was evaluated as a function of the curing stage and the corresponding water loss; strength was tested after 14 days of curing testing specimens in both dry and wet conditions to also determine the water sensitivity. As expected, the different curing conditions clearly influenced the rate of water loss of tested samples with clear effects on mechanical properties and durability.

A-V.2 Introduction

The growing consciousness on the environmental sustainability is promoting the re-use of reclaimed asphalt (RA) in road pavements to avoid disposal and preserve natural raw materials. In this regard, cold recycling in road pavements is continuously gaining interest thanks to the technical, economic and environmental advantages that could be guaranteed (Grilli et al., 2018). Cold recycling of RA is usually performed in cement-bitumen treated materials (CBTMs) produced at ambient temperature; this construction technology allows a sensible reduction of energy consumptions and emissions with respect to traditional hot mix asphalt. Successful CBTMs applications have been worldwide demonstrated, particularly in the case of base and subbase layers (Cardone et al., 2014; Hugener et al., 2014). The presence of cement and water determines an evolutive behavior of CBTMs strictly related to the curing processes which in turn are clearly affected by the adopted construction procedures (Graziani et al., 2016). Significant efforts have also been made by research-ers to properly characterize the mechanical properties of RA aggregates to be used in cold recycled mixes (Tebaldi et al., 2019). Given this background, Task Group 1 (TG1) on “Cold Recycling” of the RILEM Technical Committee TC 264-RAP on “Asphalt Pavement Recycling” launched an interlaboratory test program (ITP) investigating, among others, the effect of the curing conditions on the evolutive behavior as well as on the final properties of CBTMs prepared with different RAs and bituminous binders (foamed bitumen or bituminous emulsions). A total of 12 laboratories from 10 countries are actively involved in the TG1 activities.

A-V.3 Background and research objective

One of the crucial aspects related to the CBTM pavement layers is related to the construction procedures and, in particular, to the operations planned after the laying and compaction of such layers. The environmental site conditions, the possible different treatments of the upper surface as well as the scheduled time of the construction phases strongly affect the evolution of the moisture content within the mixtures with clear effects on the effective properties of CBTMs thus influencing the final behavior of the whole pavement. In this regard, the present paper illustrates a part of the above-mentioned ITP carried out in the framework of the activities of RILEM TG1 TC 264-RAP and specifically aimed at investigating the influence of curing conditions on the performance of CBTMs. CBTMs were produced using the same physical raw materials: single source of RA (RA1) and foamed bitumen (FB). The experimental results were collected by a restricted group of the TG1 participants, i.e. the University of Padova (Italy), the École de Technologie Supérieure (Canada) and the University of Parma (Italy), using a specific sample size compacted with the same technology: 150 mm cylinder from Shear Gyratory Compactor (SGC).

A-V.4 Experimental approach

A-V.4.1 Materials and mixtures

TG1 provides the same constituent raw materials (RA, filler, cement and bitumen for foaming) to all the involved laboratories along with a specific mix design to be followed. Based on the volumetric approach described in Grilli et al. (2012), the total solid part of the studied CBTMs was composed of RA, filler and cement. For this research, a RA1 with maximum aggregate size of 16 mm was used. The RA1 was characterized by a target gradation whose envelope is reported in Table-A V-1. In the final aggregate composition, the RA1 was integrated with filler (particle size < 0.063 mm) dosed at 5.5% of the total solid weight. A cement GU type (CSA A3000) with compressive strength at 28 days of 43.9 MPa dosed at 1.5% of the total solid weight was selected as co-binder. A bitumen for foaming was used at 3.0% by the total solid

weight. Such a 2:1 bitumen to cement ratio avoided excessive brittleness of the mixture (Grilli et al., 2012). Figure-A V-1 shows linear viscoelastic properties in terms of master curves of complex modulus G^* and phase angle δ of the base binder. The basic binder characteristics provided by the producer are shown in Table-A V-2. Mix design also required 3.0% added water by the total solid weight. The overall mix design is summarized in Table-A V-3.

Table-A V-1 RA1 target gradation envelope

Size [mm]	20	16	8	4	2	1	0.5	0.25	0.125	0.063
Min. passing [%]	96	93	73	49	31	17	9.5	7.5	5	3
Max. passing [%]	100	100	79	53.5	37	25	17.5	10	5.5	4

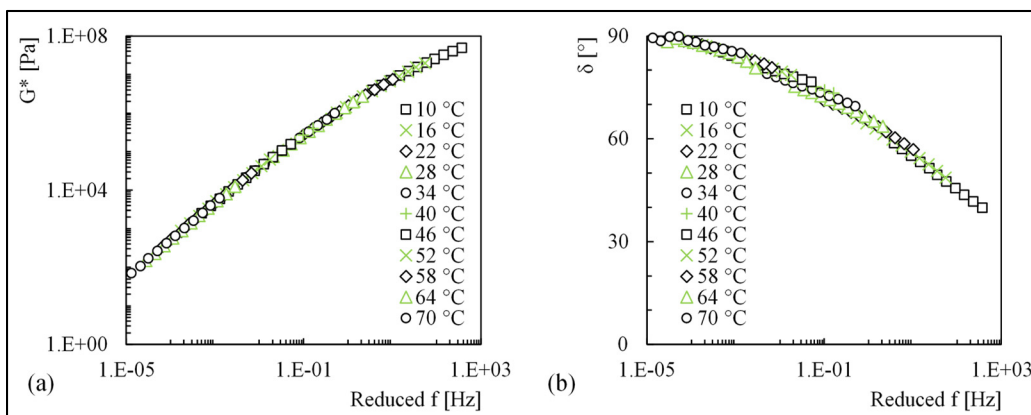


Figure-A V-1 Foamed bitumen master curves (34 °C): shear complex modulus G^* (a) and phase angle δ (b)

Table-A V-2 Basic properties of bitumen for foaming

Property	Standard	Unit	Value
Penetration	EN 1426	0.1·mm	64
Softening point	EN 1426	°C	52

A-V.4.2 Mixing, compaction and curing

After oven-drying at 40 °C, the selected RA1 was adequately mixed with filler and cement according to the mix design formulation achieving a homogeneous blend which was then accurately mixed with the added water. At the mixing time, the foamed bitumen was added to the wet aggregate blend immediately before the final mixing process carried out by an automatic equipment. In particular, the foamed bitumen was produced using a foaming unit adopting standardized temperature and water flow rate (170 °C and 1.9% of the bitumen content, respectively) based on a preliminary optimization study. In this regard, the spraying time was set to obtain an expansion ratio of 10 and a half-time of about 6 s. Lab_1 used a mortar mixer while pugmill mixing unit was used by Lab_2 and Lab_3.

Table-A V-3 CBTM adopted mix design

Component	RA1	Filler	Cement	Bitumen	Water
Dosage [%]	93.0*	5.5*	1.5*	3.0**	3.0**
* of the total solid weight (RA1 + filler + cement)					
** by the total solid weight (RA1 + filler + cement)					

The 150-mm diameter samples were compacted using an undrained SGC mold to target void content of 14.3% (pressure of 600 kPa; rotation speed of 30 rpm; angle of inclination of 1.25 °). In this regard, the following Table-A IV-4 reports the actual average bulk densities (G_{mb}) measured by the different laboratories based on the geometric dimensions of specimens at the beginning of curing. The theoretical maximum specific gravity (G_{mm}) of the CBTM is also reported. Samples were then subjected to a curing period of 14 days at 40 °C with a relative humidity of 55±5% in three different conditions. In particular, the so-called Free-Surface Drying (FSD) allows free evaporation from the lateral and top specimens' surfaces whereas the Partial-Surface Drying (PSD) was achieved by sealing the lateral surface of cylindrical samples, thus allowing evaporation only from the top surfaces. Finally, Restricted-Surface

Drying (RSD) was also evaluated by curing the specimens wrapped in sealed bags to avoid any free evaporation.

Table-A V-4 Volumetric properties of CBTM samples

Property	Lab_1	Lab_2	Lab_3
Average bulk densities (G_{mb}) [g/cm ³]	2.124	2.035	2.035
Maximum specific gravity (G_{mm}) [g/cm ³]	2.396	2.396	2.396

A-V.4.3 Experimental plan and testing methods

Indirect Tensile Stiffness Modulus (ITSM) tests were carried out at 25 °C at different curing stages (from 1 to 14 days) in order to relate the evolution of the material properties with the corresponding moisture loss (ML). ML is the percentage of mass loss in accordance to the initial sample weight (fresh). At the end of the curing stage (14 days) ITSM was also measured at 2, 10 and 20 °C to evaluate the temperature sensitivity of the mixture. Tests were executed according to EN 12697-26/Annex C applying load pulses with 124 ms of rise-time at a target peak horizontal deformation of 7 µm (Poisson's ratio was fixed at 0.35). Stiffness properties at 25 °C at the different curing stages were also assessed using the Ultrasonic Pulse Velocity (UPV) non-destructive test according to ASTM C 597. The pulse waves propagation through the mix was used to estimate the dynamic modulus of elasticity at a resonant frequency of 54 kHz. Prior to the test, samples were conditioned 3 hours at the testing temperature.

The cured specimens were also subjected to indirect tensile strength ITS tests (EN 12697-23). ITS was evaluated at 25 °C for all samples. Wet conditioning was 3 days in water at 40 °C according to EN 12697-12. This allowed calculating the Indirect Tensile Strength Ratio (ITSR) as an indicator of the water resistance of the tested CBTMs. A summary of experimental plan is schematized in Figure-A V-2.

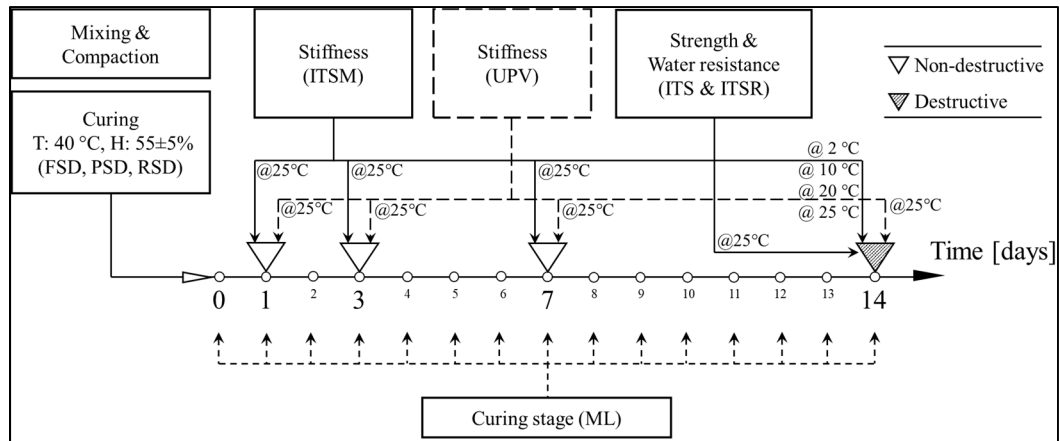


Figure-A V-2 Schematic summary of the experimental plan

A-V.5 Results and discussion

A-V.5.1 Moisture loss

Figure-A V-3 shows the evolution of the moisture loss ML in accordance to the curing time. Figure-A V-3a depicts the results obtained by different laboratories in the case of FSD cured samples (6 specimens for Lab_1 and 10 specimens for Lab_2; Lab_3 did not assess ML) whereas Figure-A V-3b shows the comparison among the different curing procedures (FSD, PSD and RSD) by reporting the average data along with the corresponding error bars at 90% confidence level.

It can be clearly observed that the curing condition strongly influenced the ML evolution. Obviously, the higher the “restrictions” to the water evaporation is, the lower the moisture loss is during time. This happened till the end of the fixed curing phase. After 14 curing days at 40 °C, the residual water content by the mix weight was 0.60% for FSD, 1.25% for PSD and 1.93% for RSD samples bearing in mind that the total water content (w_{mix}) is 2.83% by mix weight. Indeed, specimens in a completely-cured state are expected to exhibit a ML equal to the w_{mix} minus the water of ce-ment hydrated products, thus not countable for evaporation. Therefore, in the case that 0.53% of the total water would be part of the hydrate products

(cement hydration degree of 90%), a maximum water loss could be estimated around 2.30% by mix weight (Cardone et al., 2014). In this respect, regardless the testing laboratories, FSD specimens (Figure-A V-3b) effectively approached such value also showing a quasi-constant behavior after 7 days curing at 40 °C (after one curing day the ML is already more than 50%). This finding suggests that the ML can be considered sub-stantially concluded after 14 days in this curing condition. On the other hand, lower ML values and more progressive evolution of ML during the whole curing phase can be observed for PSD and RSD denoting that water is still remaining in samples even after 14 days curing in the established conditions. Comparable findings were obtained by other researchers testing similar materials under analogous curing conditions (Pasetto et al., 2019).

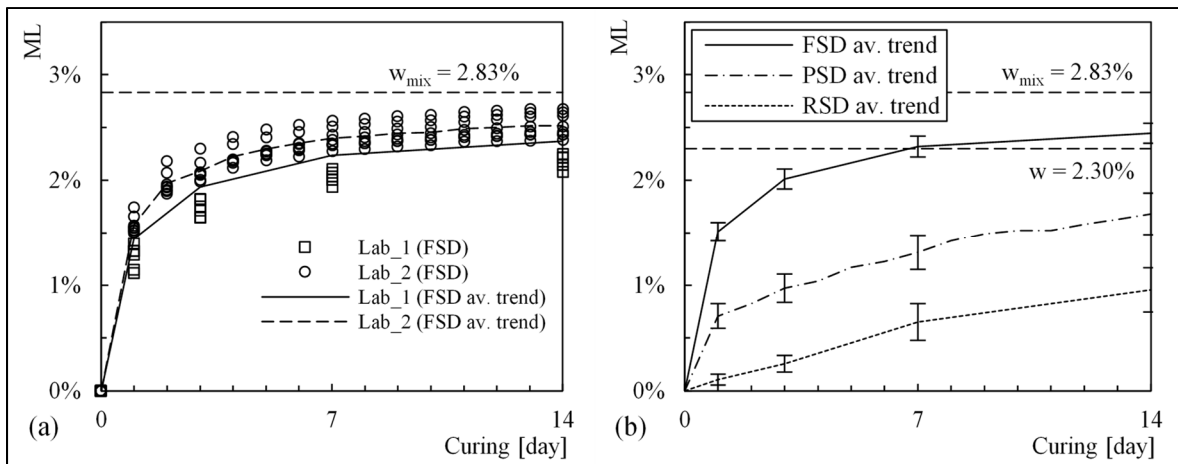


Figure-A V-3 Evolution of the ML in accordance to the curing time (40 °C): FSD samples (a); average trend of Lab_1 and Lab_2 for the three surface drying conditions tested (b)

A-V.5.2 Stiffness properties

The effect of curing on the CBTMs stiffness properties is depicted in Figure-A V-4 in terms of ITSM (Figure-A V-4a) and UPV (Figure-A V-4b) test results; for each data group the average ML is also reported. Results from both tests show similar trend and values (between 3000 and 7000 MPa) also consistent with field measurements from literature (Godenzoni et

al., 2017; Graziani et al., 2017). As regards ITSM data, no difference was found between the two methods of drying. In contrast, UPV data seem to show some differences. Based on UPV data, RSD conditioning generally led to higher average stiffness values than the FSD during the whole curing process, even if the experimental points are scattered. In this regard, it is worth noting that the curing time affects the stiffness development of cold mixes due in particular to the cement hydration process. Higher water content into CBTMs cured in RSD conditions during the curing process could reasonably encourage cement hydration process that could be beneficial to stiffness increase.

At the same time, specimens cured in FSD condition could be characterized by an incomplete cement hydration and a slight oxidation process of the virgin binder. In this way, both FSD and RSD conditions were able to reach similar stiffness values, despite the very different residual water.

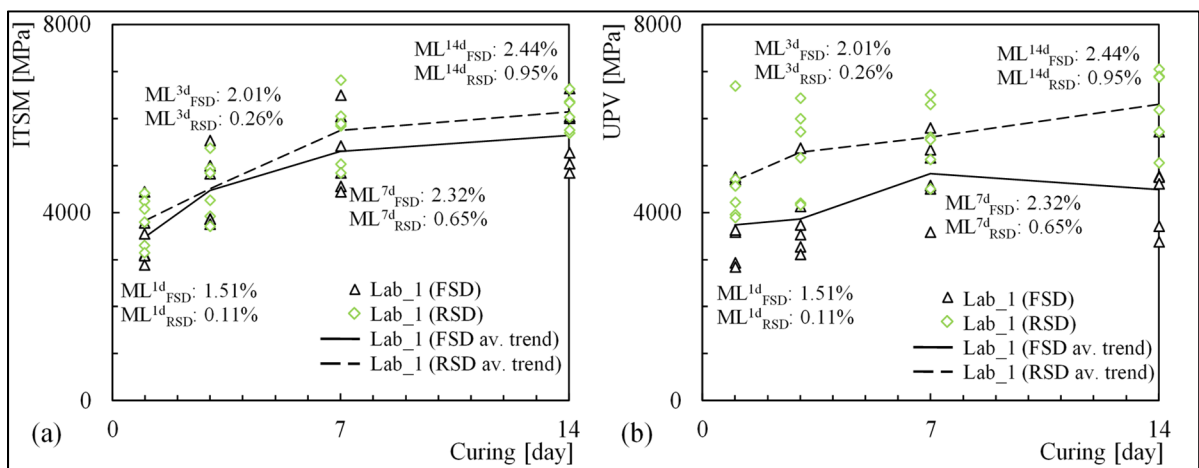


Figure-A V-4 ITSM (a) and UPV (b) stiffness test results vs. curing time (test temperature = 25 °C)

Figure-A V-5 depicts the same stiffness data as a function of the corresponding ML. Results show that RSD samples were characterized by higher stiffness at a given moisture loss level. Moreover, the rate of stiffness increase seems similar in both FSD and RSD curing conditions thus demonstrating the crucial role of the moisture loss. According to previous studies

(Dulaimi et al., 2015), the experimental data also show that stiffness was still increasing at the end of the curing period (14 days) at the given curing conditions, suggesting a still incomplete development of the ultimate mix properties.

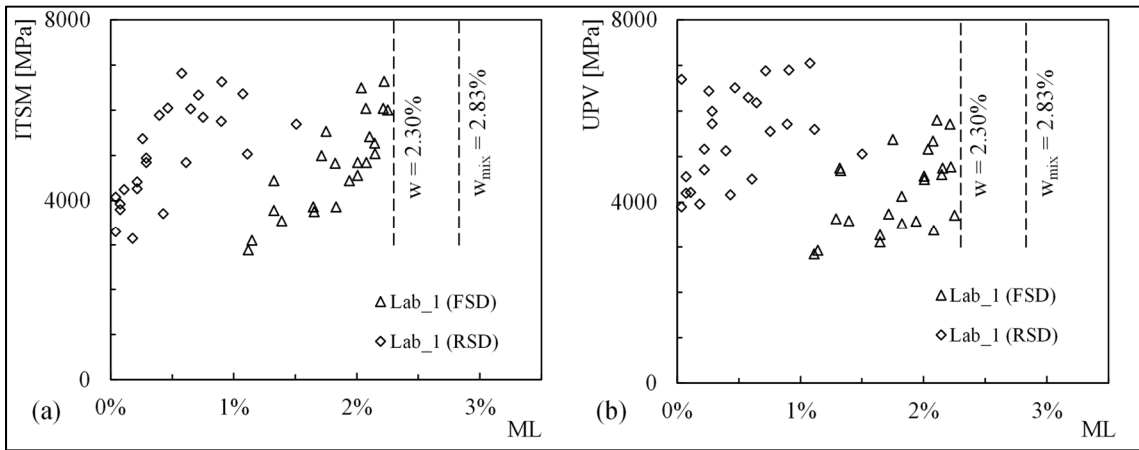


Figure-A V-5 ITSM (a) and UPV (b) test results vs. ML (tests temperature = 25 °C)

The influence of test temperature on the stiffness properties can be observed in Figure-A V-6.

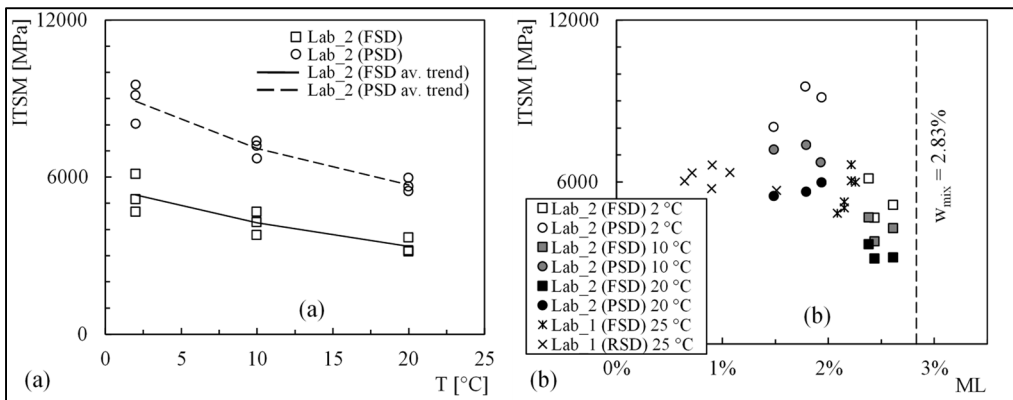


Figure-A V-6 ITSM test results after 14 days curing at 40 °C: influence of temperature (a) and ML (b)

In particular, Figure-A V-6a plots ITSM at 2, 10 and 20 °C test temperature for 14 days cured FSD and PSD specimens. Again, PSD specimens were characterized by higher stiffness than

FSD ones but the temperature sensitivity of the two samples appears almost equivalent. Moreover, Figure-A V-6b summarizes the stiffness properties of the selected CBTM tested at the end of curing by the different laboratories. Besides the already discussed aspects concerning the influence of test temperature, curing conditions and moisture loss, it is worth highlighting the higher stiffness measured by Lab_1 at 25 °C in FSD conditions with respect to that detected by Lab_2 at the same curing conditions but at lower temperature (20 °C). This fact can be likely explained by the higher bulk density of specimens tested by Lab_1 (Table-A V-3).

A-V.5.3 Strength and moisture resistance

Strength and moisture resistance characteristics of 14 days cured samples are illustrated in Figure-A V-7. Firstly, it is worth noting that the measured ITS values were similar to those recently presented by other researchers investigating analogous materials in similar conditions (Gandi et al., 2019).

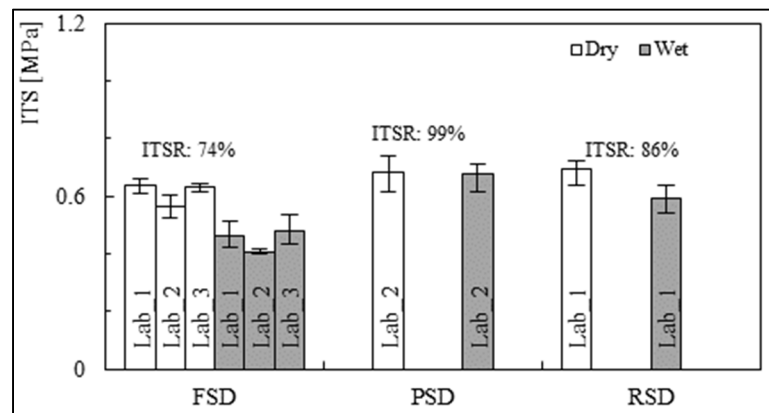


Figure-A V-7 ITS and ITSR results at 14 days

Moreover, a good repeatability among the three involved laboratories can be detected by observing the average dry ITS of specimens cured in FSD conditions. In this sense, Table-A V-5 reports the main outcomes of the ANalysis Of VAriance (ANOVA) carried out at 95%

confidence level in order to assess the statistical significance of the different measured average values.

Table-A V-5 ANOVA test: laboratory's reliability for dry ITS at 14 curing days (FSD samples)

Property	Lab_1 vs. Lab_2		Lab_1 vs. Lab_3		Lab_2 vs. Lab_3	
	Signif.?	<i>p</i> -value	Signif.?	<i>p</i> -value	Signif.?	<i>p</i> -value
ITS _{dry} (FSD)	Yes	0.046	No	0.552	Yes	0.049

On the other hand, the different curing procedures did not seem to strongly influence the tensile strength of the CBTM tested in dry condition whereas a higher influence can be clearly observed for wet conditioned samples, thus deeply affecting the related moisture resistance in terms of ITSR. Reasonably, the greater wet ITS determined for PSD and RSD specimens could be ascribed to the higher residual moisture at the time of wet conditioning. In any case, it is worth specifying that the water resistance of the tested material can be considered still acceptable in all the investigated conditions since an ITSR of 70% is commonly recognized as threshold value for material acceptance (Kennedy & Anagnos, 1984).

A-V.6 Summary and conclusions

The present paper discusses a part of the results achieved during the first phase of the ITP carried out in the framework of the activities of TG1 on “Cold Recycling” of RILEM TC 264-RAP on “Asphalt Pavement Recycling”. Specifically, the influence of different curing conditions (free, partial and restricted-surface drying) on the evolution of stiffness, strength and moisture resistance properties of CBTMs with foamed bitumen was analyzed. Results from three involved laboratories testing 150 mm diameter specimens prepared with SGC using common source of RA, cement and filler were used to accomplish this objective. Based on the experimental findings, the following main conclusions can be drawn:

- CBTMs mechanical properties strongly depend on curing and water evaporation conditions.

- Well-designed cured CBTMs are able to achieve noticeable stiffness and strength properties, particularly when the curing conditions allow for a “controlled” water evaporation with beneficial effects on cement hydration.
- The studied CBTMs in cured state demonstrate an acceptable water resistance, regardless the curing conditions.

Findings mainly highlighted that a “restrained” curing (e.g. early laying down of the upper layer during field construction) causes a higher amount of water in the mixture at the end of the process compared to the free-surface drying condition (i.e. extended field curing time without restrictions). Nevertheless, this is not affecting mechanical properties in terms of stiffness, strength and water sensitivity. More studies are encouraged to further investigate the role of water and cement in CBTM mixtures, especially when foamed bitumen is used.

ANNEX VI

THERMO-RHEOLOGICAL MODELLING IN THE SMALL STRAIN DOMAIN OF CEMENT-BITUMEN TREATED MATERIALS

Table-A VI-1 Generalized Kelvin-Voigt (GKV) parameters for 40 elements

Element	A_Unsealed		A_Sealed		B_Unsealed	
	E _i	η _i	E _i	η _i	E _i	η _i
0	6.90E+03	-	6.85E+03	-	7.85E+03	-
1	2.73E+06	1.92E-12	3.35E+06	2.35E-12	8.64E+06	6.08E-12
2	4.28E+06	1.33E-11	5.17E+06	1.61E-11	1.23E+07	3.82E-11
3	2.90E+06	3.99E-11	3.54E+06	4.87E-11	9.43E+06	1.30E-10
4	2.97E+06	1.81E-10	3.76E+06	2.29E-10	1.31E+07	7.95E-10
5	3.86E+06	1.04E-09	4.76E+06	1.28E-09	7.62E+06	2.05E-09
6	2.57E+06	3.06E-09	2.96E+06	3.52E-09	7.00E+06	8.33E-09
7	2.40E+06	1.26E-08	2.88E+06	1.51E-08	4.66E+06	2.45E-08
8	1.75E+06	4.07E-08	2.00E+06	4.66E-08	3.96E+06	9.21E-08
9	1.55E+06	1.59E-07	1.81E+06	1.86E-07	2.79E+06	2.87E-07
10	1.18E+06	5.34E-07	1.33E+06	6.06E-07	2.27E+06	1.03E-06
11	1.01E+06	2.02E-06	1.15E+06	2.32E-06	1.66E+06	3.33E-06
12	7.84E+05	6.97E-06	8.79E+05	7.81E-06	1.31E+06	1.17E-05
13	6.58E+05	2.59E-05	7.40E+05	2.91E-05	9.77E+05	3.84E-05
14	5.21E+05	9.06E-05	5.76E+05	1.00E-04	7.63E+05	1.33E-04
15	4.32E+05	3.32E-04	4.77E+05	3.67E-04	5.73E+05	4.41E-04
16	3.45E+05	1.17E-03	3.76E+05	1.28E-03	4.43E+05	1.51E-03
17	2.84E+05	4.27E-03	3.08E+05	4.63E-03	3.35E+05	5.04E-03
18	2.28E+05	1.52E-02	2.45E+05	1.63E-02	2.57E+05	1.71E-02
19	1.86E+05	5.48E-02	1.99E+05	5.85E-02	1.95E+05	5.72E-02

20	1.50E+05	1.95E-01	1.59E+05	2.06E-01	1.48E+05	1.93E-01
21	1.22E+05	7.00E-01	1.28E+05	7.36E-01	1.12E+05	6.44E-01
22	9.78E+04	2.49E+00	1.02E+05	2.59E+00	8.47E+04	2.15E+00
23	7.88E+04	8.86E+00	8.17E+04	9.17E+00	6.35E+04	7.13E+00
24	6.29E+04	3.12E+01	6.46E+04	3.21E+01	4.74E+04	2.36E+01
25	5.00E+04	1.10E+02	5.12E+04	1.12E+02	3.51E+04	7.71E+01
26	3.92E+04	3.81E+02	4.00E+04	3.89E+02	2.57E+04	2.50E+02
27	3.05E+04	1.31E+03	3.11E+04	1.34E+03	1.86E+04	7.99E+02
28	2.34E+04	4.44E+03	2.39E+04	4.53E+03	1.33E+04	2.52E+03
29	1.77E+04	1.48E+04	1.81E+04	1.52E+04	9.34E+03	7.85E+03
30	1.31E+04	4.87E+04	1.36E+04	5.05E+04	6.47E+03	2.40E+04
31	9.64E+03	1.58E+05	1.01E+04	1.66E+05	4.43E+03	7.27E+04
32	7.05E+03	5.12E+05	7.53E+03	5.47E+05	3.01E+03	2.19E+05
33	5.21E+03	1.67E+06	5.66E+03	1.82E+06	2.06E+03	6.61E+05
34	3.99E+03	5.66E+06	4.39E+03	6.23E+06	1.45E+03	2.06E+06
35	3.27E+03	2.05E+07	3.61E+03	2.26E+07	1.08E+03	6.80E+06
36	2.98E+03	8.28E+07	3.24E+03	9.00E+07	9.05E+02	2.51E+07
37	3.10E+03	3.80E+08	3.27E+03	4.01E+08	8.81E+02	1.08E+08
38	3.62E+03	1.97E+09	3.65E+03	1.98E+09	1.02E+03	5.54E+08
39	4.55E+03	1.09E+10	4.34E+03	1.04E+10	1.37E+03	3.28E+09
40	4.37E+03	4.64E+10	3.64E+03	3.86E+10	9.48E+02	1.01E+10

LIST OF BIBLIOGRAPHICAL REFERENCES

- AIPCR-PIARC. (2002). Cold in-place recycling of pavements with emulsion or foamed bitumen (Vol. Draft rep.). France: Association Mondiale de la Route and World Road Association.
- AkzoNobel. (2017). Introduction to Asphalt Emulsions: AkzoNobel.
- Al-Qadi, I. L., Elseifi, M., & Carpenter, S. H. (2007). Reclaimed asphalt pavement—a literature review.
- Anderson, T. L. (2017). *Fracture mechanics: fundamentals and applications*: CRC press.
- ARRA. (2001). *Basic asphalt recycling manual*.
- ARRA. (2016). Recommended Construction Guidelines For Cold In-place Recycling (CIR) Using Bituminous Recycling Agents.
- Ashmawy, A. K., Salgado, R., Guha, S., & Drnevich, V. P. (1995). Soil damping and its use in dynamic analyses.
- Asphalt Academy, A. (2009). *Technical Guideline (TG2): Bitumen Stabilised Materials*.
- . ASTM D6931 - 12: Standard Test Method for Indirect Tensile (IDT) Strength of Bituminous Mixtures, American Society for Testing and Materials. (2012).
- Attia, T. (2020). *Interfaces between pavement layers in bituminous mixtures*. (Doctor of Philosophy), École Nationale des Travaux Publics de l'État.
- Bailey, A. (2002). Bailey Method for Gradation Selection in Hot-Mix Asphalt Mixture Design. *Transportation Research Board Circular. USA*.

- Batista, F., Valentin, J., Čížková, Z., Valentová, T., Simnofske, D., Mollenhauer, K., . . . Engels, M. (2014). Report on available test and mix design procedures for coldrecycled bitumen stabilised materials (D1. 1). *Project CoRePaSol, Prague, 89*.
- Bayomy, F. M., Dessouky, S., & Masad, E. (2002). *EXPERIMENTAL PROCEDURES FOR EVALUATING ASPHALT MIX STABILITY USING THE SUPERPAVE GYRATORY COMPACTOR*. Paper presented at the PROCEEDINGS OF THE 6TH INTERNATIONAL CONFERENCE ON THE BEARING CAPACITY OF ROADS AND AIRFIELDS, LISBON, PORTUGAL, 24-26 JUNE 2002.
- Bennert, T., Reinke, G., Mogawer, W., & Mooney, K. (2010). Assessment of workability and compactability of warm-mix asphalt. *Transportation Research Record: Journal of the Transportation Research Board*(2180), 36-47.
- Bergeron, G. (2005). Performance des techniques de retraitement en place et de recyclage à froid au Québec. *Congrès annuel de 2005 de l'Association des transports du Canada*.
- Blanc, M., Di Benedetto, H., & Tiouajni, S. (2011). Deformation characteristics of dry Hostun sand with principal stress axes rotation. *Soils and foundations, 51*(4), 749-760.
- Bocci, M., Grilli, A., Cardone, F., & Graziani, A. (2011). A study on the mechanical behaviour of cement-bitumen treated materials. *Construction and Building Materials, 25*(2), 773-778. doi: 10.1016/j.conbuildmat.2010.07.007
- Bowering, R. (1970). *Properties and behaviour of foamed bitumen mixtures for road building*. Paper presented at the Proceedings of the 5th Australian Road Research Board Conference.
- Bowering, R., & Martin, C. (1976). *Foamed bitumen production and application of mixtures evaluation and performance of pavements*. Paper presented at the Association of Asphalt Paving Technologists Proc.
- Brouwers, H. J. H. (2004). The work of Powers and Brownyard revisited: Part 1. *Cement and Concrete Research, 34*(9), 1697-1716.

- Brouwers, H. J. H., & Radix, H. J. (2005). Self-compacting concrete: theoretical and experimental study. *Cement and Concrete Research*, 35(11), 2116-2136.
- Brown, S., & Needham, D. (2000). A study of cement modified bitumen emulsion mixtures. *Asphalt Paving Technology*, 69, 92-121.
- Butcher, M. (1998). Determining gyratory compaction characteristics using servopac gyratory compactor. *Transportation Research Record*, 1630(1), 89-97.
- Cardone, F., Grilli, A., Bocci, M., & Graziani, A. (2014). Curing and temperature sensitivity of cement-bitumen treated materials. *International Journal of Pavement Engineering*, 16(10), 868-880. doi: 10.1080/10298436.2014.966710
- Cardone, F., Virgili, A., & Graziani, A. (2018). Evaluation of bonding between reclaimed asphalt aggregate and bitumen emulsion composites. *Construction and Building Materials*, 184, 565-574.
- Carret, J.-C., Pedraza, A., Di Benedetto, H., & Sauzeat, C. (2018). Comparison of the 3-dim linear viscoelastic behavior of asphalt mixes determined with tension-compression and dynamic tests. *Construction and Building Materials*, 174, 529-536.
- Carter, A., Fiedler, J., Kominek, Z., Vacin, O., Barberi, A., & Perraton, D. (2007). *Influence of Accelerated Curing on Cold In-Place Recycling*. Paper presented at the PROCEEDINGS OF THE FIFTY-SECOND ANNUAL CONFERENCE OF THE CANADIAN TECHNICAL ASPHALT ASSOCIATION (CTAA): NIAGARA FALLS, ONTARIO, NOVEMBER 2007.
- Chandra, R., Veeraragavan, A., & Krishnan, J. M. (2013). Evaluation of Mix Design Methods for Reclaimed Asphalt Pavement Mixes with Foamed Bitumen. *Procedia - Social and Behavioral Sciences*, 104, 2-11. doi: 10.1016/j.sbspro.2013.11.092
- Chesner, W., Stein, C., Justus, H., Kearney, E., & Cross, S. (2011). Evaluation of factors affecting long-term performance of cold in-place recycled pavements in New York State. *Transportation Research Record: Journal of the Transportation Research Board*(2227), 13-22.

Circular, T. R. (2006). *Asphalt Emulsion Technology* (Vol. E-C102).

Čížková, Z., Valentin, J., Suda, J., Krpálek, O., Simnofske, D., & Batista, F. (2014). Report on Durability of cold-recycled mixes: Test procedures for stiffness determination. *no. September*.

Colleparidi, M. (1991). *Scienza e tecnologia del calcestruzzo*: Hoepli Editore.

Cominsky, R. J., Huber, G. A., Kennedy, T. W., & Anderson, M. (1994). *The superpave mix design manual for new construction and overlays*: Strategic Highway Research Program Washington, DC.

Copeland, A. (2011). Reclaimed Asphalt Pavement in Asphalt Mixtures: State of the Practice. 29 Publication FHWA-HRT-11-021. *Turner-Fairbank Highway Research Center, Federal Highway, 30*.

Corte, F., & Di Benedetto, H. (2004). Matériaux routiers bitumineux 2: constitution et propriétés thermomécaniques des mélanges. *HERMES/LAVOISIER, 283*.

Cross, S. (1999). Experimental cold in-place recycling with hydrated lime. *Transportation Research Record: Journal of the Transportation Research Board*(1684), 186-193.

Cross, S. (2003). Determination of Superpave® gyratory compactor design compactive effort for cold in-place recycled mixtures. *Transportation Research Record: Journal of the Transportation Research Board*(1819), 152-160.

Dal Ben, M., & Jenkins, K. J. (2014). Performance of cold recycling materials with foamed bitumen and increasing percentage of reclaimed asphalt pavement. *Road Materials and Pavement Design, 15*(2), 348-371. doi: 10.1080/14680629.2013.872051

Davidson, J. K. (2005). Progress in Cold Mix Processes in Canada. *Canadian Technical Asphalt Association*.

Davidson, J. K., & Eng, J.-M. C. P. (2003). Best practices in cold in-place recycling.

- De Larrard, F. (1999). *Concrete Mixture Proportioning—A Scientific Approach*. E & FN Spon. *New York, NY*.
- Dessouky, S., Masad, E., & Bayomy, F. (2004). Prediction of hot mix asphalt stability using the superpave gyratory compactor. *Journal of Materials in Civil Engineering*, *16*(6), 578-587.
- Dessouky, S., Pothuganti, A., Walubita, L. F., & Rand, D. (2012). Laboratory evaluation of the workability and compactability of asphaltic materials prior to road construction. *Journal of Materials in Civil Engineering*, *25*(6), 810-818.
- Di Benedetto, H., Blanc, M., Tiouajni, S., & Ezaoui, A. (2014). Elastoplastic model with loading memory surfaces (LMS) for monotonic and cyclic behaviour of geomaterials. *International Journal for Numerical and Analytical Methods in Geomechanics*, *38*(14), 1477-1502.
- Di Benedetto, H., Delaporte, B., & Sauzéat, C. (2007). Three-dimensional linear behavior of bituminous materials: experiments and modeling. *International Journal of Geomechanics*, *7*(2), 149-157.
- Di Benedetto, H., Mondher, N., Sauzéat, C., & Olard, F. (2007). Three-dimensional thermo-viscoplastic behaviour of bituminous materials: the DBN model. *Road Materials and Pavement Design*, *8*(2), 285-315.
- Di Benedetto, H., Olard, F., Sauzéat, C., & Delaporte, B. (2004). Linear viscoelastic behaviour of bituminous materials: From binders to mixes. *Road Materials and Pavement Design*, *5*(sup1), 163-202.
- Di Benedetto, H., Partl, M. N., Francken, L., & Saint André, C. D. L. R. (2001). Stiffness testing for bituminous mixtures. *Materials and Structures*, *34*(2), 66-70.
- Di Benedetto, H., Tatsuoka, F., & Ishihara, M. (2002). Time-dependent shear deformation characteristics of sand and their constitutive modelling. *Soils and foundations*, *42*(2), 1-22.

- Dolzycki, B., Jaczewski, M., & Szydłowski, C. (2017). The long-term properties of mineral-cement-emulsion mixtures. *Construction and Building Materials*, 156, 799-808. doi: 10.1016/j.conbuildmat.2017.09.032
- Dongre, R., Sharma, M. G., & Anderson, D. A. (1989). Development of fracture criterion for asphalt mixes at low temperatures. *Transportation Research Record*, 1228, 94-105.
- Du, S. (2014). Effect of Different Fillers on Performance Properties of Asphalt Emulsion Mixture. *Journal of Testing and Evaluation*, 42. doi: 10.1520/jte20130020
- Du, S. (2018). Effect of curing conditions on properties of cement asphalt emulsion mixture. *Construction and Building Materials*, 164, 84-93.
- Dulaimi, A., Al Nageim, H., Ruddock, F., & Seton, L. (2015). A novel cold asphalt concrete mixture for heavily trafficked binder course. *World Acad. Sci. Eng. Technol. Int. J. Civ. Environ. Struct. Constr. Archit. Eng.*, 9(8), 945-949.
- . EN 1097-6: Test for mechanical and physical properties of aggregates - Part 6: Determination of particle density and water absorption. (2013).
- . EN 12697-23: Bituminous Mixtures - Test methods for hot Mix Asphalt Part 23: Determination of the indirect tensile strength of bituminous specimens, European Committee for Standardization. (2006). Brussels, Belgium.
- . EN 12697-26: Bituminous Mixtures - Test methods for hot Mix Asphalt Part 26: Stiffness, European Committee for Standardization. (2004). Brussels, Belgium.
- Enomoto, T., Kawabe, S., Tatsuoka, F., Di Benedetto, H., Hayashi, T., & Duttine, A. (2009). Effects of particle characteristics on the viscous properties of granular materials in shear. *Soils and foundations*, 49(1), 25-49.
- Esenwa, M., Davidson, J. K., Kucharek, A. S., & Moore, T. (2013). 100% Recycled Asphalt Paving, Our Experience. *Canadian Technical Asphalt Association*.

- . Evaluation of Asphalt Mixture Cracking Resistance using the Semi-Circular Bend Test (SCB) at Intermediate Temperatures, American Society for Testing and Materials. (2016) *ASTM D8044 - 16: Standard Test Method for*.
- Fang, X., Garcia, A., Winnefeld, F., Partl, M. N., & Lura, P. (2016). Impact of rapid-hardening cements on mechanical properties of cement bitumen emulsion asphalt. *Materials and Structures*, 49(1-2), 487-498.
- Ferry, J. D. (1980). *Viscoelastic properties of polymers*: John Wiley & Sons.
- Francken, L., Vanelstraete, A., Léonard, D., & Pilate, O. (2003). *New developments in the PRADO volumetric mix design*. Paper presented at the Proc. Of the 6th RILEM Symposium on Performance Testing and Evaluation of Bituminous Materials, PTEBM.
- Frigio, F., & Canestrari, F. (2018). Characterisation of warm recycled porous asphalt mixtures prepared with different WMA additives. *European Journal of Environmental and Civil Engineering*, 22(1), 82-98.
- Frigio, F., Raschia, S., Steiner, D., Hofko, B., & Canestrari, F. (2016). Aging effects on recycled WMA porous asphalt mixtures. *Construction and Building Materials*, 123, 712-718.
- Fuller, H. B., & Thompson, S. E. (1907). The laws of proportioning concrete. *Trans. Am. Soc. Civ. Engrs*, 59, 67-193.
- Gaestel, C. (1967). The breaking mechanism of cationic bitumen emulsions. *Chemistry and Industry*.
- Galobardes, I., Cavalaro, S. H., Goodier, C. I., Austin, S., & Rueda, Á. (2015). Maturity method to predict the evolution of the properties of sprayed concrete. *Construction and Building Materials*, 79, 357-369.
- Gandi, A. (2018). *Laboroatory characterization of bitumen treated full depth reclamation materials*. (Eng. Ph.D.), Ecole de tecnología supérieure.

- Gandi, A., Cardenas, A., Sow, D., Carter, A., & Perraton, D. (2019). Study of the impact of the compaction and curing temperature on the behavior of cold bituminous recycled materials. *Journal of Traffic and Transportation Engineering (English Edition)*, 6(4), 349-358.
- Gandi, A., Carter, A., & Singh, D. (2017). Rheological behavior of cold recycled asphalt materials with different contents of recycled asphalt pavements. *Innovative Infrastructure Solutions*, 2(1), 45.
- García, A., Lura, P., Partl, M. N., & Jerjen, I. (2013). Influence of cement content and environmental humidity on asphalt emulsion and cement composites performance. *Materials and Structures*, 46(8), 1275-1289.
- Gaufrey, V., Wendling, L., Odie, L., Fabre, J., De La Roche, C., Horny, P., & Dubois, V. (2008, 2008-05-21). *Laboratory characterization of cold mix treated with bitumen emulsion*. Paper presented at the 4th Europhalt and eurobitume Congress, France.
- Gayte, P. (2016). *Modélisation du comportement thermo-viscoplastique des enrobés bitumineux*.
- Gayte, P., Di Benedetto, H., Sauzéat, C., & Nguyen, Q. T. (2016). Influence of transient effects for analysis of complex modulus tests on bituminous mixtures. *Road Materials and Pavement Design*, 17(2), 271-289.
- Genta, G. (2009). *Vibration dynamics and control*: Springer.
- Gergesova, M., Zupančič, B., Saprunov, I., & Emri, I. (2011). The closed form tTP shifting (CFS) algorithm. *Journal of Rheology*, 55(1), 1-16.
- Giani, M. I., Dotelli, G., Brandini, N., & Zampori, L. (2015). Comparative life cycle assessment of asphalt pavements using reclaimed asphalt, warm mix technology and cold in-place recycling. *Resources, Conservation and Recycling*, 104, 224-238. doi: 10.1016/j.resconrec.2015.08.006
- Giuliani, F. (2001). *X-ray diffraction method for studying cement-modified bitumen-emulsion mixtures in asphalt pavement cold recycling*. Paper presented at the International

Symposium on Subgrade Stabilisation and In Situ Pavement Recycling Using Cement, 1st, 2001, Salamanca, Spain.

- Godenzoni, C. (2017). *Multiscale Rheological and Mechanical characterization of Cold Mixtures*. (Doctoral dissertation), Università Politecnica delle Marche, Ancona.
- Godenzoni, C., Cardone, F., Graziani, A., & Bocci, M. (2016). The Effect of Curing on the Mechanical Behavior of Cement-Bitumen Treated Materials. *11*, 879-890. doi: 10.1007/978-94-017-7342-3_70
- Godenzoni, C., Graziani, A., Bocci, E., & Bocci, M. (2017). The evolution of the mechanical behaviour of cold recycled mixtures stabilised with cement and bitumen: field and laboratory study. *Road Materials and Pavement Design*, 1-22. doi: 10.1080/14680629.2017.1279073
- Godenzoni, C., Graziani, A., & Bocci, M. (2015). *Influence of reclaimed asphalt content on the complex modulus of cement bitumen treated materials*. Paper presented at the 6th International conference bituminous mixtures and pavements, Thessaloniki (Greece).
- Godenzoni, C., Graziani, A., & Perraton, D. (2016). Complex modulus characterisation of cold-recycled mixtures with foamed bitumen and different contents of reclaimed asphalt. *Road Materials and Pavement Design*, 18(1), 130-150. doi: 10.1080/14680629.2016.1142467
- Graziani, A., Godenzoni, C., Cardone, F., Bocci, E., & Bocci, M. (2017). An application of the Michaelis–Menten model to analyze the curing process of cold recycled bituminous mixtures. *International Journal of Pavement Research and Technology*, 10(1), 62-74.
- Graziani, A., Godenzoni, C., Cardone, F., & Bocci, M. (2016). Effect of curing on the physical and mechanical properties of cold-recycled bituminous mixtures. *Materials & Design*, 95, 358-369.
- Graziani, A., Iafelice, C., Raschia, S., Perraton, D., & Carter, A. (2018). A procedure for characterizing the curing process of cold recycled bitumen emulsion mixtures. *Construction and Building Materials*, 173, 754-762.

- Graziani, A., Mignini, C., Bocci, E., & Bocci, M. (2020). Complex Modulus Testing and Rheological Modeling of Cold-Recycled Mixtures. *Journal of Testing and Evaluation*, 48(1), 20180905. doi: 10.1520/jte20180905
- Graziani, A., Virgili, A., & Cardone, F. (2018). Testing the bond strength between cold bitumen emulsion composites and aggregate substrate. *Materials and Structures*, 51(1), 14.
- Grilli, A., Cardone, F., & Bocci, E. (2018). Mechanical behaviour of cement-bitumen treated materials containing different amounts of reclaimed asphalt. *European Journal of Environmental and Civil Engineering*, 22(7), 836-851.
- Grilli, A., Graziani, A., Bocci, E., & Bocci, M. (2016). Volumetric properties and influence of water content on the compactability of cold recycled mixtures. *Materials and Structures*, 49(10), 4349-4362. doi: 10.1617/s11527-016-0792-x
- Grilli, A., Graziani, A., & Bocci, M. (2012). Compactability and thermal sensitivity of cement-bitumen-treated materials. *Road Materials and Pavement Design*, 13(4), 599-617. doi: 10.1080/14680629.2012.742624
- Grilli, A., Mignini, C., & Graziani, A. (2019). *FIELD BEHAVIOUR OF COLD-RECYCLED ASPHALT MIXTURES FOR BINDER COURSES*. Paper presented at the International Conference on Sustainable Materials, Systems and Structures (SMSS 2019) - New Generation of Construction Materials, Rovinj, Croatia.
- Gu, F., Ma, W., West, R. C., Taylor, A. J., & Zhang, Y. (2019). Structural performance and sustainability assessment of cold central-plant and in-place recycled asphalt pavements: A case study. *Journal of Cleaner Production*, 208, 1513-1523.
- Guatimosim, F. V., Vasconcelos, K. L., Kuchiishi, A. K., & Bernucci, L. L. B. (2019). Field Evaluation of High Level Roads with Foamed Bitumen Stabilized Base Layers *Airfield and Highway Pavements 2019: Testing and Characterization of Pavement Materials* (pp. 549-559): American Society of Civil Engineers Reston, VA.
- Gudimettla, J. M., Cooley, L., & Brown, E. R. (2003). *Workability of hot mix asphalt*: NCAT.

- Hodgkinson, A., & Visser, A. T. (2004). *The role of fillers and cementitious binders when recycling with foamed bitumen or bitumen emulsion*. Paper presented at the 8th Conference on Asphalt Pavements for Southern Africa, Sun City, South Africa.
- Hugener, M., Partl, M. N., & Morant, M. (2014). Cold asphalt recycling with 100% reclaimed asphalt pavement and vegetable oil-based rejuvenators. *Road Materials and Pavement Design*, 15(2), 239-258.
- Institute, A., & Association, A. E. M. (1979). *A basic asphalt emulsion manual*: Department of Transportation, Federal Highway Administration.
- Israelachvili, J. N. (2015). *Intermolecular and surface forces*: Academic press.
- Jacobson, T. (2002). *Cold recycling of asphalt pavement-mix in plant*. Paper presented at the Seminar on Road Pavement Recycling.
- Jenkins, K. J. (2000a). *Mix design considerations for cold and half-warm bituminous mixes with emphasis of foamed bitumen*. Stellenbosch: Stellenbosch University.
- Jenkins, K. J. (2000b). *Mix Design Considerations for Cold and Half-Warm Bituminous Mixes With Emphasis On Foamed Bitumen*. (Doctoral dissertation), Stellenbosch University, Stellenbosch.
- Jenkins, K. J., & Moloto, P. K. (2008). Updating Bituminous Stabilized Materials Guidelines: Mix Design Report, Phase II.
- Jensen, O. M., & Hansen, P. F. (2001). Water-entrained cement-based materials: I. Principles and theoretical background. *Cement and Concrete Research*, 31(4), 647-654.
- Jiang, Y., Lin, H., Han, Z., & Deng, C. (2019). Fatigue Properties of Cold-Recycled Emulsified Asphalt Mixtures Fabricated by Different Compaction Methods. *Sustainability*, 11(12), 3483.
- Kandhal, P. S., & Mallick, R. B. (1998). Pavement recycling guidelines for state and local governments participant's reference book.

- Karray, M., Carter, A., Ethier, Y., & Lecuru, Q. (2019). Characterization of Cold In-Place Recycled Materials at Young Age Using Shear Wave Velocity. *Advances in Civil Engineering Materials*, 8(1), 336-354.
- Kavussi, A., & Modarres, A. (2010). A model for resilient modulus determination of recycled mixes with bitumen emulsion and cement from ITS testing results. *Construction and Building Materials*, 24(11), 2252-2259. doi: 10.1016/j.conbuildmat.2010.04.031
- Kennedy, T. W., & Anagnos, J. N. (1984). Wet-dry indirect tensile test for evaluating moisture susceptibility of asphalt mixtures.
- Kim, S., Guarin, A., Roque, R., & Birgisson, B. (2008). Laboratory evaluation for rutting performance based on the DASR porosity of asphalt mixture. *Road Materials and Pavement Design*, 9(3), 421-440.
- Kim, Y., Im, S., & Lee, H. (2011). Impacts of Curing Time and Moisture Content on Engineering Properties of Cold In-Place Recycling Mixtures Using Foamed or Emulsified Asphalt. *Journal of Materials in Civil Engineering*, 23(5), 542-553. doi: 10.1061/(asce)mt.1943-5533.0000209
- Kim, Y., & Lee, H. D. (2006). Development of Mix Design Procedure for Cold In-Place Recycling with Foamed Asphalt. *Journal of Materials in Civil Engineering*. doi: 10.1061//asce/0899-1561/2006/18:1/116
- Komacka, J., Remisova, E., Liu, G., Leegwater, G., & Nielsen, E. (2014). Influence of reclaimed asphalt with polymer modified bitumen on properties of different asphalts for a wearing course. *Proc. ICTI*, 3, 179-185.
- Kowalski, T. E., & Starry, D. W. (2007, October 14-17, 2007). *Cold Recycling Using Foam Bitumen*. Paper presented at the Annual Conference of the Transportation Association of Canada, Saskatoon, Saskatchewan.
- Kuleshov, A. (2018). COMPARATIVE ANALYSIS OF PAVEMENT RECONSTRUCTION METHODS. *Architecture and Engineering*, 3(1).

- Lachance-Tremblay, É., Perraton, D., Vaillancourt, M., & Di Benedetto, H. (2017). Degradation of asphalt mixtures with glass aggregates subjected to freeze-thaw cycles. *Cold Regions Science and Technology*, *141*, 8-15.
- Lachance, E., Carter, A., & Tate, M. (2012). *Hydrated Lime and Lime Kiln Dust as Additives for CIR and FDR Materials Treated with Asphalt Emulsion and Foamed Asphalt*. Paper presented at the Fifty-seventh annual conference of the canadian technical asphalt association (ctaa).
- Lamothe, S., Perraton, D., & Benedetto, H. D. (2017). Degradation of hot mix asphalt samples subjected to freeze-thaw cycles and partially saturated with water or brine. *Road Materials and Pavement Design*, *18*(4), 849-864. doi: 10.1080/14680629.2017.1286442
- Lauter, K. A., & Corbett, M. A. (1998). *Developing gyratory compacter guidelines for use with cold in-place recycled material*. Paper presented at the Proceedings of the... Annual conference of canadian technical asphalt association.
- Lee, D. (1980). *Treating marginal aggregates and soils with foamed asphalt*: Iowa State University College of Engineering.
- Lee, K. W., Brayton, T. E., & Harrington, J. (2002). New Mix-Design Procedure of Cold In-Place Recycling for Pavement Rehabilitation. *Transportation Research Record*.
- Lesueur, D., & Potti, J. J. (2004). Cold mix design: A rational approach based on the current understanding of the breaking of bituminous emulsions. *Road Materials and Pavement Design*, *5*(sup1), 65-87. doi: 10.1080/14680629.2004.9689988
- Li, W., Zhu, X., Hong, J., She, W., Wang, P., & Zuo, W. (2015). Effect of anionic emulsifier on cement hydration and its interaction mechanism. *Construction and Building Materials*, *93*, 1003-1011.
- Lim, I. L., Johnston, I. W., & Choi, S. K. (1993). Stress intensity factors for semi-circular specimens under three-point bending. *Engineering Fracture Mechanics*, *44*(3), 363-382.

- Lin, J., Wei, T., Hong, J., Zhao, Y., & Liu, J. (2015). Research on development mechanism of early-stage strength for cold recycled asphalt mixture using emulsion asphalt. *Construction and Building Materials*, *99*, 137-142.
- Mahmoud, A. F. F., & Bahia, H. U. (2004). Using gyratory compactor to measure mechanical stability of asphalt mixtures: Wisconsin Highway Research Program.
- Mangiafico, S., Di Benedetto, H., Sauzéat, C., Olard, F., Pouget, S., & Planque, L. (2014). New method to obtain viscoelastic properties of bitumen blends from pure and reclaimed asphalt pavement binder constituents. *Road Materials and Pavement Design*, *15*(2), 312-329.
- Martínez-Echevarría, M. J., Recasens, R. M., del Carmen Rubio Gámez, M., & Ondina, A. M. (2012). In-laboratory compaction procedure for cold recycled mixes with bituminous emulsions. *Construction and Building Materials*, *36*, 918-924. doi: <https://doi.org/10.1016/j.conbuildmat.2012.06.040>
- Martínez, A., Miró, R., & Pérez-Jiménez, F. (2007). Spanish experience with gyratory compactor and indirect tensile test in design and control of cold recycled asphalt pavement. *Transportation Research Record: Journal of the Transportation Research Board*(2001), 163-168.
- Meocci, M., Grilli, A., La Torre, F., & Bocci, M. (2017). Evaluation of mechanical performance of cement-bitumen-treated materials through laboratory and in-situ testing. *Road Materials and Pavement Design*, *18*(2), 376-389.
- Michaelis, L., & Menten, M. L. (2007). *Die kinetik der invertinwirkung*: Universitätsbibliothek Johann Christian Senckenberg.
- Mignini, C., Cardone, F., & Graziani, A. (2018a). Experimental study of bitumen emulsion-cement mortars: mechanical behaviour and relation to mixtures. *Materials and Structures*.
- Mignini, C., Cardone, F., & Graziani, A. (2018b). Experimental study of bitumen emulsion-cement mortars: mechanical behaviour and relation to mixtures. *Materials and Structures*, *51*(6), 149. doi: 10.1617/s11527-018-1276-y

- Miljković, M., Poulikakos, L., Piemontese, F., Shakoorioskooie, M., & Lura, P. (2019). Mechanical behaviour of bitumen emulsion-cement composites across the structural transition of the co-binder system. *Construction and Building Materials*, 215, 217-232.
- Miljković, M., & Radenberg, M. (2014). Fracture behaviour of bitumen emulsion mortar mixtures. *Construction and Building Materials*, 62, 126-134.
- Miljković, M., Radenberg, M., Fang, X., & Lura, P. (2017). Influence of emulsifier content on cement hydration and mechanical performance of bitumen emulsion mortar. *Materials and Structures*, 50(3), 185.
- Miller, T., Greyling, A., Bahia, H. U., & Jenkins, K. J. (2010). *Development of a test method for determining emulsion bond strength using the bitumen bond strength (BBS) test: A South African perspective*. Paper presented at the INTERNATIONAL SPRAYED SEALING CONFERENCE, 2ND, 2010, MELBOURNE, VICTORIA, AUSTRALIA.
- Moghaddam, T. B., & Baaj, H. (2018). Application of compressible packing model for optimization of asphalt concrete mix design. *Construction and Building Materials*, 159, 530-539.
- Mohammad, L. N., Wu, Z., & Aglan, M. (2004). *Characterization of fracture and fatigue resistance on recycled polymer-modified asphalt pavements*. Paper presented at the 5th RILEM International Conference on Cracking in Pavements.
- Molenaar, J. M. M., Liu, X., & Molenaar, A. A. A. (2003). *Resistance to crack-growth and fracture of asphalt mixture*. Paper presented at the 6th International RILEM Symposium on Performance Testing and Evaluation of Bituminous Materials, Zurich, Switzerland.
- Montepara, A., & Giuliani, F. (2001). *The role of cement in the recycling of asphalt pavement cold-stabilized with bituminous emulsions*. Paper presented at the Second International Symposium on Maintenance and Rehabilitation of Pavements and Technological Control, Alabama (USA).
- Nady, R. M. (1997). THE QUALITY OF RANDOM RAP. SEPARATING FACT FROM SUPPOSITION. *HMAT: Hot Mix Asphalt Technology*, 2(2).

- NAPA. (2009-2010). *Asphalt Pavement Mix Production Survey*.
- Navarro, F. M., & Gámez, M. C. R. (2011). Influence of crumb rubber on the indirect tensile strength and stiffness modulus of hot bituminous mixes. *Journal of Materials in Civil Engineering*, 24(6), 715-724.
- Needham, D. (1996). *Developments in bitumen emulsion mixtures for roads*. University of Nottingham.
- Neifar, M., & Di Benedetto, H. (2001). Thermo-viscoplastic law for bituminous mixes. *Road Materials and Pavement Design*, 2(1), 71-95.
- Neville, A. M. (1995). *Properties of concrete* (Vol. 4): Longman London.
- Niazi, Y., & Jalili, M. (2009). Effect of Portland cement and lime additives on properties of cold in-place recycled mixtures with asphalt emulsion. *Construction and Building Materials*, 23(3), 1338-1343. doi: 10.1016/j.conbuildmat.2008.07.020
- No., A.-A.-A. J. C. C. T. F. (1998). Report on cold recycling of asphalt pavements: American Association of State Highway and Transportation Officials.
- Ojum, C., Kuna, K., Thom, N., & Airey, G. (2014). An investigation into the effects of accelerated curing on cold recycled bituminous mixes.
- Olard, F. (2012). GB5 mix design: high-performance and cost-effective asphalt concretes by use of gap-graded curves and SBS modified bitumens. *Road Materials and Pavement Design*, 13(sup1), 234-259.
- Olard, F., & Di Benedetto, H. (2003). General “2S2P1D” model and relation between the linear viscoelastic behaviours of bituminous binders and mixes. *Road Materials and Pavement Design*, 4(2), 185-224.
- Olard, F., & Perraton, D. (2010). On the optimization of the aggregate packing characteristics for the design of high-performance asphalt concretes. *Road Materials and Pavement Design*, 11(sup1), 145-169.

- Oruc, S., Celik, F., & Akpinar, M. V. (2007). Effect of Cement on Emulsified Asphalt Mixtures. *Journal of Materials Engineering and Performance*, 16(5), 578-583. doi: 10.1007/s11665-007-9095-2
- Ouchi, M., & Okamura, H. (1999). *Self-compacting concrete development, Present and future*. Paper presented at the Proc. 1st Int. Symposium on Self-compacting Concrete, RILEM, Sweden.
- Ouyang, J., Hu, L., Li, H., & Han, B. (2018). Effect of cement on the demulsifying behavior of over-stabilized asphalt emulsion during mixing. *Construction and Building Materials*, 177, 252-260. doi: 10.1016/j.conbuildmat.2018.05.141
- . Part 44: Crack Propagation by Semi-Circular Bending Test, European Committee for Standardization. (2010) *EN 12697-44: Bituminous Mixtures - Test methods for hot Mix Asphalt*. Brussels, Belgium.
- Pasetto, M., Baliello, A., Giacomello, G., & Pasquini, E. (2019). Cold recycling of reclaimed asphalt: analysis of alternative procedures. *Bituminous Mixtures and Pavements VII*, 551-559.
- Perraton, D., Di Benedetto, H., Sauzéat, C., Hofko, B., Graziani, A., Nguyen, Q. T., . . . Grenfell, J. (2016). 3Dim experimental investigation of linear viscoelastic properties of bituminous mixtures. *Materials and Structures*, 49(11), 4813-4829.
- Perraton, D., Meunier, M., & Carter, A. (2007). Application of granular packing methods to the mix design of Stone Matrix Asphalts (SMA). *Bulletin de Liaison des Ponts et Chaussées*(270-271).
- Perraton, D., Tebaldi, G., Dave, E. V., Bilodeau, F., Giacomello, G., Grilli, A., . . . Muraya, P. (2016). *Tests campaign analysis to evaluate the capability of fragmentation test to characterize recycled asphalt pavement (RAP) material*. Paper presented at the 8th RILEM International Symposium on Testing and Characterization of Sustainable and Innovative Bituminous Materials.
- Pigeon, M. (1981). Composition et hydratation du ciment Portland. *Séminaire progrès dans le domaine du béton, Québec, (septembre 1981) p*, 36-72.

- Plotnikova, I. A. (1993). *Control of the interaction process between emulsion and mineral aggregate by means of physico-chemical modification of their surfaces*. Paper presented at the First world Congress on Emulsion, Paris.
- Powers, T. C. (1958). Structure and physical properties of hardened Portland cement paste. *Journal of the American Ceramic Society*, 41(1), 1-6.
- Pronk, A. C. (2006). The Huet-Sayegh Model; A simple and excellent rheological model for master curves of asphalt mixes. *Asphalt Concrete*, 73-82.
- Québec, M. d. T. d. (2018). LC 26-045: Détermination de la densité maximale.
- Raschia, S., Badeli, S., Carter, A., Graziani, A., & Perraton, D. (2018). *Recycled Glass Filler in Cold Recycled Materials Treated with Bituminous Emulsion*. Paper presented at the Transportation Research Board 97th Annual Meeting, Washington, D.C. (USA).
- Raschia, S., Graziani, A., Carter, A., & Perraton, D. (2019a). *Influence of RAP Source and Nominal Maximum Size on Volumetric and Physical Properties of Cement-Bitumen Treated Materials*. Paper presented at the Transportation Research Board (TRB) 98th Annual Meeting, Washington D.C. (USA).
- Raschia, S., Graziani, A., Carter, A., & Perraton, D. (2019b). Laboratory mechanical characterisation of cold recycled mixtures produced with different RAP sources. *Road Materials and Pavement Design*, 20(sup1), S233-S246. doi: 10.1080/14680629.2019.1588775
- Raschia, S., Mignini, C., Graziani, A., Carter, A., Perraton, D., & Vaillancourt, M. (2019). Effect of gradation on volumetric and mechanical properties of cold recycled mixtures (CRM). *Road Materials and Pavement Design*, 1-15.
- Raschia, S., Perraton, D., Graziani, A., & Carter, A. (2020). Influence of low production temperatures on compactability and mechanical properties of cold recycled mixtures. *Construction and Building Materials*, 232, 117169.
- Richardson, I. G. (1999). The nature of CSH in hardened cements. *Cement and Concrete Research*, 29(8), 1131-1147.

- Rodezno, C., Brown, R., Julian, G., & Prowell, B. (2017). *Variability of Ignition Furnace Correction Factors*.
- Rutherford, T., Wang, Z., Shu, X., Huang, B., & Clarke, D. (2014). Laboratory investigation into mechanical properties of cement emulsified asphalt mortar. *Construction and Building Materials*, 65, 76-83.
- Saleh, M. F. (2007). Effect of rheology on the bitumen foamability and mechanical properties of foam bitumen stabilised mixes. *International Journal of Pavement Engineering*, 8(2), 99-110.
- Salomon, D. R. (2006). *Asphalt emulsion technology*: Transportation Research Board.
- Sangiorgi, C., Tataranni, P., Simone, A., Vignali, V., Lantieri, C., & Dondi, G. (2017). A laboratory and field evaluation of Cold Recycled Mixture for base layer entirely made with Reclaimed Asphalt Pavement. *Construction and Building Materials*, 138, 232-239.
- Sauzeat, C. (2003). *Comportement du sable dans le domaine des petites et moyennes déformations: rotations" d'axes" et effets visqueux*. Lyon, INSA.
- Sebaaly, P., Bazi, G., Hitti, E., Weitzel, D., & Bemanian, S. (2004). Performance of cold in-place recycling in Nevada. *Transportation Research Record: Journal of the Transportation Research Board*(1896), 162-169.
- Serfass, J. P., Poirier, J. E., Henrat, J. P., & Carbonneau, X. (2004). Influence of curing on cold mix mechanical performance. *Materials and Structures*, 37(5), 365-368.
- SFERB. (1991). *Bitumen Emulsions - General Information applications*: SFERB.
- Shoenberger, J. E. (1992). User's guide: Cold-mix recycling of asphalt concrete pavements. Final report: Army Engineer Waterways Experiment Station, Vicksburg, MS (United States

- Stimilli, A., Virgili, A., & Canestrari, F. (2017). Warm recycling of flexible pavements: Effectiveness of Warm Mix Asphalt additives on modified bitumen and mixture performance. *Journal of Cleaner Production*, *156*, 911-922.
- Stimilli, A., Virgili, A., Giuliani, F., & Canestrari, F. (2016). *In plant production of hot recycled mixtures with high reclaimed asphalt pavement content: a performance evaluation*. Paper presented at the 8th RILEM International Symposium on Testing and Characterization of Sustainable and Innovative Bituminous Materials.
- Stroup-Gardiner, M. (2011). *Recycling and Reclamation of Asphalt Pavements Using In-Place Methods*.
- Tan, Y., Ouyang, J., Lv, J., & Li, Y. (2013). Effect of emulsifier on cement hydration in cement asphalt mortar. *Construction and Building Materials*, *47*, 159-164.
- Task, F. (1998). Report on Cold Recycling of Asphalt Pavements: AASHTO-AGC-ARTBA Joint Committee, American Association of State Highway and Transportation Officials, Washington, DC.
- Tatsuoka, F., Di Benedetto, H., Kongkitkul, W., Kongsukprasert, L., Nishi, T., & Sano, Y. (2008). Modelling of ageing effects on the elasto-viscoplastic behaviour of geomaterial. *Soils and foundations*, *48*(2), 155-174.
- Tebaldi, G., Dave, E. V., Falchetto, A. C., Hugener, M., Perraton, D., Grilli, A., . . . Jenkins, K. (2018). Recommendation of RILEM TC237-SIB: protocol for characterization of recycled asphalt (RA) materials for pavement applications. *Materials and Structures*, *51*(6), 142.
- Tebaldi, G., Dave, E. V., Falchetto, A. C., Hugener, M., Perraton, D., Grilli, A., . . . Jenkins, K. (2019). Recommendation of RILEM TC237-SIB on fragmentation test for recycled asphalt. *Materials and Structures*, *52*(4), 82.
- Tebaldi, G., Dave, E. V., Marsac, P., Muraya, P., Hugener, M., Pasetto, M., . . . Canestrari, F. (2014). Synthesis of standards and procedures for specimen preparation and in-field evaluation of cold-recycled asphalt mixtures. *Road Materials and Pavement Design*, *15*(2), 272-299. doi: 10.1080/14680629.2013.866707

- Thenoux, G., González, Á., & Dowling, R. (2007). Energy consumption comparison for different asphalt pavements rehabilitation techniques used in Chile. *Resources, Conservation and Recycling*, 49(4), 325-339. doi: 10.1016/j.resconrec.2006.02.005
- Thomas, J. J., & Jennings, H. M. (2009). *Materials of cement science primer: The science of concrete*.
- Tierrie, J., Baaj, H., & Darnedru, P. (2016). Modeling the relationship between the shape and flowing characteristics of processed sands. *Construction and Building Materials*, 104, 235-246.
- Timm, D. H., Diefenderfer, B. K., & Bowers, B. F. (2018). Cold Central Plant Recycled Asphalt Pavements in High Traffic Applications. *Transportation Research Record*, 2672(40), 291-303.
- Tiouajni, S., Di Benedetto, H., Sauzéat, C., & Pouget, S. (2011). Approximation of linear viscoelastic model in the 3 dimensional case with mechanical analogues of finite size: application to bituminous materials. *Road Materials and Pavement Design*, 12(4), 897-930.
- Underwood, B. S., & Kim, Y. R. (2013). Effect of volumetric factors on the mechanical behavior of asphalt fine aggregate matrix and the relationship to asphalt mixture properties. *Construction and Building Materials*, 49, 672-681.
- Valentin, J., Čížková, Z., Suda, J., Batista, F., Mollenhauer, K., & Simnofske, D. (2016). Stiffness Characterization of Cold Recycled Mixtures. *Transportation Research Procedia*, 14, 758-767. doi: 10.1016/j.trpro.2016.05.065
- Van de Ven, M. F. C., Voskuilen, J. L. M., & Tolman, F. (2003). *The spatial approach of hot mix asphalt*. Paper presented at the Sixth International RILEM Symposium on Performance Testing and Evaluation of Bituminous Materials.
- Wang, Z., Wang, Q., & Ai, T. (2014). Comparative study on effects of binders and curing ages on properties of cement emulsified asphalt mixture using gray correlation entropy analysis. *Construction and Building Materials*, 54, 615-622.

- Wates, J. M., & James, A. D. (1993). *Zeta potential measurements on bitumen emulsions and road aggregates*. Paper presented at the 1st World Congress on Emulsions, Bordeaux.
- Wendling, L., Gaudefroy, V., Gaschet, J., Ollier, S., & Gallier, S. (2014). Evaluation of the compactability of bituminous emulsion mixes: experimental device and methodology. *International Journal of Pavement Engineering*, 17(1), 71-80. doi: 10.1080/10298436.2014.925553
- West, R. C. (2009). Keys to managing RAP variability. *Better roads*.
- Wu, Z., Mohammad, L. N., Wang, L. B., & Mull, M. A. (2005). Fracture resistance characterization of superpave mixtures using the semi-circular bending test. *Journal of ASTM International*, 2(3), 1-15.
- Xiao, F., Yao, S., Wang, J., Li, X., & Amirkhanian, S. N. (2018). A literature review on cold recycling technology of asphalt pavement. *Construction and Building Materials*, 180, 579-604.
- Xu, O., Wang, Z., & Wang, R. (2017). Effects of aggregate gradations and binder contents on engineering properties of cement emulsified asphalt mixtures. *Construction and Building Materials*, 135, 632-640.
- Yan, J., Leng, Z., Li, F., Zhu, H., & Bao, S. (2017). Early-age strength and long-term performance of asphalt emulsion cold recycled mixes with various cement contents. *Construction and Building Materials*, 137, 153-159.
- Yan, J., Ni, F., Yang, M., & Li, J. (2010). An experimental study on fatigue properties of emulsion and foam cold recycled mixes. *Construction and Building Materials*, 24(11), 2151-2156. doi: 10.1016/j.conbuildmat.2010.04.044
- Yan, J., Zhu, H., Zhang, Z., Gao, L., & Charmot, S. (2014). The theoretical analysis of the RAP aged asphalt influence on the performance of asphalt emulsion cold recycled mixes. *Construction and Building Materials*, 71, 444-450. doi: 10.1016/j.conbuildmat.2014.09.002

Zaumanis, M., Oga, J., & Haritonovs, V. (2018). How to reduce reclaimed asphalt variability: A full-scale study. *Construction and Building Materials*, 188, 546-554.